STUDIES OF FLUID MOVEMENT IN THE EYE

Thesis presented to the University of Glasgow
for the degree of Ph.D.

Henry Moseley, B.Sc.
West of Scotland Health Boards
Department of Clinical Physics and Bio-Engineering
11 West Graham Street
Glasgow G4 9LF

August, 1980

ProQuest LLC.
789 East Eisenhower Parkway
P.O. Box 1346
Ann Arbor, MI 48106 – 1346

CONTENTS

ILLUSTRATIONS

Chapter 6

Chapter 7

ACKNOWLEDGEMENTS

I should like to thank Professor W.S. Foulds, Tennent Institute of Ophthalmology, University of Glasgow and Dr F.C. Gillespie, Top Grade Physicist, and Dr R. Strang, Principal Physicist, West of Scotland Health Boards, Department of Clinical Physics and Bio-Engineering, for their stimulation, help and advice during these studies.

The experiments described in Section 2.3 and 3.3 were performed in collaboration with Professor W.S. Foulds. Results in Chapter 7 are based on electronmicrographic data of Dr I Grierson, Tennent Institute of Ophthalmology. Surgical assistance was given by Dr I Grierson, Dr N.F. Johnson and Mr N.M. McKechnie, Tennent Institute of Ophthalmology, University of Glasgow, in experiments described in Sections 2.4 and 6.2.

I should also like to thank Professor J.M.A. Lenihan, Director, West of Scotland Health Boards, Department of Clinical Physics and Bio-Engineering, for his continued support.

Finally, my thanks go to Miss A.K. Wotherspoon for typing the manuscript.

Some of the work described in this thesis has been published or presented before learned societies. At the time of submission these papers are:

Moseley, H. (1977). Movement of fluid across the outer layers of the eye. Experimental Eye Research 25: 536 (Abs.)

Moseley, H. (1977). A mathematical analogue of the posterior blood ocular barriers. Transactions of the Ophthalmological Society (U.K.) 97: 565-568.

Moseley, H. (1978). Mathematical modelling of the giant vacuole in the lining endothelium of Schlemm's canal. Ophthalmic Research 7: 250 (Abs.)

Moseley, H., Johnson, N.F. & Foulds, W.S. (1978). Vitreo-scleral fluid transfer in the rabbit. Acta Ophthalmologica 56: 769-776.

Moseley, H. (1978). A geometric method for measuring the distance between a point on the surface of the eye and the tip of a needle or instrument within the eye. Vision Research 18: 1697-1699.

Grierson, I., Lee, W.R., Moseley, H. & Abraham, S. (1979). The trabecular wall of Schlemm's canal: a study of the effect of pilocarpine by scanning electron microscopy. British Journal of Ophthalmology 63: 9-16.

Moseley, H. & Foulds, W.S. Water movement between the vitreous and the choroid. Ophthalmic Research (Abs. in press).

Moseley, H. & Foulds, W.S. Tracer movement across the rabbit retina. Documenta Ophthalmologica (In press).

SUMMARY

Although much work has been carried out on the movement of many substances into and out of the vitreous, very little is known about the transfer of water. In order to facilitate subsequent analysis, studies were performed using an inert tracer, xenon-133 dissolved in saline, as well as tritiated water.

Chapter 1 forms an introduction to the thesis. It details relevant anatomy and summarises previous work in the field, drawing attention to gaps in present knowledge.

Chapter 2 describes experiments in which xenon-133 was injected into the vitreous of rabbits and subsequently collected in one of the vortex veins draining the choroid, on the sclera and in the anterior chamber. It was found that most of the xenon-133 was removed in the blood of the choroid.

The experiments outlined in Chapter 3 are analogous to those of the previous chapter, but in this case, tritiated water was the tracer under study. As with xenon-133, most of the tritiated water from the vitreous left the eye in the blood of the choroid. The rates of removal of the two isotopes were also comparable. It is evident that the ordinary water molecules in the vitreous are being changed rapidly with a mean transit time from mid-vitreous to choroid of approximately 30 minutes.

A mathematical model of diffusion is developed in Chapter 4. The model is based on three-dimensional diffusion from the vitreous through the eye with removal occurring in the choroid. Because of symmetry, only a two-dimensional solution is required.

The results of the mathematical model are given in Chapter 5. It is shown that xenon-133 experimental results are consistent

with a diffusional explanation. The model is then applied to tritiated water where there is also good agreement between experiment and the diffusional model.

The above chapters relate to fundamental properties of water in the vitreous. It has been suggested in the literature that because of hydrostatic pressure differences, a flow exists across the retina. This is examined in Chapter 6. The existing model for hydrostatic pressure-induced flow across the posterior layers of the eye is shown to be inadequate and a new model presented. No firm conclusion may be drawn concerning the magnitude and direction of this flow but it is thought that pressures are likely to equalise and prevent such a flow occurring.

Aqueous humour leaves the eye through pores in the lining endothelium of Schlemm's canal. In Chapter 7, calculations of the pore fluid resistance are presented, based on different pore geometries. The contribution of the pore to the total outflow resistance is determined at different intraocular pressures and with and without treatment using pilocarpine.

A final discussion and conclusions are presented in Chapter 8.

CHAPTER I

INTRODUCTION

1.1 Anatomy

1.1.1 General Description

The structures and fluids of the eye are contained within a tough outer coating which is divided into the clear cornea in the anterior third of the eye and the opaque sclera over the rest of the eye. The eye fluids are separated into two compartments by the lens which is a variable focusing element (fig. 1.1). The aqueous humour is found in front of the lens and the vitreous humour is located in the vitreous cavity behind it. The aqueous humour, which is formed in the ciliary processes, moves into the posterior chamber and passes through the pupil into the anterior chamber. Its drainage is chiefly into Schlemm's canal although other routes also exist. Behind the lens, the fluid is a gel which is in contact with the inner limiting membrane of the retina. The retina is the layer of tissue which converts the optical image which it receives into electrical signals which are partly processed within the retina itself and partly within the brain. Between the retina and the vascular layer of the choroid there lies a monocellular layer called the retinal pigment epithelium.

1.1.2 Aqueous Humour

Aqueous humour is a clear, colourless liquid; in man, the volume is some 0.35 ml while in rabbits the anterior chamber volume is about 0.25 ml and the posterior chamber volume is about 0.06 ml; its viscosity is 1.025 to 1.040 relative to water and its osmotic pressure is 3 to 5 milliosmols per litre hyperosmotic to plasma (Levene, 1958; Moses, 1970).

Aqueous humour is produced in the ciliary processes partly as a secretion and partly as an ultrafiltration (Cole, 1974).

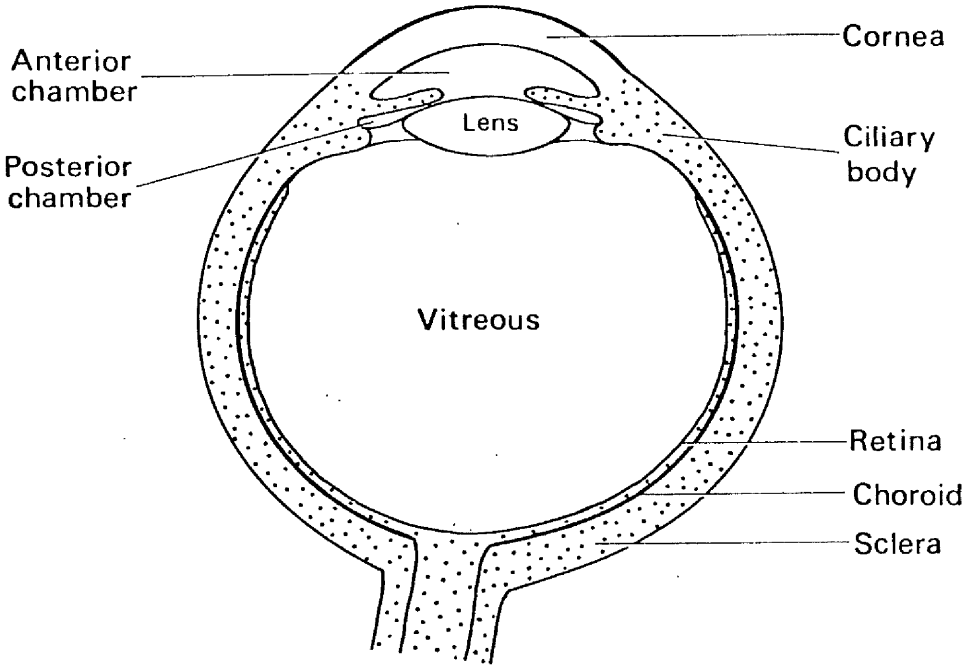

Figure 1.1

Diagrammatic cross-section of the eye.

Secretion is independent of pressure whereas ultrafiltration is pressure-dependent. While some investigations show the importance of ultrafiltration (Green and Pederson, 1973) others indicate that it is of little (Cole, 1966) or no (Bill, 1973) significance. Levene et al (1976) found a decrease in aqueous production as pressure was increased in glaucomatous eyes but not in normal eyes. From this they concluded that the relative importance of filtration and secretion depended on the pathological state of the eye. Mathematical considerations relating to the rate of aqueous production have been developed by Kinsey and Palm (1955) and Friedenwald and Becker (1956). They calculated a turnover rate for rabbit aqueous of 0.0125 to 0.0175 min^{-1}.

The conventional drainage of aqueous humour is through the trabecular meshwork into Schlemm's canal which is located at the angle between the iris and the cornea (fig. 1.2). In rabbits, there is no single canal as in primates but, rather, a series of drainage vessels (Tripathi, 1971b). The aqueous is then led into the venous system, either in the aqueous veins or the episcleral veins (Ascher, 1942; Ashton, 1951; 1952; Ruskell, 1961; Jocson and Grant, 1965). The conventional drainage system has been shown to contain a pressure-sensitive mechanism and is the major exit route (Cole, 1974).

Another drainage pathway is the uveo-scleral route whereby aqueous enters the iris root and passes between the muscle bundles in the ciliary body to the choroid and out through the episcleral tissues (Bill, 1966d). Its contribution to outflow is considered to be greater in primates than in rabbits (Bill, 1965; 1966a, 1966b; 1966c; 1966d; 1971; Bill and Hellsing, 1965; Bill and Wallinder, 1966; Bill and Barany, 1966; Bill and Phillips, 1971). It has been suggested that the uveo-scleral pathway is in fact a uveo-vortex route with drainage into the vortex veins rather than through the ocular tissues (Sherman et al, 1978). Unlike the conventional route, this system is relatively pressure-insensitive (Bill, 1966a).

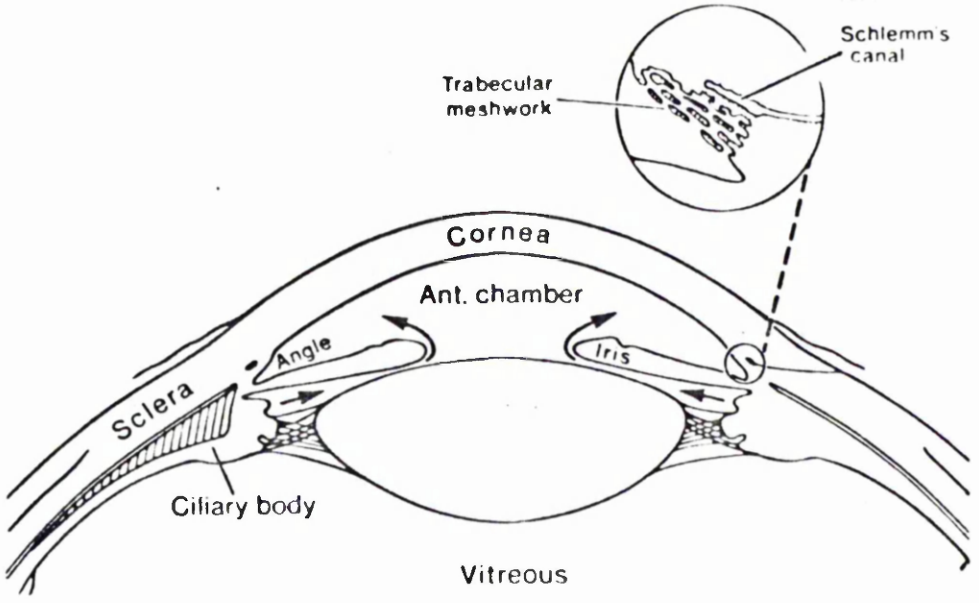

Figure 1.2

Diagram showing the formation of aqueous humour in the ciliary body and its drainage into Schlemm's canal (after Grierson, 1976).

Aqueous may also empty into the iris vessels but this does not seem to be an important route for bulk drainage (Cole, 1974). Some aqueous may exit through the cornea (Mishima and Maunce, 1961; Tönjum, 1977) while there is also a possible drainage route through the vitreous (Hayreh, 1966).

1.1.3 The Vitreous Humour

The weight of the vitreous humour in man is 3.9 g and its volume about 3.9 ml (Redslob, 1932); the water content is between 98% (Redslob, 1932) and 99.7% (Sullman, 1951); its density is between 1.0053 and 1.0089 (Visser-Heerema, 1936); the viscosity is very variable and has an intrinsic value of 4.2 cm^3/g (Balazs, 1966; Berman and Michaelson, 1964) and the refractive index is between 1.3345 (Guggenheim and Franceschetti, 1928) and 1.3348 (Paufique et al, 1959).

Points of attachment to the neighbouring tissue occur behind the lens, at the peripheral retina and around the optic disc. A layer of dense collagen fibrils forms the outermost part of the cortical vitreous (Fine and Tousimis, 1961; Fine, 1968; Hogan, 1963). Some cells, known as hyalocytes, exist in the collagen network (Szirmai and Balazs, 1958; Balazs et al, 1963). Running between the lens and optic disc is Cloquet's canal, which is a remnant of the primary vitreous which develops in embryo. A network of collagen and hyaluronic acid is responsible for the structure and viscosity of the vitreous, the hyaluronic acid preventing the collagen network of the gel from separating into solid and liquid phases.

1.1.4 The Posterior Layers

The posterior cortical layer of the vitreous is in intimate contact with the inner limiting membrane of the retina. The retina is attached to the choroid around the optic disc and at the ora serrata, which is just behind the ciliary body. It consists principally of

three layers which are, from the outside of the eye inwards, the visual cells (rods and cones), the bipolar cells and the ganglion cells (fig. 1.3). The visual cells transform light energy into nerve impulses; the bipolar cells are nerve cells which form connections between adjacent rods and cones and the ganglion cells are neurones which interconnect between the bipolar cells and the visual cortex in the brain.

The pigment epithelium is a single layer of pigmented cells joined together by tight junctions. On the outer side, it is firmly attached to the basal lamina of the choroid and, on its inner aspect, it interdigitates with the rods and cones of the retina. As observed by Foulds (1979), the intimate contact between the pigment epithelium and retina not only improves cellular adhesion but also exposes a large surface area between each tissue. The close relation facilitates molecular transfer between the two layers. The gaps between the apical processes of the pigment epithelial cells and the outer retina are filled with a mucopolysaccharide ground substance (Sidman, 1958; Zimmerman and Eastham, 1959; Fine and Zimmerman, 1963; Berman, 1969; Berman and Voaden, 1970; Rohlich, 1970; Feeney, 1973). The cells of the pigment epithelium have been shown to have facilities for active transport and are able to phagocytose material (Bairati and Orzalesi, 1963; Young and Bok, 1969; Johnson, 1975; Bassinger et al, 1976; Johnson and Foulds, 1977).

Bruch's membrane separates the pigment epithelium from the choroid which is mainly comprised of blood vessels which become increasingly larger away from the retina. The innermost vessels, called the choriocapillaris, are capillaries with membrane-covered fenestrations. These have been shown to be much leakier than the retinal capillaries (Shiose, 1969; Chioralia et al, 1976; Bellhorn et al, 1977). Vortex veins, usually four in number, remove most of the blood from the eye.

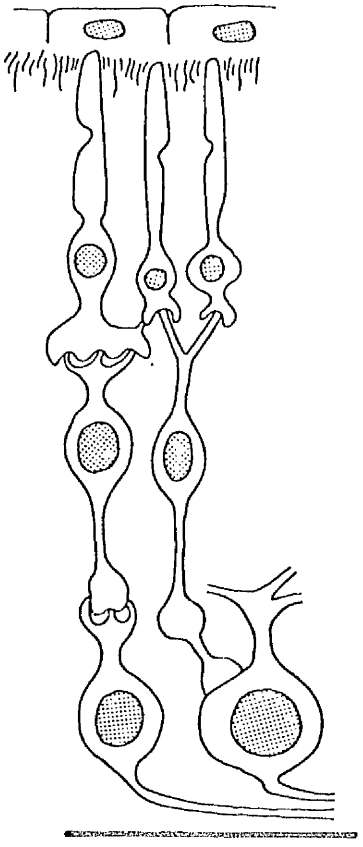

Figure 1.3

Diagram showing the three main cell types in the retina. The inner limiting membrane is in contact with the vitreous; there is inter-digitation of the pigment epithelium and outer segments of the visual cells.

The sclera is the "white"of the eye and consists of fibrous tissue which contribute to its viscoelasticity and to the viscoelastic properties of the whole eye.

1.2 Drainage of Aqueous Humour through Giant Vacuoles

There has been some controversy in relation to the route by which aqueous humour drains through the endothelium into Schlemm's canal. Sondermann's canals (Tripathi, 1974), the intercellular clefts (Feeney and Wissig, 1966; Shabo et al, 1973), micropinosomes (Fine, 1964; 1966; Feeney and Wissig, 1966; Rohen, 1969; Van der Zyphen, 1971) and intracellular channels (Tripathi, 1974; Grierson and Lee, 1975a; 1975b; 1975c) have all been proposed for the drainage of aqueous humour.

Evidence favouring intracellular channels has been given by Bill (1975), Tripathi (1977) and Grierson et al (1977; 1978). The endothelial cells on the trabecullar aspect of Schlemm's canal contain large swellings, called giant vacuoles (Garron and Feeney, 1959; Holmberg, 1959) which are usually blind invaginations but some also have an opening onto Schlemm's canal and thus form transcellular channels for the transfer of aqueous (Holmberg, 1965; Kayes, 1967; Tripathi, 1968; 1971a; 1974; Inomata et al, 1972; Grierson and Lee, 1975c; Grierson, 1976). The incidences of the vacuoles and trans-cellular channels are pressure-dependent (Johnstone and Grant, 1973; Lee and Grierson, 1974; Grierson and Lee, 1974; 1975a; 1975b; 1975c; Kayes, 1975; Grierson, 1976) and are affected by topical pilocarpine (Grierson et al, 1978; 1979).

Quantitative scanning electron microscopic studies on the endothelial lining of Schlemm's canal have been undertaken by a number of investigators (Bill, 1970; Lee, 1971; Hoffmann and Dumitrescu, 1971; Bill and Svedbergh, 1972; Segawa, 1973; Lee and Grierson, 1975; Grierson, 1976; Svedbergh, 1976; Grierson et al, 1979) and

their findings are summarized in table 1.1

McEwen (1958) applied Poiseuille's law to the flow of aqueous through the trabecular meshwork and concluded that the location of the normal barrier to outflow probably occurs in the very near vicinity of Schlemm's canal. Bill and Svedbergh (1972) investigated the resistance of the transcellular giant vacuoles lining Schlemm's canal. Their calculations showed that the paths through the giant vacuoles were sufficient to account for the flow of aqueous humour through Schlemm's canal. Svedbergh (1976) carried out a model study of the giant vacuole at a magnification of x 2,000 using aqueous humour simulated by glycerol with a viscosity 2,000 times that of water. Different shapes of the invagination were considered, but the pore openings were always modelled by a short tube. He concluded that the transcellular channels easily accounted for the bulk flow of aqueous humour.

Data on pore dimensions and incidences were obtained at different intraocular pressures in the rhesus monkey by Grierson (1976) and in human control and pilocarpine-treated tissue by Grierson et al (1979). This thesis describes an analysis of this data using different mathematical models of the pore and giant vacuole. New pore models are developed and the effect of pore geometry on fluid conductance is investigated. Application of the models to the data of Grierson (1976) and Grierson et al (1979) shows the effect of pressure and pilocarpine on fluid flow through the pore-invagination.

1.3 The Movement of Substances into and out of the Vitreous

It has been suggested (Maurice, 1957; Reddy and Kinsey, 1960) that there is free diffusion across the surface of separation between the vitreous and the aqueous and within the vitreous. However, as mentioned by Gloor (1970), account must also be taken of exchange

Table 1.1

Quantitative scanning electron microscopic studies on the lining endothelium of Schlemm's canal at normal or near-normal IOP.

Species	Number of pores per mm^2	Range of pore widths (μm)	Reference
Vervet and Rhesus monkey	1200	0.3 - 2.0	Bill (1970)
Rhesus monkey	-	0.2 - 1.0	Lee (1971)
Rhesus monkey	950	0.1 - 4.0	Lee & Grierson (1975) Grierson (1976)
Cynomolgus monkey	1640	0.25 - 5.0	Svedbergh (1976)
Human	-	$\leq$ 2.0	Hoffman and Dumitrescu (1971)
Human	1800	0.15 - 5.0	Bill & Svedbergh (1972)
Human	1000	0.15 - 1.5	Segawa (1973)
Human	350	0.2 - 3.0	Grierson et al (1979)

between the vitreous and the lens and between the vitreous and the retina. Labelled substances administered systemically reach a steady state more slowly in the vitreous than in the aqueous and different equilibrium concentration ratios between plasma, aqueous and vitreous exist for different substances (Davson et al, 1949; Maurice, 1957; Bleeker et al, 1968a; 1968b). A barrier between the vitreous and adjacent tissues has been shown to exist in the endothelium of the retinal vessels, the retinal pigment epithelium, the inner layer of the ciliary epithelium and the pigment epithelium of the ciliary body (Cunha-Vaz and Maurice, 1967; Rodriguez-Peralta and Lorenzo, 1968). The experiments of Forbes and Becker (1960) suggest a pump at the retinal vessels or pigment epithelium to remove organic anions from the vitreous. Cunha-Vaz and Maurice (1967) showed that, although fluorescein does not normally pass from the bloodstream into the vitreous, it moves out quickly from the vitreous towards the retina. They also showed that its rate of removal from the vitreous was appreciably reduced by the administration of substances which also block anion transport in the kidney.

Studies of the movement of sodium in the vitreous using ^{24}Na suggest that it enters the vitreous from the ciliary body and posterior chamber rather than across the retina and that it leaves the vitreous by way of the aqueous (von Sallmann et al, 1949; Kinsey and Reddy, 1959). The levels of potassium found by Bito and Davson (1964) in various parts of the eye indicate that it enters the vitreous from the posterior chamber and leaves across the retina. Studies of chloride exchange in the rabbit vitreous using ^{36}Cl, show that half takes place across the retina and half at the posterior chamber (Kinsey and Reddy, 1959).

Phosphate enters the anterior chamber from the ciliary body (Palm, 1949; von Sallmann and Dillon, 1950; von Sallmann and Locke, 1952; Cristiansson and Palm, 1954) and labelled phosphate

injected directly into the vitreous has been recovered mainly in the retina and choroid and, to a lesser extent, in the iris (Tronche, 1963). The relative concentrations of bicarbonate found by Davson and Luck (1956) suggest that it enters the vitreous from the posterior chamber.

A study of the distribution of proteins and amino acids led Balazs (1960) to postulate the existence of a blood-vitreous barrier and an aqueous-vitreous barrier. Protein mainly leaves the vitreous via the aqueous (Castren and Laamanen, 1963; Maurice, 1959). Amino acids are thought to move into the retina, possibly by active transport (Reddy et al, 1961; Reddy and Kinsey, 1962; Bito et al, 1965). Urea has been shown to enter the vitreous more slowly than the aqueous (Bleeker et al, 1968a) and to leave by the posterior chamber (Kinsey et al, 1960).

Some of the selective properties of the vitreous barrier were demonstrated by Bleeker et al (1968b) who studied the penetration of a number of substances from the blood into the aqueous and vitreous of the rabbit. Iodopyracet (Forbes and Becker, 1960) and fluorescein (Cunha-Vaz and Maurice, 1967; Cunha-Vaz et al, 1975) normally do not enter the vitreous from the blood but are rapidly removed from the vitreous across the retina and this movement may be obstructed by the use of probenecid which is known to block active transfer in the kidney. An active transport of iodite from the vitreous has also been proposed by Becker (1961).

From a study of the rabbit eye using a dye, Fowlks (1963) concluded that a posterior flow existed across the retina. However, Hayreh (1966) showed that colloidal iron moved from the rabbit vitreous towards the optic disc and did not cross the retina. He concluded that there was no flow across the retina but that, instead, there was a posterior flow in the direction of the optic disc. Fatt (1975) showed that some of the findings of the above investigations could be explained on the basis of diffusion combined with a posterior

flow.

With the existence of active transport mechanisms, extrapolation of the above tracer studies to the movement of water could be misleading. Moreover, conclusions based on passive modes of transfer could be erroneous because of differences in molecular size or solubility. Kinsey et al (1942) studied water movement in the vitreous using deuterium-labelled water by determining the vitreous content after systemic administration of the tracer. They found that half of the vitreous water was replaced every 10 to 15 minutes and that there was therefore a rapid turnover of water in the vitreous.

The results of previous investigations presented above are summarised in table 1.2.

This thesis describes the removal of two tracers from the vitreous to other parts of the eye. The tracers are xenon-133, an inert molecule, and tritiated water which should simulate the behaviour of the ordinary water in the vitreous. The only study of xenon-133 in the vitreous is that of Fish et al (1971) who tried to measure the choroidal blood flow by monitoring the rate of disappearance of intravitreal xenon. They concluded that other factors, besides choroidal blood flow, affected the disappearance of xenon-133 from the eye. A mathematical model based on the diffusion of these substances is developed and the predictions of the model are compared with the experimental results.

1.4 Posterior Resistance

Since the inside of the eye is at a raised pressure with respect to the outside, investigations have been carried out to measure the resistance to fluid movement across the retina, choroid and sclera and assess the hydrostatic flow across these layers. In experiments designed to show the feasibility of trans-scleral flow, Foulds (1976) reported that a radioactive tracer placed in the

Table 1.2

Previous investigations into the movement of substances into and out of the vitreous.

Substance	Transfer	Reference
Sodium	posterior chamber ► vitreous ►aqueous	von Sallmann et al (1949) Kinsey & Reddy (1959)
Potassium	posterior chamber ► vitreous ►retina	Bito & Davson (1964)
Chloride	vitreous ► retina (50%) ►aqueous (50%)	Kinsey & Reddy (1959)
Phosphate	ciliary body ► anterior chamber . vitreous►retina and choroid (most) ► iris (little)	Palm (1949) von Sallmann & Dillon (1950) von Sallmann & Locke (1952) Cristiansson & Palm (1954) Tronche (1963)
Bicarbonate	posterior chamber ► vitreous	Davson & Luck (1956)
Protein	vitreous ► aqueous	Castren & Laamanen (1963) Maurice (1959)
Amino acids	vitreous ► retina	Reddy et al (1961) Reddy & Kinsey (1962) Bito et al (1965)
Urea	vitreous ► aqueous	Kinsey et al (1960)
Iodopyracet	vitreous ► retina (active transport)	Forbes & Becker (1960)
Fluorescein	vitreous ► retina (active transport)	Cunha-Vaz & Maurice (1967) Cunha-Vaz et al (1975)
Iodite	vitreous ► retina (active transport)	Becker (1961)
India ink	vitreous ► retina (flow)	Fowlks (1963)
Colloidal iron	vitreous ► optic disc (flow)	Hayreh (1966)
Mathematical analysis	diffusion + posterior flow	Fatt (1975)
Water	systemic ► vitreous	Kinsey et al (1942)

vitreous of a living rabbit eye could be recovered in a suction chamber on the sclera. In vitro studies performed by Fatt and Hedbys (1970) and Fatt and Shantinath (1971) showed that the sclera offered much more resistance to fluid flow than the retina. They calculated that there was a flow of about 1 $\mu l.min^{-1}$ from the vitreous to the sclera. The values for resistance were supported by the in vivo experiments of Kleinstein and Fatt (1977) who used a suction cup on the sclera. However, their results are open to the criticism that the suction device altered the normal orientation of the underlying tissue.

This thesis describes experiments to measure resistance to fluid movement across the outer layers of the eye and proposes a model of the pressure-flow relations which exist at these tissues.

1.5 Discussion

There appears to be an exchange of certain substances between the aqueous, the vitreous and across the retina. The nature of this movement is not clear and its direction appears to depend on the substance in question. There appear to be selective barriers to the transfer of substances from the vitreous.

Although 99% of the vitreous is water, little is known concerning its movement. The thesis will examine the fate of both intravitreal xenon-133 and tritiated water and attempt to explain their movement. This may have relevance in the pathological condition of retinal detachment since a posterior flow has been implicated as a possible mechanism for retinal adhesion (Dobbie, 1963; Foulds, 1969; 1975; 1976; Fatt and Shantinath, 1971; Bill, 1974) and may help to explain the appearance of subretinal fluid and its disappearance without the need for a drainage operation (Weidenthal, 1967; Rosengren, 1971; Chignell, 1974; Akhmeteli et al, 1975; Leaver et al, 1976).

A better understanding of the properties of the sites of resistance both in the anterior and posterior regions of the eye may help in the understanding of some of the pathological processes which lead to glaucoma, when the intraocular pressure increases above normal.

CHAPTER 2

THE REMOVAL OF XENON-133 FROM THE VITREOUS

2.1 Introduction

The purpose of the experiments described in this chapter was to study the removal of an inert tracer from the vitreous body of the rabbit eye. An inert substance was used in order to facilitate the analysis. In the following chapter, experiments using tritiated water will be reported. A solution of xenon-133 dissolved in saline was used as the tracer. Experiments were designed to discover how much xenon-133 left the eye in the choroidal blood, how much passed through the sclera, and the extent to which it moved into the anterior chamber. The disappearance of xenon-133 from the vitreous was also monitored.

In the rabbit, most of the blood leaves the choroid through the vortex veins, of which there are usually four (Ruskell, 1964). The method adopted to assess the amount of isotope in the choroidal blood involved the collection of blood from one of the vortex veins.

2.2 Choice of Tracer

A tracer was chosen which would fulfil several criteria: 1) there should be no chemical interaction between the tracer and the material of the eye; 2) the tracer should be commercially available in liquid form; 3) in order to minimise the injected volume, it should be available in a high specific activity; 4) it should be removed rapidly from the blood pool so that the effect of recirculated tracer in the blood is minimal; 5) the diffusion coefficients and solubilities in the relevant eye tissues should be known.

Xenon-133 fulfils these criteria. It is chemically inert; 95% is removed on the first passage through the lungs (Chidsey et al, 1959) and the relevant diffusion coefficients and solubilities are

known (Strang, 1975a; 1975b; 1977). Xenon-133 has a half-life of 5.3 days, an 81 keV gamma emission and 340 keV beta emission. The isotope was obtained from the Radiochemical Centre, Amersham, U.K. and was dissolved in isotonic saline with a specific activity of 10 mCi per ml.

2.3 Movement of Xenon-133 from the Vitreous to the Vortex Veins

2.3.1 Materials and Methods

Experiments were carried out on six Dutch rabbits weighing between 1.7 kg and 2.3 kg. In order to dilate the pupil, one drop of 1% cyclopentolate and of 10% phenylephrine were placed on the eye under study. The animals were anaesthetised with an intravenous injection of 5 ml per kg of 40% ethyl carbonate in sterile distilled water (urethane) and anticoagulated with an intravenous injection of 2,500 international units of heparin in 0.5 ml (Nakamura and Goulstine, 1973). Injections were made into the marginal ear vein.

The volume of tracer injected into the vitreous was 25 µl. The introduction of such a small volume had a minimal effect on the intraocular pressure as discussed in section 2.8. The volume was measured accurately with a precision microsyringe and injected into a central position in the vitreous through the sclera using a 25G needle. The activity of xenon-133 injected was 25 µCi and a small quantity of fluorescein was mixed with the isotope to detect any leakage at the injection site.

A diagram of the experimental arrangement is shown in fig. 2.1. A vortex vein was dissected out under the operating microscope. The conjunctiva was incised and the superior oblique muscle cut through at its insertion so that no bleeding occurred. A suture was placed through the scleral tissue near the limbus and the eye was turned down to expose a vortex vein which was dissected free. The vortex vein was cut and the blood collected from it on absorbent paper tissue

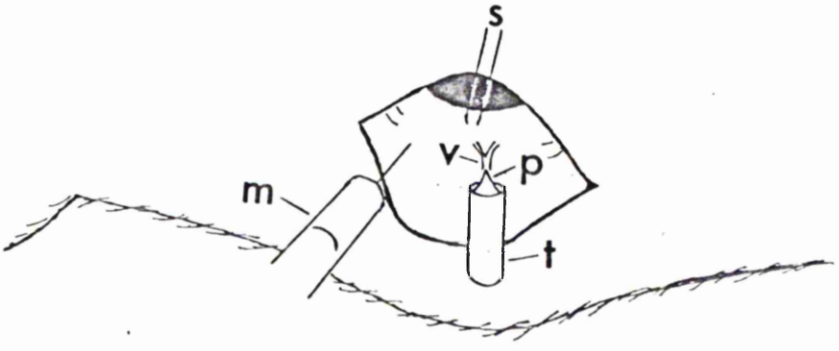

Figure 2.1

A diagram of the experimental arrangement used to collect blood from a vortex vein after the injection of xenon-133 into the vitreous. s: suture, V: vortex vein, P: paper tissue, t: glass tube, m: microsyringe.

which protruded from a small glass tube. In this way the blood was transferred rapidly from the open end of the vein into the glass tube without any loss of blood during the procedure.

At the end of each two minute period, the open end of the tube containing blood-soaked paper tissue was sealed with a piece of tape and this small tube was placed inside a larger glass tube which was heat-sealed to prevent the loss of xenon. A fresh tube with absorbent paper was placed against the open vortex vein. The collection of blood was continued for 42 mins. to 80 mins. and, at the end of the experiment, the eye was enucleated and the number of vortex veins counted.

When they had cooled, the sealed tubes were immersed for one minute in a bath of fluorescein. The tubes were then removed and inspected for the presence of fluorescein. The introduction of fluorescein within a tube would have indicated that the seal was incomplete. The tubes were then counted in a Packard Auto Gamma Counter.

Xenon-133 standards were made up after each experiment. It was necessary to divide the total activity injected into smaller units to prevent saturation of the amplifier in the counter. One way of achieving a standard would be to dilute the isotope in a known volume of distilled water. However, this could lead to an error because of the loss of xenon by diffusion into the air. The use of a single sample which was a fraction of the total 25 µl could also be inaccurate. Standards were therefore prepared by filling the 25 µl syringe with the activity of xenon which was used during the experiment. The contents of the syringe were then dispensed in approximately equal volumes into ten small tubes which were the same as used on the eye. These tubes were placed inside larger tubes which were heat-sealed and counted along with the tubes

from the eye. On summation of the counts from the standard samples, the total count for the injected activity was obtained.

For each sample, the weight of the small glass tube plus paper tissue plus tape was determined before the start of each experiment. At the end of the experiment, after the counting had been carried out, the large outer tubes were broken open and, for each sample, the weight of the small glass tube plus blood plus paper tissue plus tape was determined. The tape sealing the end of the tube prevented the loss of blood from the small tube both by evaporation and physical contact with the outer tube as well as preventing the entry of glass particles into the small tube when the outer tube was broken. The weight of blood was obtained by subtraction of the two weights and the volume calculated by dividing this by 1.067, the density of blood (Strang, 1975a).

2.3.2 Results and Discussion

No fluorescein was seen around the needle on the sclera and this indicated that little, if any, leakage occurred.

When the sealed tubes which had been immersed in a bath of fluorescein were removed from the water bath and inspected, on no occasion was fluorescein observed inside the tube and this indicated that a tight seal had been formed.

The results obtained in the six different experiments are shown in table 2.1. On each occasion xenon-133 activity was recorded from the blood in the vortex vein after the isotope had been injected into the vitreous. The range in the summation of the counts from all the tubes in each experiment was 43069 to 312001. The counts represented 7% to 32% of the injected activity, the mean being 20% and the standard error 4% (table 2.1, column 3).

Table 2.1

Results of experiments in which xenon-133 was detected in a vortex vein after injection of the isotope into the vitreous.

Experiment Number	Duration of experiment (min)	Amount of xenon in vortex vein (%)	Mean transit time (min)	Average volume of blood collected in 2 mins (ml)
1	42	25	24	0.09
2	48	7	26	0.08
3	60	22	28	0.17
4	60	13	32	0.22
5	80	32	20	0.15
6	74	19	35	0.38
Mean	61	20	28	0.18
Standard Deviation	15	9	5	0.11
Standard Error	6	4	2	0.04

Figure 2.2 shows the results from a typical experiment with the counts recorded in each tube plotted against the time when the tube collected the xenon. This shows the appearance of xenon in a vortex vein draining the choroid after injection of the tracer into a central position in the vitreous.

In order to quantify the rate as well as the extent of removal of xenon from the vitreous by the vortex vein, it is necessary to know the time it took for the isotope to reach the collecting tube from its injection site in the centre of the eye. It should be noted that the time of the appearance of the peak in the concentration-time curve would not accurately give the average appearance time since the curve is skewed. Moreover, the peak was sometimes difficult to assess because of the variability in the counts for each tube. A more accurate approach is to measure the mean rate of arrival using the formula

$$\bar{t} = \frac{\sum_{i=1}^{n} C_i \, t_i}{\sum_{i=1}^{n} C_i} \qquad (2.1)$$

where $\bar{t}$ = mean transit time

C_i = tracer counts in sample i

t_i = time from start of experiment until the mid-point of the collection of sample i

n = number of samples

The mean arrival time calculated according to equation (2.1) varied from 24 mins to 35 mins with a mean of 28 mins and a standard error of 2 mins (table 2.1, column 4).

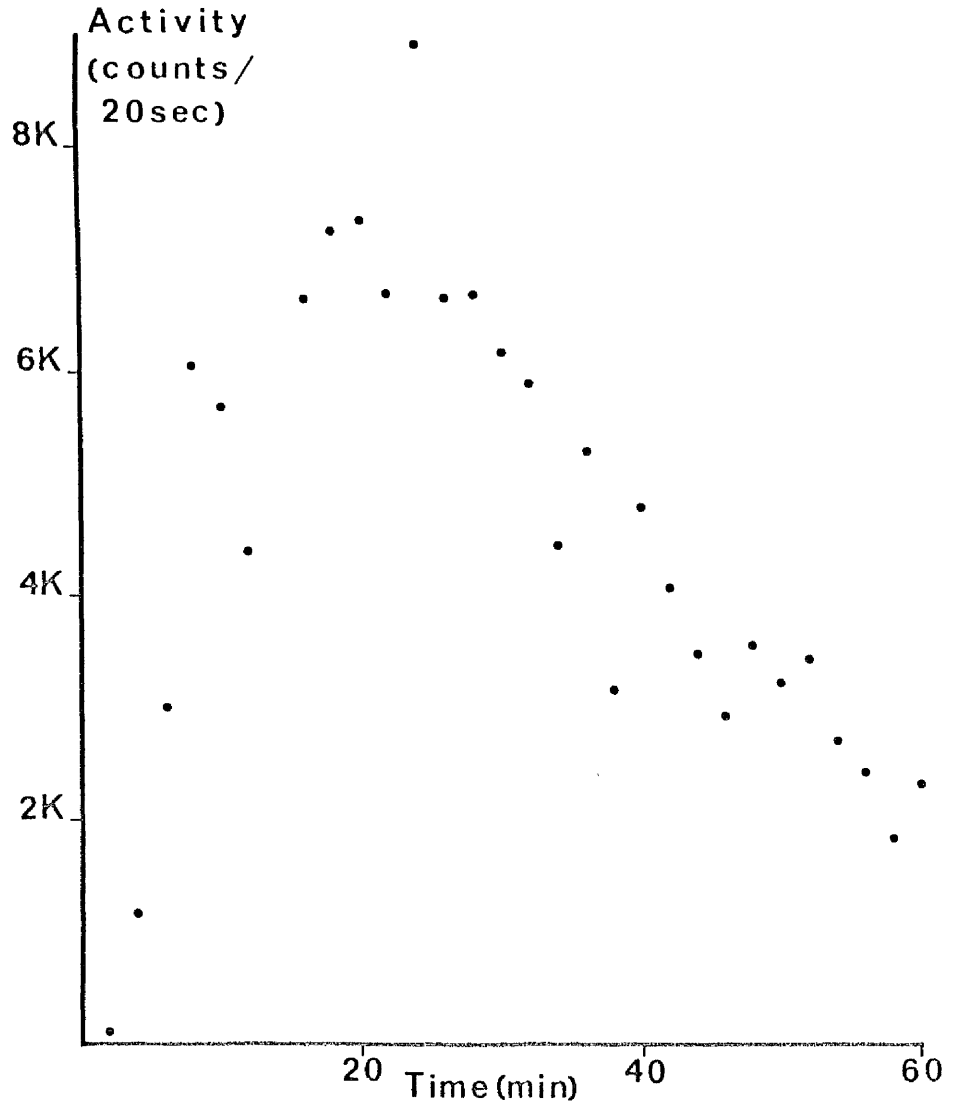

Figure 2.2

Typical result showing the appearance of xenon-133 in the blood of a vortex vein after the injection of the isotope into the vitreous.

Inspection of the enucleated eyes showed that there were four vortex veins on each occasion. The amount of blood collected in each experiment is given in table 2.1, column 5. On the assumption that each vortex vein drains one quarter of the choroid, as verified in an excised eye by Bill (1962), the mean choroidal blood flow during each experiment was 0.4 ± 0.1 ml min^{-1}. This is less than the values of 1.1 ml min^{-1} to 1.9 ml min^{-1} obtained by other investigators who also collected blood from a vortex vein (Fischer, 1930; Meesmann, 1930; Sondermann, 1932; Linner, 1952; Levene, 1957; Nakamura and Goulstine, 1973). O'Day et al (1971) found a value of 0.84 ml min^{-1} for choroidal blood flow in the rabbit using a microspheres technique and, by the inert gas clearance method, Friedman et al (1964) obtained a value of 831 to 1664 ml/min/100 g and Strang (1975a) a value of 920 ml/min/100g. In the experiments reported here, neither temperature, blood pressure nor blood gases were monitored although these factors are known to alter blood flow substantially (Strang et al, 1974). Moreover, the present study was conducted on rabbits weighing considerably less than those used by the other investigators.

A regression analysis was carried out to see if the choroidal blood flow correlated with either the amount of xenon removed by the choroid or the mean transit time. There was no correlation ($p > 0.1$) between the amount of xenon removed by the choroidal blood and the choroidal blood flow rate. A weak correlation ($0.02 < p < 0.05$) was found between the mean transit time and the choroidal blood flow rate but this weak correlation must be regarded as coincidental since it related the two parameters directly rather than inversely. It is apparent that under normal conditions the movement of an inert tracer, such as xenon-133, from the vitreous to the choroid is not limited by the rate of choroidal blood flow. This lack of

correlation explains the results of Fish et al (1971). In experiments designed to measure the choroidal blood flow, they monitored externally the amount of xenon-133 in the eye following an intra-vitreal injection. They applied the inert gas clearance method for measuring blood flow to the rate of disappearance of xenon-133 from the eye and were unable to obtain a sensible value for choroidal blood flow. The present experiments show the rate of disappearance of xenon-133 from the eye to be independent of the choroidal blood flow.

If it is assumed that each vortex vein drains one quarter of the choroid, 80 $\pm$ 16% of 25 µl of xenon-133 dissolved in saline and injected mid-vitreous is removed by the choroidal circulation with an average appearance time of 28 $\pm$ 2 mins.

2.4 Movement of Xenon-133 from the Vitreous to the Sclera

2.4.1 Materials and Method

Experiments were carried out on six Dutch rabbits weighing between 1.6 kg and 1.8 kg and the rabbits were anaesthetised with 5 ml per kg of 40% urethane. To facilitate visualisation within the eye, the pupil of the experimental eye was dilated with one drop of 1% cyclopentolate and one drop of 10% phenylephrine.

Twenty-five microlitres of xenon-133 dissolved in saline mixed with fluorescein were injected into the vitreous through the sclera using a 25G needle. The activity of xenon-133 was 250 µCi. The experimental arrangement is shown diagrammatically in fig. 2.3.

To prepare a site for the collection of any xenon which passed through the sclera, a suitable area of conjunctiva in the superior temporal quadrant was incised and reflected to expose the sclera which was kept moist with drops of isotonic saline throughout the course of the experiment. An area of sclera on the nasal side of the superior rectus muscle was prepared for the collection site

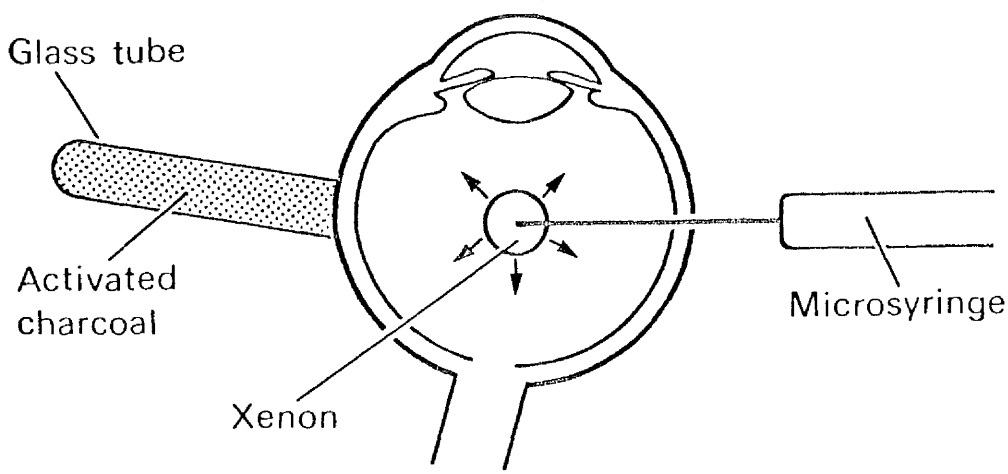

Figure 2.3

Diagram of experimental arrangement used to collect xenon-133 from the outer surface of the sclera after injection of the isotope into the vitreous.

and, on the temporal side of the superior rectus muscle, for the injection site. A threaded suture was inserted into the tendon of the insertion of the superior rectus muscle and was used to pull the eye gently downwards to facilitate access to the collection site.

It was relevant for the adoption of an appropriate collection technique to observe that the solubility of xenon in air is twenty times greater than its solubility in the sclera (Strang, 1975). This means that under equilibrium conditions, air at normal temperature and pressure will contain twenty times more xenon per unit volume than will the sclera. Thus, while any xenon surrounded by sclera or other ocular tissue will remain in solution, any in contact with air will tend to come out of solution.

For the collection of xenon in the air outside the sclera a small glass tube 2.4 cm long, 0.5 cm in diameter was filled with activated charcoal, which adsorbs xenon on its surface (Parkes, 1967), and this tube was held in contact with the exposed sclera. A thin layer of cotton wool across the open face of the tube prevented the loss of charcoal granules and provided a cushion between the charcoal and the eye without significantly impeding the passage of xenon. The nearest edge of the collection tube was always at least 1.5 cm round the sclera from the point at which the needle penetrated the eye and at least 3 mm from the limbus.

Fifteen minutes after injection, the tube was removed from the eye and a new tube containing activated charcoal was placed on the eye at the same site as the previous one. This procedure of changing the tube every 15 minutes was continued for four hours, so that 16 tubes were collected from each experiment. After its removal from the eye, each small tube packed with activated charcoal was immediately placed inside a larger glass tube which was heat-sealed.

The integrity of the seal was checked by the technique described in section 2.3.

Standards were prepared as outlined in section 2.3 and the tubes were counted for twenty minutes each in a Packard Auto Gamma Counter. The total count for each experiment was obtained by summing the activity above background in the 16 tubes.

2.4.2 Results and Discussion

The fluorescein-xenon mixture which was injected into the eye was seen to leave the end of the needle in an irregular distribution and a small amount of fluorescein could be observed along the needle. After a few minutes, the fluorescein was seen to spread through the vitreous and was not apparently leaving along the needle track. On no occasion was any fluorescein observed around the needle on the sclera and this indicated that there was little or no leakage of fluid along the needle on to the sclera.

The sealed tubes which had been immersed in a bath of fluorescein were examined. The absence of dye within the tubes indicated that the seal was effective.

The results of the six separate experiments are shown in table 2.2. The counts recorded ranged between 7766 and 136547 for the total of the 16 tubes in each experiment. Xenon activity was recorded from the sclera after it had been injected into the vitreous on each occasion.

The results expressed as a percentage of the injected activity are also given in table 2.2, with a spread in values of 0.004% to 0.031%.

One way to estimate the total amount of xenon passing through the whole sclera would be to multiply the percentage at the collection site by the ratio of the scleral area to the collecting

Table 2.2

Results of experiments in which xenon-133 was detected on the sclera following injection of isotope into the vitreous.

Experiment number	Total activity in collection tubes		Estimated activity through whole sclera	Mean transit time
	(counts)	(% of injected activity)	(% of injected activity)	(min)
1	7766	0.010	3	70
2	7898	0.005	1	87
3	13325	0.004	1	77
4	77476	0.010	2	59
5	136547	0.031	4	84
6	71643	0.009	1	93
Mean			2	78
Standard deviation			1.3	12
Standard error			0.5	5

area. However this would be incorrect since the amount collected in each experiment would depend on the distance between the tip of the needle and the collection site.

This distance was measured using a geometric method described in section 2.7. There was a tendancy that the shorter the distance between the collection site and the tip of the needle the greater the amount of activity obtained at the collection site, although this relation did not achieve statistical significance. If it is assumed that the concentration of xenon spreads out in a spherical fashion, the amount of xenon that passes through the whole sclera may be obtained from the activity at one collecting site by using the equation

$$I_s = \frac{I_c}{A} \, 4\pi r^2 \qquad (2.2)$$

where I_s = amount of indicator through the whole sclera

I_c = amount of indicator at the collecting site

A = area of collecting site

r = distance between tip of needle and collecting site

This equation may be used provided the area of the collection site and its distance from the injection point in the vitreous are known. Using this method of calculation it may be shown that the amount of xenon that passed through the whole sclera varied between 1% and 4% with a mean of 2% and standard error of 0.5% (table 2.2).

Figure 2.4 shows the results from a typical experiment with the activity recorded in each tube plotted against the time when the tube collected the xenon. This graph is a concentration-time curve for the passage of xenon from the vitreous through the sclera.

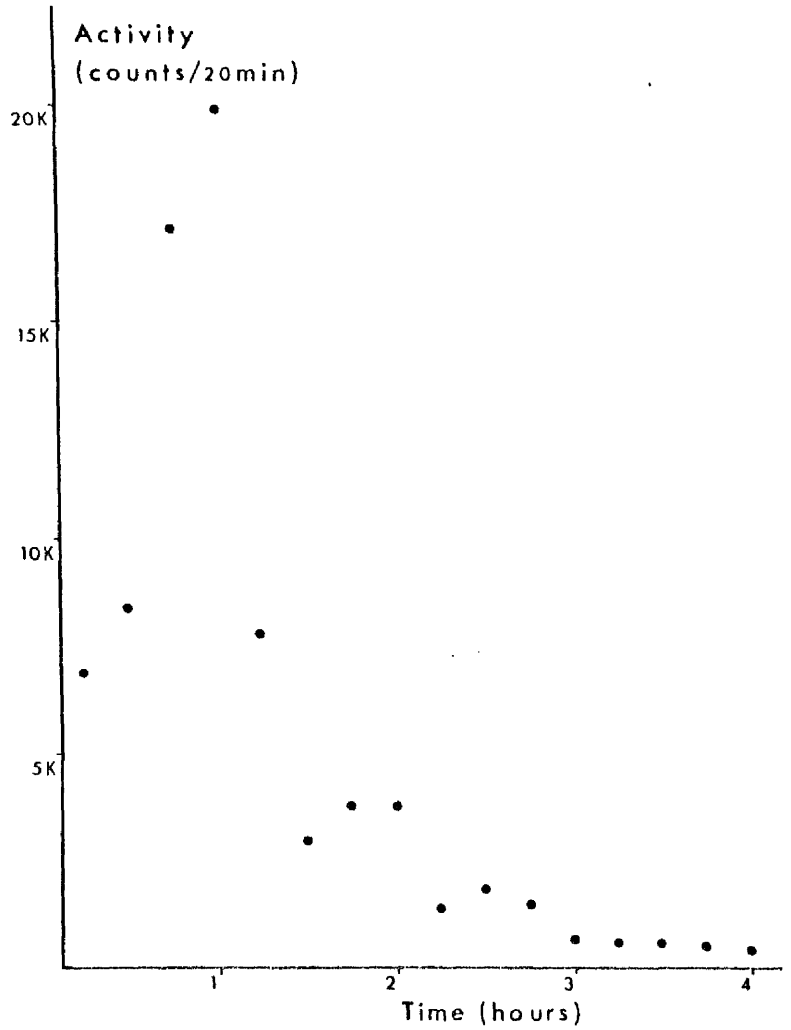

Figure 2.4

Typical result from experiment in which xenon-133 was detected on the sclera after injection of the isotope into the vitreous.

The mean transit time, calculated according to equation 2.1, varied from 59 mins to 93 mins with a mean of 78 mins and a standard error of 5 mins (table 2.2).

Bill (1966) has reported that following cyclodialysis in the living rabbit, substantial amounts of aqueous humour penetrated the sclera. Consequently it would be incorrect to regard the sclera as an impenetrable barrier. This is supported by the present findings where it is shown that 2 $\pm$ 0.5% from a 25 µl volume of an inert tracer, xenon-133 dissolved in saline, injected into the vitreous passed out through the sclera with a mean transit time of 78 $\pm$ 5 mins.

2.5 Movement of Xenon-133 from the Vitreous into the Anterior Chamber

2.5.1 Materials and Method

Experiments were carried out on four Dutch rabbits, weighing between 1.7 kg and 2.4 kg which were anaesthetised with 5 ml per kg of 40% urethane. In order to dilate the pupil and anaesthetise the cornea, each eye under study received one drop of 1% cyclopentalate, 10% phenylephrine and either benoxinate or amethocaine.

The anterior chamber was cannulated with a 25G heparinised needle attached to a syringe containing 1 ml heparinised saline (fig. 2.5). The heparin prevented fibrin formation around and within the needle in the anterior chamber.

Twenty-five microlitres containing a mixture of fluorescein and xenon-133 dissolved in saline were injected into a central position in the vitreous through the sclera using a 25G needle.

After 15 mins, 0.2 ml of the fluid in the anterior chamber was withdrawn by the syringe containing the 1 ml of heparinised saline. This syringe was removed from the needle in the anterior

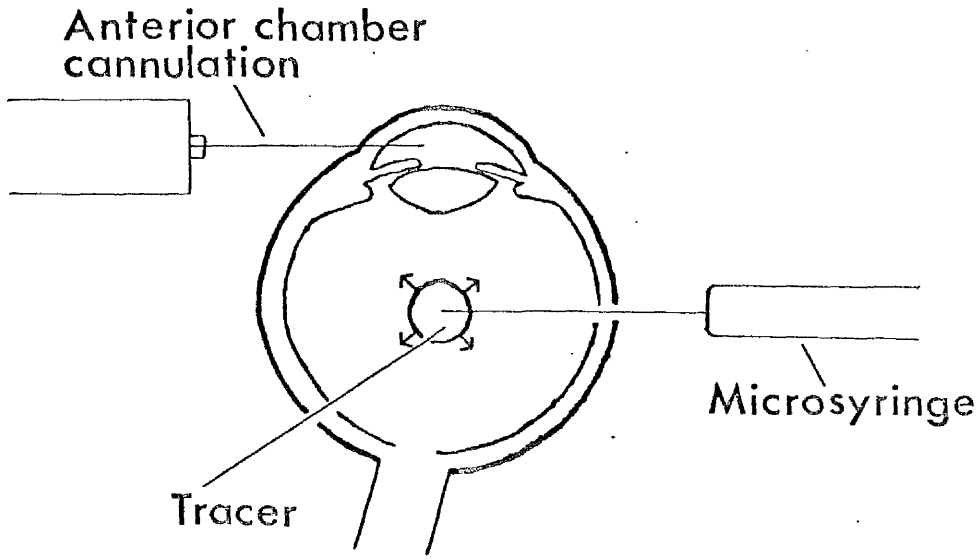

Figure 2.5

Diagram of experimental arrangement used to study the appearance of xenon-133 in the anterior chamber after its injection into the vitreous.

chamber which was re-formed using a fresh syringe containing 1 ml of heparinised saline. Any fluid around the connection between the new syringe and the needle was drawn into the old syringe which was then emptied into a glass tube 5 cm long and 0.8 cm in diameter. This tube was immediately heat-sealed to prevent the loss of xenon to the air and the tubes were checked for leakage as described in section 2.3.

The anterior chamber was emptied and re-formed every 15 minutes for 4 hours thus providing 16 collections per experiment. Fifty microcuries of xenon-133 were injected on each occasion. After each experiment, standards were made by dispensing 25 µl of xenon-133 into ten tubes as described in section 2.3.1. The tubes each contained 1 ml of heparinised saline and were identical to those used in the experiment.

2.5.2 Results and Discussion

The fluorescein was distributed in the eye in a similar manner to that described in section 2.3.2 and was not visible around the needle on the sclera. Moreover, no fluorescein was taken up by the sealed tubes in a bath of fluorescein and this showed that the seal was effective.

The results for the four separate experiments are shown in table 2.3. The total counts obtained on each occasion ranged between 7581 and 40612 (table 2.3, column 2). When compared to the prepared standards the results were equivalent to 1.7% to 6.8% of the injected activity (table 2.3, column 3). The mean value was 2.2% and the standard error of the mean was 1.2%.

A typical curve which shows the appearance of xenon-133 in the anterior chamber after its injection into the vitreous is shown in fig. 2.6. The results were analysed for the mean arrival time, using equation 2.1. The values are given in table 2.3, column 4 and may be seen to vary from 59 mins to 119 mins with a mean of

Table 2.3

Results of experiments in which xenon-133 was detected in the anterior chamber following injection of the isotope into the vitreous.

Experiment Number	Total activity in samples		Mean transit time
	(counts)	(% of injected activity)	(min.)
1	13619	1.8	106
2	40612	6.8	59
3	7581	2.3	119
4	8815	1.7	72
	Mean	2.2	89
	Standard Deviation	2.4	28
	Standard Error	1.2	14

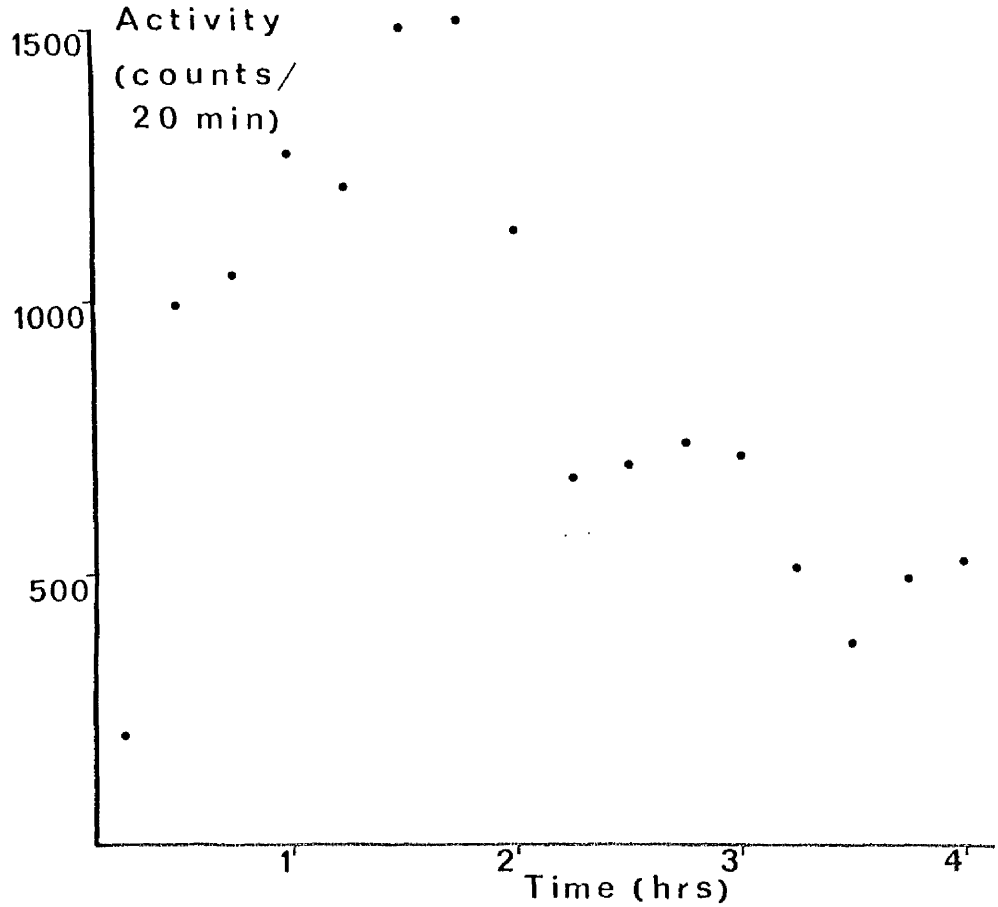

Figure 2.6

Results of typical experiment in which xenon-133 was detected in the anterior chamber after injection of the isotope into the vitreous.

89 mins and a standard error of 14 mins.

It was noted that the experiment which gave the highest percentage of xenon-133 in the anterior chamber, experiment 3, had a short mean arrival time. In this case, the peak appeared in the first sample. This may have been due to a greater than usual anterior movement of the tracer which would give both a high percentage of xenon in the anterior chamber and also a rapid rate of appearance or, since entry to the anterior chamber is via the posterior chamber in an annulus around the lens, it may have been due to an injection which was in closer proximity to the posterior chamber.

It was found that the rabbit anterior chamber contained approximately 0.24 ml of aqueous humour. However, if the anterior chamber were completely emptied, after draining and re-forming the anterior chamber a few times, the pupil would contract and the lens would be liable to come forward. However, if the anterior chamber were not completely emptied, then with very careful manipulation, it was possible to carry out the emptying and re-forming procedure many times on the same eye and still maintain an open pupil and normally placed lens. Removing a volume of 0.2 ml on each occasion allowed for a successful experiment, and still amounted to the removal of over 80% of the anterior chamber volume. Moreover, the fluid left in the anterior chamber would mix with the fresh heparinised saline once the anterior chamber was re-formed so that the only fluid loss by this means would be that left in the eye after the collection of the last sample.

The average time between the formation and drainage of the aqueous humour by the normal outflow mechanism in the rabbit is 100 minutes (Prince, 1964b). In 15 minutes, 15% of the fluid in the anterior chamber would have left the eye by this route and this

fluid might have contained some xenon. However, the amount of fluid which would reach the outflow channels from the posterior chamber is likely to be negligible. Some xenon may also have diffused into the blood vessels of the iris. According to O'Rourke (1976), in the human eye the mean xenon clearance time by this method was 5.22% min^{-1}. This would give a decay pattern as shown in table 2.4. If the isotope is assumed to have entered the anterior chamber continuously at a constant rate during each collection period and to have left according to the decay pattern of table 2.4, the amount of isotope present after 15 minutes would be the average of the decay scheme over this period, i.e. 63% of the isotope which had entered the anterior chamber. Assuming the rabbit behaviour is similar to the human, the loss of xenon to the iris would be 37%. In the present experiments, the pupil was dilated and so the surface area for diffusion into the iris was reduced to, at most, 10% of normal. Thus the loss of xenon by diffusion into the iris was probably no more than about 4%. Another source of error could be the diffusion of xenon through the cornea. Since O'Rourke (1976) found that this was significantly less than removal by the iris in the normal eye, it is thought reasonable to regard the two clearance routes as comparable in the dilated eye for the present estimation of errors. Hence the total loss of xenon by the aqueous outflow, blood flow in the iris and diffusion through the cornea was probably less than 10%.

Since the aqueous humour was collected in 1 ml of heparinised saline rather than into an empty syringe, the xenon from the eye mixed with a volume of 1 ml instead of just the 0.2 ml removed from the eye. This reduced the surface to volume ratio and lowered the concentration gradient at the liquid-air interface. The loss of xenon-133 by diffusion into the air, both from the syringe after its removal from

Table 2.4

Clearance of xenon from the anterior chamber, after O'Rourke (1976)

Time (min)	Relative amount of xenon in anterior chamber
0	100
1	94.8
2	89.8
3	85.2
4	80.7
5	76.5
6	72.5
7	68.7
8	65.1
9	61.7
10	58.5
11	55.5
12	52.6
13	49.8
14	47.2
15	44.8

the eye and also from the tube into which the syringe was emptied before the tube was sealed, was thereby reduced. Moreover, it also decreased the amount of xenon left in the syringe after it was emptied into the tube since any small liquid droplet left contained proportionately less xenon.

The constant agitation of the anterior chamber is known to cause a breakdown of the blood-aqueous barrier. This results in the secretion of plasma into the posterior chamber. Since, under the conditions of the experiments, the anterior chamber is formed mainly of isotonic saline it is unlikely that changes in the concentration of certain substances from the normal aqueous production would appreciably affect the present results.

This study has shown that when 25 µl of xenon-133 dissolved in saline was placed in the mid-vitreous of a rabbit eye, 2.2 $\pm$ 1.0% entered the anterior chamber with a mean appearance time of 108 $\pm$ 11 minutes.

2.6 Clearance of Xenon-133 from the Vitreous

2.6.1 Materials and Methods

In relation to the movement of xenon-133 from the vitreous to various ocular tissues, it is of interest to monitor the clearance of the isotope from the vitreous to see how this relates to its appearance elsewhere in the eye. Dutch rabbits weighing between 1.7 kg and 2.1 kg were anaesthetised with 5 ml/kg of 40% urethane and the pupil was dilated with one drop of 1% cyclopentalate and 10% phenylephrine. Twenty-five microlitres of xenon-133 dissolved in saline and mixed with fluorescein was injected through the sclera, using a 25G needle, into the vitreous. The activity used was 25 µCi. Three animals were left for two hours and then killed using an over-dose of anaesthetic and another three were left for four hours and then

killed by the same method.

The vitreous was removed using a freezing technique described by Forrester et al (1976). After the rabbit was killed the eye was quickly enucleated and the anterior chamber cannulated, its contents withdrawn into a syringe containing 1 ml of saline. The syringe containing saline and aqueous humour was emptied into a glass tube which was heat-sealed to prevent the loss of xenon. The eye was placed in a polythene bag and immersed in a bath containing a mixture of solid CO_2 and acetone for 1.5 minutes. The eye was then removed from the bag and the lens cut out. The outer coats of the eye were peeled back with a blade leaving only frozen vitreous which was placed in a tube and heat-sealed. Activity in the vitreous and aqueous humour were measured in a well counter and compared with standards made up as described in section 2.3.1.

2.6.2. Results and Discussion

No leakage of fluorescein was seen around the needle on the sclera.

The results obtained are given in table 2.5. The rabbits killed after two hours had, on average, 17% of the xenon-133 still in the vitreous. After four hours the average amount of xenon-133 for the remaining rabbits was 9%. These results would not be consistent with a simple mono-exponential clearance.

In section 2.4 where xenon was measured on the sclera and in section 2.5.where it was collected in the aqueous humour, the experiments lasted four hours. After four hours there was 9% of the injectate remaining in the vitreous so that a correction to the sclera and aqueous results would be less than 10%. In the case of the collection of xenon-133 from the vortex vein, described in section 2.3, the experiments lasted up to 80 minutes when there was

Table 2.5

Results of experiments in which xenon-133 was left in an undisturbed eye.

Experiment number	% of injected activity in vitreous	% of injected activity in aqueous
at 2 hrs		
1	22	0.3
2	17	0.4
3	12	0.3
at 4 hrs		
4	9	0.2
5	9	0.4
6	8	0.3

at least 17% of the injected xenon-133 still in the vitreous. Taking this into account, the total amount of xenon-133 leaving the eye in the choroidal vessels should be increased by 17%, giving a figure of 97%.

As shown in table 2.5, on average, 0.3% of the injected xenon was present in the aqueous at both of the times investigated, viz. two hours and four hours. This is less than the total amount of xenon-133 found to have entered the anterior chamber from the vitreous as described in section 2.5. The quantity of xenon-133 present in the aqueous humour at any time is less than the total amount which has entered the anterior chamber up to that time because some of it will have left the anterior chamber by the various routes described in section 2.5. Since the present results were obtained without any previous physical interference with the front of the eye, the figure of 0.3% may be taken as a lower limit for the amount of xenon-133 entering the anterior chamber from the mid-vitreous under normal physiological conditions.

2.7 Geometric method to measure the distance between the tip of a needle in the eye and a point on the surface of the eye

A geometric method is outlined which allows the distance between the tip of a needle inside the eye and the collection point on the surface of the eye to be calculated. In fig. 2.7, AC is the length of the needle, which penetrates the eye at the point B, and D is the point on the surface of the eye. A reference grid is set up at any convenient position beside the eye. A centre "O" is marked on the grid and 3 mutually perpendicular axes X, Y and Z are centred at O. Perpendiculars are dropped from the reference grid to the points A, B and D and these perpendiculars meet the reference grid at the points A^1, B^1 and D^1 respectively. The X and

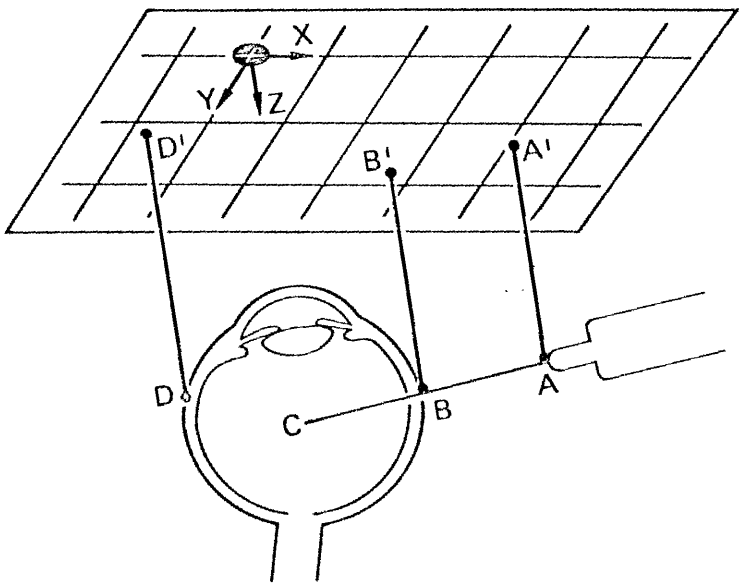

Figure 2.7

Diagram to show co-ordinate points referred to in text.

Y co-ordinates of A are identical with those of A^1, which may be obtained from the reference grid, and the perpendicular distance A^1A provides the Z co-ordinate of the point A. Thus the 3 co-ordinates of A (Xa, Ya, Za) are obtained. The co-ordinates of B (Xb, Yb, Zb) are obtained in a similar manner.

Since the needle AC is a straight line in 3 dimensions, the X co-ordinate of the point C, Xc, is given by

$$Xc = Xb + \frac{(AC - AB)}{AB} (Xb - Xa) \qquad (2.3)$$

where AC = the total length of the needle

AB = the length of that part of the needle which is outside the eye.

Similarly, the Y co-ordinate, Yc, and the Z co-ordinate, Zc, are obtained.

It is then a simple matter to determine the length of DC, since

$$DC = \sqrt{(Xc - Xd)^2 + (Yc - Yd)^2 + (Zc - Zd)^2} \qquad (2.4)$$

DC is the distance between the tip of the needle, C, and the point, D, on the surface of the eye.

The co-ordinates and perpendicular distances may be obtained quite simply and rapidly by using graph paper fixed to a board and a slider of variable length on a right-angled base (fig. 2.8). The graph paper and board, which function as a reference frame, are positioned conveniently with respect to the eye. The slider is placed with its base on the frame such that it extends perpendicularly from the frame and its position and length are adjusted until its tip is just touching the desired point (e.g. A). The position of the slider is marked on the graph paper (e.g. A^1), and its length measured

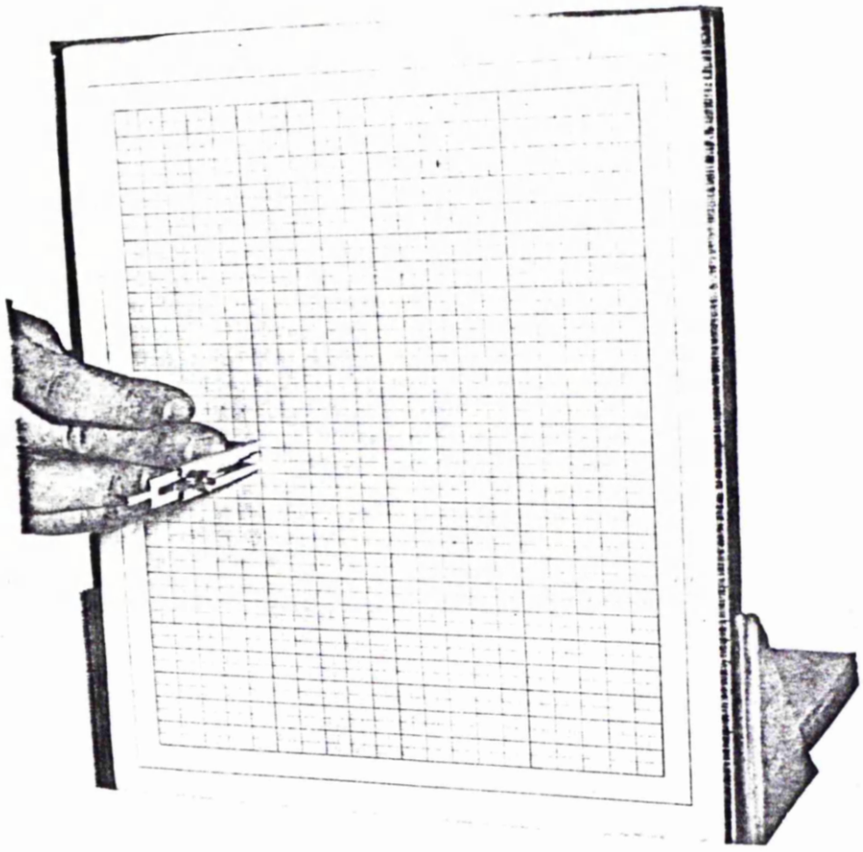

Figure 2.8

Apparatus used to obtain co-ordinate points.

(e.g. A'A). The accuracy of the measurement is limited primarily by the graph paper and slider.

2.8 Effect on the intraocular pressure of injecting 25 µl into the vitreous

In order to measure the effect on the intraocular pressure (IOP) of injecting 25 µl into the vitreous, experiments were carried out in which the IOP was monitored during the injection procedure. The anterior chamber of three living rabbit eyes was cannulated using a 25G needle attached via a short manometer line to a Bell and Howell pressure transducer and a Devices chart recorder. After allowing a few minutes for the pressure to stabilise, 25 µl of isotonic saline was injected from a microsyringe through the sclera using a 25G needle into the vitreous while continuously monitoring the pressure. The results are given in table 2.6. In one experiment the pressure rose from 20 mm Hg to 35 mm Hg and returned to 20 mm Hg in 7 minutes; in another it rose from 22 mm Hg to 32 mm Hg and returned to 20 mm Hg in 2 minutes and in the final experiment it rose from 18 mm Hg to 40 mm Hg and returned to 20 mm Hg in 16 minutes. On average, the starting pressure of 20 mm Hg rose to 36 mm Hg and returned to 20 mm Hg in 8 minutes. The injection of 25 µl into the vitreous, therefore, causes a brief rise in pressure which returns to normal in a time which is considerably shorter than the duration of the experiments reported in other sections of the present study.

Investigations into the pressure-volume relation in the eye have been reported in the literature. Perkins and Gloster (1957) conducted experiments on rabbit eyes and found a mean pressure rise from 20 mm Hg to 47 mm Hg on five successive injections of 5 µl into the anterior chamber. Eisenlohr, Langham and Maumenee (1962) reported an average increase from 27 to 48 mm Hg when 25 µl was added

Table 2.6

Effect on the IOP of introducing 25 µl into the vitreous.

Experiment number	Initial IOP (mmHg)	Raised IOP (mmHg)	Final IOP (mmHg)	Time between initial and final IOP (min)
1	20	35	20	7
2	22	32	20	2
3	18	40	20	6
Mean	20	36	20	5

to three human eyes. From the results of Hosni (1964) an increase from 20 to 45 mm Hg would be predicted for a volume increment of 25 µl in the rabbit eye. Berggren (1967) found a pressure rise from 19 mm Hg to 45 mm Hg when he injected 50 µl into the rabbit eye. The results published by Viernstein and Cowan (1969) would lead to a rise in pressure from 20 to 51 mm Hg to be expected on adding 25 µl. Finally, Blumenthal, Best, Galin and Wald (1971) reported a pressure rise from 20 to 40 mm Hg when 25 µl was injected into the cat eye.

Berggren (1967) found that the high pressure of 45 mm Hg was sustained for 45 minutes while Blumenthal et al (1971) although not giving a time, reported a rapid decline from the increased pressure.

The present results are in fairly good agreement with the published studies when it is considered that much of the early work was carried out before strain gauge transducers were available. Moreover, only Blumenthal et al (1971) and Eisenlohr et al (1962), whose results are very similar to those of the present study, gave a direct result for a single injection of 25 µl.

2.9 Movement of Xenon-133 from the Needle into the Vitreous during the Experiment

When the plunger of the syringe, used to inject the xenon-133 into the eye, is fully depressed there still remains a dead space at the tip of the syringe and within the needle. It is necessary to investigate the likelihood of the isotope in this dead space diffusing out into the eye during the course of the experiment. The volume within the dead space depended on the firmness of the attachment of the needle to the syringe. It varied from 7 µl when the needle was attached firmly to 22 µl when the attachment was loose. In the experiments described in the present and subsequent

chapter care was taken to ensure that the needle was firmly attached to the syringe. To assess the error from diffusion of xenon out of the dead space, at the end of three experiments the volume of the dead space was measured and expressed as a percentage of the injected volume, and the dead space contents were washed into a vial, heat-sealed and counted in a well counter and the counts expressed as a percentage of the injected counts.

In an experiment in section 2.3 where xenon was detected in a vortex vein, the volume of the dead space amounted to 68% of the injected volume and the activity washed out came to 72% of the total injected activity. In an experiment in section 2.5, where xenon-133 was detected in the anterior chamber, the dead space volume was 88% of the injected volume while the washed out activity was 70% of the injected activity. In an experiment in section 2.6 where the eye was left undisturbed, both the dead space volume and activity were 30% of the injected quantities. The mean dead space volume was 62% of the injected quantity and the mean dead space count was 57% of the injected activity. This indicated a mean leakage of 5% into the vitreous. However, there was an inevitable loss of xenon-133 when it was being washed from the dead space into the vial since some would be left on the walls of the syringe and needle and some would diffuse into the air. These experiments, therefore, probably overestimate the error so that 5% may be regarded as an upper limit for the average error from this source.

CHAPTER 3

REMOVAL OF TRITIATED WATER FROM THE VITREOUS

3.1 Introduction

The purpose of the experiments described in this chapter was to study the removal of water from the vitreous since water accounts for a large proportion of the volume of the vitreous. To do this, a tracer was injected into the vitreous and its presence detected elsewhere in the eye.

In the experiments described in this chapter, a small amount of tritiated water was injected into the vitreous of rabbits' eyes and detected on the sclera, in the aqueous humour and in one of the vortex veins. These are the veins which drain the choroid and, in the rabbit, they are usually four in number. The amount of tritiated water remaining in the vitreous of the eye at various times was also determined.

If tritiated water in the eye behaves in the same way as the ordinary water molecules in the eye, the movement of the tracer will reflect that of the water which is normally present. Since water constitutes 99% of the vitreous by volume (Süllmann, 1951), a knowledge of its movement is fundamental to an understanding of fluid dynamics in the vitreous. The experiments were designed to provide some basic information about the fate of water in the vitreous

3.2 Choice of Tracer

Possible tracers are heavy water or tritiated water. Heavy water is a non-radioactive form of water in which one or more of the hydrogen atoms is replaced by deuterium. Its detection is by gravimetric means. Tritiated water is radioactive and is formed when one or more of the hydrogen atoms is replaced by tritium.

Tritium is a simple beta emitter; there are no gamma-rays given off. The electrons emitted have a maximum energy of 0.018 MeV and an average energy of 0.005 MeV. They have a range of up to 0.007 mm in water. The isotope has a physical half-life of 12.26 years and tritiated water in the body has a biological half-life typically between 7.5 days and 11.5 days (Fallot, Aeberhardt and Masson, 1956 ; Pinson and Langham, 1957 ; Foy and Schnieden, 1960 ; Richmond, Langham and Trujillo, 1962). When injected in normal man it reaches approximate equilibrium with the body water within eight hours (Udekwu, Kozell and Meyer, 1963). The isotope is detected by liquid scintillation spectrometry. It is inexpensive, commercially available in high specific activities, easily detected and is the tracer of choice for water studies in the body. The tritiated water used in this study was obtained from the Radiochemical Centre, Amersham, U.K. with a specific activity of 5 Ci per ml and diluted to the concentrations required in the different experiments.

According to Leibman, Gotch and Edelman (1960), the dilution spaces of heavy water and tritiated water are identical and it would be reasonable to assume, therefore, that the movement of tritiated water in the body is the same as ordinary water.

3.3 Movement of Tritiated Water from the Vitreous to the Vortex Veins

3.3.1 Materials and Methods

Six Dutch rabbits weighing between 1.6 kg and 2.2 kg were anaesthetised with 5 ml/kg of 40% urethane. One drop each of 1% cyclopentalate and 10% phenylephrine were instilled into the eye under study.

The experimental arrangement is shown diagrammatically in fig. 3.1. The conjunctiva was incised and the superior rectus muscle cut. A threaded suture placed in the episcleral tissue allowed the

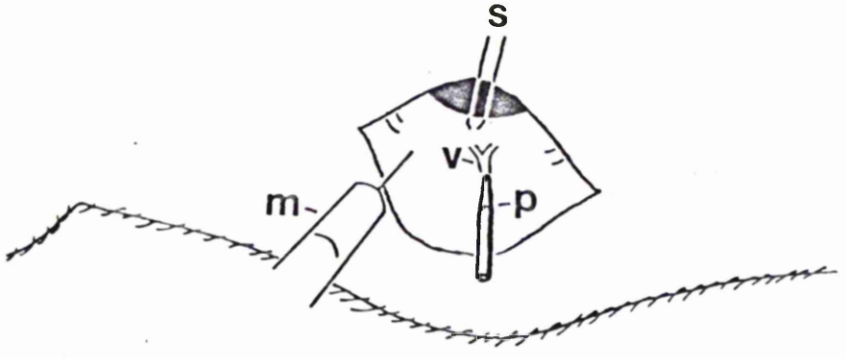

Figure 3.1

Diagrammatic representation of the experimental arrangement used to collect blood from a vortex vein after the injection of tritiated water into the vitreous. s: suture; v: vortex vein, P: capillary pipette, m: microsyringe.

eye to be turned down to facilitate access to the vortex veins. The muscle was cut at the insertion to prevent bleeding, and coagulation was prevented by the intravenous administration of 2500 International Units of Heparin in 0.5 ml, in accordance with the 1500 International Units/kg recommended by Nakamura and Goulstine (1973). The surgical procedure was carried out under an operating microscope. A dissection of the vortex vein nasal to the superior rectus muscle was performed.

Twenty-five μCi of tritiated water in 25 μl was measured accurately using a precision microsyringe and injected through the sclera using a 25G needle into a mid-vitreal position. The vortex vein was cut and the blood collected in a long form Pasteur capillary pipette. The narrow end of the pipette was placed against the open end of the vein and the pipette was inclined downwards, away from the eye, at a slight angle. As the blood left the vein it was taken into the pipette by the capillary force and it then travelled down the pipette by gravity-assisted capillary action. After two minutes the pipette was removed and a new one placed on the eye. The contents of the pipette taken from the eye were blown into a pre-weighed scintillation vial. After this, the pipette still contained some blood and so it was then washed through with one ml of water into another scintillation vial. On some occasions, the pipette was filled with blood before the two minute collection period was completed and, in these cases, the sample changes were carried out more frequently. The blood leaving the vortex vein during the changeover of the Pasteur pipettes formed a pool in the conjunctival sac and was easily taken into the new pipette. There was no blood loss during the procedure; all the blood leaving the vortex vein was collected in the pipettes.

The scintillation vial containing the blood samples was weighed and the weight of the blood was the difference between the weights of the vial with and without blood. From the weight of blood and its known density (Strang, 1975a) the volume of blood collected was obtained. The vials were kept capped throughout to prevent contamination and evaporative losses.

The amount of blood in each vial was approximately 0.2 ml. Without further sample preparation, the counting efficiency in liquid scintillator was low because of the quenching effect of the blood. To overcome this, the wet oxidation procedure described by Mahin and Lofberg (1966) was employed. Up to 0.2 ml blood was placed at the bottom of a borosilicate glass counting vial. 0.2 ml of 60% perchloric acid was added to the sample in the vial followed by 0.4 ml of 30% hydrogen peroxide, with the contents being swirled after each addition. The vials were tightly secured using caps with an inert polyethylene disc liner and the vials were then incubated in a temperature-regulated oven at 70-75^{o}C for up to three hours. Occasional agitation of the vials accelerated the solubilisation process. A clear, colourless digest resulted which, on cooling to room temperature, completely dissolved in 10 ml of NE 260 liquid scintillator (Nuclear Enterprises (G.B.) Ltd.) which was added to the vial. NE 260 is a multi-purpose xylene-based liquid scintillator for counting aqueous, aqueous salt and non-aqueous samples and accepts at least 1 ml of water, plasma, urine, etc. per 10 ml scintillator. Mahin and Lofberg (1966) observed no significant change in counting rate or absolute counting efficiency when samples containing tritium were counted again four weeks after preparation. The contents of the vials were mixed using a Rotamixer.

Samples were counted in a Packard Scintillation Counter and a channels-ratio quench correction procedure was carried out (Belcher,

1971). Quenching refers to the reduced counting efficiency which results from interference with the generation or emission of light pulses in the scintillator. In the channels-ratio method, counting is performed on three separate channels. One channel covers the complete energy spread of the pulses, another records counts from the lower energy pulses only and a third detects the higher energy pulses. Both the lower energy channel and the upper energy channel combine to cover the whole energy range of the first channel. The ratio of counts in the lower energy channel to counts in the channel covering the total energy spectrum is affected by the degree of quenching since, if quenching occurs, some of the larger pulses are converted into smaller pulses and the channels ratio is shifted. The relation between the channels ratio and the counting efficiency was determined by counting samples containing equal, known quantities of isotope and graded amounts of a quenching agent.

In the present study, Bromoform was used as the quenching agent and the counting efficiency of each experimental sample determined. Samples were counted to a maximum of 100,000 counts up to 20 minutes and relative counting efficiences of around 90% compared with the standard samples were obtained from the blood samples using the wet oxidation procedure. A standard solution was made by diluting 25 µl containing 25 µCi in 500 ml and withdrawing 1 ml into each sample.

After each experiment was completed, the eye was enucleated and the number of vortex veins counted.

3.3.2 Results and Discussion

All experiments lasted 80 minutes save one, which was of 60 minutes duration.

The blood content of each vial was obtained as described and the average blood flow calculated for each experiment. This showed

a wide variation from 0.05 ml min^{-1} to 0.21 ml min^{-1} with a mean of 0.13 ml min^{-1} and a standard error of 0.03 ml min^{-1} (table 3.1). If this is one quarter of the total choroidal blood flow, the average choroidal blood flow in these experiments was 0.52 ml min^{-1}. This is less than the values normally quoted in the literature and may be due to hypotension following urethane anaesthesia as discussed in section 2.3.

The summation of the counts from the samples in each experiment was determined, with a spread in total counts from 923920 to 5099471. When these counts were compared to the standards, the percentage of injected tritiated water collected in the blood samples of each experiment was obtained and this is shown in table 3.1. It varied between 10% and 38% with a mean of 25% and a standard error of 4%. The spread in values obtained in different experiments may have been due to different positions of the injection site within the vitreous or to a variation in the configuration of the capillary bed which is the "catchment area" of each vortex vein. The counting error due to the random nature of the radioactive disintegration process is described by the Poisson probability distribution according to which the standard deviation is equal to the square root of the counts recorded. In the case of the present experiments, this was less than 0.1%.

It is relevant to consider whether the amount collected bore any relation to the vortex vein blood flow. This is plotted in fig. 3.2 and there was no correlation ($p > .1$). Thus the amount of tritiated water collected in a single vortex vein was not dependent on the blood flow within the limits measured in the present experiments. The change in blood flow from one experiment to another may have either reflected the change in the total choroidal blood flow or simply the change in flow in the single vein under investigation and may have

Table 3.1

Results of experiments in which tritiated water was detected in the blood of a vortex vein after the isotope had been injected into the vitreous.

Experiment Number	Duration of Experiment	Amount of $^{3}H_2O$ in vortex vein	Mean Transit Time	Average volume of blood collected in 2 mins.
	(min)	(%)	(min)	(ml)
1	60	10	26	0.14
2	80	18	36	0.22
3	80	38	24	0.10
4	80	23	36	0.42
5	80	35	27	0.28
6	80	27	32	0.38
Mean	77	25	30	0.26
Standard deviation	8	11	5	0.13
Standard error	3	4	2	0.05

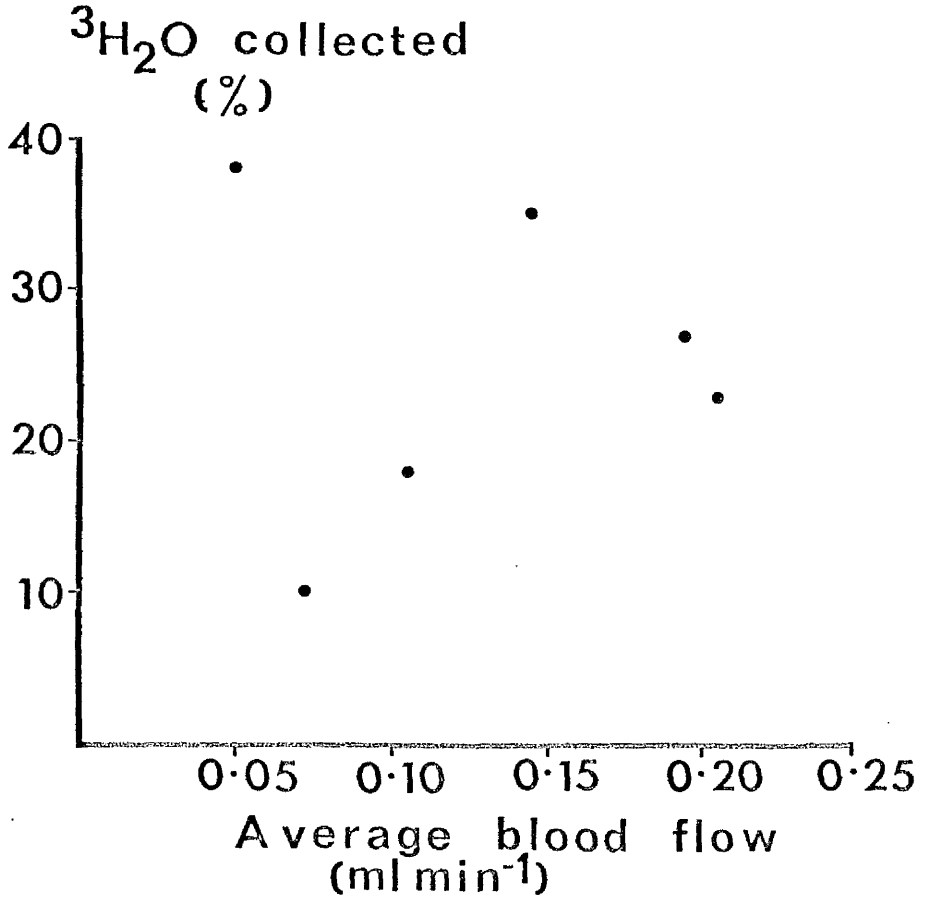

Figure 3.2

Percentage of tritiated water collected from a vortex vein v average blood flow in the vortex vein during the experiment.

been a manipulative artefact. In the former situation, one may conclude that, for a choroidal blood flow between 0.20 ml min^{-1} and 0.84 ml min^{-1}, the movement of tritiated water from the vitreous to the choroidal vessels was not dependent on the blood flow. In the latter case, a local change of blood flow in a single vortex vein between 0.05 ml min^{-1} and 0.21 ml min^{-1} did not affect the uptake of tritiated water from the vitreous. If such a variation in regional flow did not affect the tritiated water uptake, it is unlikely that a similar change in the total choroidal blood flow would affect the uptake.

The results from a typical experiment, showing the appearance of isotope in the vortex vein at different times after injection is given in fig. 3.3. For each experiment, the mean transit time for the movement of tritiated water from a central position in the viteous to the choroidal vasculature was calculated according to equation 2.1 and is given in table 3.1. The mean transit times varied between 26 minutes and 36 minutes with a mean of 30 minutes and a standard error of 2 minutes.

Since the mean transit time is the average time taken for the tracer to reach the vortex vein in each experiment, it is of interest to see if any relation exists between this and the percentage of tritiated water collected in the vortex vein. This is plotted in fig. 3.4 and, with the exception of one point, the two variables are clearly related. The reason for the aberrant point being different from the others is not apparent. This particular experiment lasted 60 minutes whereas the others were 80 minute experiments and this shorter time would slightly reduce the calculated mean transit time. A regression analysis carried out on the other five points showed that they correlated well ($.001 < p < .01$). The spread in points along the regression line may have been due to inter-experimental

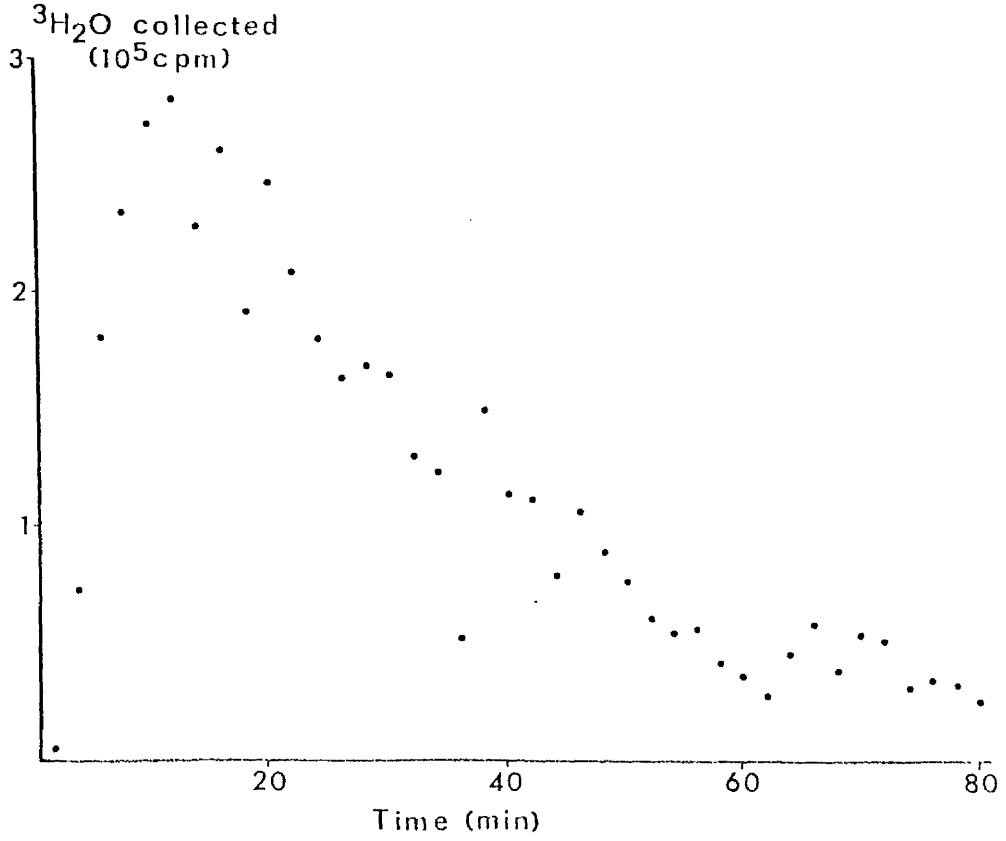

Figure 3.3

Typical result showing the appearance of tritiated water in the blood of a vortex vein following its injection into the vitreous.

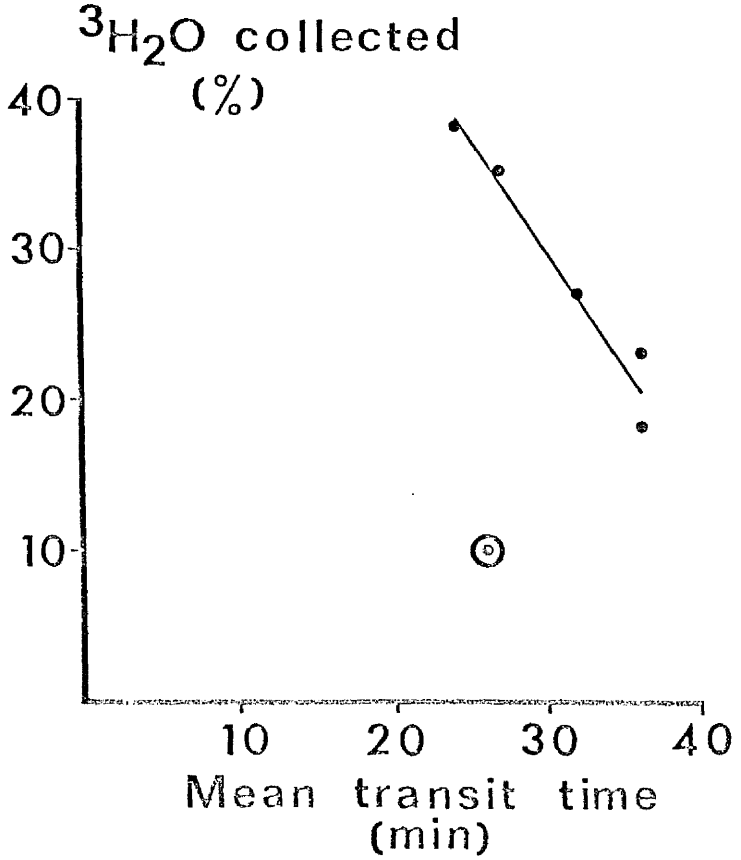

Figure 3.4

Percentage of tritiated water collected from a vortex vein v mean transit time between the middle of the vitreous and the vortex vein. Regression line excludes ringed point.

differences in the rate of movement of the tracer towards the particular vortex vein studied or it may have resulted from inter-experimental differences in the initial injection point within the vitreous and a similar rate of movement of the isotope. The latter explanation seems the more likely and, if this is so, the spread in results about the mean is due to variations in the solid angle subtended by the region of the choriocapillaris which is drained by the vortex vein. The average value of the mean transit time of the five points statistically analysed is 31 minutes. Since the spread in mean transit time values was probably due to variations in the position of the injection site, along with other factors, the spread in the mean transit times should indicate the constancy or otherwise of the distance between injection site and choriocapillaris. Of the five points, the maximum deviation from the mean was 16%. Since other factors will have contributed to the mean transit time differences, this value indicates the upper limit of the positioning error. Moreover, the relation between percentage collected and mean transit time suggests that the tracer moved directly from the vitreous to the choroid and not by some other route, e.g. into the anterior chamber and from there into the iris vessels.

Great care must be taken in interpretation of a curve which has been extrapolated since no evidence has been produced to show that a similar relation exists outwith the experimentally-verified limits. When the regression equation $y = -1.55x + 76$, where y is the percentage of isotope collected from the vortex vein and x is the mean transit time, is extrapolated to $x = 0$, a value of 76 is obtained for the percentage of water in the vortex vein. For a mean transit time of zero, one might expect the uptake to be around 100%. On the other hand, for a point close to the choroid where half the tracer enters the choroid and the rest diffuses off into

the vitreous, one would expect a very low value of mean transit time and an uptake of the order of 50%. Clearly the $y = -1.55x + 76$ equation does not apply at very low values of x. Nevertheless, extrapolation down to low values of x gives a percentage uptake which is a reasonably sensible value. Extrapolation to $y = 0$ gives $x = 49$. Since the injections were made in the centre of the vitreous, the mean transit time, x, from the most distant point in the vitreous where the uptake, y, will be a minimum, will be of the order of twice the average value, i.e. 60 mins. In view of the uncertainties involved these two mean transit times are sufficiently close to indicate the reasonableness of the relation. The extrapolated values, therefore, add support to the argument that the variations found were due to different injection points and that the isotope moved directly between the vitreous and the choroid.

On each occasion four vortex veins were counted in the rabbit eye under investigation. If it is assumed that each vortex vein drains one quarter of the choroid, the total amount of tritiated water removed by the choroid was four times 25%, i.e. 100% with a standard error of 16%.

Since it is believed that tritiated water and normal water behave in a similar fashion, the present study shows that, to an accuracy of 16%, the water in the vitreous is entirely removed by the choroid. Moreover, the mean transit time for the movement of water from the mid-vitreous is 30 ± 2 minutes.

From experiments in which heavy water was injected intraperitoneally and subsequently detected in the vitreous of two rabbits, Kinsey et al (1942) calculated that one half of the vitreous volume is replaced every 10 to 15 minutes, i.e. 75% to 87.5% is replaced in 30 minutes. The findings of the present experiments are in agreement with those of Kinsey et al (1942).

3.4 Movement of Tritiated Water from the Vitreous to the Sclera

3.4.1 Materials and Methods

Experiments were carried out on six Dutch rabbits weighing between 1.3 kg and 1.8 kg. The rabbits were anaesthetised with 5 ml per kg of 40% urethane. In order to dilate the pupil one drop of 1% cyclopentalate and one drop of 10% phenylephrine were instilled into the conjunctival sac of the eye under study.

A diagram of the experimental arrangement is given in fig. 3.5. The conjunctiva was cut on the superior temporal aspect of the eye to expose the sclera. An area of sclera was prepared on the nasal side of the superior rectus muscle for the collection of any isotope which appeared on the sclera and, on the other side of the superior rectus muscle, the conjunctiva was opened for the injection site. A suture was placed in the sclera at the insertion of the superior rectus muscle and this was used to pull the eye gently downwards to facilitate access to the collection site.

During the experiment, drops of isotonic saline were placed on the eye periodically from a syringe to prevent dehydration of the sclera. Co-ordinate points were obtained to measure the distance between the tip of the needle in the eye and the collection site on the sclera, as described in section 2.7. The experiment was continued for four hours.

Twenty-five microlitres containing 1.25 mCi of tritiated water were drawn into a precision microsyringe and injected through a 25G needle into the vitreous body. Any isotope which came through the sclera at the collection site was absorbed on a small disc of glass fibre filter paper of a suitable grade for radioassay of weak beta-emitters by scintillation counting. The discs were circular and covered an area of 0.25 cm^2. Identical discs were made using a paper punch. The filter disc on the eye was placed in an envelope

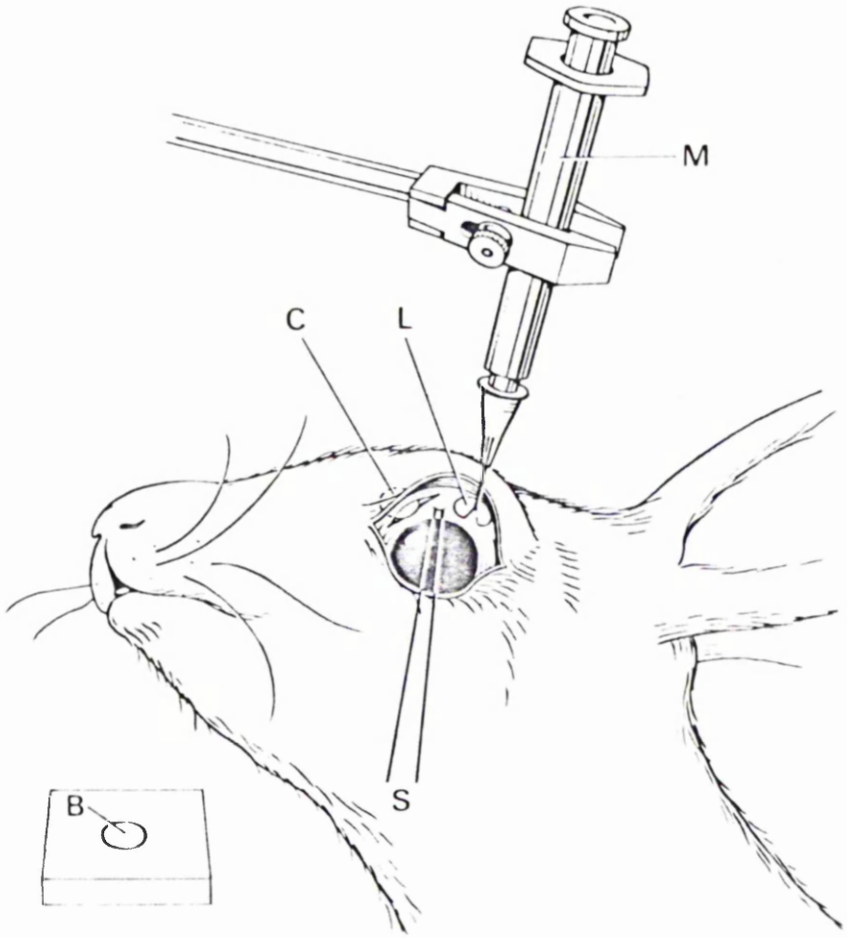

Figure 3.5

Diagram of experimental arrangement to detect tritiated water on the sclera after the isotope had been injected into the vitreous.
M: microsyringe, C: collection disc on sclera, L: disc to collect any leakage around needle, S: suture, B: disc to monitor background activity.

between the sclera and the conjunctiva and this prevented the loss of tritiated water from the filter disc by evaporation during the collection period. To prevent the tritiated water from diffusing through the filter disc and subsequently being left on the conjunctiva when the filter disc was removed from the eye, the filter disc was covered on the outside by an identical-size disc of cellophane. When a filter disc containing 10 µl of water was situated on the weighing pan of a balance only 20% of the water remained after 15 mins at room temperature. When the experiment was repeated with the cellophane disc on top of the wet filter disc, there was no detectable weight loss after 15 mins. This provided confirmation that the cellophane constituted an effective barrier to the penetration of water. Moreover, in the experimental situation, any tritiated water collected on the filter disc from the eye was absorbed on the inside of the disc and must pass through the disc before it reached the outer face.

A disc of filter paper with a "V" notch cut out was placed around the needle on the sclera. This was used to check whether there was any leakage of isotope around the needle. Another disc of filter paper was placed beside the head of the rabbit. This was used to assess the degree of contamination from the tritiated water breathed out by the rabbit or from any other source. Since the disc was positioned flat with half its total surface area exposed, it may be expected to provide an upper limit for the amount of contamination which is present on the scleral samples.

The filter discs were all replaced every 15 mins for four hours. The discs were handled with forceps which were rinsed and dried after each removal or replacement of a disc to prevent contamination between samples. The filter disc samples were placed directly in vials containing 10 ml of NE 260 liquid

scintillator and mixed with a Rotamixer. The filter paper became transparent in the scintillator fluid. It was found that when a small disc containing isotope was placed in four different positions at the bottom of the vial, counts were within 2%. It was further observed that the average count from three vials containing a filter disc to which isotope had been added was within 5% of the average from three vials containing the identical quantity of isotope alone. These checks showed that the presence of the small glass fibre disc at the bottom of the vial did not lead to significant counting errors.

Each sample was counted for up to twenty minutes to a maximum of 100,000 counts. A standard solution was made by diluting 25 µl containing 1.25 mCi of tritiated water in 2 l of distilled water and withdrawing 1 ml into each standard sample.

3.4.2 Results and Discussion

On each occasion, counts were obtained from the scleral samples after injection of tritiated water into the vitreous. These showed that transfer of water had occurred from the vitreous to the outer surface of the sclera. The results are given in table 3.2. The total counts obtained in each experiment from the summation of the sixteen samples varied from 1944831 to 7219464. Quench corrections were applied although the samples were all close to the 100% relative counting efficiency of the unquenched standards.

Using the standards, the results were expressed as percentages of the amount of tritiated water injected into the vitreous. This is given in table 3.2 and varied between 0.017% and 0.052%. Using equation 2.2 and the co-ordinates taken during the experiment, the amount of tritiated water which passed through the whole sclera was calculated to be between 1.0% and 3.1% of the quantity injected into the eye (table 3.2). The mean value was 1.5% and the standard error was 0.4%.

Table 3.2

Results of experiments in which tritiated water was detected on the outer surface of the sclera following injection of the isotope into the vitreous.

Experiment Number	Total Activity at Collection Site (counts)	(%)	Estimated Activity over Whole Sclera (%)	Mean Transit Time (min)
1	1944831	0.017	1.0	118
2	3594403	0.024	1.3	103
3	7219464	0.052	1.6	81
4	2802549	0.018	0.6	86
5	4745100	0.038	3.1	74
6	4679680	0.035	1.3	79
Mean			1.5	90
Standard deviation			0.9	17

A typical plot of the activity collected at different times after the start of the experiment is shown in fig. 3.6. The mean appearance time of tritiated water on the sclera was calculated by equation 2.1 and varied from 74 minutes to 118 minutes with a mean of 90 minutes and standard error of 7 minutes.

The average counts recorded from the background filter paper was less than 1% of the scleral counts and, since this is an upper limit for the background activity on the scleral samples, it shows that the scleral counts were very little affected by atmospheric contamination. It also implies that there was little or no transfer of isotope between the filter discs, as would have occurred if the forceps were contaminated.

When a similar analysis was carried out on the filter samples around the needle, the estimated amount of tritiated water over the whole sclera was between 0.5% and 2.4% with a mean of 1.3% and a standard error of 0.6%. Since the mean obtained from the samples around the needle was comparable to that obtained from the scleral samples, it may be deduced that there was no significant leakage around the needle. This means that there was little activity lost from the eye so that the percentages quoted are substantially correct and, also, that it is unlikely that the isotope collected on the scleral samples arrived by tracking along the needle and then running across the sclera. There was a greater scatter of results around the needle as shown by the higher standard deviation. This may have been due to the greater difficulty in positioning the filter disc around the needle at the same site as the previous sample.

It may be supposed that the tritiated water behaved in an analogous fashion to the ordinary water in the eye. If this is the case, and, if 1.5% of the whole vitreous water passes through the

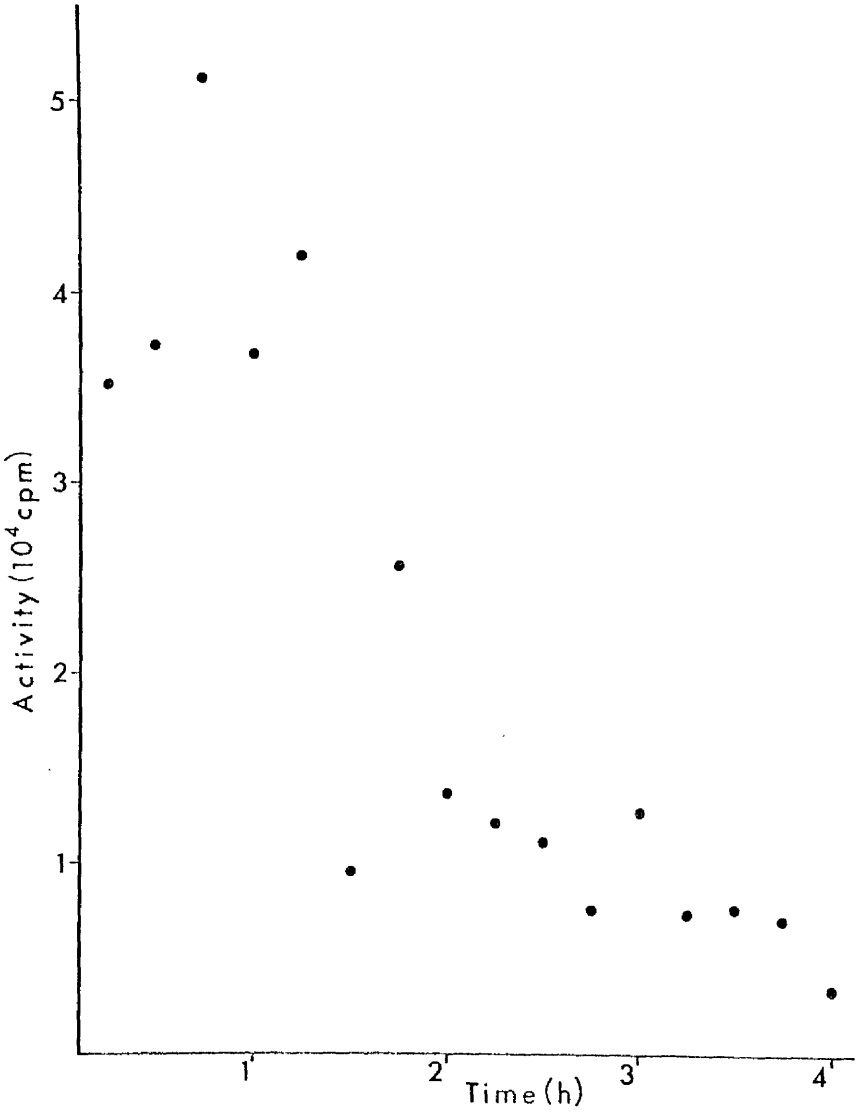

Figure 3.6

Typical result showing the appearance of tritiated water on the sclera after injection of the isotope into the vitreous.

sclera in 90 mins, then, assuming a vitreous volume of 1.47 ml (Prince, 1964a), this is equivalent to a movement of 0.25 $\pm$ 0.07 µl min^{-1}. This average rate of movement of the whole vitreous may not be valid if there exist regional differences in the water movement within the vitreous, since the average of the six experiments may not then give a representative result. From the results of experiments in which nitro blue tetrazolium chloride and India ink were injected into rabbits' vitreous, Fowlks (1963) concluded that there exists a stream of fluid in the pararetinal vitreous flowing posteriorly from the corona ciliaris across the retina. Studies with colloidal iron led Hayreh (1966) to suggest that fluid from the peripheral part of the vitreous travels towards the optic disc. Other tracer studies have been carried out and these have been reviewed by Hayreh (1977). However, there is, as yet, no direct evidence of regional variations of water movement within the vitreous. It is, therefore, reasonable to regard the six results in the present study as typical of the vitreous as a whole. Moreoever, the amount of tritiated water passing through the whole sclera would still remain valid provided the tracer could cross the sclera at any point.

The value of 0.25 µl min^{-1} is not the trans-scleral flow rate. It includes water movement by diffusion and does not take account of diffusion of water in the opposite direction, from the sclera to the vitreous. Therefore, the net transfer of water by pressure-dependent bulk flow from the vitreous across the sclera must be less than this value.

Other investigations of fluid movement across the sclera in the living rabbit eye have been undertaken (Bill, 1966; Kleinstein and Fatt, 1971). Using tracers, Bill (1966) found that there was a drainage of aqueous from the anterior chamber

through the sclera of 0.1 µl min^{-1}. Kleinstein and Fatt (1971) found a trans-scleral flow rate of 1.1 µl min^{-1} using a suction cup technique on the sclera. Kleinstein and Fatt (1971) did not demonstrate the source of the fluid which they collected. However, in view of the present findings, it is unlikely that the fluid which they collected was derived directly from the vitreous.

These experiments show that a small amount of water is transferred from the vitreous to the outer surface of the sclera in the rabbit eye. Since the outer surface of the filter disc was covered with cellophane, it is unlikely that the tritiated water collected was derived from the conjunctiva. Some of the isotope may have been removed in the choroidal blood and transferred back into the choroidal tissue in subsequent circulations round the body. In this case, the result would still be valid with respect to vitreo-scleral transfer, since this makes no assumptions on the mechanism involved. Exchange of tritiated water in and out of the choroidal blood would merely introduce a "dead time" in the choroid, during which the isotope was in the circulation. Consideration of experiments carried out using xenon-133, however, shows that the amount of recirculated isotope collected on the sclera was probably insignificant. Ninety-five percent of xenon is removed on the first passage through the lungs (Chidsey et al, 1959). The amount of recirculated xenon in the choroidal blood, following an intravitreal injection is, therefore, insignificant. It follows that the xenon collected on the sclera was essentially unaffected by recirculation of the tracer. Since the percentages of xenon-133 and tritiated water on the sclera are comparable, it is unlikely that the tritiated water result was significantly affected by recirculated isotope.

3.5 Movement of Tritiated Water from the Vitreous into the Anterior Chamber

3.5.1 Materials and Methods

Six Dutch rabbits weighing between 1.7 kg and 2.3 kg were anaesthetised with 5 ml/kg of 40% urethane injected into the marginal ear vein. One drop each of 1% cyclopentalate, 10% phenylephrine and amethocaine were instilled into the eye under investigation to dilate the pupil and anaesthetise the cornea.

The method used was similar to that described in section 2.5.1 and the experimental arrangement is shown diagrammatically in fig. 3.7. The anterior chamber was cannulated with a 25G needle connected to a syringe containing 1 ml of isotonic saline. Twenty-five microlitres containing 25 μCi of tritiated water was injected into the vitreous through a 25G needle using a precision microsyringe. The isotope was placed in an approximately central position in the vitreous under direct vision. Every 15 mins for four hours, the anterior chamber was emptied of 0.2 ml and re-formed with isotonic saline. With practice, this procedure did not distort the appearance of the anterior chamber and, at the end of the experiment, the pupil was still fully dilated and the lens in its normal position. Sixteen samples were obtained from each experiment and these were placed in vials containing NE 260 liquid scintillator. The samples were counted in a Packard Scintillation Counter along with a series of quenched standards.

3.5.2 Results and Discussion

The total counts collected from the sixteen samples in each experiment amounted to between 3111284 and 8882254 (table 3.3). When compared to the standard samples, these were equivalent to 1.2% to 5.2% with a mean of 2.8% and a standard error of 0.6% (table 3.3).

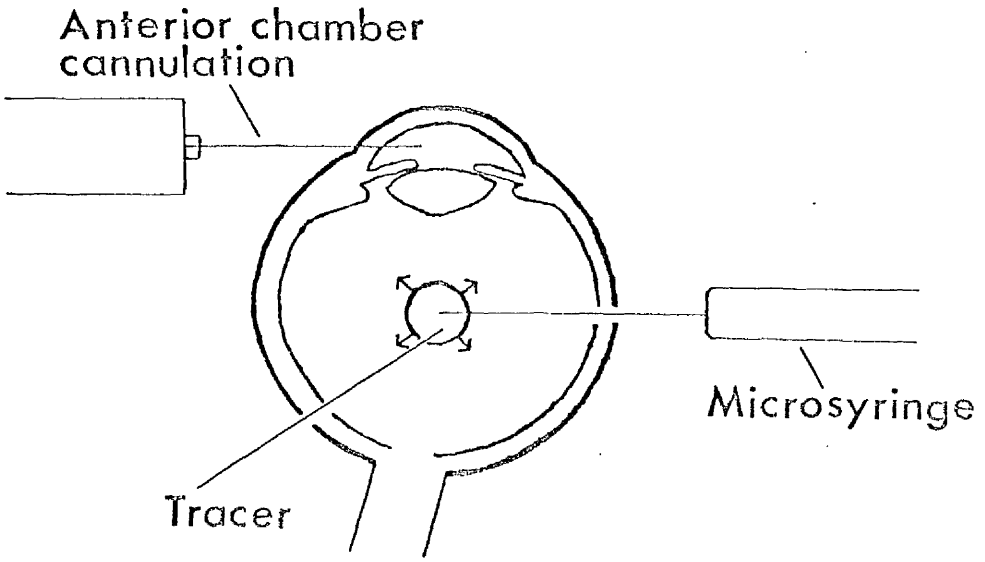

Figure 3.7

Diagram to show injection of tracer into the vitreous using a micro-syringe and cannulation of the anterior chamber.

Table 3.3

Results of experiments in which tritiated water was recovered in the anterior chamber after it had been injected into the vitreous.

Experiment Number	Total activity in samples		Mean Transit Time
	(counts)	(% of injected activity)	(min)
1	3111284	1.2	90
2	8882254	5.2	72
3	5417760	2.0	93
4	6848820	3.0	86
5	3114838	1.6	78
6	7581614	3.5	83
Mean		2.8	84
Standard deviation		1.5	8
Standard error		0.6	3

A typical curve showing the appearance of tritiated water in the anterior chamber after injection into the vitreous is given in fig. 3.8. Similar curves were obtained for each experiment and, from these, the mean appearance time was calculated according to equation 2.2. This is given in table 3.3 and varies from 72 mins to 93 mins with a mean of 84 mins and a standard error of 3 mins.

In an experiment reported by Kinsey, Grant and Cogan (1942), there was no detectable tracer in the aqueous after 11 mins when 70 µl of 80% heavy water was injected into the rabbit vitreous. Kinsey et al (1942) claimed to be able to detect a concentration of 0.05% of heavy water in normal water. This means that in an average rabbit anterior chamber of 0.25 ml, they should have been able to detect 0.125 µl of heavy water. Since they injected 70 µl of 80% heavy water, i.e. 56 µl of heavy water, they would have been able to detect 0.22% of the injected tracer. The values obtained in the first sample of the present study are the amounts of tritiated water in the aqueous after 15 mins and are shown in table 3.4. There is a large scatter in these results, going from 0.04% to 0.42% with a mean and standard error of 0.20% and 0.07% respectively. Kinsey et al (1942) do not report on the number of experiments they performed but, if this was small, they may easily have been unable to find more than 0.22% in the aqueous after 11 mins so that there is no disagreement between the findings of the present experiments and theirs.

Von Sallmann, Evans and Dillon (1949) injected ^{24}Na into the vitreous of rabbit eyes. They tracked its movement by killing the rabbits at various times after the injection of the isotope and then opening the eye and obtaining autoradiographs. They found traces of ^{24}Na in the aqueous humour one hour after the intra-vitreal injection. The findings of the present experiments are

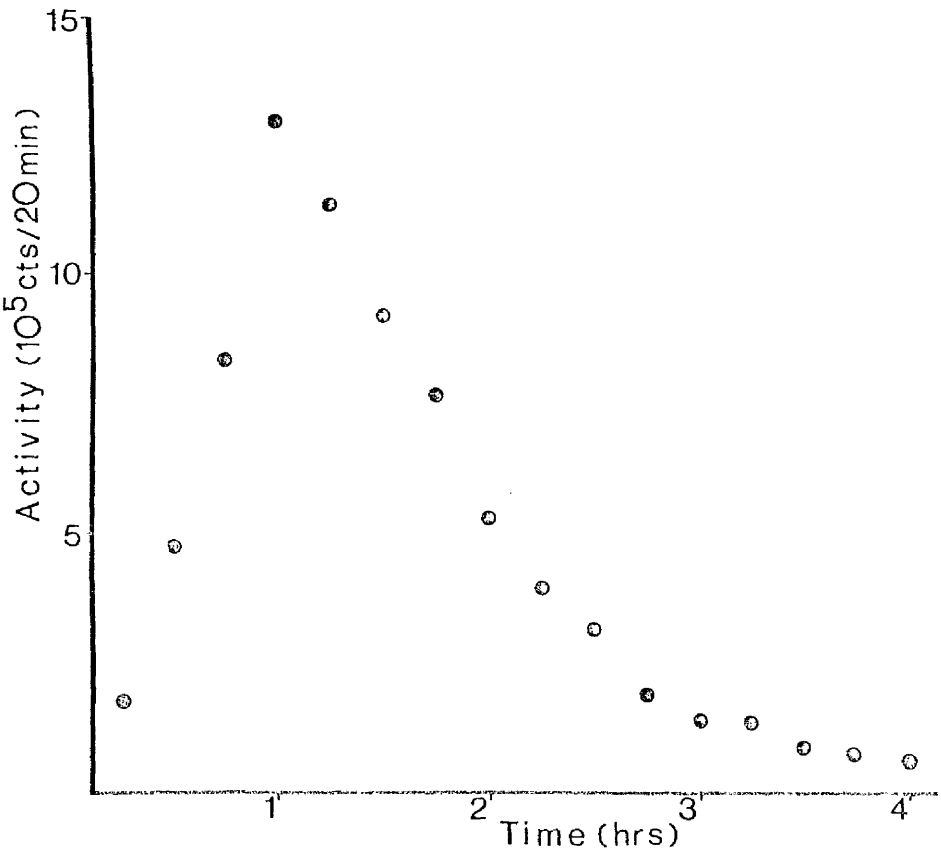

Figure 3.8

Results from a typical experiment showing the appearance of tritiated water in the anterior chamber following its injection into the vitreous.

Table 3.4

Percentage of tritiated water in the first fifteen minute sample taken from the anterior chamber.

Experiment Number	Activity in first 15 min. sample (%)
1	0.04
2	0.42
3	0.11
4	0.37
5	0.15
6	0.08
Mean	0.20
Standard deviation	0.16
Standard error	0.07

consistent with this.

3.6 Clearance of tritiated water from the vitreous

3.6.1 Materials and Methods

Experiments were carried out on Dutch rabbits weighing between 1.6 kg and 2.2 kg. The rabbits were anaesthetised with 5 ml per kg body weight of 40% urethane and, to facilitate comparison with other experiments, the pupil of the eye under study was dilated by the instillation of one drop each of 1% cyclopentalate and 10% phenylephrine.

Twenty-five microcuries of tritiated water in 25 µl was injected into the rabbit vitreous through a 25G needle using a precision microsyringe. Two rabbits were left for two hours and then killed while another three were left for four hours then killed. Death was by an overdose of anaesthetic. The eyes were enucleated, the aqueous withdrawn and the vitreous was removed by a freezing technique described in section 2.6. The samples from the eyes were placed in a scintillation vial containing 10 ml of NE 260 liquid scintillation fluid and counted in a Packard Scintillation Counter. A series of quenched standards was prepared as discussed in section 3.3 and counted along with the ocular samples. In some cases lens and ocular coat, comprising retina, choroid and sclera, were also counted for comparison. Quench corrections were carried out.

3.6.2 Results and Discussion

The results obtained are shown in table 3.5. The amount of tritiated water in the vitreous after two hours was found to be 2.6% and 1.8% with a mean of 2.2%. After four hours, this had fallen to 0.6%, 0.2% and 0.6% (mean = 0.5%). In the investigations described in section 3.4, where tritiated water was detected on the sclera and, in section 3.5, in the aqueous, the experiments

Table 3.5

Results of experiments in which animals were killed two hours or four hours after injection of tritiated water into the vitreous.

Experiment Number	Activity in vitreous (%)	Activity in aqueous (%)	Activity in lens (%)	Activity in ocular coat (%)
at 2 hrs				
1	2.6	0.2		
2	1.8	0.2		
at 4 hrs				
3	0.6	0.2		
4	0.2	0.03	0.1	
5	0.6	0.1	0.4	0.1

were continued for four hours, by which time the present results show that there was very little isotope left in the vitreous. In the series described in section 3.3 where tritiated water was collected in a vortex vein, the experiments lasted 80 mins. The present results show that at two hours there is only 2.2% of tracer left in the vitreous so that any correction to the vortex vein results would probably be very small.

In both two hour experiments 0.2% of the injectate was detected in the aqueous. At four hours there was 0.2%, 0.03% and 0.1% in the aqueous in the three separate experiments with a mean of 0.1%. In two of the four hour experiments 0.1% and 0.4% (mean = 0.3%) was recovered in the lens and 0.1% was found in one occasion in the ocular coats at four hours. Thus, the tritiated water in the eye after four hours was distributed as follows: outer coat 0.1%, vitreous 0.6%, lens 0.3% and aqueous 0.1%. According to Prince (1964a) the volume of the vitreous, lens and aqueous are 1.47 ml, 0.5 ml and 0.24 ml respectively. The volume ratio for vitreous:lens: aqueous is approximately 6:2:1 and this is close to the tritiated water ratio of 6:3:1. This shows that at four hours there is an approximately uniform concentration of tritiated water in the vitreous, lens and aqueous and suggests that some of the isotope may have transferred from the vitreous to the aqueous via the lens.

CHAPTER 4

MATHEMATICAL MODEL OF DIFFUSION IN THE EYE: DESCRIPTION

4.1 Introduction

In the preceding chapters, experimental results have been given for the movement of tracers from the vitreous to other parts of the eye. These experiments were designed to provide basic information on the removal of water from the vitreous. Having quantified the movement and determined its rate, there still remained the need to understand the reason for the tracer movement observed. Since most of the xenon-133 and tritiated water were removed by the choroidal blood flow, it was decided to investigate more thoroughly the nature of the movement between the vitreous and the choriocapillaris.

The most fundamental movement of the tracer to consider is its movement by diffusion. Diffusion is the process by which matter is transported from one part of a system to another as a result of random molecular motions. In order to study this, a mathematical model is developed in which tracer in the eye may diffuse from the vitreous into the surrounding tissue with removal occurring in the choriocapillaris.

In the next chapter, the results of the model will be presented and these will be compared with the experimental results.

4.2 The Differential Diffusion Equation

The equation of heat conduction derived by Fourier (1822) was applied to the process of diffusion by Fick in 1855. The basis of the theory of diffusion in isotropic substances is that the rate of transfer of a diffusing substance through unit cross-sectional area is proportional to the partial pressure gradient

(Carslaw and Jaeger, 1947; Crank, 1956). In one dimension, Fick's first law of diffusion states that

$$J_x = - D \frac{\partial \rho}{\partial x} \qquad (4.1)$$

where J_x is the rate of transfer per unit cross-sectional area in the x-direction (g sec^{-1} cm^{-2})

ρ is the partial pressure (g ml^{-1})

x is the space co-ordinate normal to the section (cm)

D is the diffusion coefficient (cm^2 sec^{-1})

ρ = ksc

where k is a constant of proportionality

s is the solubility

c is the concentration (g ml^{-1})

By application of the law of conservation of matter to an element of volume around a point

$$\frac{\partial \rho}{\partial t} + \frac{\partial J_x}{\partial x} + \frac{\partial J_y}{\partial y} + \frac{\partial J_z}{\partial z} = 0 \qquad (4.2)$$

where J_y and J_z are the rates of transfer per unit cross-sectional area in the y and z directions respectively (g sec^{-1} cm^{-2})

x, y, z form the axes of a rectangular co-ordinate system.

J_y and J_z are given by equations similar to 4.1, and 4.2 becomes

$$\frac{\partial \rho}{\partial t} = D \left(\frac{\partial^2 \rho}{\partial x^2} + \frac{\partial^2 \rho}{\partial y^2} + \frac{\partial^2 \rho}{\partial z^2} \right) \qquad (4.3)$$

If $\frac{\partial}{\partial y}$ and $\frac{\partial}{\partial z}$ are zero, this reduces to the one-dimensional diffusion equation

$$\frac{\partial \rho}{\partial t} = D \frac{\partial^2 \rho}{\partial x^2} \qquad (4.4)$$

Equation (4.3) is Fick's second law of diffusion and, by its application, the diffusion of a substance in an isotropic medium may be predicted in a rectangular co-ordinate system.

In a cylindrical co-ordinate system (fig. 4.1)

$$x = r \cos\theta$$

$$y = r \sin\theta$$

$$z = z$$

and $$ds^2 = dr^2 + r^2 \, d\theta^2 + dz^2 \qquad (4.5)$$

where ds is the volume of a small element of sides dr, $rd\theta$ and dz.

Equation 4.3 becomes

$$\frac{\partial \rho}{\partial t} = D \left(\frac{\partial^2 \rho}{\partial r^2} + \frac{1}{r} \frac{\partial \rho}{\partial r} + \frac{1}{r^2} \frac{\partial^2 \rho}{\partial \theta^2} + \frac{\partial^2 \rho}{\partial z^2} \right) \qquad (4.6)$$

This permits the calculation of the rate of diffusion of a substance in an isotropic medium in a cylindrical co-ordinate system which will be used in the eye model.

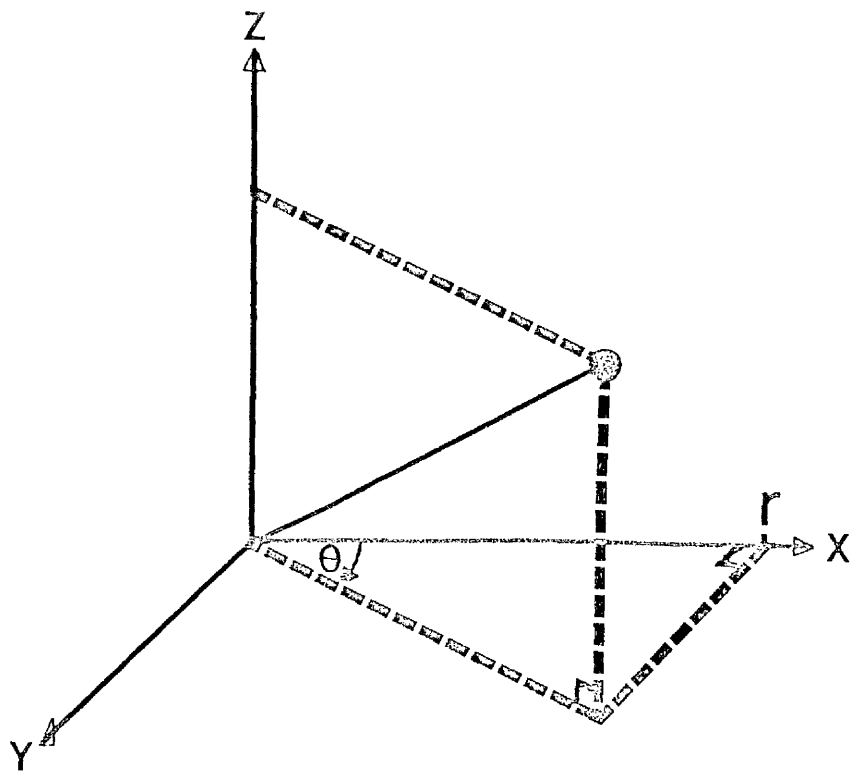

Figure 4.1

Cylindrical co-ordinate system: r is the distance from the origin to the projection of the point on the X-axis; Θ is the angle between the X-axis and the line joining the origin to the projection of the point on the X-Y plane and Z is the distance along the Z-axis.

4.3 Boundary Conditions

Consider two adjacent media of different diffusion coefficients. The suffix 1 will denote properties relating to medium 1 and, similarly, the suffix 2 for medium 2. The flux of particles leaving medium 1 is

$$J_{n1} = D_1 \frac{\partial \rho_1}{\partial n} \tag{4.7}$$

where n is the normal to the surface of separation.
The flux of particles entering medium 2 is

$$J_{n2} = D_2 \frac{\partial \rho_2}{\partial n} \tag{4.8}$$

The flux is continuous over the surface of separation. Thus at the boundary

$$D_1 \frac{\partial \rho_1}{\partial n} = D_2 \frac{\partial \rho_2}{\partial n} \tag{4.9}$$

Moreover, at the surface of separation, the partial pressures in the two media are the same, i.e.

$$\rho_1 = \rho_2 \tag{4.10}$$

4.4 Methods of solution of the diffusion equation

Analytical solutions for the diffusion equation exist for a variety of initial and edge conditions (Carslaw and Jaeger, 1947; Crank, 1956). They usually use a series of error functions or related integrals or a trigonometrical series and are restricted to a narrow range of problems. However, numerical solutions of the diffusion equations are applicable in many different situations (Crank, 1956; Forsythe and Wasow, 1960; von Rosenberg, 1969). Using these

methods, approximate solutions are obtained at discrete points by replacing the differential equations by finite-difference approximations.

4.5 Finite-Difference Formulae

Consider a function, y, of a variable, x. If the range of x is divided into discrete points each separated by a distance, δx, and, if values of y are known for each discrete value of x (fig. 4.2), an approximate value of the first-order derivative at an arbitrary point x_1 is

$$\left.\frac{\partial y}{\partial x}\right|_{x_1} = \frac{y(x_1 + \delta x) - y(x_1)}{\delta x} \tag{4.11}$$

An equally valid approximation is

$$\left.\frac{\partial y}{\partial x}\right|_{x_1} = \frac{y(x_1) - y(x_1 - \delta x)}{x} \tag{4.12}$$

A better approximation is one which weights equally both points around x_1, viz.,

$$\left.\frac{\partial y}{\partial x}\right|_{x_1} = \frac{y(x_1 + \delta x) - y(x_1 - \delta x)}{2\,\delta x} \tag{4.13}$$

Because of the advantages of 4.13 over 4.11 or 4.12, it is the preferred equation for first-order differentiation.

The second-order differential equation may be similarly obtained

$$\left.\frac{\partial^2 y}{\partial x^2}\right|_{x_1} = \frac{y(x_1 + \delta x) - 2\,y(x_1) + y(x_1 - \delta x)}{(\delta x)^2} \tag{4.14}$$

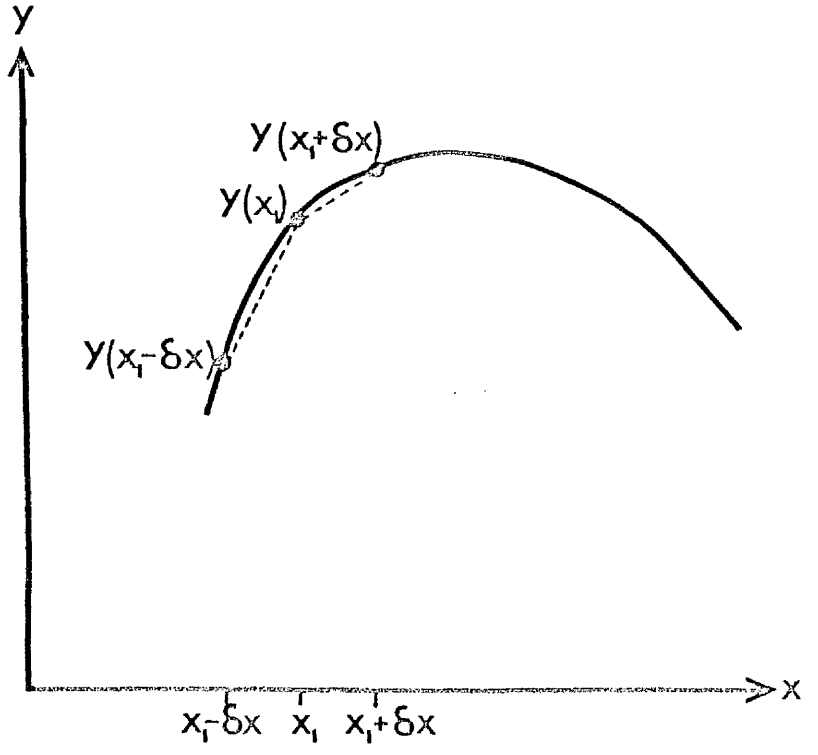

Figure 4.2

A general function $y(x)$ where values of y are known for discrete values of x at intervals of δx; dashed lines indicate approximations for the gradient at $y(x_1)$.

These equations may be alternatively derived using Taylor's expansion theorem

$$y(x_1 + \delta x) = y(x_1) + \delta x \left.\frac{\partial y}{\partial x}\right|_{x_1} + \frac{1}{2}(\delta x)^2 \left.\frac{\partial^2 y}{\partial x^2}\right|_{x_1} + \frac{1}{6}(\delta x)^3 \left.\frac{\partial^3 y}{\partial x^3}\right|_{x_1} \cdots \quad (4.15)$$

$$y(x_1 - \delta x) = y(x_1) - \delta x \left.\frac{\partial y}{\partial x}\right|_{x_1} + \frac{1}{2}(\delta x)^2 \left.\frac{\partial^2 y}{\partial x^2}\right|_{x_1} - \frac{1}{6}(\delta x)^3 \left.\frac{\partial^3 y}{\partial x^3}\right|_{x_1} \cdots \quad (4.16)$$

Neglecting higher than second-order terms in δx

$$\left.\frac{\partial^2 y}{\partial x^2}\right|_{x_1} = \frac{y(x_1 + \delta x) - 2y(x_1) + y(x_1 - \delta x)}{(\delta x)^2} \quad (4.17)$$

which is the same as 4.14, and

$$\left.\frac{\partial y}{\partial x}\right|_{x_1} = \frac{y(x_1 + \delta x) - y(x_1 - \delta x)}{2\,\delta x} \quad (4.18)$$

which is the same as 4.13. Equation 4.11 and 4.12 may be obtained from 4.15 and 4.16 respectively but these would have a leading error term of $\frac{1}{2}(\delta x)^2 \left.\frac{\partial^2 y}{\partial x^2}\right|_{x_1}$ and thus 4.18 is more accurate.

4.6 The Finite-Different Approximations of the Diffusion Equation

In the one-dimensional diffusion equation, values of partial pressure are obtained at discrete values of x separated by a distance h and at successive time intervals of 1 secs. This may be represented by intersections, called nodal points, between $x = ih$ and $t = kl$ where i and k are integers (fig. 4.3).

The finite-difference approximation of the one-dimensional diffusion equation is obtained by substituting 4.11 and 4.13 into 4.4.

$$\frac{\rho_{i,k+1} - \rho_{ik}}{1} = D \frac{\rho_{i+1,k} - 2\rho_{ik} + \rho_{i-1,k}}{h^2} \quad (4.19)$$

where ρ_{ik} is the partial pressure at the nodal point (i,k) (and similar notation for $\rho_{i,k+1}$, $\rho_{i+1,k}$ and $\rho_{i-1,k}$),

from which the recursion equation

$$\rho_{i,k+1} = \left(1 - 2\frac{D\,1}{h^2}\right)\rho_{ik} + \frac{D\,1}{h^2}\left(\rho_{i+1,k} + \rho_{i-1,k}\right) \quad (4.20)$$

is obtained.

By the application of 4.20, solutions for the partial pressure are obtained at $t = (k + 1)\,1$ and $x = ih$ from the values at $x = (i-1)h$, $x = ih$ and $x = (i + 1)h$ at the previous time step $t = k\,1$ (fig. 4.3).

The finite-difference method may be applied to diffusion in more than one dimension. The finite-difference form of the cylindrical co-ordinate diffusion equation will be obtained with $\frac{\partial}{\partial \theta} = 0$ and this will be used in the eye model. Used in this

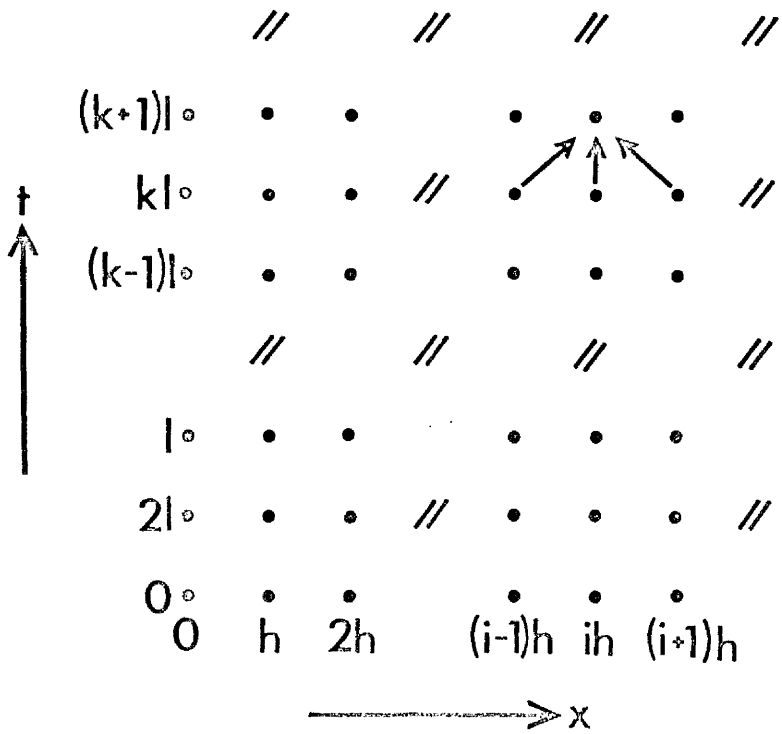

Figure 4.3

A two-dimensional matrix of nodal points with inter-point separation of h along the x-axis and l along the t-axis. Solution at distance ih and time (k+1)l is obtained from known solutions at time kl and distances (i-1)h, ih and (i+1)h.

way, the cylindrical co-ordinate system maintains a constant inter-nodal point spacing irrespective of distance from the origin, which would not be the case with a spherical polar co-ordinate system.

Solutions are obtained at points $r = ih$ and $z = pq$ where h and q are the distances between discrete points along the r-axis and z-axis respectively and i and p are integers. Successive solutions are obtained at times kl (fig. 4.4)

$$\frac{\partial \rho}{\partial t} = \frac{\rho_{ip,k+1} - \rho_{ipk}}{l} \tag{4.21}$$

where ρ_{ipk} is the partial pressure ar $r = ih$, $z = pq$ and $t = kl$ (and similar notation for all other ρ's)

$$\frac{\partial \rho}{\partial r} = \frac{\rho_{i+1,pk} - \rho_{i-1,pk}}{2\,h} \tag{4.22}$$

$$\frac{\partial^2 \rho}{\partial r^2} = \frac{\rho_{i+1,pk} - 2\,\rho_{ipk} + \rho_{i-1,pk}}{h^2} \tag{4.23}$$

and

$$\frac{\partial^2 \rho}{\partial z^2} = \frac{\rho_{i,p+1,k} - 2\,\rho_{ipk} + \rho_{i,p-1,k}}{q^2} \tag{4.24}$$

The solution is simplified by choosing the same distance increment in the r and z directions. Thus $q = h$ and

$$\frac{\partial^2 \rho}{\partial z^2} = \frac{\rho_{i,p+1,k} - 2\rho_{ipk} + \rho_{i,p-1,k}}{h^2} \tag{4.25}$$

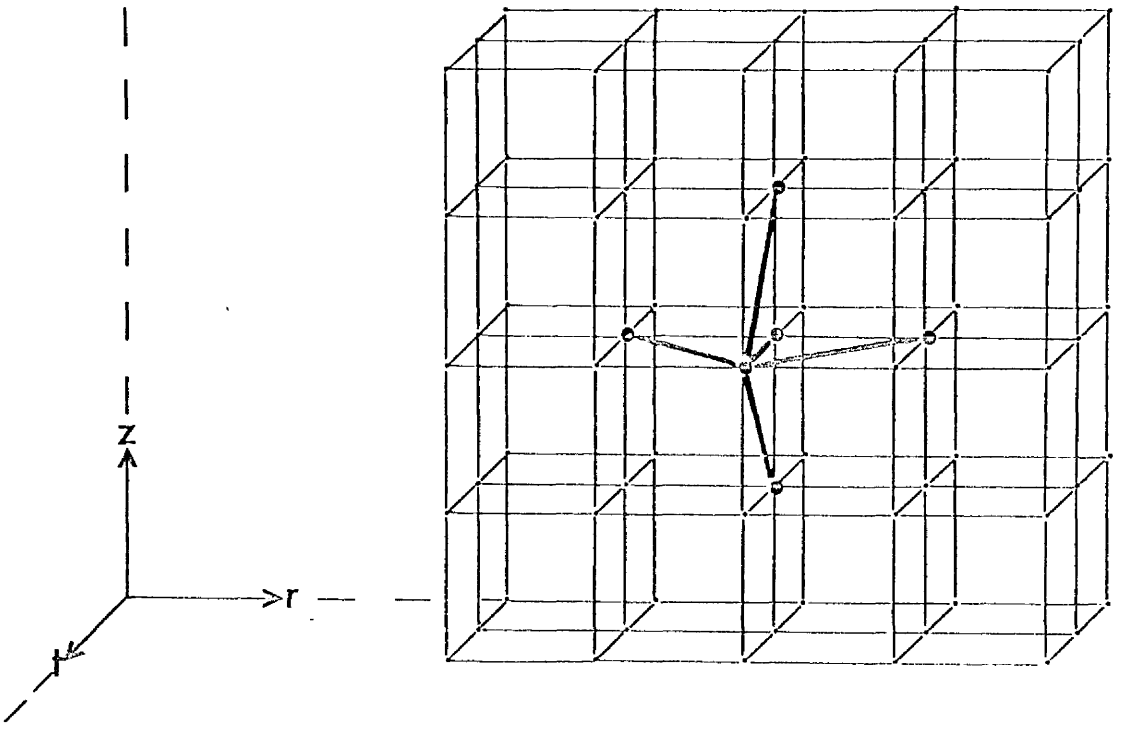

Figure 4.4

Three-dimensional matrix where solutions for points at successive time intervals are derived from known solutions for points at the previous time interval with the same space co-ordinates, and its four neighbouring points.

Equations 4.22, 4.23 and 4.25 are now used to solve the two-dimensional diffusion equation in cylindrical co-ordinates when

$\frac{\partial}{\partial \theta} = 0$, i.e.

$$\frac{\partial \rho}{\partial t} = D \left(\frac{\partial^2 \rho}{\partial r^2} + \frac{1}{r} \frac{\partial \rho}{\partial r} + \frac{\partial^2 \rho}{\partial z^2} \right) \qquad (4.26)$$

$$\frac{\rho_{ip,k+1} - \rho_{ipk}}{1} = D \left(\frac{\rho_{i+1,pk} - 2\rho_{ipk} + \rho_{i-1,pk}}{h^2} + \frac{\rho_{i+1,pk} - \rho_{i-1,pk}}{2\,i\,h^2} \right.$$

$$\left. + \frac{\rho_{i,p+1,k} - 2\rho_{ipk} + \rho_{i,p-1,k}}{h^2} \right) \qquad (4.27)$$

Setting $\lambda = \frac{1\,D}{h^2}$ and re-arranging the terms gives

$$\rho_{ip,k+1} = (1 - 4\lambda)\rho_{ipk} + \lambda \left[\left(1 + \frac{1}{2i}\right) \rho_{i+1,pk} + \left(1 - \frac{1}{2i}\right) \rho_{i-1,pk} \right.$$

$$\left. + \rho_{i,p+1,k} + \rho_{i,p-1,k} \right] \qquad (4.28)$$

For a system which is symmetrical about the z-axis, as is the case in the eye model,

$$\rho_{i-1} = \rho_{i+1} \qquad (4.29)$$

and, by definition, i=1 on the z-axis in the model. On the z-axis, equation (4.28) reduces to

$$\rho_{1p,k+1} = (1 - 4\lambda)\rho_{1pk} + \lambda \left[2\rho_{2pk} + \rho_{1,p+1,k} + \rho_{1,p-1,k} \right] \qquad (4.30)$$

Equations 4.28 and 4.30 are recursion equations which permit the value of the partial pressure at the point (i,p) to be obtained at $t = (k + 1)\,l$ from the values of the partial pressure at $t = kl$ at the points (i,p), (i+1,p), (i-1,p), (i,p+1) and (i,p-1) (fig. 4.4).

For a solution of the equations, it is necessary to specify initial conditions and edge conditions.

4.7 Finite-Difference Format of the Boundary Conditions

In the situation which is applicable to the eye model, the boundary points between two media are on spherical surfaces around a point on the z-axis, (1, C) say. Equation 4.9 stated that the flux was continuous along the outward normal. It is necessary, therefore, to interpolate the values of the concentration at points in the two media on the outward normal passing through the boundary point. In the eye model, there are three different representations of the boundary condition, equation 4.9, depending on the angle between the outward normal and the axes of the matrix. These three cases give the appropriate method of interpolation according to the position of the boundary point.

Case 1: Boundary point (I, P) : $|I - 1| < |C - P|$ and $P < C$

Consider the boundary point (I, P) between medium 1 and medium 2 as shown in fig. 4.5. In order to apply the boundary condition 4.9, it is necessary to know the change of partial pressure along the outward normal. The values of the partial pressure at points A and B of fig. 4.5 are calculated.

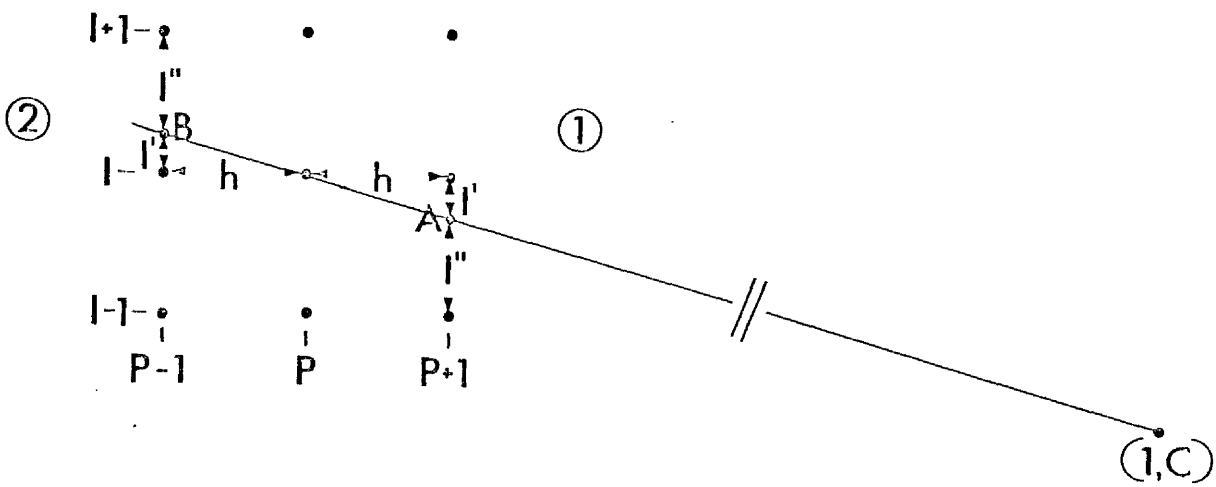

Figure 4.5

Boundary point (I,P) between medium 1 and medium 2. The outward normal from the centre (1,C) passes through the points A and B. The case shown is that where $|I-1| < |C-P|$ and $P < C$.

Distance between (I, P+1) and A = distance between (I, P-1) and B = I'

Distance between (I-1, P+1) and A = distance between (I+1,P-1) and B = I"

Distance between (I,P-1) and (I,P)= distance between (I,P) and (I,P+1) = h

(4.31)

By similar triangles,

$$\frac{I-1}{C-P} = \frac{I'}{h} \tag{4.32}$$

$$I' = h\left(\frac{I-1}{C-P}\right) \tag{4.33}$$

$$\begin{aligned} I'' &= h - I' \\ &= h\left(1 - \frac{I-1}{C-P}\right) \end{aligned} \tag{4.34}$$

$$\begin{aligned} \rho_A &= \frac{I'}{h}\,\rho_{I-1,P+1} + \frac{I''}{h}\,\rho_{I,P+1} \\ &= \frac{I-1}{C-P}\,\rho_{I-1,P+1} + \left(1 - \frac{I-1}{C-P}\right)\rho_{I,P+1} \end{aligned} \tag{4.35}$$

$$\begin{aligned} \rho_B &= \frac{I'}{h}\,\rho_{I+1,P-1} + \frac{I''}{h}\,\rho_{I,P-1} \\ &= \frac{I-1}{C-P}\,\rho_{I+1,P-1} + \left(1 - \frac{I-1}{C-P}\right)\rho_{I,P-1} \end{aligned} \tag{4.36}$$

Since the distance along the normal between B and (I,P) = distance between (I,P) and A, the boundary equation (4.9) may be approximated by

$$D_1\,(\rho_{IP} - \rho_A) = D_2\,(\rho_B - \rho_{IP}) \tag{4.37}$$

$$(D_1 + D_2)\,\rho_{IP} = D_2\,\rho_B + D_1\,\rho_A \tag{4.38}$$

$$\rho_{IP} = \frac{D_2\,\rho_B + D_1\,\rho_A}{D_1 + D_2} \tag{4.39}$$

$$\rho_{IP} = \left\{ D_2 \left[\frac{I-1}{C-P} \rho_{I+1,P-1} + \left(1 - \frac{I-1}{C-P}\right) \rho_{I,P-1} \right] + D_1 \left[\frac{I-1}{C-P} \rho_{I-1,P+1} + \left(1 - \frac{I-1}{C-P}\right) \rho_{I,P+1} \right] \right\} \Big/ (D_1 + D_2) \tag{4.40}$$

Case 2: Boundary point (I,P): $|I - 1| > |C - P|$ and $P < C$

Consider the boundary point (I,P) between medium 1 and medium 2 as shown in fig. 4.6. As in case 1, the values of the partial pressure at points A and B are found.

Distance between (I-1,P) and A = distance between (I+1,P) and B = Z'

Distance between (I-1,P+1) and A = distance between (I+1,P-1) and B = Z"

Distance between (I-1,P) and (I,P) = distance between (I+1,P) and (I,P) = h

(4.41)

$$\frac{Z'}{h} = \frac{C-P}{I-1} \tag{4.42}$$

$$Z' = \left(\frac{C-P}{I-1}\right) h \tag{4.43}$$

$$Z'' = h - Z' = h \left(1 - \frac{C-P}{I-1}\right) \tag{4.44}$$

$$\rho_A = \frac{Z'}{h} \rho_{I-1,P+1} + \frac{Z''}{h} \rho_{I-1,P}$$

$$= \frac{C-P}{I-1} \rho_{I-1,P+1} + \left(1 - \frac{C-P}{I-1}\right) \rho_{I-1,P} \tag{4.45}$$

$$\rho_B = \frac{Z'}{h} \rho_{I+1,P-1} + \frac{Z''}{h} \rho_{I+1,P}$$

$$= \frac{C-P}{I-1} \rho_{I+1,P-1} + \left(1 - \frac{C-P}{I-1}\right) \rho_{I+1,P} \tag{4.46}$$

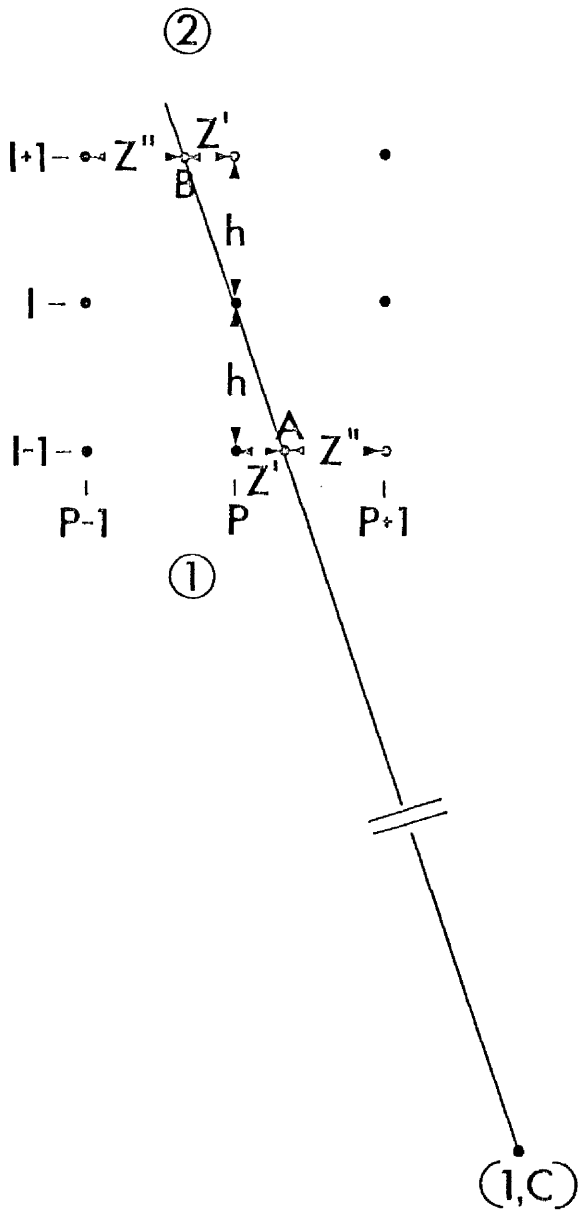

Figure 4.6

The boundary point (I,P) between medium 1 and medium 2. The outward normal from the centre (1, C) passes through A and B. The case shown is that where $|I-1| > |C-P|$ and $P < C$.

According to 4.39

$$\rho_{IP} = \frac{D_2 \rho_B + D_1 \rho_A}{D_1 + D_2}$$

Hence

$$\rho_{IP} = \left\{ D_2 \left[\frac{C-P}{I-1} \rho_{I+1,P-1} + \left(1 - \frac{C-P}{I-1}\right) \rho_{I+1,P} \right] + D_1 \left[\frac{C-P}{I-1} \rho_{I-1,P+1} + \left(1 - \frac{C-P}{I-1}\right) \rho_{I-1,P} \right] \right\} \Big/ (D_1 + D_2) \tag{4.47}$$

Case 3: Boundary Point (I,P): $|I - 1| > |C - P|$, $P > C$

Consider the boundary point (I,P) between medium 1 and medium 2 as shown in fig. 4.7.

The distance relationships (4.41) are still true but now

$$\frac{Z'}{h} = \frac{P-C}{I-1} \tag{4.48}$$

$$Z' = \left(\frac{P-C}{I-1}\right) h \tag{4.49}$$

$$Z'' = h - Z' = h \left[1 - \left(\frac{P-C}{I-1}\right)\right] \tag{4.50}$$

$$\rho_A = \frac{Z'}{h} \rho_{I-1,P-1} + \frac{Z''}{h} \rho_{I-1,P}$$

$$= \frac{P-C}{I-1} \rho_{I-1,P-1} + \left(1 - \frac{P-C}{I-1}\right) \rho_{I-1,P} \tag{4.51}$$

$$\rho_B = \frac{Z'}{h} \rho_{I+1,P+1} + \frac{Z''}{h} \rho_{I+1,P}$$

$$= \frac{P-C}{I-1} \rho_{I+1,P+1} + \left(1 - \frac{P-C}{I-1}\right) \rho_{I+1,P} \tag{4.52}$$

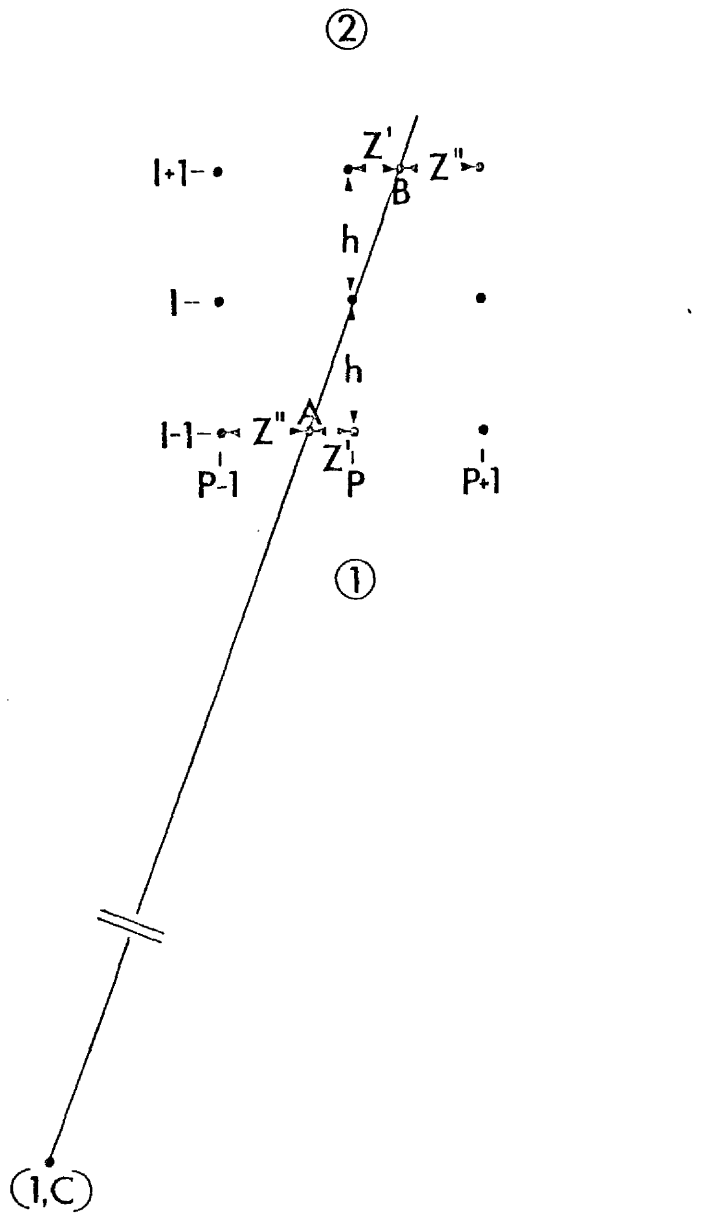

Figure 4.7

The boundary point (I, P) between medium 1 and medium 2. The outward normal from the centre (1, C) passes through the points A and B. The case shown is that where $|I-1| > |C-P|$ and $P > C$.

Cases 1, 2 and 3 cover all the necessary conditions in the eye model.

4.8 The Eye Model

In the model of the eye, the x-y plane is situated at the back of the eye with the z-axis pointing forwards towards the lens (fig. 4.8). For convenience, a section is taken through the centre of the eye along the x- and z-axes so that r = x, the perpendicular distance between a point and the z-axis. Moreover $\Theta = 0$, and the z co-ordinate is the distance along the z-axis. Since there is symmetry about the z-axis, for initial distributions centred along the z-axis, only half of this section need be considered. The dimensions of the eye model are from Prince (1964a), Hughes (1972) and Strang (1975a). The outer eye is regarded as a sphere of diameter 16 mm and the posterior lens is modelled as a sphere of diameter 11 mm with its nearest edge 6.7 mm from the retina. The vitreous is limited by the lenticular fibres which provide an anterior cut-off line as shown in fig. 4.9. The thickness of the sclera, choroid and retina are 0.024 cm, 0.012 cm and 0.015 cm respectively with respective diffusion coefficients for xenon of 1.3×10^{-5} cm^2 sec^{-1}, 0.61×10^{-5} cm^2 sec^{-1} and 0.64×10^{-5} cm^2 sec^{-1}. Further, the diffusion coefficient of xenon in the vitreous is 0.96×10^{-5} cm^2 sec^{-1}. Since the diffusion coefficients of choroid and retina are within 5%, they were replaced by a single structure with diffusion coefficient of 0.63×10^{-5} cm^2 sec^{-1}. The xenon is removed by blood flow in the choroid over a thickness of 0.009 cm and this value provides the upper limit for the distance interval, h. In the model, h = 0.009 cm.

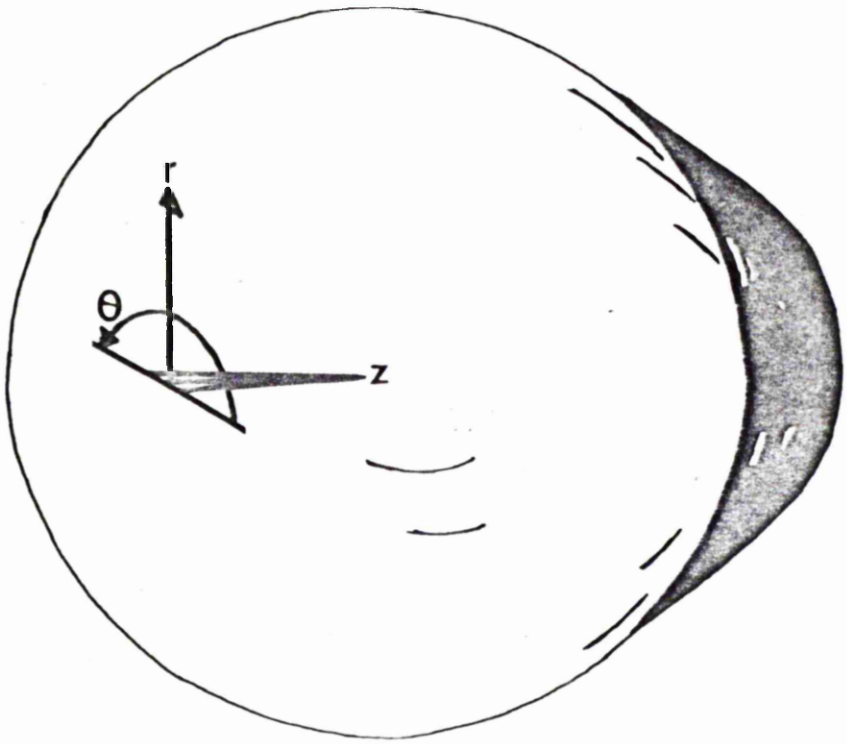

Figure 4.8

Cylindrical co-ordinate system with origin at back of eye and Z-axis pointing forwards.

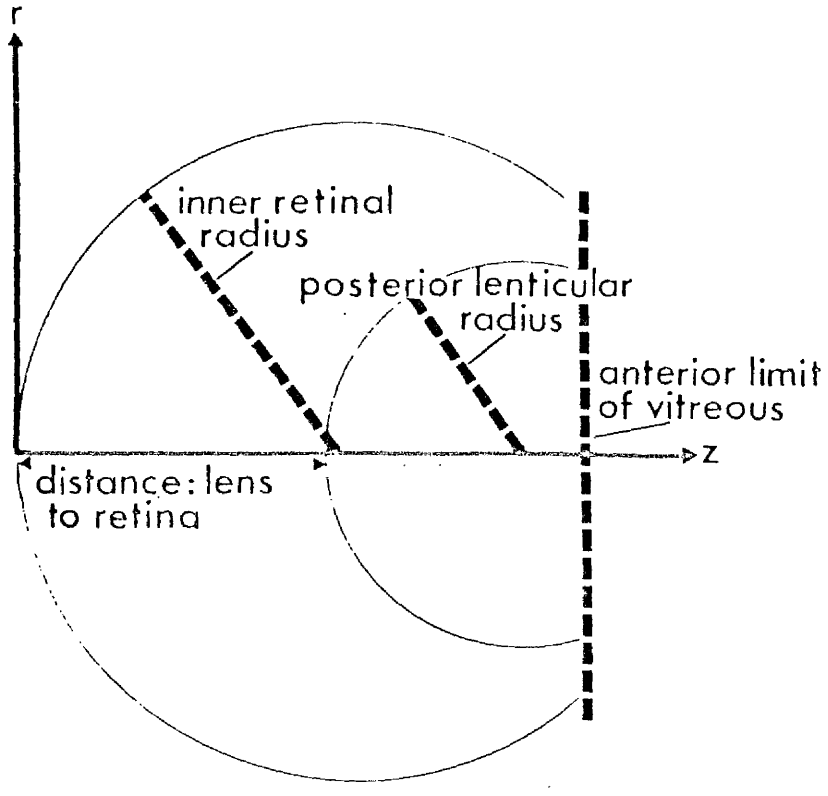

Figure 4.9

Limits of vitreous used in eye model.

In terms of the nodal points, the centre is the point (1,89) with the eye points such that

$$(I-1)^2 + (P-89)^2 \leq 7744 \tag{4.53}$$

Furthermore $$P \leq 113 \tag{4.54}$$

and $$(I-1)^2 + (P-143)^2 \geq 3844 \tag{4.55}$$

Equation (4.54) defines the anterior limit of the vitreous at the edge of the lens and equation (4.55) is the anterior limit of the vitreous behind the lens.

Edge points fall into the following categories:

$$\begin{aligned} &(I-1)^2 + (P-89)^2 \leq 7744 \\ \text{and either } &I^2 + (P-89)^2 > 7744 \\ \text{or } &(I-2)^2 + (P-89)^2 > 7744 \\ \text{or } &(I-1)^2 + (P-90)^2 > 7744 \\ \text{or } &(I-1)^2 + (P-92)^2 > 7744 \end{aligned} \tag{4.56}$$

which are the edge points on the sclera;

$$P = 113 \tag{4.57}$$

are the anterior points at the edge of the lens;

$$3844 \leq (I-1)^2 + (P-143)^2 < 3969 \tag{4.58}$$

which are the edge points behind the lens; and

$$I = 1 \tag{4.59}$$

which are the points on the z axis.

The order of calculation of partial pressures is as follows:

(1) points on the z-axis in the sclera, neither edge nor boundary

(2) points on the z-axis in the retina + choroid, neither edge nor boundary

(3) points on the z-axis in the vitreous, neither edge nor boundary

(4) other points in the sclera, neither edge nor boundary

(5) other points in the retina + choroid, neither edge nor boundary

(6) other points in the vitreous, neither edge nor boundary

(7) boundary points between the sclera and the retina + choroid

(8) boundary points between the retina + choroid and the vitreous

(9) edge points round the sclera

(10) edge points at the anterior face of the vitreous

(11) edge points behind the lens

(12) removal takes place at blood flow points.

Scleral points are those with $P \leq 112$ which do not satisfy (4.56) but for which

$$7310.25 \leq (I-1)^2 + (P-89)^2 \leq 7744 \qquad (4.60)$$

Choroidal + retinal points are those for which $p \leq 112$

and

$$6806.25 \leq (I-1)^2 + (P-89)^2 < 7140.25 \qquad (4.61)$$

Points in the vitreous have $P \leq 112$ and

$$(I-1)^2 + (P-89)^2 < 6642.25$$

and $$(I-1)^2 + (P-143)^2 \geq 3969 \qquad (4.62)$$

Boundary points between the sclera and choroid + retina are those with $P \leq 112$ and

$$7140.25 \leq (I-1)^2 + (P-89)^2 < 7310.25 \qquad (4.63)$$

Boundary points between the choroid + retina and the vitreous have $P \leq 112$ and

$$6642.25 \leq (I-1)^2 + (P-89)^2 < 6806.25 \qquad (4.64)$$

The nodal points in the eye model are shown in fig. 4.10.

Blood flow removal points satisfy the inequality

$$6972.25 \leq (I-1)^2 + (P-89)^2 < 7140.25 \qquad (4.65)$$

Blood flow is assumed to remove a constant fraction of the partial pressure from such points.

Edge points are obtained by a linear extrapolation from the two nearest points.

For points which satisfy (4.56), if $I-1 < 89-P$

$$\rho_{ip,k+1} = 2\,\rho_{i,p+1,k+1} - \rho_{i,p+2,k+1} \qquad (4.66)$$

and if $I-1 > 89-P$

$$\rho_{ip,k+1} = 2\,\rho_{i-1,p,k+1} - \rho_{i-2,p,k+1} \qquad (4.67)$$

For points such that $P = 113$

$$\rho_{i,113,k+1} = 2\,\rho_{i,112,k+1} - \rho_{i,111,k+1} \qquad (4.68)$$

For points satisfying equation (4.58), if $I-1 < P-143$ equation (4.66) applies and if $I-1 > P-143$ equation (4.67) is used.

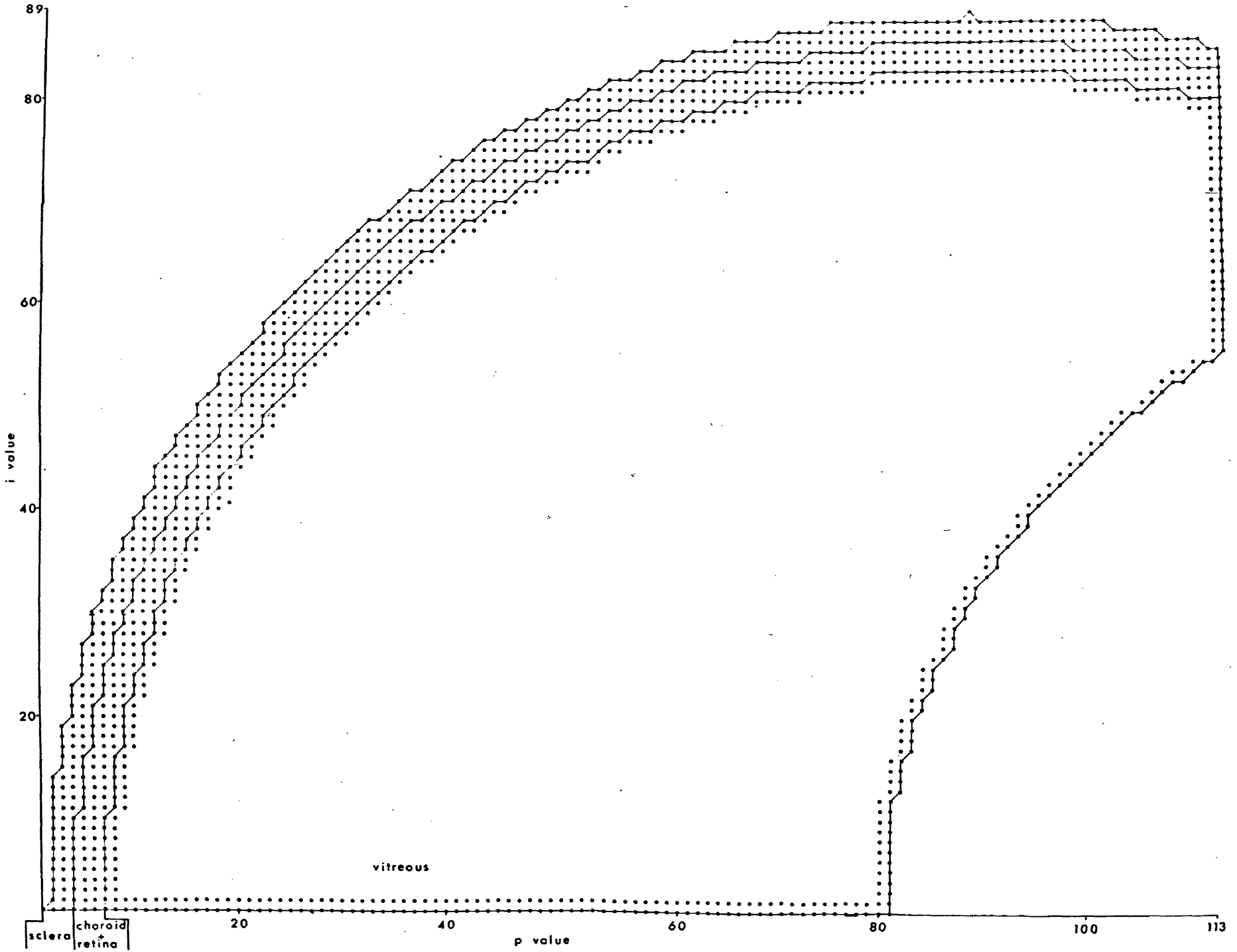
89
80
60
40
20
i value
vitreous
sclera
choroid
+
retina
20
40
60
80
100
113
p value

Figure 4.10

4.9 Stability

From the recursion equations (4.31), for points on the z-axis, and (4.28), for all other points, values of the partial pressure at $t = 1, 21 \ldots$ may be successively calculated starting with the initial values $\rho_{ipo} = f(r,z)$.

If $\lambda \leq \frac{1}{4}$, the right members of equations (4.31) and (4.28) are a weighted average of ρ_{ipk}. It follows that ρ_{ipk} satisfies at all grid points the inequalities

$$m \leq \rho_{ipk} \leq M$$

provided $m \leq f(r,z) \leq M$. According to Forsythe and Wasow (1960) this constitutes stable behaviour.

Thus

$$\lambda \leq \frac{1}{4} \qquad (4.69)$$

must be satisfied and so $1 \leq \frac{h^2}{4D}$. Since h cannot be more than 0.009 and D in the sclera is 1.3×10^{-5}, $1 \leq 1.56$ sec. 1 was set at 1.5 sec in the programme. The equations were solved using an IBM 370/168 computer which provided partial pressure profiles and blood uptake curves. A listing of the programme appears in Appendix I.

CHAPTER 5

MATHEMATICAL MODEL OF DIFFUSION IN THE EYE: RESULTS

5.1 Introduction

A mathematical model was described in the previous chapter for the diffusion of a tracer through the vitreous to the other tissues in the eye and its subsequent removal in the choroid. The results of the model are given in the present chapter. The distribution of partial pressure throughout the eye at different times and the appearance curve for the tracer in the choroidal circulation are obtained. The model is initially applied to the diffusion of xenon in order to reduce the effect of complex interactions between the tracer and the surrounding matter. The effects of changing the position of the initial distribution of tracer in the vitreous and of different rates of blood flow in the choroid, are observed. The results of the model are compared with those obtained experimentally. Having established the validity of the model for the diffusion of xenon, it is then applied to water.

5.2 Analytical Solution

Analytical solutions of partial differential equations are more accurate than those obtained by numerical methods. In order to assess the accuracy of the model, solutions were obtained using the finite difference format of the model in a situation where an analytical solution exists. Carslaw and Jaeger (1947) obtained an analytical solution for the flow of heat in a sphere under specific conditions. They calculated the temperature distribution at various times after zero initial temperature and a surface temperature which is constant with time. This calculation has a direct application

to the theory of time-lag in thermometers and, since diffusion and heat conduction are analogous phenomena, it may be used to test the finite difference approximation in the model. The solution is

$$v = V + \frac{2aV}{\pi r} \sum_{n=1}^{\infty} \frac{(-1)^n}{n} \sin \frac{n\pi r}{a} \; e^{-Kn^2\pi^2 t/a^2} \qquad (5.1)$$

where v = temperature at r (^{o}C)

r = distance from origin (cm)

a = radius of sphere (cm)

V = constant surface temperature (^{o}C)

K = thermal conductivity ($cm^2\ sec^{-1}$)

t = time (sec)

The finite difference equations developed in the previous chapter are applied to the diffusion of xenon from a constant surface partial pressure of 100 units through the vitreous, which was regarded as a sphere. This is analogous to the problem solved by equation (5.1) where v is now the partial pressure of xenon in the vitreous, V is 100, a is the radius of the vitreous and K is the diffusion coefficient of xenon in the vitreous.

Figure 5.1 shows the temperature distribution both by the analytical solution of Carslaw and Jaeger (1947) and the finite difference approximations of the previous chapter after a time of 327 s. The finite difference solutions plotted were obtained from the values on the nodal points along a radial line from the origin of the sphere at a 45^{o} angle to the Z-axis so that the r- and z-axes of the model were equally weighted. The two partial pressure profiles are practically identical and this indicates good agreement between the two solutions.

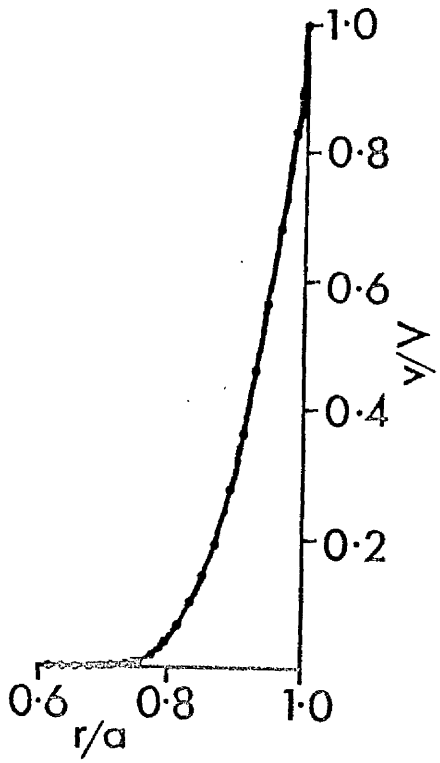

Figure 5.1

Temperature distribution by the analytical solution of Carslaw and Jaeger (1947) (continuous line) and by the numerical method of the present model (dots).

This agreement was further investigated by summing the values of v/V as obtained by each solution at values of r/a at discrete intervals of 0.02 up to and including 0.98. The finite difference values were obtained for the different values of r/a by interpolation between the two closest nodal points. Only values of v/V greater than 0.01 were included in this comparison since accurate analytical solutions were unobtainable for less than this. The two summated values were found to be within 0.2% which may be regarded as the order of magnitude of the errors involved in the finite difference approximations used in the model. This error is much less than the experimental errors, e.g. the standard deviation in the amount of xenon collected in the vortex vein was 45% of the mean (Chapter 2).

5.3 Diffusion Coefficients

The diffusion coefficient of xenon in ocular tissue was measured by Strang (1975a; 1977) using a technique described by Gillespie and Unsworth (1968). They showed that if one face of a slab of a medium containing a dissolved gas at uniform initial partial pressure is suddenly exposed to, and maintained at, zero partial pressure, for large values of time the partial pressure at all points decreases at the same exponential rate described by

$$T_{\frac{1}{2}} = \frac{0.282\ L^2}{D} \qquad (5.2)$$

where $T_{\frac{1}{2}}$ = half-life of exponential partial pressure decrease (sec)

L = thickness of material (cm)

D = diffusion coefficient ($cm^2\ sec^{-1}$)

The results obtained by Strang (1975a; 1977) for the diffusion coefficient of xenon in various tissues were: sclera $1.3 \times 10^{-5}\ cm^2 sec^{-1}$

$\pm$ 0.3 (S.D.), choroid 0.61 x 10^{-5} $\pm$ 0.14, retina 0.64 x 10^{-5} $\pm$ 0.05, vitreous 0.96 x 10^{-5} $\pm$ 0.12. Since the diffusion coefficients of xenon in choroid and retina were within 5%, which was less than the standard deviation of each, the choroid and retina were combined in the present model and the diffusion coefficient of xenon taken to be 0.63 x 10^{-5} cm^2 sec^{-1}. The values obtained by Strang (1975a; 1977) for the diffusion coefficients in the other ocular tissues were adopted.

The diffusion coefficients for tritiated water in the various ocular tissues were taken to be the values for xenon times the ratio of the self-diffusion coefficient of water to that of xenon in water. Taking the self-diffusion coefficient of water as measured by Wang (1965) and the diffusion coefficient of xenon in water as measured by Unsworth and Gillespie (1970) this ratio has the value of 1.8 between 20°C and 37°C. Water is a suitable medium for comparison because of the high water content of eye tissue (Gloor, 1970) as shown by the value for the diffusion coefficient of xenon in water of 1.6 x 10^{-5} cm^2 sec^{-1} which is similar to those obtained by Strang (1975a) in eye tissue. The diffusion coefficients of tritiated water in the various tissues were thus taken to be 2.34 x 10^{-5} cm^2 sec^{-1} in sclera, 1.13 x 10^{-5} cm^2 sec^{-1} in combined choroid and retina and 1.73 x 10^{-5} cm^2 sec^{-1} in vitreous.

5.4 Effect of Changing the Position of the Initial Distribution

The purpose of the present section is to determine the effect, by use of the diffusional model, of changing the initial distribution of tracer on its removal in the choroid. The model is applied to initial distributions situated at different positions along the Z-axis. Distributions centred off the Z-axis are beyond the scope of the model in its present form since they would introduce asymmetry. This is not

considered a serious limitation since results may still be presented, showing the effect of positional changes of initial distribution on the rate of appearance in the choroid based on a diffusional mechanism and these may be compared in a later section with the experimental results obtained.

Figure 4.10 showed the distribution of nodal points used in the model. Since the xenon was introduced as a volume of 25 µl in the mid-vitreous, it is assumed to have an initial distribution of radius 1.8 mm centred on the Z-axis. The programme was written in such a way as to allow the distance of the initial distribution along the Z-axis to be varied by choosing a different value for the mid-point of the distribution. This was achieved by adjusting the p-value of the mid-nodal point (section 4.6). A p-value of 37 was considered to be realistic for the mid-point of the initial distribution and two other p-values, 27 and 47, chosen to illustrate the effect of changing the position of the distribution. The blood flow removal rate which corresponded to that used by Strang (1975a) for the normal rabbit was 0.225 per incremental time step of 1.5 seconds.

The diffusion coefficients of xenon were used in the model and the partial pressures at the nodal points of the eye model (fig. 4.10) were calculated. As an example, they are given after 20 minutes for an initial mid-point p-value of 37 in Appendix 2.

The programme gave the amount of isotope removed by the choroidal blood flow every two minutes. The appearance curves for xenon in the vortex vein for mid-point p-values of 27, 37 and 47 are shown in figs. 5.2, 5.3 and 5.4 respectively.

Inspection of the blood appearance curves, fig. 5.2, fig. 5.3 and fig. 5.4 reveals the considerable change in shape which occurs as a result of initial injections at different points along the Z-axis.

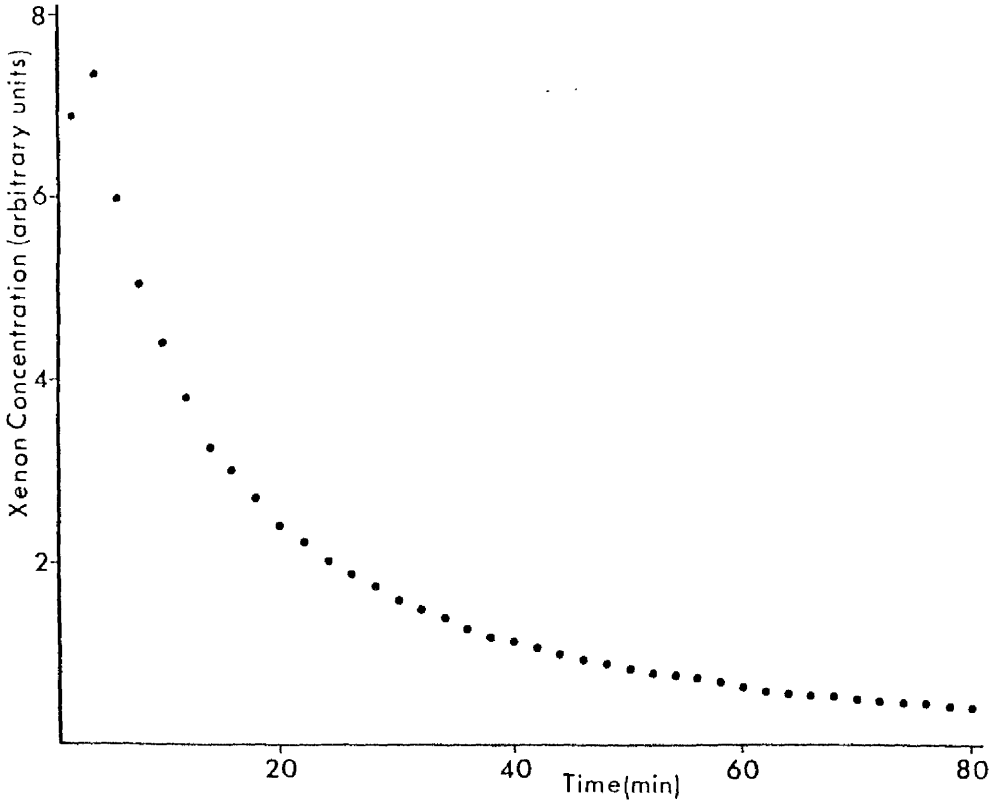

Figure 5.2

Relative concentration of xenon in the choroidal blood according to the model for an initial mid-point p-value of 27 and normal blood flow.

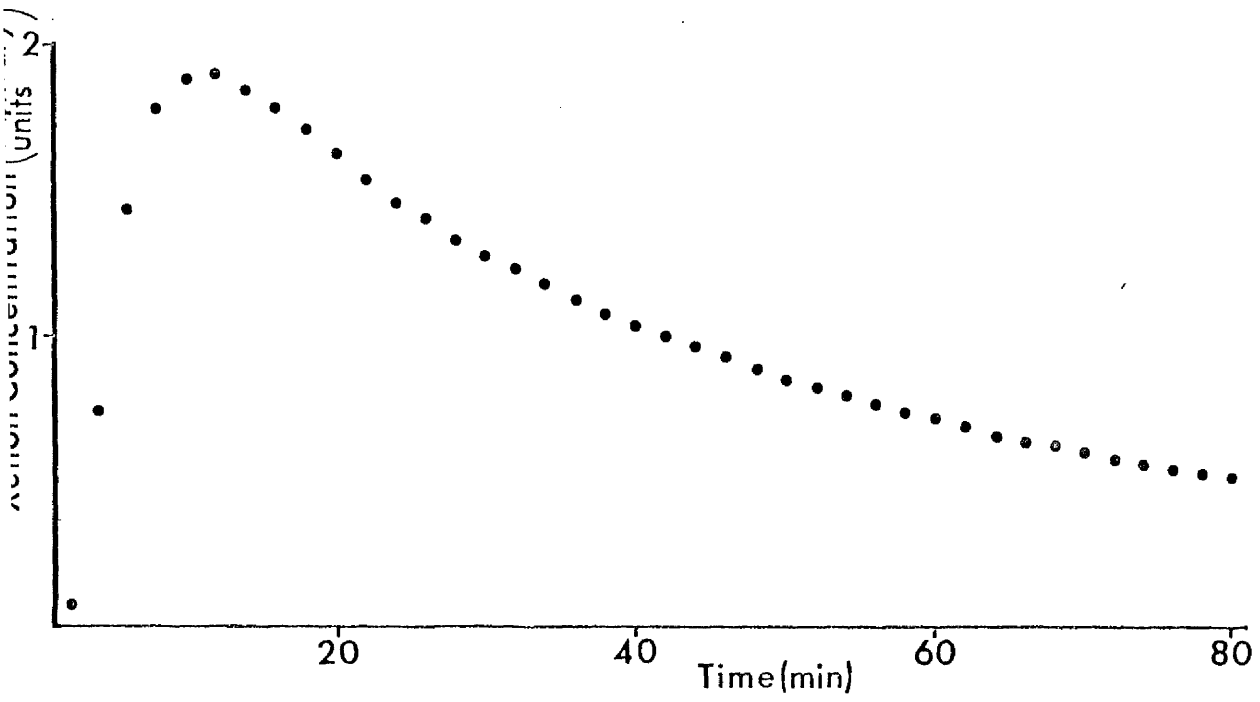

Figure 5.3

Relative concentration of xenon in the choroidal blood according to the model for an initial mid-point p-value of 37 and normal blood flow.

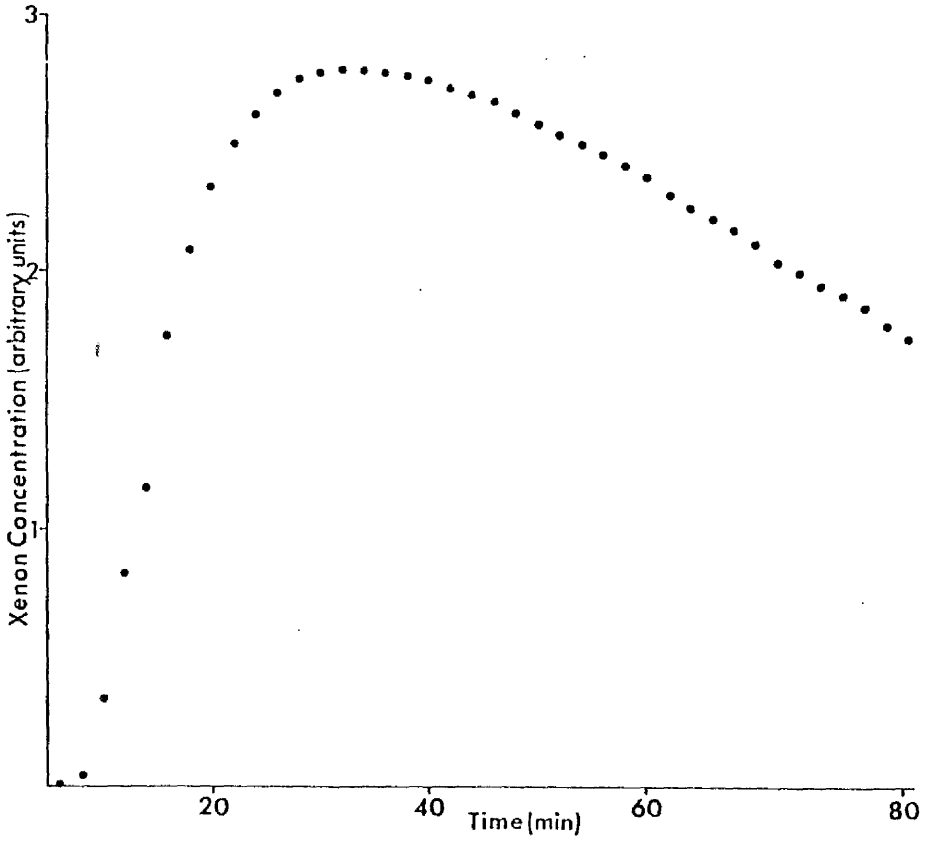

Figure 5.4

Relative concentration of xenon in the choroidal blood according to the model for an initial mid-point p-value of 47 and normal blood flow.

For mid-point p-values of 27, 37 and 47, the time to the peak is 4 mins, 12 mins and 30 mins respectively and the interval on the downslope between the peak and half peak value is 8 mins, 34 mins and greater than 50 mins respectively. These changes are due to injections which are centred $\pm$ 0.9 mm about a point 3.33 mm from the posterior scleral surface along the Z-axis of the eye.

The mean transit times computed from these curves at 40 mins, 60 mins and 80 mins are given in table 5.1. This shows the effect of an initial distribution at different points along the Z-axis on the mean transit time. For an initial mid-point p-value of 27, the mean transit time at 80 minutes was 20 minutes, for a p-value of 37 it was 33 minutes and, for the mid-point p equal to 47, the mean transit time was 42 minutes. Thus, a change of $\pm$ 0.9 mm in the initial position along the Z-axis produced $\pm$ 27% variation about a mean transit time of 33 minutes.

5.5 Effect of changing the blood flow

The effect of altering the blood flow removal term was investigated using an initial distribution with a mid-point p-value of 37 and three different blood flow removal terms, viz. half normal: 0.113 per time step, normal: 0.225 per time step and twice normal: 0.45 per time step. The diffusion coefficients of xenon were used.

The partial pressures at the nodal points shown in fig. 4.10 for the three different blood flow removal terms were calculated and the amount of isotope removed by the blood obtained.

The appearance of the isotope in the blood at half normal, normal and twice normal blood flow is shown in figs. 5.5, 5.6 and 5.7 respectively. The peak occurs at 12 mins for half normal and normal blood flow and at 10 mins for twice normal blood flow while the time on the downslope between the peak and half peak value is

Table 5.1

Effect of mid-point p-value on the mean transit time

Central p co-ordinate of initial distribution	Time (min.)	Mean transit time (min.)
47	40	25
	60	34
	80	42
37	40	20
	60	27
	80	33
27	40	13
	60	18
	80	20

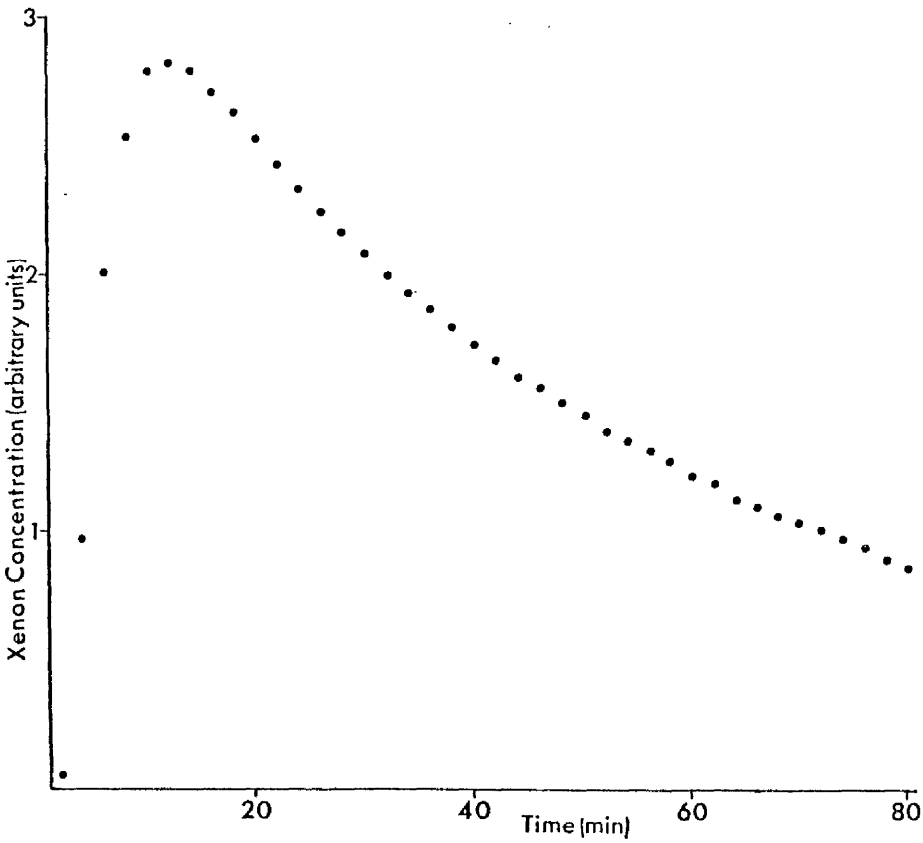

Figure 5.5

Relative concentration of xenon in the choroidal blood according to the model for an initial mid-point p-value of 37 and half normal blood flow.

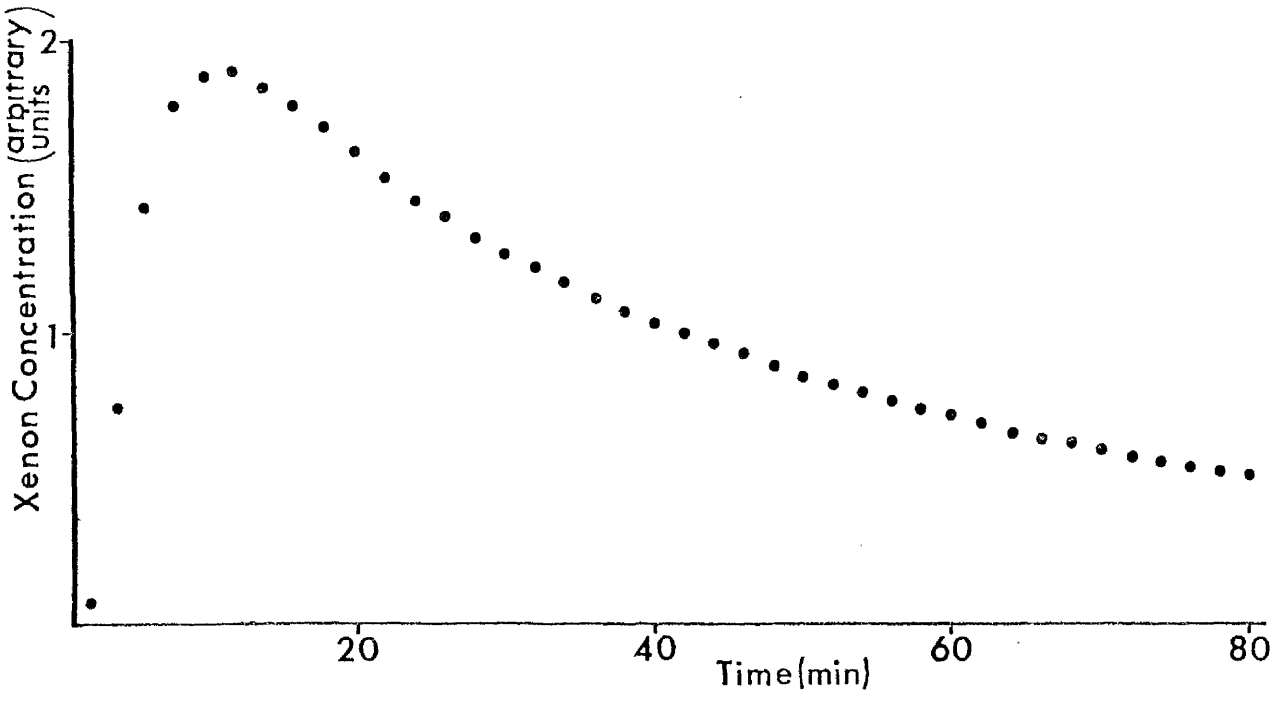

Figure 5.6

Relative concentration of xenon in the choroidal blood according to the model for an initial mid-point p-value of 37 and normal blood flow.

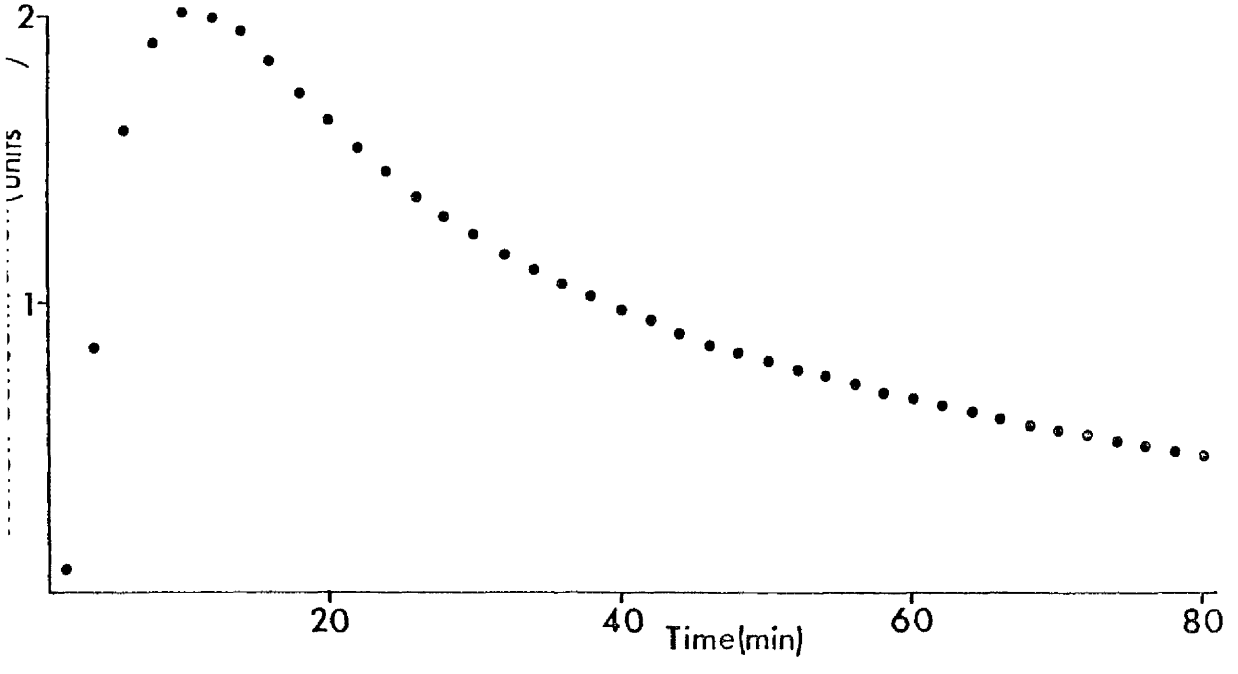

Figure 5.7

Relative concentration of xenon in the choroidal blood according to the model for an initial mid-point p-value of 37 and twice normal blood flow.

36 mins, 34 mins and 30 mins for the three respective situations. Despite a fourfold difference in blood flow, the appearance of isotope in the choroidal blood is very similar.

The mean transit times at 40 minutes, 60 minutes and 80 minutes are given in table 5.2 for the different blood flow terms. At 80 minutes, the mean transit time was 34 minutes for half normal blood flow, 33 minutes for normal blood flow and 32 minutes for twice normal blood flow. It may be seen, therefore, that the alterations in blood flow used in the model had very little effect on the rate of appearance of tracer in the choroidal blood.

5.6 Comparison between model and experimental results

5.6.1 Xenon

The experimental curve which was shown in fig. 2.2 for the appearance of xenon in a vortex vein is reproduced in fig. 5.8. This may be seen to be similar to the xenon model curve given above for an initial distribution centred at p = 37 and normal blood flow (fig. 5.3). The similarity between experiment and model is substantiated by a comparison of the mean transit times (table 5.3). The model mean was calculated for a time equal to the average experimental duration. The experimental mean transit time of 28 $\pm$ 2 minutes corresponded closely to the model result of 27 minutes.

The effect of a change in the position of the initial distribution predicted by the model is consistent with the range in experimental values. Further, the observation made during the experiments, that a change in blood flow had no apparent effect on the rate of appearance of isotope in the vortex vein was also a feature of the model.

Table 5.2

Effect of blood flow removal term on the mean transit time.

Blood flow removal term	Time (min.)	Mean transit time (min.)
0.113	40	20
	60	28
	80	34
0.225	40	20
	60	27
	80	33
0.45	40	19
	60	26
	80	32

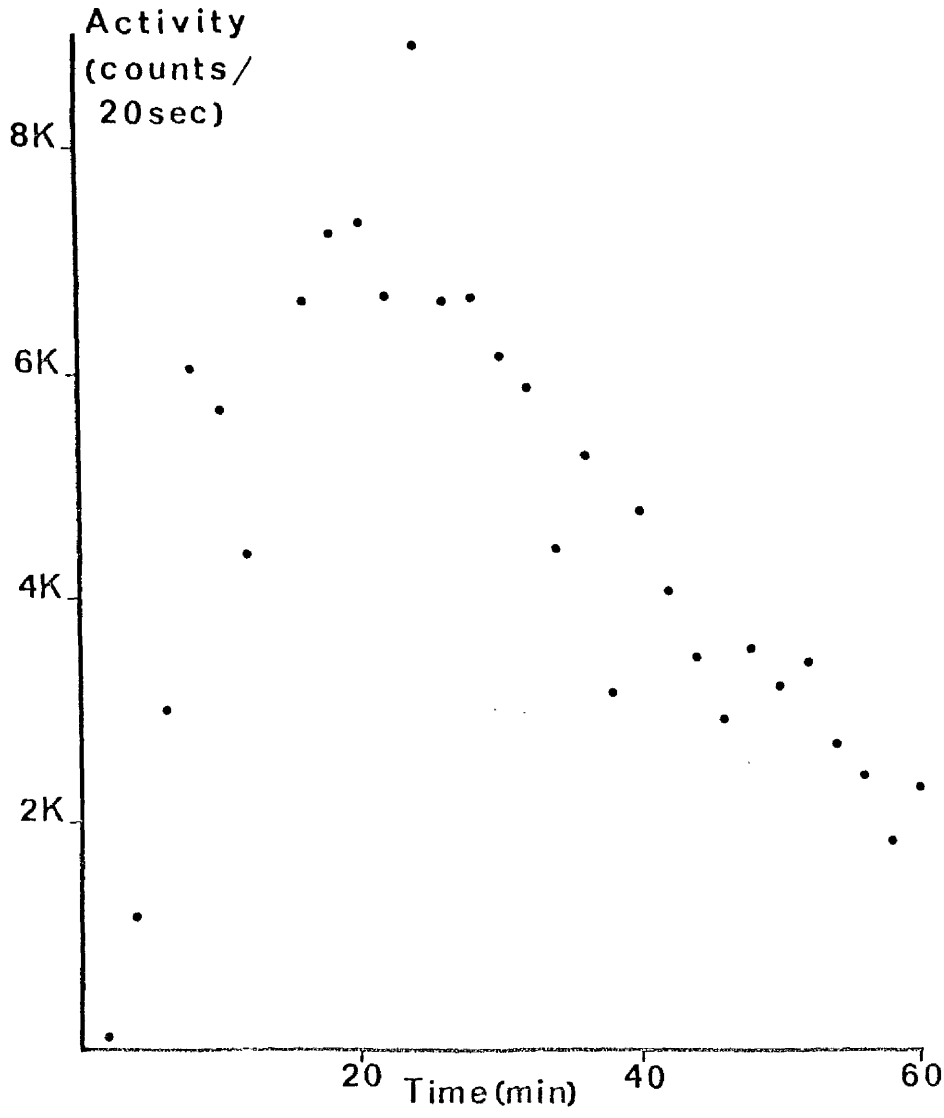

Figure 5.8

Experimental curve for the appearance of xenon-133 in the choroidal blood following its injection into the vitreous.

Table 5.3

Comparison of experimental mean transit time (mins.) ± S.E. and the model value for xenon-133.

Experiment	Model
28 ± 2	27

There is, therefore, good agreement between the model and the experimental results for xenon. The model may be used with some confidence to study the diffusion of a tracer from the mid-vitreous of the eye with removal occurring in the choroid.

5.6.2 Tritiated Water

The model was used to calculate the partial pressures at the nodal points shown in fig. 4.10 using the diffusion coefficients of water. For an initial distribution with a mid-point p-value of 37 and normal blood flow, the partial pressure distribution was computed and rate of appearance of the isotope in the blood obtained. The removal of tritiated water by the choroidal blood, according to the model, is shown in fig. 5.9. The mean transit times at 40 minutes, 60 minutes and 80 minutes are given in table 5.4. The effect of the higher diffusion coefficient of water compared to xenon is to spread the tracer more quickly throughout the vitreous and into the choroid.

The experimental curve for the appearance of tritiated water in the vortex vein (fig. 3.3) is reproduced in fig. 5.10 for comparison. The model and experimental curves are in reasonable agreement. The mean transit time was calculated from the rate of appearance of tritiated water in the choroidal blood according to the model for an initial distribution with a mid-point p-value of 37, normal blood flow and for a time which was equal to the average duration of the experiments (table 5.5). The model result of 28 minutes is in good agreement with the experimental value of 30 ± 2 minutes.

The effects of altering the position of the initial distribution and varying the blood flow which were demonstrated using the diffusion coefficients of xenon in the model are also applicable

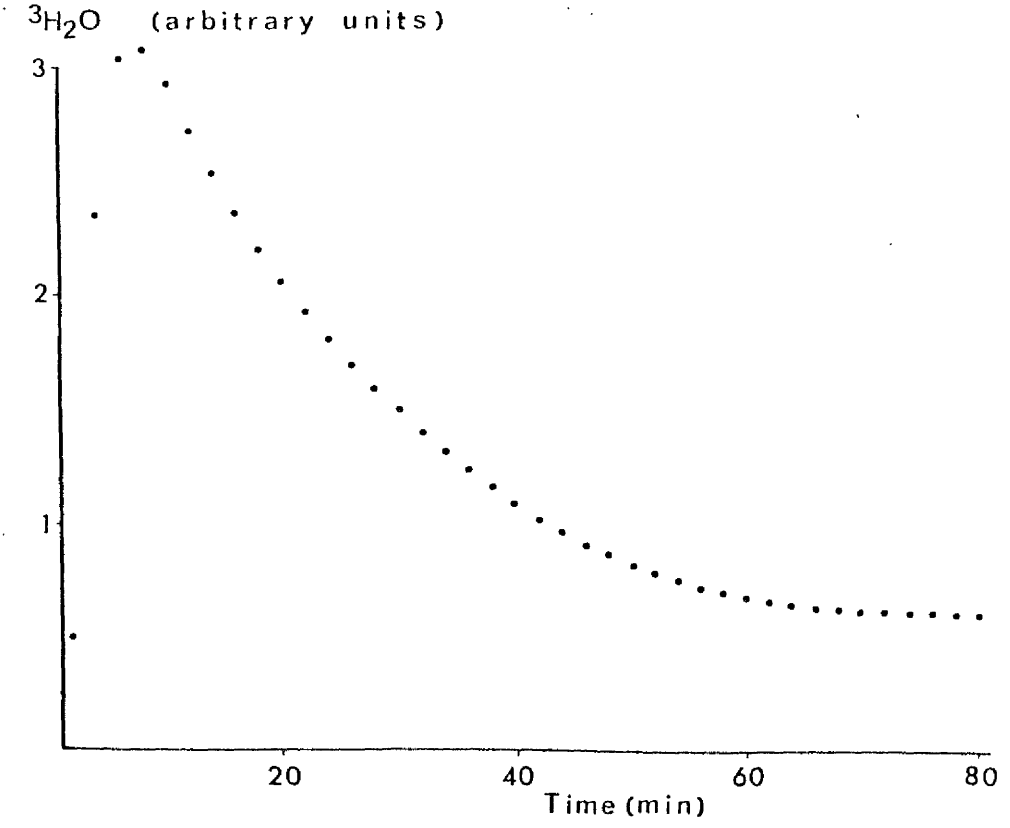

Figure 5.9

Relative concentration of tritiated water in the choroidal blood according to the model for an initial mid-point p-value of 37 and normal blood flow.

Table 5.4

Mean transit times according to the model for diffusion of tritiated water at 40, 60 and 80 minutes for a mid-point p-value of 37 and normal blood flow.

Time (min.)	Mean Transit Time (min.)
40	17
60	22
80	28

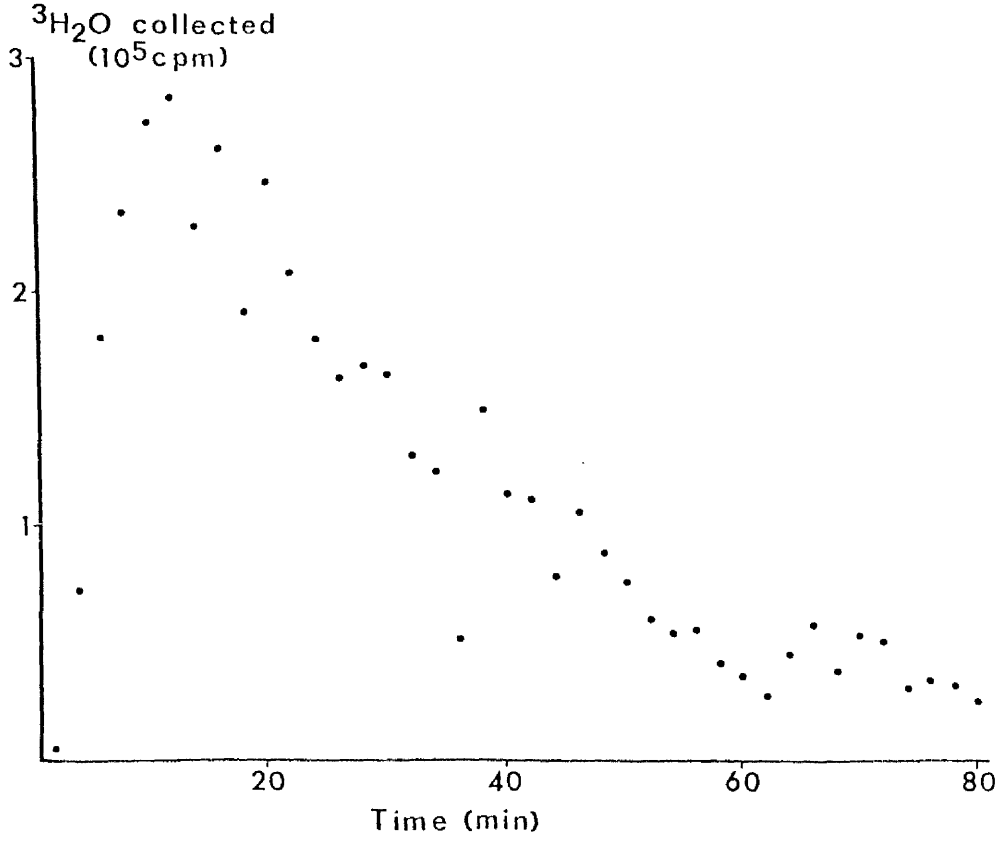

Figure 5.10

Experimental curve for the appearance of tritiated water in the choroidal blood following its injection into the vitreous.

Table 5.5

Comparison of experimental mean transit time (mins.) ± S.E. and the model value for tritiated water.

Experiment	Model
30 ± 2	28

to the diffusion of tritiated water. These provide further agreement between experiment and model.

It is considered, therefore, that the model has provided a satisfactory explanation for the experimental results obtained with tritiated water. The results are consistent with the movement of water from the vitreous by diffusion with removal occurring principally in the blood which flows in the choroid.

CHAPTER 6

RESISTANCE TO FLUID FLOW INDUCED BY HYDROSTATIC PRESSURE : I. POSTERIOR SITES

6.1 Introduction

In the earlier chapters, the removal of fluid from the vitreous was investigated. The experimental results were consistent with a mathematical model of diffusion from the vitreous into the choroid where removal was effected by the blood flow. Since the contents of the eye are normally some 15 mm.Hg above atmospheric pressure, a pressure difference exists which will tend to drive fluid out of the eye. In this and the subsequent chapter, two possible routes for this hydrostatic pressure-induced flow will be considered, viz. fluid movement across the posterior layers of the eye and the flow of fluid into Schlemm's canal in the anterior region of the eye.

In the present chapter, fluid movement from the vitreous across the retina, choroid and sclera is studied. Previous investigators have discussed the possible importance of a posterior flow, particularly in relation to retinal adhesion (see Chapter 1), and a model of this flow has been published (Fatt and Hedbys, 1970). Since this model will be shown to be inadequate, a superior model will be presented in the present chapter. Measurements of the conductivity of fluid flow across the posterior layers of the eye have also been published (Fatt and Hedbys, 1970; Fatt and Shantinath, 1971). These measurements are repeated and will be described before a discussion of the models.

6.2 Measurement of Conductivity

6.2.1 Materials and Methods

Resistance per unit area to fluid flow through tissue is the pressure drop across the tissue divided by the rate of flow through the tissue. Since Fatt and Hedbys (1970) and Fattand Shantinath

(1971) quote their results in fluid conductivity rather than resistance the results of the present study are also presented in units of fluid conductivity for comparison. By definition,

$$C = \frac{Q\ l}{f\ A} \qquad (6.1)$$

where C = tsssue fluid conductivity ($cm^4\ dyn^{-1}\ sec^{-1}$)

Q = rate of flow of fluid ($cm^3\ sec^{-1}$)

l = tissue thickness (cm)

f = differential force across tissue (dyn)

A = tissue cross-sectional area (cm^2)

Figure 6.1 shows a diagram of the experimental arrangement. Perfusion fluid was passed through tissue from a reservoir which maintained a constant pressure during each experiment. The tissue sample was held in a chamber and the rate of fluid flow measured using a microlitre scale against a mirror. The perfusion chamber is shown in more detail in fig. 6.2. This is a modified version of that used by Oakley (1977) to measure electrical properties of the frog retinal epithelium. Tissue was placed on X-ray film, with an aperture of known central diameter, which had been previously lightly covered on the tissue-facing surface with a cyanoacrylate tissue adhesive. The other surface of the film was lightly greased and the film and tissue were securely fixed between the two faces of the lucite chamber. Temperature in the chamber was maintained at $37^{o}C$ by immersion of the chamber in a water bath.

Retinal samples were perfused using the solution of Barany (1964) in order to maintain them in as near a physiological condition as possible. Scleral samples were perfused with 0.9% saline since cell viability was of little importance with this tissue. The difference

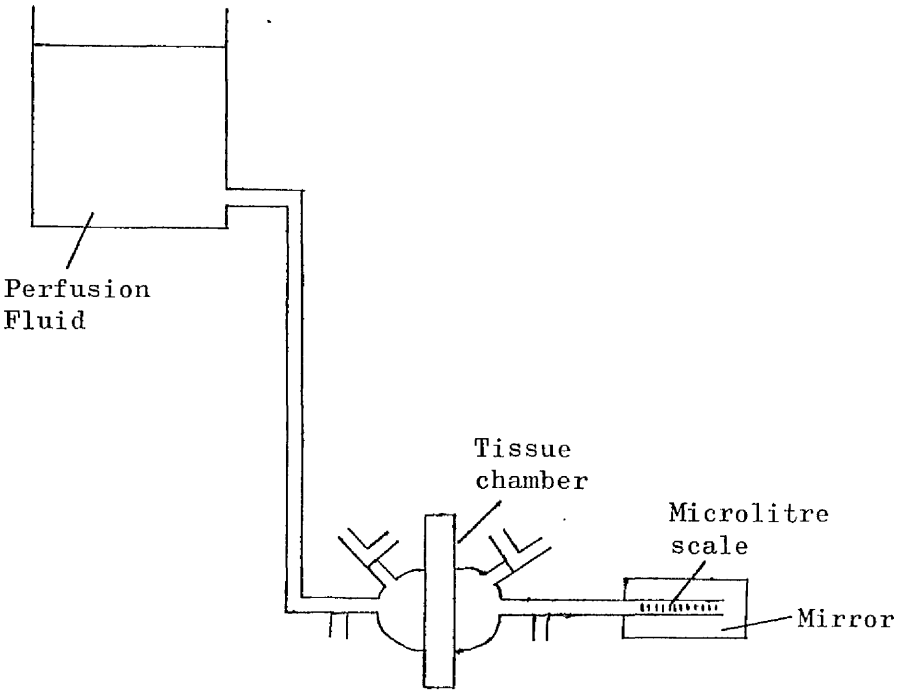

Figure 6.1

Diagram of equipment used in fluid conductivity experiments.

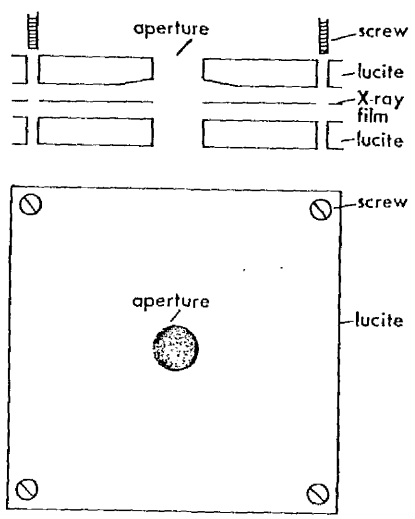

Figure 6.2

Perfusion chamber used in fluid conductivity experiments. Tissue samples were placed between the X-ray film and upper lucite plate.

in the values of resistance between the two tissues was so large as to make the effect of the different viscosity of the two fluids negligible in the future discussion.

Tissue was obtained from Dutch rabbits which were killed by an overdose of Urethane anaesthetic. The eye was removed within several seconds and placed in a bath of perfusion fluid. The eye was quickly transferred to a dissecting microscope where discs of tissue were obtained using a corneal trephine. Measurements were made on retina, pigment epithelium and choroid together or on sclera alone.

The rate of flow through the tissue was measured by timing the movement of the fluid along a microlitre scale using a stopwatch. A mirror was used when reading the scale to avoid any errors due to parallax. The thickness of the scleral samples used was measured with a micrometer and this instrument was used to measure thickness of several samples of retina, pigment epithelium and choroid. The retinal samples used in thickness measurements were not used in the measurement of fluid conductivity since unfixed retina is fragile and easily damaged. The differential force was calculated from a measurement of the height of the reservoir above the outflow tube from the perfusion chamber, and the known central diameter of the X-ray film within the chamber. A pressure difference of 39 to 57 mm.Hg was used in the determination of scleral fluid conductivity but, to avoid damage to tissue, measurements were made on retinal samples using only 1 to 6 mm.Hg.

6.2.2 Results

The tissue fluid conductivity results for sclera are given in table 6.1. In six samples, the mean conductivity of the sclera was 110×10^{-13} cm^4 dyn^{-1} sec^{-1} with a standard deviation of 45×10^{-13}.

Table 6.1

Results for rabbit sclera

	Conductivity ($cm^4\ dyn^{-1}\ sec^{-1}$)
	80 $\times 10^{-13}$
	61
	136
	71
	160
	155
Mean	110
Standard deviation	45
Standard error	18

This is similar to the value of 19 x 10^{-13} cm^4 dyn^{-1} sec^{-1} obtained by Fatt and Hedbys (1970) on four scleral samples. Fatt and Hedbys (1970) used a flow conductivity-hydration relation and the different results may be due to the different methods employed. Both methods indicate a value of around 10^{-11} cm^4 dyn^{-1} sec^{-1} for the scleral conductivity.

The tissue fluid conductivity measurements for retina, pigment epithelium and choroid are given in table 6.2. The mean value of six measurements on three samples was 0.93 x 10^{-9} cm^4 dyn^{-1} sec^{-1} (standard deviation 0.40 x 10^{-9}). Fatt and Shantinath (1971) obtained a value of 9.4 x 10^{-9} cm^4 dyn^{-1} sec^{-1} from two fresh retinae and three frozen retinae. Since the tissue of the present series includes pigment epithelium and choroid whilst Fatt and Shantinath used retina alone, a difference between the two sets of results would be expected. Retina, pigment epithelium and choroid samples were used in the present study for two reasons, (1) to avoid manipulative artefact and (2) for inclusion in the model. The retina in its unfixed state tears very easily, in contrast to the sclera which forms the tough outer coat of the eye. The chance of tearing the retina would be increased if it were to be separated from the underlying pigment epithelium. In the model to be described in the following section, two resistance values are required, viz. that of the retina, pigment epithelium and choroid together and the scleral resistance.

6.3 Model of Hydrostatic Pressure-Flow Situation across the Posterior layers of the Eye

6.3.1 Introduction

The hydrostatic pressure sources which exist across the outer layers of the eye are shown in fig. 6.3. The vitreous is at the intraocular pressure. A pressure source exists in the choroid

Table 6.2

Results for rabbit retina + pigment epithelium + choroid

	Conductivity ($cm^4\ dyn^{-1}\ sec^{-1}$)
	0.62 $\times 10^{-5}$
	0.57
	0.59
	1.49
	1.04
	1.31
Mean	0.93
Standard deviation	0.40
Standard error	0.17

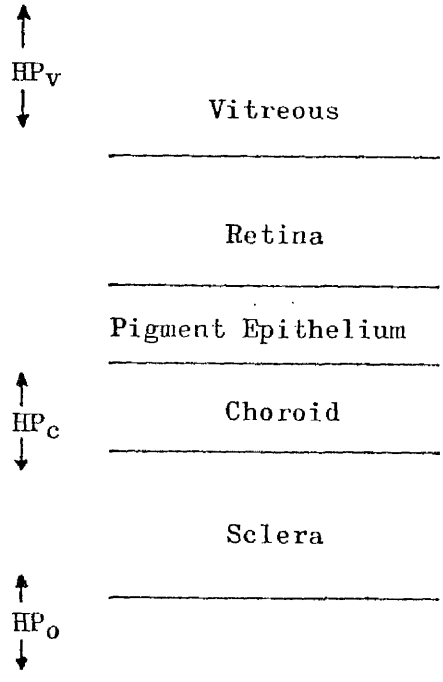

Figure 6.3

Hydrostatic pressure sources in the posterior layers of the eye.

HP_V = pressure in the vitreous; HP_C = pressure in the choroid and

HP_O = pressure outside the eye.

because of the blood vessels, e.g. the choriocapillaris has been shown to leak peroxidase (Peyman, Spitznas and Straatsma, 1971; Johnson, McNaught and Foulds, 1977), a molecule with an effective diffusion radius of 3 mm (Bellhorn, Bellhorn and Poll, 1977). The pressure outside the eye is atmospheric or a little above it. As indicated by the arrows, hydrostatic pressure acts equally in all directions. Although the results described above refer to fluid conductivity, it is resistance per unit area which is used in the models to be described. This eliminates the error in the measurement of tissue thickness as the parameter is not needed.

A pressure-flow model has been proposed by Fatt and Hedbys (1970) and Fatt and Shantinath (1971) and is illustrated in fig. 6.4. In this model the pressure difference between intraocular pressure and the pressure outside the eye acts across the retina and sclera in series. The flow from the eye is described by

$$F = \frac{HP_v - HP_o}{R_r + R_s} \qquad (6.2)$$

where F = flow rate

HP_v = pressure in the vitreous

HP_o = pressure outside the eye

R_r = retinal resistance per unit area

R_s = scleral resistancer per unit area

Since the resistance of the sclera is several orders of magnitude greater than the retinal resistance, its value determines the flow from the vitreous. Fatt and Hedbys (1970) obtained a flow rate of 0.74 µl min^{-1} from their model when the intraocular pressure is 18 mm.Hg. The flow rate by this model using the resistance measurements of the present study would be 3.5 µl min^{-1}. The model

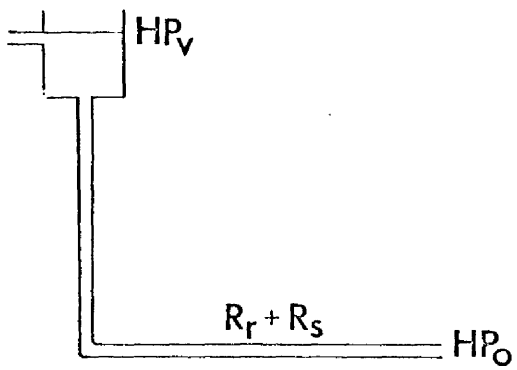

Figure 6.4

Fatt's model of hydrostatic pressures and resistances across the posterior layers of the eye. HP_v = pressure in the vitreous; HP_o = pressure outside the eye; $R_r + R_s$ = retinal + scleral resistance.

implies that there is a flow of 1 to 3 $\mu l\ min^{-1}$ of fluid across the retina and sclera. However, the model must be faulted due to its failure to take account of the choroid as a pressure source and fluid reservoir. A superior model which incorporates these features is presented in the following section.

6.3.2 Description of Model

The model is illustrated in fig. 6.5. Here the resistance between the vitreous and the choroid is that due to the combined retina, pigment epithelium and choroid. The vitreal and choroidal pressures are represented as reservoirs a given height above the outside pressure. The flow across the retina depends on the pressure difference between the vitreous and the choroid and the resistance between the two regions.

$$F_r = \frac{HP_v - HP_c}{R_r} \qquad (6.4)$$

where F_r = flow across the retina

HP_c = pressure in the choroid

R_r = resistance of retina + pigment epithelium + choroid

The flow from the choroid through the sclera depends on the pressure difference between the choroid and the external pressure and on the scleral resistance.

$$F_s = \frac{HP_c - HP_o}{R_s} \qquad (6.5)$$

where F_s = flow across the sclera.

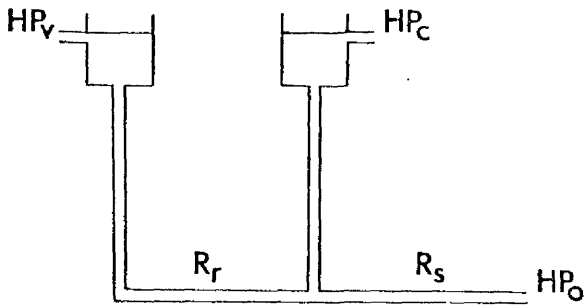

Figure 6.5

Model representing the hydrostatic pressures and resistances across the posterior layers of the eye. HP_V = pressure in vitreous; HP_C = pressure in choroid; HP_O = pressure outside eye= R_r = retinal resistance; R_S = scleral resistance.

An important aspect of this model is that since the choroid acts as a reservoir with an independent supply and exit route, the flow through the retina is not the same as the flow through the sclera. The difference between the retinal flow and the scleral flow is the net flow into or out of the choroid.

$$F_x = F_r - F_s \tag{6.6}$$

where F_x = net flow into or out of the choroid,

i.e. $$F_x = \frac{HP_v - HP_c}{R_r} - \frac{HP_c - HP_o}{R_s} \tag{6.7}$$

$$F_x = \frac{R_s\, HP_v + R_r\, HP_o - (R_r + R_s)\, HP_c}{R_r\, R_s} \tag{6.8}$$

If F_x is positive there is a net flow into the choroid which functions as a sink; if F_x is negative the net flow is out of the choroid which acts as a source of fluid.

6.3.3 Application and Discussion of Model

Assuming the surface area of the rabbit eye to be 7 cm^2, the value of R_s obtained from the results of the present experiments would give a scleral flow of 0.2 µl min^{-1} $mm.Hg^{-1}$. If the pressure difference across the sclera were 18 mm.Hg the scleral flow would be 3.6 µl min^{-1}.

The value of R_r obtained from the present experiments would give a retinal flow of 43 µl min^{-1} $mm.Hg^{-1}$. Van Alphen (1961) measured the choroidal pressure to be between 1 and 3 mm.Hg below the intraocular pressure. His measurements were obtained by inserting a cannula through the sclera into the choroid and sealing it in place. Due to the technical difficulties involved, this cannot be considered a reliable measurement and it is doubtful if such could be achieved with present techniques. Maurice, Salmon and Zauberman (1971) were

unable to detect any pressure difference between the intraocular pressure and the pressure in the sub-retinal space in an experiment similar to Van Alphen's (1961).

It is unlikely that a significant pressure difference exists across the retina since the pressure will be transmitted across the retina and tend to equalise the tissue pressure on either side. It is likely that HP_v and HP_c are approximately equal. Any small disparity between HP_v and HP_c may produce significant retinal flow because of the low retinal resistance, and affect the sign of F_x. The model underlines the need for an accurate simultaneous pressure measurement in the vitreous and in the choroid, before one can predict with confidence the magnitude and direction of the retinal flow induced by hydrostatic pressure.

CHAPTER 7

RESISTANCE TO FLUID FLOW INDUCED BY HYDROSTATIC PRESSURE : II. ANTERIOR SITES

7.1 Introduction

Under normal conditions, there exists a continuous flow of aqueous humour from the ciliary processes in the posterior chamber into Schlemm's canal or equivalent at the angle of the anterior chamber. This is the major route by which fluid leaves the anterior chamber (Cole, 1974). The anatomy of this region was described in Chapter 1. There is considerable evidence that, in primates at least, fluid enters Schlemm's canal through pores in invaginations or giant vacuoles which line the canal endothelium (fig. 7.1). (Inomata, Bill and Smelser, 1972; Segawa, 1973; Grierson, 1976).

The size and incidence of these pores have been shown to vary with pressure (Grierson & Lee, 1975a; 1975b; Grierson, 1976), so that the conductance of the pore and vacuole system is not a fixed quantity but is pressure-dependent. Pilocarpine is a drug which is used to reduce intraocular pressure in the treatment of glaucoma. It has been shown (Grierson, Lee and Abraham, 1978; 1979; Grierson, Lee, Moseley and Abraham, 1979) that pilocarpine alters the size and incidence and hence the conductance of the pore-invagination system.

It is of interest, therefore, to calculate the fluid conductance of the pore-invagination in normal tissue and to see the effect of pressure and pilocarpine on this value. A model of the pore has been published (Bill and Svedbergh, 1972) and this over-estimates the pore resistance. This model will be considered along with two others developed in the present chapter - an aperture model and a Venturi tube model. Based on electron micrographs of pore

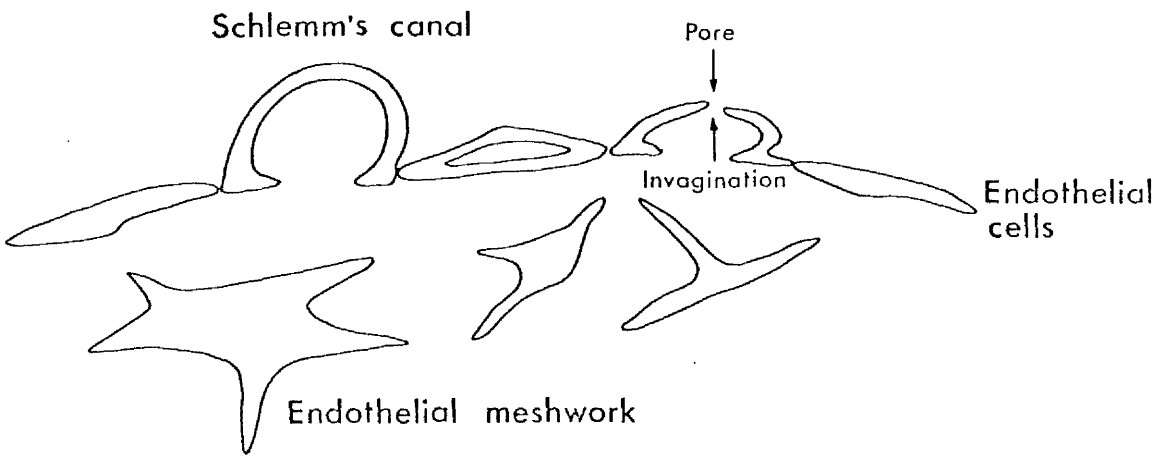

Figure 7.1

Diagram of endothelial cells lining Schlemm's canal showing an invagination with a pore opening and underlying endothelial meshwork.

openings (fig. 7.2) the Venturi tube seems a particularly appropriate model. The invagination is considered as a tube in series with the pore and its conductance is derived from Poiseuille's law.

The models are applied to data from the scanning electron microscope studies of rhesus monkey eye tissue at 8 mm Hg and 15 mm Hg and of human eye tissue, pilocarpine-treated and untreated (Grierson, 1976; Grierson et al, 1979).

7.2 Quantification of Pore Incidence

7.2.1. Human: pilocarpine-treated and untreated

Data on the size and frequency of the luminal openings were obtained from a study performed by Grierson, Lee, Moseley and Abraham (1979) in which the endothelium lining the trabecular aspect of Schlemm's canal was examined with the scanning electron microscope (S.E.M.). The tissue for this investigation came from ten patients with an ostensibly normal anterior segment, and each eye was enucleated in treatment of a choroidal melanoma. With five patients, the eye to be enucleated was subjected to a topical application of 2 to 4% pilocarpine on four separate occasions at six-hourly intervals before surgery. The remaining five patients in an age-matched group were untreated, and the tissue served as a control. The tissue was processed for electron microscopy using standard techniques. The pore widths were measured from sets of prints which corresponded to a surface area of 100,000 μm^2 from each eye with the use of a X7 magnifier which incorporated a graticule. In each eye, the numbers of pores in a 0.5 μm diameter range up to the maximum pore size were obtained.

The results are given in figs 7.3 and 7.4. Frequency versus pore width is plotted for the five pilocarpine-treated eyes in figs. 7.3 a to e and for the untreated eyes in figs. 7.4 a to e. In the pilocarpine-treated tissue there are more pores and there is also a

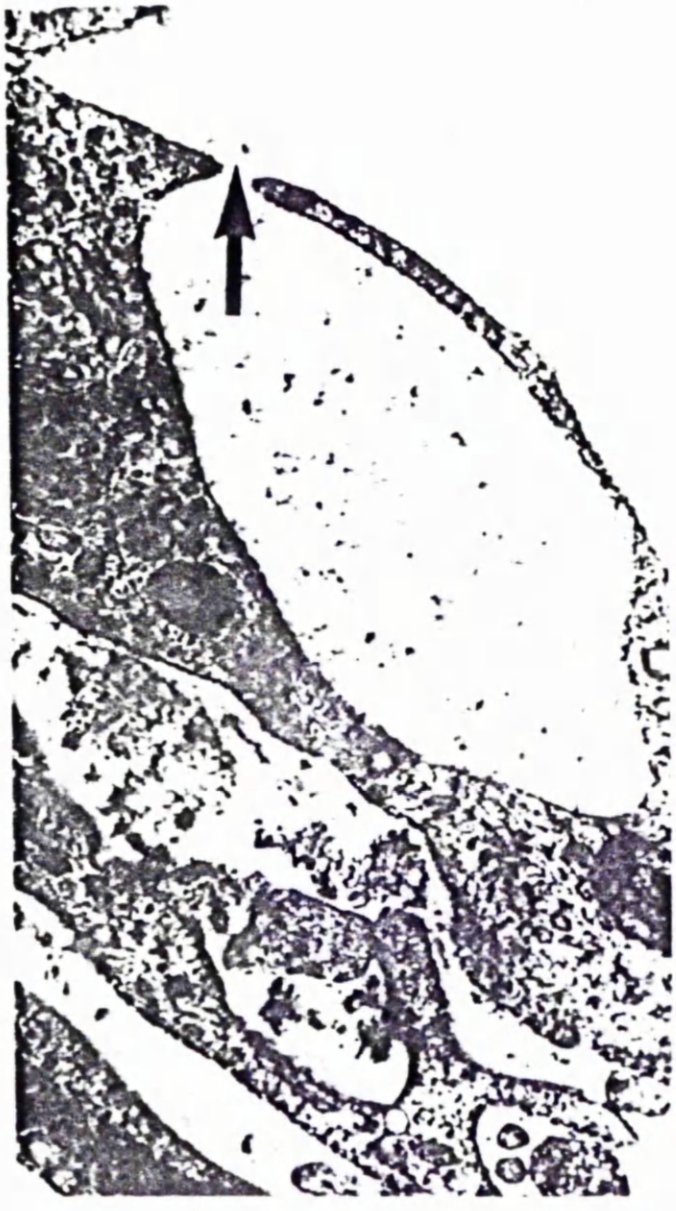

Figure 7.2

Electron micrograph of a pore opening (arrow) in the lining endothelium of Schlemm's canal in a Rhesus monkey at IOP of 15 mm Hg (photograph courtesy of Dr I Grierson).

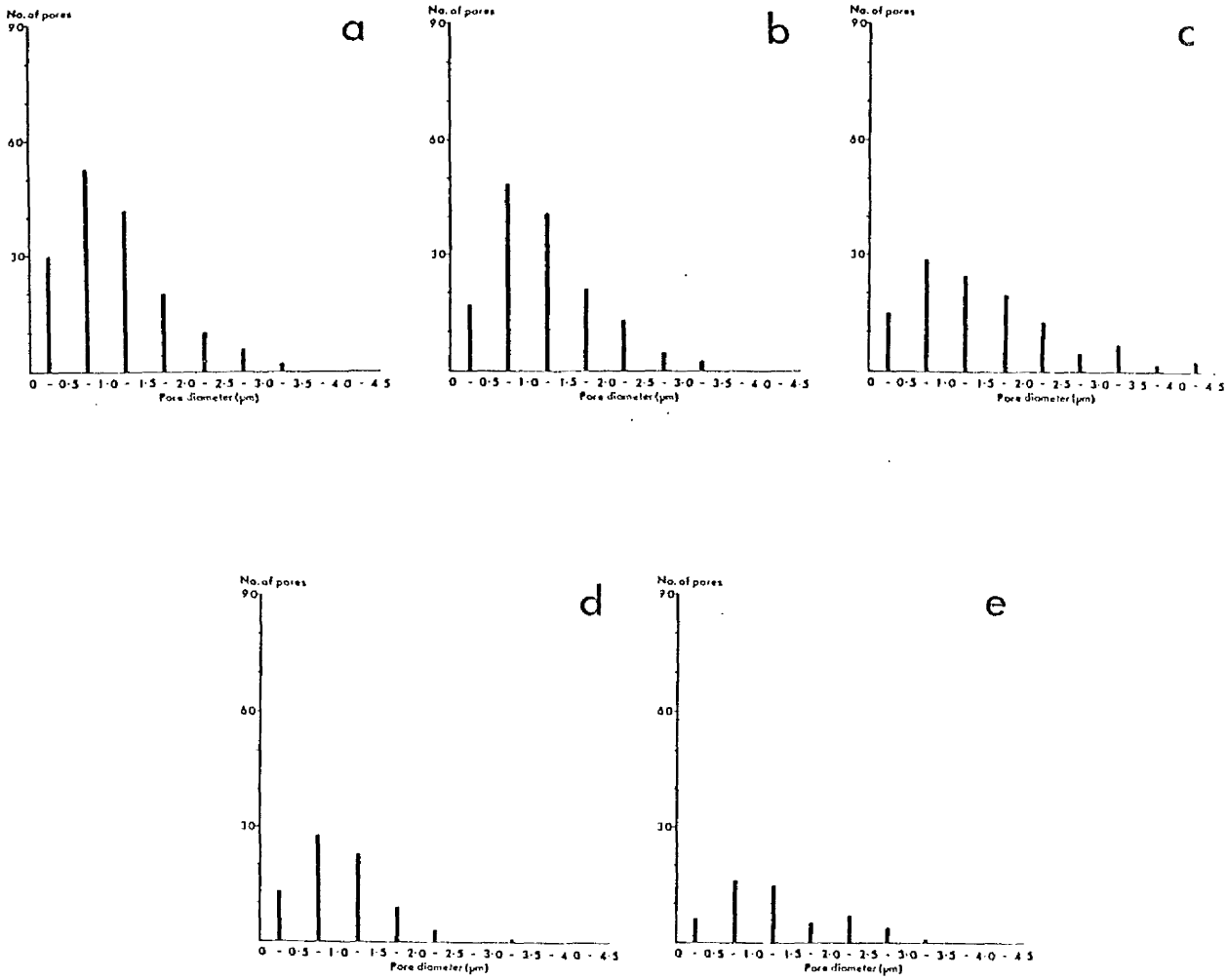

Figure 7.3

Number of pores of different diameters from electron micrographs of 100,000 μm^2 of lining endothelium of Schlemm's canal. Tissue from pilocarpine-treated human eyes, a: P/1, b: P/2, c: P/3, d: P/4, e: P/5.

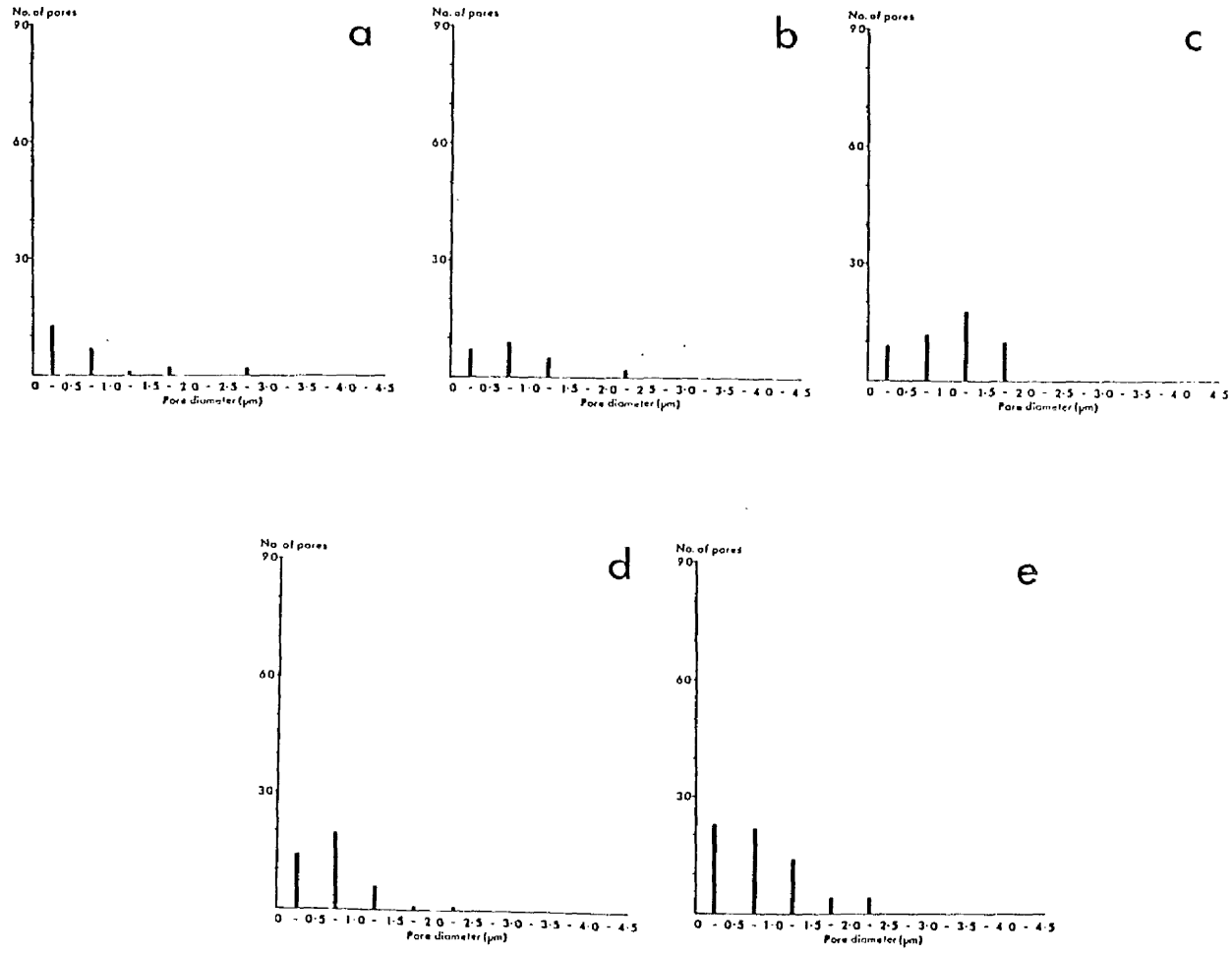

Figure 7.4

Numbers of pores of different diameters from electron micrographs of 100,000 μm^2 of lining endothelium of Schlemm's canal. Tissue from untreated human eyes. a: U/1, b: U/2, c: U/3, d: U/4, e: U/5.

shift in the pore distribution towards larger pores.

7.2.2 Rhesus monkey: 8 mm Hg and 15 mm Hg

In the experiments conducted by Grierson (1976) on rhesus monkeys, intraocular pressure was controlled by an intracameral 25 gauge needle attached to a manometer system which contained an aqueous replacement solution (Barany, 1964). In three animals, one eye was maintained at 8 mm Hg and the other at 15 mm Hg which was 2 mm Hg higher than the mean value for spontaneous pressure obtained from nine eyes (13 $\pm$ 3 mm Hg). Tissue was prepared for S.E.M. studies by freeze-drying (Lee and Grierson, 1975). Electron micrographs covering an area of 100,000 μm^2 of the lining endothelium of Schlemm's canal were obtained from each eye and pore diameters measured as described above.

The results are given in figs. 7.5 and 7.6. In fig. 7.5 a to c the number of pores versus pore width for the three eyes at 8 mm Hg is plotted and in fig. 7.6 a to c the same is given for the eyes maintained at 15 mm Hg.

7.3 Aperture Model

Since, on initial inspection of the electron micrographs, the pore may be regarded as simply a hole in the invagination, an aperture model will be developed in this section (fig. 7.7). The pressure drop experienced by a fluid flowing through an aperture (Happel and Brenner, 1965), is

$$P = \frac{3\,Q\,u}{R^3} \qquad (7.1)$$

where P = pressure drop across aperture (dyn cm^{-2})

Q = flow (ml sec^{-1})

u = viscosity (Poise)

R = aperture radius (cm)

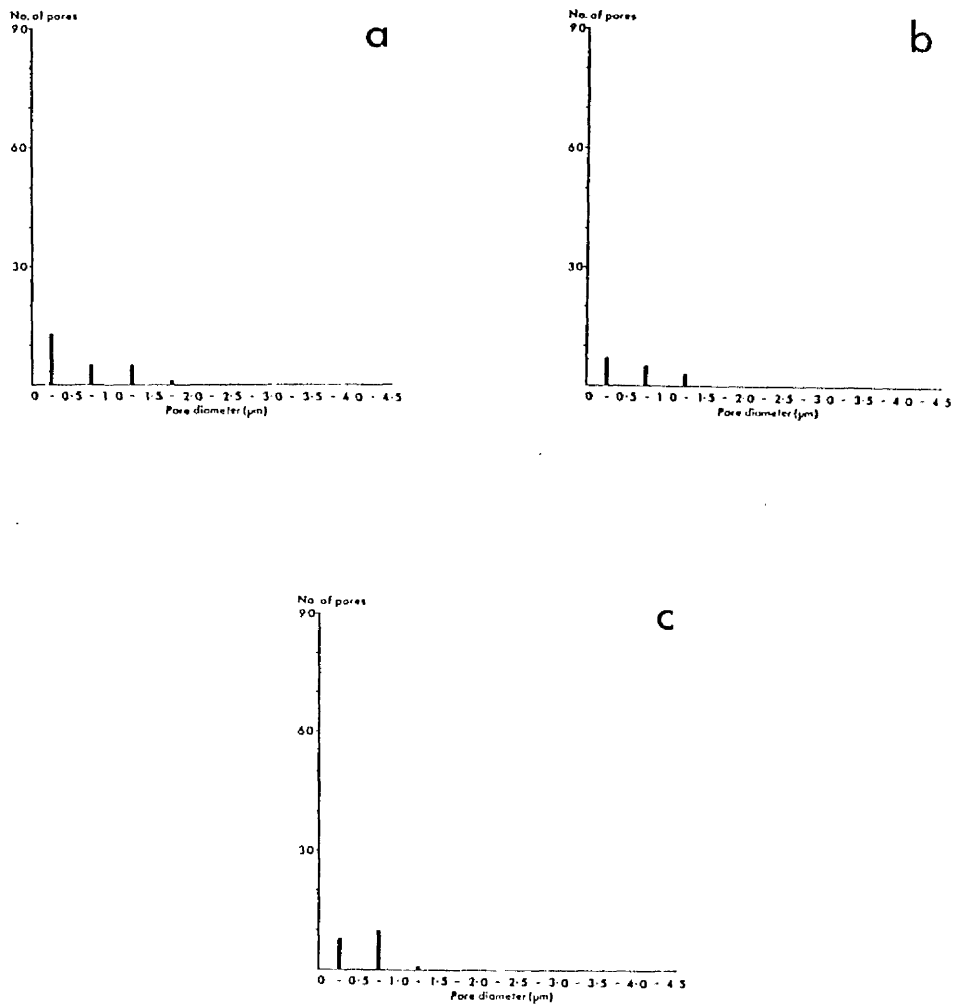

Figure 7.5

Numbers of pores of different diameters from electron micgraphs of 100,000 μm^2 of lining endothelium of Schlemm's canal. Tissue from Rhesus monkeys at IOP of 8 mm Hg, a: 8/1, b: 8/2, c: 8/3.

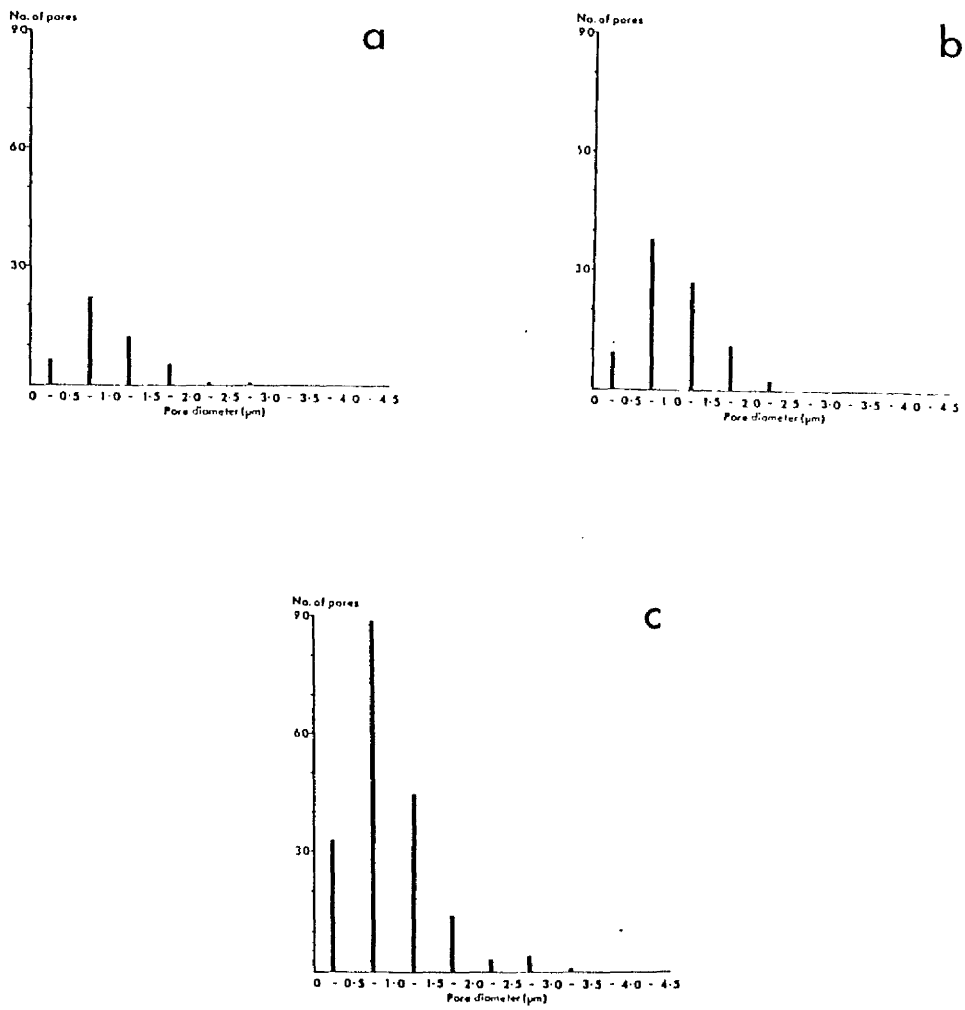

Figure 7.6

Numbers of pores of different diameters from electron micrographs of 100,000 μm^2 of lining endothelium of Schlemm's canal. Tissue from Rhesus monkeys at IOP of 15 mm Hg. a: 15/1, b: 15/2, c: 15/3.

APERTURE MODEL

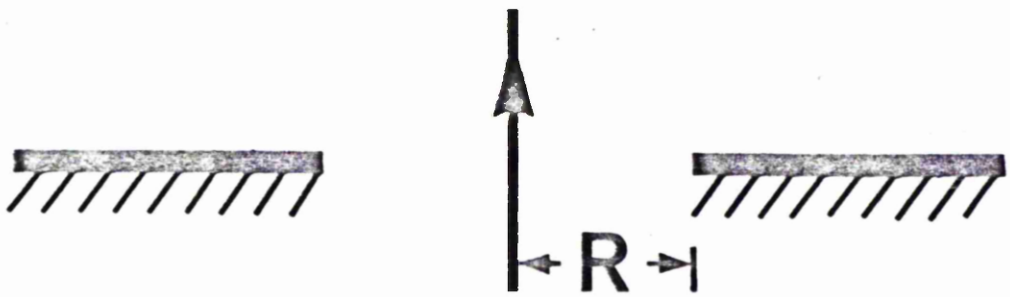

$$P = \frac{3\,Q\,u}{R^3}$$

Figure 7.7

Aperture model. P = pressure drop; Q = flow; u = viscosity and R = radius.

By definition,

$$C = \frac{Q}{P} \tag{7.2}$$

where C = conductance ($cm^5\ dyn^{-1}\ sec^{-1}$)

and

$$c = \frac{q}{p} \tag{7.3}$$

where c = conductance ($\mu l\ min^{-1}\ mm\ Hg^{-1}$)

q = flow ($\mu l\ min^{-1}$)

p = pressure (mm Hg)

The conversion between (7.2) and (7.3) is

$$c = C \times 8.005 \times 10^7 \tag{7.4}$$

From (7.1) and (7.2)

$$C = \frac{R^3}{3\ u} \tag{7.5}$$

Replacing the radius, R (cm), by the diameter, d (μm), and assuming a viscosity of 0.007 Poise, which is the viscosity of water at 37^oC (McEwen, 1958), substitution of equation (7.5) into (7.4) leads to

$$c = \frac{d^3}{2099} \tag{7.6}$$

Equation (7.6) permits the conductance of the pore openings to be calculated, provided the diameter of the pores is known.

7.4 Bill and Svedbergh (1972) Model

A model of the pore-invagination was published by Bill and Svedbergh (1972). Their model was developed to provide an upper limit for the pore resistance. They treated the pore as an aperture in series with a short tube so that the pore resistance is the sum of the aperture resistance and the tube resistance. Although the Bill and Svedbergh (1972) model overestimates the pore resistance it is useful to include it for a comparison with the two models of the present study.

Poiseuille's law for flow through a tube is

$$Q = \frac{P\pi R^4}{8\ L\ u} \qquad (7.7)$$

where L = tube length (cm).

From (7.2) and (7.7),

$$C = \frac{\pi R^4}{8\ L\ u} \qquad (7.8)$$

On changing units,

$$c = \frac{\pi R^4}{8\ L\ u} \times 8.005 \times 10^7 \qquad (7.9)$$

and, again taking u equal to 0.007 Poise as in the aperture model

$$c = \frac{d^4}{1 \times 3563} \qquad (7.10)$$

where l = length (μm).

In this model, the pore resistance is the resistance of the equivalent aperture plus the resistance of the equivalent tube. The conductance by this model is therefore obtained from equations (7.6) and (7.10) and is

$$c = \left(\frac{2099}{d^3} + \frac{1 \times 3563}{d^4} \right)^{-1} \qquad (7.11)$$

Another aspect of this model is that a diameter of 2 μm is ascribed to all pores which are larger than this, i.e.

$$\begin{aligned} d &= dm \qquad 0 \leqslant dm \leqslant 2 \\ d &= 2 \qquad\quad dm \geqslant 2 \end{aligned} \qquad (7.12)$$

where dm = measured diameter (μm).

Equation (7.11) gives the conductance, provided the pore diameter and length are known in μm and the condition of equation (7.12) is adhered to.

7.5 Venturi Tube Model

7.5.1 Theory

The analysis of flow in a Venturi tube is described in detail elsewhere (Happel and Brenner, 1965). A Venturi tube is a confocal hyperboloid of revolution (fig. 7.8). The pressure drop experienced by fluid flowing through a Venturi tube is

$$P = \frac{3 Q u}{R^3 (1 + 2 \cos a) (1 - \cos a)^2} \qquad (7.13)$$

where a = angle of convergence.

From equation (7.2) and (7.13)

$$C = \frac{R^3 (1 + 2 \cos a) (1 - \cos a)^2}{3 u} \qquad (7.14)$$

From equation (7.4) and (7.14)

$$c = \frac{R^3 (1 + 2 \cos a) (1 - \cos a)^2}{3 u} \times 8.005 \times 10^7 \qquad (7.15)$$

Substituting the numerical value of 0.007 for u and replacing R with d leads to

$$c = \frac{d^3}{2099} (1 + 2 \cos a) (1 - \cos a)^2 \qquad (7.16)$$

Equation (7.16) permits the conductance in $\mu l\ min^{-1}\ mm\ Hg^{-1}$ of the pores to be calculated provided their diameters in μm are known and their angle of convergence.

VENTURI TUBE MODEL

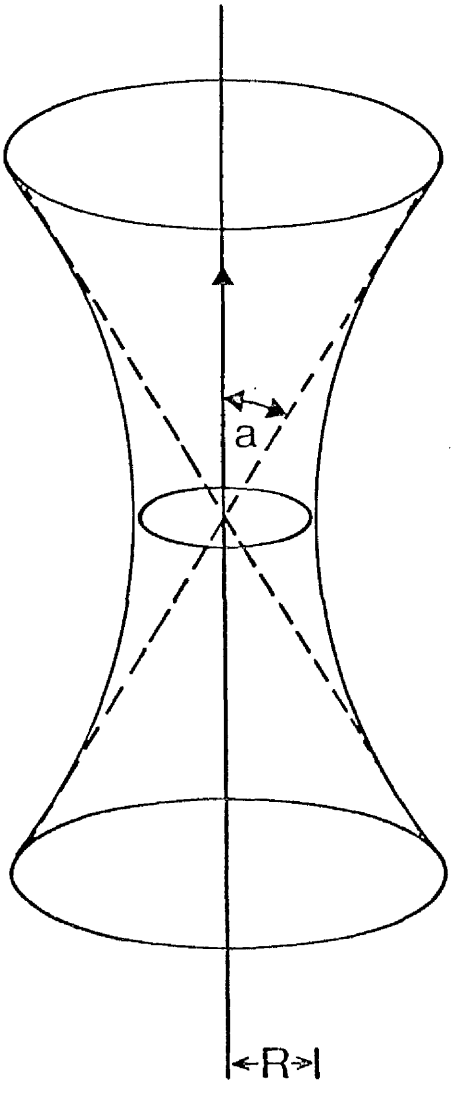

$$P = \frac{3\,Q\,u}{R^3\,(1 + 2\cos a)\,(1 - \cos a)^2}$$

Figure 7.8

Venturi tube model. P = pressure drop; Q = flow; u = viscosity; R = radius and a = angle of convergence.

7.5.2 Angle of Convergence

It may be seen by inspection of equation (7.16) that the pore conductance is a function of the angle of convergence. The relation between conductance and angle of convergence is shown in fig. 7.9, where it is seen to possess a sigmoid shape. The conductance is within 10% of the maximum conductance for angles of convergence between 90^{o} and 79^{o}. As the angle of convergence decreases, there is an increasingly rapid fall in the conductance. It has dropped by 20% at 73^{o}, 30% at 68^{o}, 40% at 64^{o} and 50% at 60^{o}. The similarity of equations (7.6) and (7.16) is apparent and is a result of the fact that equation (7.6) is derived as a special case of equation (7.16) when cos a = 0, i.e. a = 90^{o}, at which point the Venturi tube becomes an aperture.

The angle of convergence was measured from transmission electron micrographs of twelve different pores (table 7.1) from which the mean of 70^{o} and a standard deviation of 9^{o} were obtained. This sample may contain more small pores than large ones because of the technical difficulty in obtaining serial sections of large pores. Moreover, since the structures are biological, they do not all fit the Venturi tube model equally well. The mean value was used as the angle of convergence in the model. This means that the conductance of a pore by the aperture model and Venturi tube model bear a constant ratio to each other.

7.6 Application of the Models

7.6.1 Total Pore Conductance

The results of the electron micrograph investigations described in section 7.2 gave the number of pores in 0.5 μm bands. The value of the mid-diameter of each band was used in the conductance calculations. The conductance of all the pores in a particular diameter range is the number of pores in that range times the

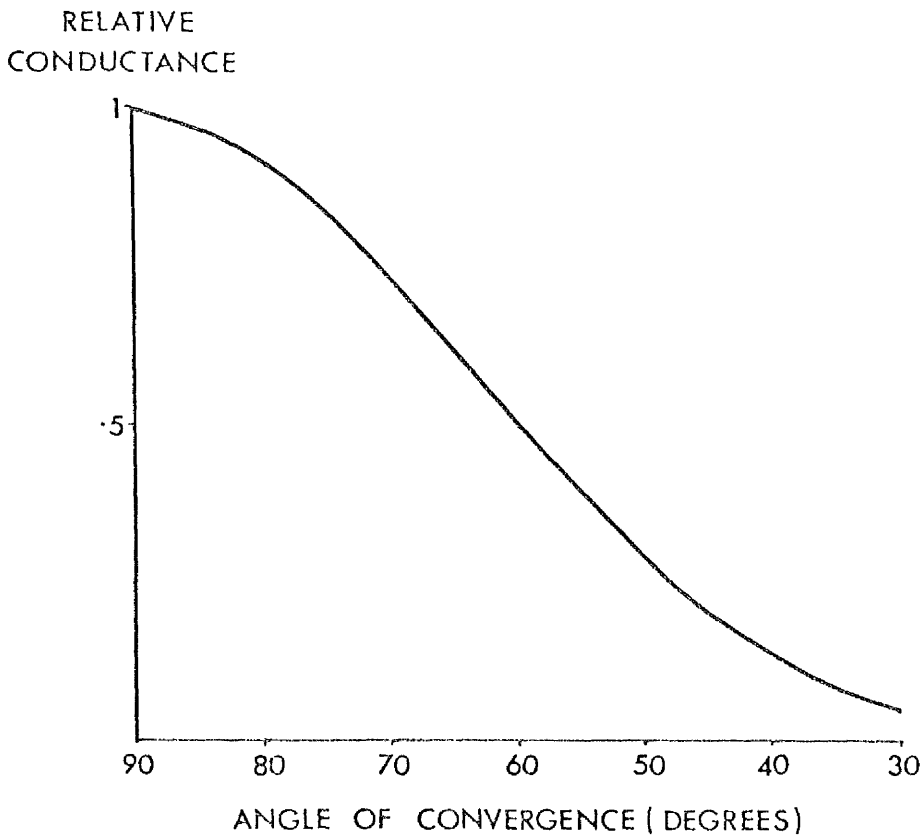

Figure 7.9

Effect of angle of convergence on the conductance according to the Venturi tube model.

Table 7.1

The angle of convergence of the Venturi tube - equivalent of 12 different pores measured from electron micrographs.

Angle of Convergence (degrees)	
	75
	61
	72
	78
	85
	76
	70
	65
	72
	56
	57
	72
Mean	70
Standard deviation	9
Standard error	3

conductance at the mid range diameter. The total conductance of all the pores observed in the eye is then the sum of the conductance values for each diameter band. The total pore conductance of the entire lining endothelium in the eye is the conductance of the observed pores multiplied by the ratio of the area of the endothelium to the area of tissue covered by the micrographs.

Resistance at all times is the inverse of conductance.

7.6.2 Pore-Invagination Conductance

The conductance of the pore-invagination unit is obtained by considering the pores and invaginations in series. The conductance of the invagination is calculated by treating it as a tube of radius 1 μm and length 3 μm (Bill and Svedbergh, 1972) and applying Poiseuille's law (equation 7.10) so that

$$c_I = n/668 \qquad (7.17)$$

where c_I = conductance of invagination ($\mu l\ min^{-1}\ mm\ Hg^{-1}$)

n = number of invaginations with pores

Although equation (7.17) does not take account of any possible variation in shape or size of the invagination with pore width it is used to provide an order of magnitude figure for the invagination conductance. The number of invaginations which contribute to the conductance is equal to the number of pores counted in the tissue since, although there are more invaginations than pores (Grierson, 1976), only those with pore openings have a flow of fluid and, hence, a non-zero conductance. The pore-invagination conductance is given by

$$\frac{1}{c_{pI}} = \frac{1}{c_p} + \frac{1}{c_I} \qquad (7.18)$$

where c_{pI} = pore-invagination conductance

c_p = pore conductance

7.7 Results of Models

7.7.1 Effect of Pore Diameter on Pore Conductance

Results were obtained using an IBM 370/168 computer. Since none of the models predicts a linear relation between conductance and diameter, it is of interest to observe the effect of diameter on the conductance calculated by each model. This is plotted in fig. 7.10 where it is seen that the large pores contribute greatly to the conductance by the aperture and Venturi tube models but, because of the 2 μm cut-off, in the Bill and Svedbergh (1972) model their effect is greatly diminished.

7.7.2 Rhesus Monkey: 8 mm Hg

The number of pores at different pore widths found by Grierson (1976) in rhesus monkeys maintained at 8 mm Hg was shown in fig. 7.5. The pore conductance for each eye by the three models is given in fig. 7.11. The eyes of figs. 7.11 a, b and c are the same as those of fig. 7.5 a, b and c respectively. Table 7.2 gives the total pore conductance and resistance, and the values of the pore-invagination conductance and resistance for each eye by the three different models for the measured area of 100,000 μ^2. The values in this table have also been extrapolated to the whole of the lining endothelium (table 7.3).

7.7.3 Rhesus Monkey: 15 mm Hg

The experimental data for this section was shown in fig. 7.6. The pore conductances for the eyes of fig. 7.6 a, b and c are plotted in fig. 7.12 a, b and c respectively according to the three models. The total pore conductance and resistance for the area investigated in each eye, together with the resultant pore-invagination conductance and resistance are given in table 7.4. These figures have also been extrapolated to whole lining endothelium (table 7.5).

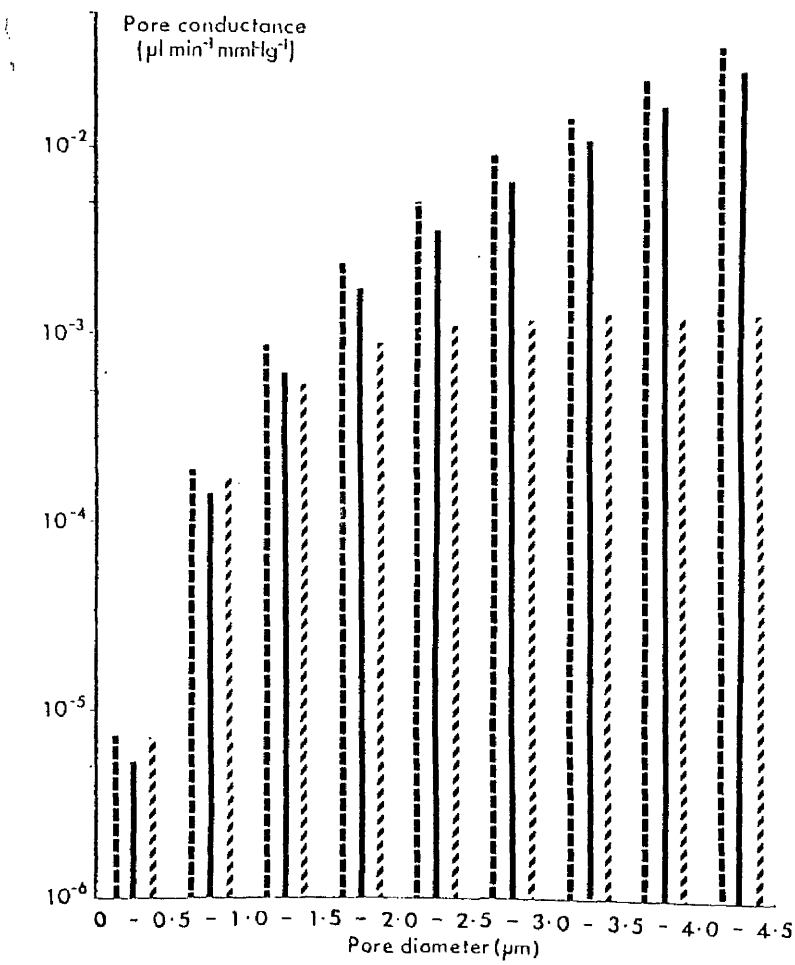

Figure 7.10

Effect of pore diameter on conductance. (- - -) Aperture; (———) Venturi tube; (⌐ ⌐ ⌐) Bill & Svedbergh (1972).

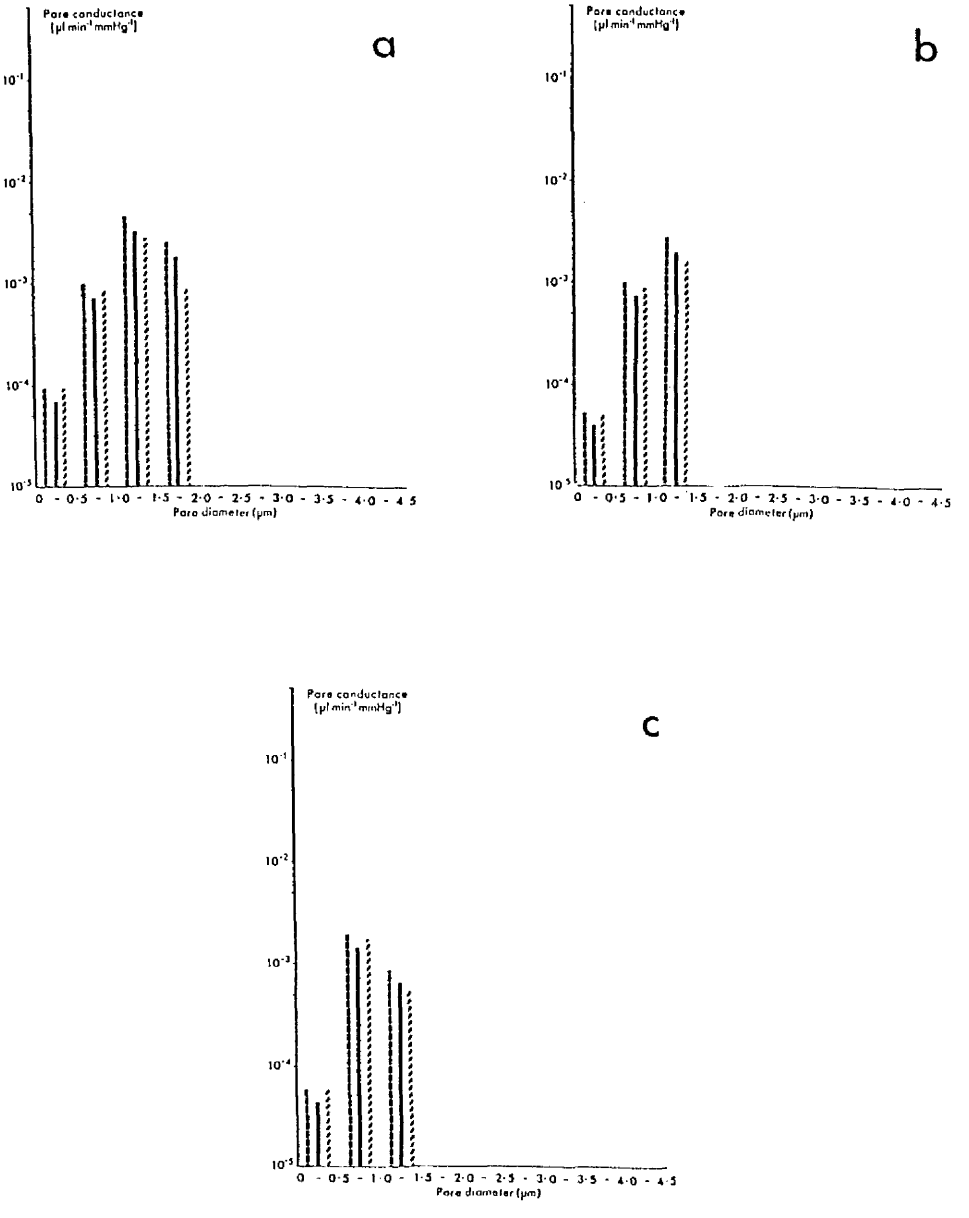

Figure 7.11

Pore conductance by each model from pores within the specified diameter range from 100,000 μ^2 of Rhesus monkey eyes at 8 mm Hg. (- - -) aperture; (——) Venturi tube; (/ / /) Bill and Svedbergh (1972). a: 8/1, b: 8/2, c: 8/3.

Table 7.2

Results of application of the models to data from electron micrographs which corresponded to 100,000 μm^2 of tissue from rhesus monkeys at an IOP of 8 mm Hg. Ap. = Aperture; V.T. = Venturi tube; B & S = Bill & Svedbergh (1972).

Experiment Number	Model	Conductance ($\mu l\ min^{-1}\ mm\ Hg^{-1}$)		Resistance (mm Hg min μl^{-1})	
		Pore	Pore-Invagination	Pore	Pore-Invagination
8/1	Ap.	0.008	0.007	120	148
	V.T.	0.006	0.005	166	193
	B & S	0.005	0.004	209	236
8/2	Ap.	0.004	0.003	260	304
	V.T.	0.003	0.003	358	402
	B & S	0.003	0.002	376	421
8/3	Ap.	0.003	0.003	333	368
	V.T.	0.002	0.002	456	494
	B & S	0.002	0.002	416	451

Table 7.3

Extrapolated values from table 7.2 for the whole lining endothelium of Schlemm's canal in rhesus monkeys at an IOP of 8 mm Hg. Ap = Aperture; V.T. = Venturi tube; B & S = Bill and Svedbergh (1972).

Experiment Number	Model	Conductance ($\mu l\ min^{-1}\ mm\ Hg^{-1}$)		Resistance ($mm\ Hg\ min\ \mu l^{-1}$)	
		Pore	Pore-Invagination	Pore	Pore-Invagination
8/1	Ap.	0.91	0.74	1.09	1.35
	V.T.	0.66	0.57	1.51	1.76
	B & S	0.53	0.47	1.89	2.15
8/2	Ap.	0.42	0.36	2.36	2.77
	V.T.	0.31	0.27	3.25	3.66
	B & S	0.29	0.26	3.41	3.82
8/3	Ap.	0.33	0.30	3.03	3.35
	V.T.	0.24	0.22	4.17	4.49
	B & S	0.27	0.24	3.77	4.10
Mean	Ap.	0.56	0.47	2.16	2.49
	V.T.	0.40	0.36	2.98	3.30
	B & S	0.30	0.32	3.02	3.36

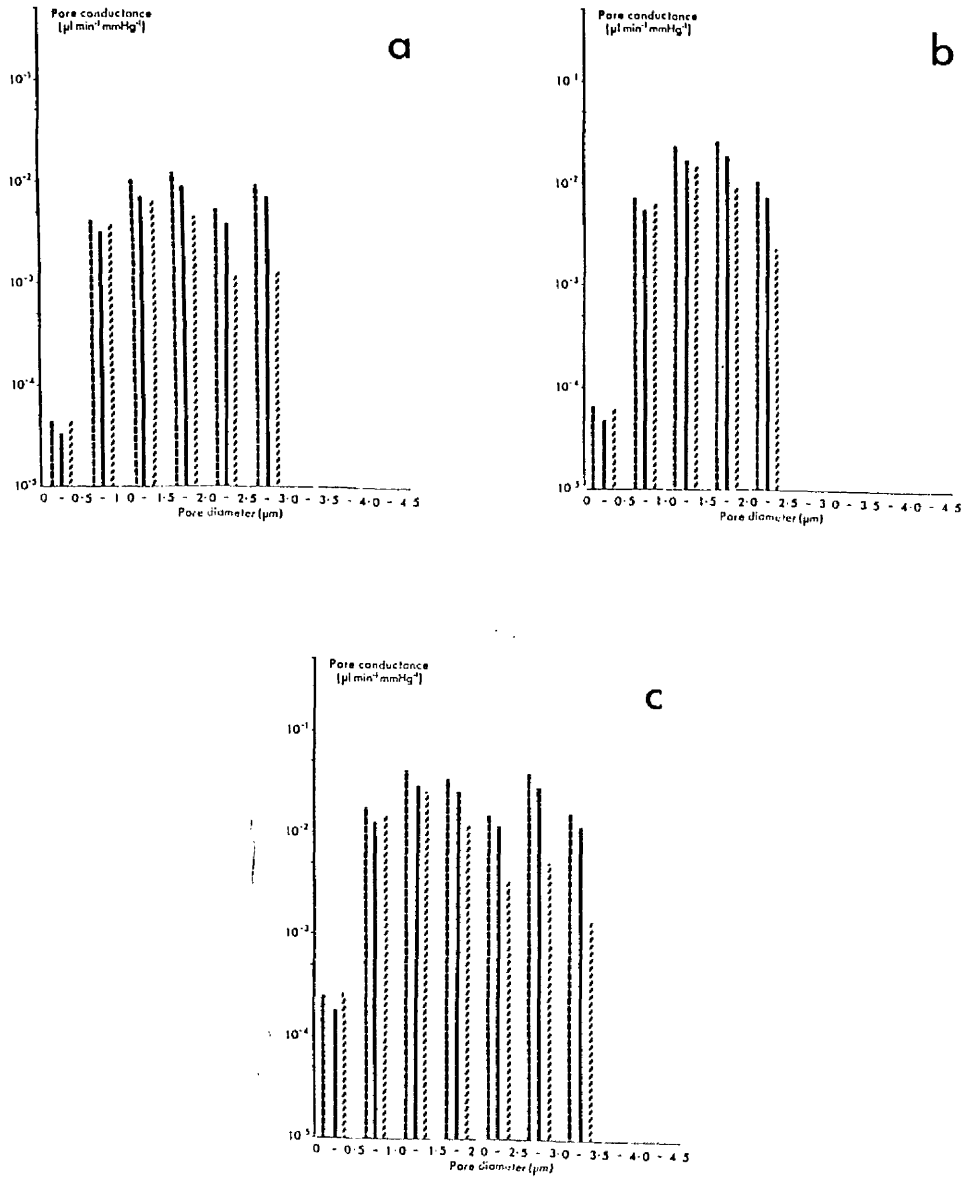

Figure 7.12

Pore conductance by each model from pores within the specified diameter range from 100,000 μ^2 of Rhesus monkey eyes at 15 mm Hg. (- - -) Aperture; (——) Venturi tube; (/ / /) Bill & Svedbergh (1972). a: 15/1, b: 15/2, c: 15/3.

Table 7.4

Results of application of the models to data from electron micgraphs which corresponded to 100,000 μm^2 of tissue from rhesus monkeys at an IOP of 15 mm Hg. Ap = Aperture; V.T. = Venturi tube; B & S = Bill and Svedbergh (1972).

Experiment Number	Model	Conductance ($\mu l\ min^{-1}\ mm\ Hg^{-1}$)		Resistance (mm Hg min μl^{-1})	
		Pore	Pore-Invagination	Pore	Pore-Invagination
15/1	Ap	0.044	0.027	23	37
	V.T.	0.032	0.022	31	46
	B & S	0.018	0.014	56	70
15/2	Ap	0.072	0.046	14	22
	V.T.	0.052	0.037	19	27
	B & S	0.035	0.028	29	36
15/3	Ap	0.168	0.105	6	10
	V.T.	0.122	0.085	8	12
	B & S	0.065	0.053	15	19

Table 7.5

Extrapolated values from table 7.4 for the whole lining endothelium of Schlemm's canal in rhesus monkeys at an IOP of 15 mm Hg. Ap = Aperture; V.T. = Venturi tube; B & S = Bill & Svedbergh (1972).

Experiment Number	Model	Conductance ($\mu l\ min^{-1}\ mm\ Hg^{-1}$)		Resistance ($mm\ Hg\ min\ \mu l^{-1}$)	
		Pore	Pore-Invagination	Pore	Pore-Invagination
15/1	Ap	4.8	3.0	0.21	0.34
	V.T.	3.5	2.4	0.29	0.42
	B & S	2.0	1.6	0.51	0.63
15/2	Ap	7.9	5.1	0.13	0.20
	V.T.	5.7	4.1	0.17	0.24
	B & S	3.9	3.0	0.26	0.33
15/3	Ap	18.5	11.6	0.05	0.09
	V.T.	13.4	9.4	0.07	0.11
	B & S	7.2	5.8	0.14	0.17
Mean	Ap	10.4	6.6	0.13	0.21
	V.T.	7.6	5.3	0.18	0.26
	B & S	4.3	3.5	0.30	0.38

7.7.4 Human: Pilocarpine-treated

The results of pore frequency and incidence in human eyes treated with pilocarpine obtained by Grierson et al (1979) were shown in fig. 7.3. The values of the pore conductances of the five eyes of fig. 7.3 a to e are plotted in fig. 7.13 a to e respectively according to the three pore models. The total pore conductance for the area of tissue investigated, together with the pore-invagination conductance are given in table 7.6. The extrapolated values for the whole of the lining endothelium have also been calculated (table 7.7).

7.7.5 Human: Untreated

The experimental results for the age- and sex-matched human control group have been given earlier (fig. 7.4). The pore conductances for these eyes are plotted in fig. 7.14 where the eyes of fig. 7.14 a to e correspond to those in fig. 7.4 a to e respectively. The total pore conductance and resultant pore-invagination conductances for the 100,000 μm^2 investigated are given in table 7.8 while the values have been extrapolated to the whole lining endothelium in table 7.9.

7.8 Discussion

Bill and Svedbergh (1972) developed their model in order to find an upper limit for the pore resistance. Their value is an over-estimate since the resistance is effectively calculated twice: once with the pore as an aperture and again as a tube. The tube resistance is calculated from Poiseuille's law which is only applicable when the length is considerably greater than the width. Since this situation does not exist in the pore, the use of Poiseuillé's law is inappropriate. The Bill and Svedbergh (1972) model further

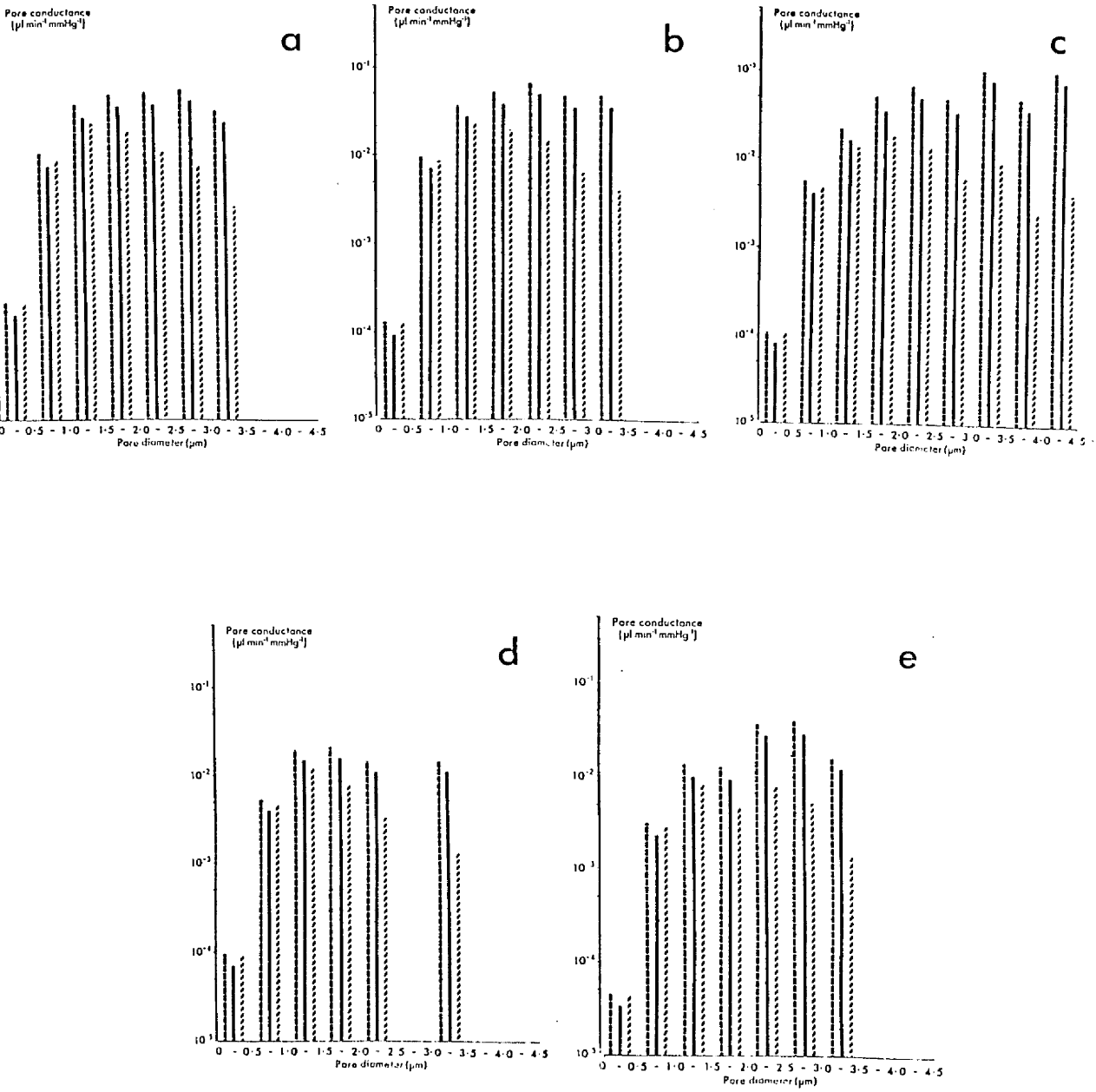

Figure 7.13

Pore conductance by each model from pores within the specified diameter range from 100,000 μ^2 of pilocarpine-treated human eyes. (- - -) Aperture; (——) Venturi tube; (/ / /) Bill & Svedbergh (1972).

a: P/1, b: P/2, c: P/3, d: P/4, e: P/5.

Table 7.6

Results of application of the models to data from electron micrographs which correspond to 100,000 μm^2 of tissue from pilocarpine-treated human eyes. Ap. = Aperture; V.T. = Venturi tube; B & S = Bill and Svedbergh (1972).

Experiment Number	Model	Conductance ($\mu l\ min^{-1}\ mm\ Hg^{-1}$)		Resistance ($mm\ Hg\ min\ \mu l^{-1}$)	
		Pore	Pore-Invagination	Pore	Pore-Invagination
P/1	Ap.	0.247	0.123	4	8
	V.T.	0.180	0.104	6	10
	B & S	0.075	0.057	13	18
P/2	Ap.	0.271	0.122	4	8
	V.T.	0.197	0.105	5	10
	B & S	0.078	0.058	13	17
P/3	Ap.	0.475	0.121	2	8
	V.T.	0.345	0.111	3	9
	B & S	0.077	0.052	13	19
P/4	Ap.	0.083	0.048	12	21
	V.T.	0.060	0.040	17	25
	B & S	0.032	0.025	32	40
P/5	Ap.	0.124	0.049	8	20
	V.T.	0.090	0.043	11	24
	B & S	0.031	0.022	32	45

Table 7.7.

Extrapolated values from table 7.6 for the whole lining endothelium of Schlemm's canal in pilocarpine-treated human eyes. Venturi tube figures in parenthesis exclude pores greater than 3 μm.

Ap. = Aperture; V.T. = Venturi tube; B & S = Bill & Svedbergh (1972)

Experiment Number	Model	Conductance ($\mu l\ min^{-1}\ mm\ Hg^{-1}$)		Resistance ($mm\ Hg\ min\ \mu l^{-1}$)	
		Pore	Pore-Invagination	Pore	Pore-Invagination
P/1	Ap.	27.2	13.5	0.037	0.074
	V.T.	19.8 (12.4)	11.4 (8.4)	0.051(0.081)	0.088 (0.120)
	B & S	8.2	6.3	0.121	0.159
P/2	Ap.	29.8	13.5	0.034	0.074
	V.T.	21.7 (13.8)	11.5 (8.7)	0.046(0.073)	0.087 (0.116)
	B & S	8.6	6.4	0.117	0.157
P/3	Ap.	52.3	13.4	0.019	0.075
	V.T.	38.0 (12.1)	12.2 (6.8)	0.026(0.083)	0.082 (0.148)
	B & S	8.5	5.8	0.118	0.174
P/4	Ap.	9.1	5.3	0.110	0.189
	V.T.	6.6 (5.3)	4.4 (3.7)	0.151(0.189)	0.230 (0.268)
	B & S	3.5	2.7	0.288	0.367
P/5	Ap.	13.6	5.4	0.073	0.186
	V.T.	9.9 (5.4)	4.7 (3.2)	0.101(0.184)	0.213 (0.308)
	B & S	3.4	2.5	0.293	0.406
Mean ± S.D.	Ap.	26.4±16.9	10.2±4.5	0.055±0.037	0.120±0.062
	V.T.	19.2±12.3 (9.8±4.1)	8.8±4.0 (6.2±2.6)	0.075±0.051 (0.122±0.059)	0.140±0.075 (0.192±0.090)
	B & S	6.4±2.7	4.7±2.0	0.187±0.094	0.253±0.123

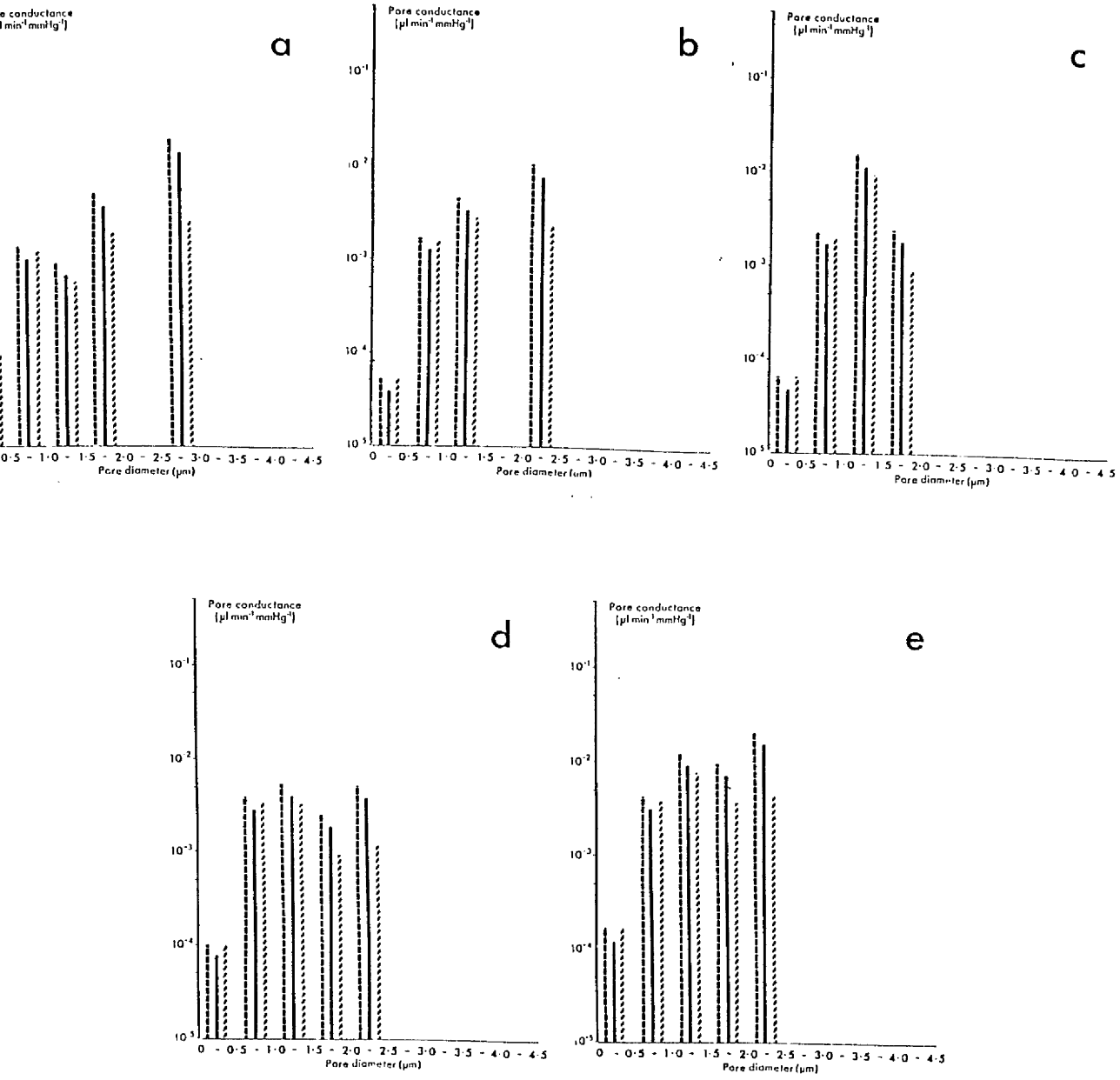

Figure 7.14

Pore conductance by each model from pores within the specified diameter range from 100,000 μ^2 of untreated human eyes. (- - - -) Aperture; (———) Venturi tube; (/ / /) Bill & Svedbergh (1972).

a: U/1, b: U/2, c: U/3, d: U/4, e: U/5.

Table 7.8

Results of application of the models to data from electron micrographs which corresponded to 100,000 μm^2 of tissue from untreated human eyes. Ap = Aperture; V.T. = Venturi tube; B & S = Bill and Svedbergh (1972).

Experiment Number	Model	Conductance ($\mu l\ min^{-1}\ mm\ Hg^{-1}$)		Resistance ($mm\ Hg\ min\ \mu l^{-1}$)	
		Pore	Pore-Invagination	Pore	Pore-Invagination
U/1	Ap.	0.027	0.016	37	63
	V.T.	0.020	0.013	50	77
	B & S	0.006	0.005	156	183
U/2	Ap.	0.017	0.012	58	87
	V.T.	0.013	0.009	79	108
	B & S	0.007	0.006	146	175
U/3	Ap.	0.022	0.016	46	63
	V.T.	0.016	0.013	63	80
	B & S	0.014	0.011	74	91
U/4	Ap.	0.018	0.014	57	72
	V.T.	0.013	0.011	78	94
	B & S	0.009	0.008	109	125
U/5	Ap.	0.050	0.033	20	30
	V.T.	0.036	0.027	28	38
	B & S	0.021	0.017	49	59

Table 7.9

Extrapolated values from table 7.8 for the whole lining endothelium of Schlemm's canal in untreated human eyes. Venturi tube figures in parenthesis exclude pores greater than 3 μm. Ap. = Aperture; V.T. = Venturi tube; B & S = Bill & Svedbergh (1972)

Experiment Number	Model	Conductance ($\mu l\ min^{-1}\ mm\ Hg^{-1}$)		Resistance ($mm\ Hg\ min\ \mu l^{-1}$)	
		Pore	Pore-Invagination	Pore	Pore-Invagination
U/1	Ap.	3.01	1.74	0.33	0.58
	V.T.	2.19 (0.61)	1.43 (0.52)	0.46 (1.64)	0.70 (1.92)
	B & S	0.70	0.60	1.42	1.66
U/2	Ap.	1.91	1.27	0.52	0.79
	V.T.	1.39	1.02	0.72	0.98
	B & S	0.76	0.63	1.33	1.59
U/3	Ap.	2.40	1.76	0.42	0.57
	V.T.	1.74	1.38	0.58	0.73
	B & S	1.49	1.21	0.67	0.83
U/4	Ap.	1.95	1.52	0.51	0.66
	V.T.	1.42	1.17	0.71	0.85
	B & S	1.01	0.88	0.99	1.13
U/5	Ap.	5.45	3.65	0.18	0.27
	V.T.	3.96	2.92	0.25	0.34
	B & S	2.27	1.88	0.44	0.53
Mean ± S.D.	Ap.	2.94±1.47*	1.99±0.95**	0.39±0.14	0.57±0.19
	V.T.	2.14±1.07* (1.82±1.26)	1.58±0.77** (1.40±0.91)	0.54±0.20 (0.78±0.52)	0.72±0.24 (0.96±0.59)
	B & S	1.25±0.65**	1.04±0.53**	0.91±0.49	1.15±0.48

Levels of significance by Student t test, pilocarpine-treated v untreated:

* $0.01 < P < 0.05$; ** $0.001 < P < 0.005$.

overestimates resistance by ascribing a diameter of 2 μm to all pores larger than this. This was done in order to reduce any error which would occur from including "pores" which are due to artefactual tearing of the tissue which may occur during processing. The inclusion of large tears could significantly alter the total calculated value of conductance because of the high value of the conductance through openings with a large diameter.

An alternative approach to that of Bill and Svedbergh's (1972) is to develop a model which will produce the correct value for the conductance. Two models have been presented in the previous sections. The aperture model was developed since, at first sight, the pore resembles an aperture. However, it allows no consideration to be taken of the pore thickness and thus underestimates its resistance. Of the models presented, the Venturi tube is considered the most appropriate since it most closely resembles the appearance of the pores in the lining endothelium of Schlemm's canal. In the Venturi tube model a constant value is used for angle of convergence. If a relation exists between angle of convergence and pore size, the use of a constant value will fail to take account of this. Nevertheless, the values of conductance determined by the Venturi tube model are probably closest to the actual pore conductances.

In tables 7.7 and 7.9, the total pore conductance was given when all the pores counted were included and, also, when pores above a diameter of 3 μm were omitted. It is believed that it is better to show the effect of large pores, which may be artefactual, in this way than to include it as part of the model, as with the Bill and Svedbergh (1972) model. Thus, in human tissue, while pores of diameter greater than 3 μm represent only 3% of the total number in the pilocarpine-treated group, they contribute 15% to the fluid conductance. No pores greater than 3 μm in diameter were observed in the Rhesus monkeys.

According to Grant (1958), the total resistance of the normal, human outflow system is 3 mm Hg μl^{-1} min. This implies that the pore and pore-invagination contribute 12% and 24% respectively in the normal human eye according to the Venturi tube model. These observations are in agreement with those of Bill and Svedbergh (1972) who considered that the bulk of the trabecular resistance is outside the canal endothelium and is probably in the underlying endothelial meshwork of the drainage wall.

Table 7.10 gives the ratios of pore resistance and of pore-invagination resistance at 15 mm Hg to their respective values at 8 mm Hg in the rhesus monkey. The pore resistance at 8 mm Hg is some 17 times greater than that at 15 mm Hg. The ratio of the pore-invagination resistances at the two pressures is 13. It is evident, therefore, that the resistances of the pore-invagination and, more especially, of the pore itself are decreased substantially with pressure. Corresponding ratios are also shown for the human untreated and treated tissue where, it may be seen, the effect of pilocarpine is to decrease the resistance of the pore and pore-invagination by a factor of 7 and 5 respectively. As shown, the ratios are only slightly affected if pores greater than 3 μm are excluded. Since artefactual tears resulting from tissue processing are equally likely to occur in all four types of tissue, it is unlikely that the ratios in table 7.10 would be appreciably altered from this cause.

Table 7.10

Ratio of resistance at 8 mm Hg to that at 15 mm Hg and of untreated to pilocarpine-treated resistance, according to the three different models. Venturi tube figures in parenthesis exclude pores greater than 3 μm.

Model	Resistance, 8 mm Hg / Resistance, 15 mm Hg		Resistance, untreated / Resistance, pilocarpine-treated	
	Pore	Pore-invagination	Pore	Pore-invagination
Aperture	17	12	7	5
Venturi tube	17	13	7(6)	5(5)
Bill & Svedbergh (1972)	10	9	5	5

CHAPTER 8

CONCLUSIONS

Some experiments have been conducted (Chapter 1) and considerable speculation has surrounded the subject of fluid movement across the retina. It has been suggested that such a flow may assist in the normal apposition of the retina against the underlying tissues. Moreover, the existence or otherwise of fluid movement across the retina has obvious implications in the drainage of sub-retinal fluid. Some investigators advocate an operational procedure to drain this fluid while others do not, observing that fluid often disappears without any intervention (Weidenthal, 1967; Rosengren, 1971; Chignell, 1974; Chisholm et al, 1975; Witmer, 1975; Leaver et al, 1976; Chawla, 1977). These, and other, observers have been more inclined to speculate than experiment.

Studies have been carried out by several investigators who have looked at the movement of a variety of substances into and out of the vitreous and these were reviewed in Chapter 1. Sodium, potassium, chloride and phosphate have been studied, as well as proteins, urea and other substances. However there has been very little done to determine the movement of water from the vitreous into the surrounding tissue. Since water accounts for approximately 99% of the vitreous, a knowledge of its movement is basic to an understanding of fluid dynamics in the vitreous.

Experiments described in this thesis were designed to answer fundamental questions regarding the behaviour of water in the vitreous. As well as water, an inert tracer, xenon-133, was studied to facilitate the subsequent analysis. Three possible exit routes from the vitreous were studied: 1. the blood in the choroid, 2. the sclera,

3. the anterior chamber. The aims of the experiments were:

1. to determine if there is any movement of dissolved xenon or tritiated water from the vitreous into the three tissues listed above,
2. to quantify this movement if it exists,
3. to calculate the rate of transfer, and
4. to investigate the nature of this movement and provide an explanation for the results obtained.

Following injection into the vitreous, both isotopes were detected in the choroidal blood, on the sclera and in the anterior chamber. Movement of an inert tracer and of water from the vitreous into the surrounding tissues has therefore been demonstrated.

Quantification of this movement was carried out and the results for xenon are given in fig. 8.1. The figures shown are those obtained from the means of the different experimental situations described in Chapter 2, corrected so that the total percentage equals one hundred. Ninety-five per cent was removed by the choroidal vasculature; 2.4% passed through the sclera and 2.6% moved into the anterior chamber. This shows that most of the xenon left the eye in the choroidal blood. This is in agreement with Strang (1975a) who injected an inert tracer, krypton-85, into the afferent choroidal circulation and showed that its removal from the tissue surrounding the choroid, into which it diffused, was principally in the efferent choroidal blood.

The distribution of tritiated water from the vitreous into the surrounding tissue was investigated in Chapter 3. These results are corrected to give a total percentage of one hunred and displayed in fig. 8.2. Ninety-six per cent of the isotope was removed by the blood flowing through the choroid; 1.4% passed through the sclera

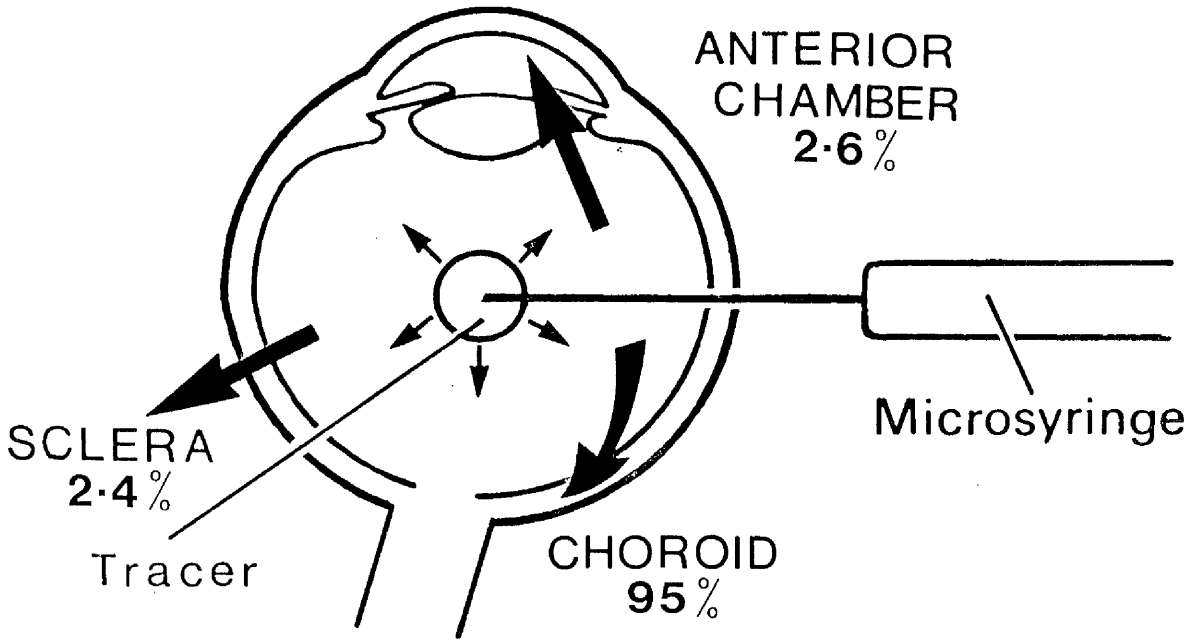

Figure 8.1

Relative distribution of xenon-133 following injection of 25 µl into the vitreous.

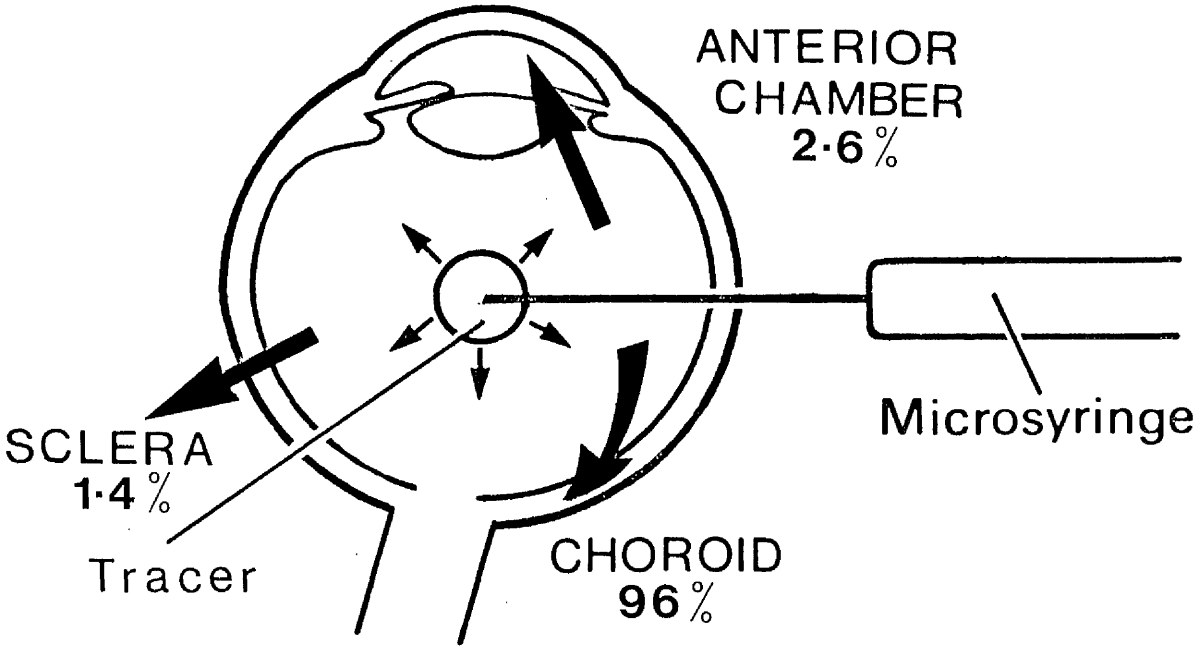

Figure 8.2

Relative distribution of tritiated water following injection of 25 µl into the vitreous.

and 2.6% into the anterior chamber. As discussed in Chapter 3, it is expected that the tritiated water behaves in a similar fashion as the ordinary water molecules of the vitreous. Therefore, almost all of the ordinary water from the mid-vitreous leaves the eye by the choroidal blood.

The mean transit times for the passage of the two tracers to the three collection sites are given in table 8.1. The mean transit time of 28 $\pm$ 2 mins for movement of xenon-133 into the choroidal blood was obtained from experiments which lasted, on average, 61 min while that of 30 $\pm$ 2 min. for tritiated water refers to experiments of 77 min average duration. The average mean transit times for the passage of both isotopes to the outside surface of the sclera, and into the anterior chamber ranged between 78 and 90 mins.

The value of 30 minutes for the mean transit time for water movement from the mid-vitreous to the choroidal blood, which is the main exit route, is in good agreement with Kinsey, Grant and Cogan (1942) who studied water movement in the opposite direction, i.e. from the blood into the vitreous. From an intraperitoneal injection of heavy water, they found that half of the vitreous was replaced in less than 26 minutes in one rabbit and less than 16 minutes in another. There is evidently a rapidly changing population of water molecules in the vitreous.

A mathematical model was developed to determine the cause of this transfer of water from the vitreous into the choroidal vessels. In the model, a 25 µl volume, representing the tracer, was allowed to move by diffusion from the vitreous into the surrounding tissue with removal occurring in the choroidal blood. Good agreement was demonstrated between the model and experiment for the inert tracer, xenon. Small differences in injection position accounted for the

Table 8.1

Experimental Mean Transit Times

Tracer	Collection Site	Mean Transit Time (± S.E.)
^{133}Xe	choroid	28 ± 2
	sclera	78 ± 5
	anterior chamber	89 ± 14
$^{3}H_2O$	choroid	30 ± 2
	sclera	90 ± 7
	anterior chamber	84 ± 3

range in mean transit times observed and the lack of dependency of mean transit time with blood flow was a feature of both experiment and model. The experimental mean transit time for xenon was 28 $\pm$ 2 minutes and according to the model it is 27 minutes (table 8.2). Since the difference is small compared to the uncertainties of experiment and model, the mathematical analogue appears to be valid for the diffusion of xenon. The model was then applied to the diffusion of water. The mean transit time for tritiated water by experiment was 30 $\pm$ 2 minutes and according to the model it is 28 minutes. These results also show good agreement between the model and experiment. From this it is concluded that the experimental results are consistent with the movement of water by diffusion.

The model may be extended to other situations where the experimental work is beyond the scope of the present thesis. For example, it may be applied to the rate of removal of the whole of the vitreous water by the choroid. This has been done by taking a uniform concentration throughout the vitreous and finding the time at which the average concentration in the vitreous is half of the initial value. The $T_{\frac{1}{2}}$ obtained by this method is approximately 20 minutes by the model.

The consistency of the results with a diffusional model does not prove that there were no other processes involved in the transfer of water. Some evidence has been presented for the existence of active transport of certain substances, such as organic anions, from the vitreous in vivo (Forbes and Becker, 1960). Moreover, in vitro experiments on the retinal pigment epithelium of frogs and toads have shown the likelihood of an active transport system within this layer (Lasansky and de Fisch, 1966; Steinberg and Miller, 1973; Miller and Steinberg, 1977). If the water molecules were actively transported

Table 8.2

Mean Transit Time (± S.E.)

Tracer	Experiment	Model
^{133}Xe	28 ± 2	27
$^{3}H_2O$	30 ± 2	28

at any stage, this was not the limiting factor under the conditions of the experiment.

The results have shown the extent of a diffusional-limited movement from the vitreous into the choroid. It is not yet known if the outward diffusion across the retina is matched by an equal inward diffusion along the same route. It may be, for example, that the pigment epithelium exhibits diode-like properties in which an easy passage in one direction is not matched in the opposite direction. The basis for this suggestion is as follows. Sodium ions are normally actively pumped from cells to maintain their correct osmotic concentration. Chloride ions follow the sodium ions and water follows, by diffusion, to maintain the ionic concentrations. However, retinal pigment epithelium cells from frogs have been shown in vitro to pump more sodium ions away from the retina than towards it (Miller and Steinberg, 1977). There is, therefore, a net transport of sodium ions, and perhaps also, by passive diffusion, of water molecules out in the direction from the retina towards the choroid. The associated movement of water is assisted by the basal infoldings of the pigment epithelium which may allow high salt concentrations to develop. The existence of tight junctions prevents inter-cellular passage of water, while the high lipid content of cell walls slows the normal unassisted diffusion of water. This proposed mechanism is consistent with the present experiments provided the limiting factor was elsewhere. This was probably diffusion through the vitreous. Such a hypothesis could be tested by introducing the isotope into the blood and measuring its rate of entry into the vitreous in an experiment which distinguishes entrance from the choroid from that which arrives anteriorly. The experiments of Kinsey et al (1942) failed to make this distinction. If such a net uni-directional movement exists, knowledge of its

mechanism could have important consequences in the understanding and treatment of retinal detachment and glaucoma.

Fluid flow across the retina has been proposed as a result of a hydrostatic pressure gradient (Fatt and Hedbys, 1970; Fatt and Shantinath, 1971). The proposed model has been shown in the present thesis to be inadequate. A better model has been developed which shows that the flow across the retina is different from that across the sclera. The magnitude and direction of the retinal flow is dependent on the pressure difference between the vitreous and the choroid. A pressure difference of less than 0.1 mm.Hg. could lead to a significant flow. The application of the model awaits the development of a sufficiently accurate measuring technique. It is, however, unlikely that a pressure difference exists across the retina. It is more probable that pressure is transmitted across the retina so that the pressure equalises on either side.

Another hydrostatic pressure-induced flow in the eye is the passage of aqueous humour from the anterior chamber into Schlemm's canal. Aqueous humour has been shown to enter the canal of Schlemm through pore openings in invaginations in the lining endothelium. The size and frequency of these pores were shown to vary with pressure (Grierson and Lee, 1975a) and also to increase after the administration of pilocarpine (Grierson et al, 1978).

A model had been proposed to calculate the conductance of the pore and pore-invagination (Bill and Svedbergh, 1972). This model, however, overestimated the pore resistance. New models have, therefore, been developed in the present thesis. A simple aperture model was considered, as well as a more complex model based on the geometry of a Venturi tube. The Venturi tube was considered to be the model of choice, since it most closely resembled the appearance

of pores in transmission electron micrographs. This showed that the pore contributed 12% and the pore-invagination 24% to the normal human outflow resistance. This implies that the main site of resistance in the normal human eye lies elsewhere. Studies are now being conducted to investigate the muco-polysaccharide content in the endothelial meshwork since the presence of such intercullalar material may offer appreciable resistance to fluid movement. The model also showed that the resistance of the pore was 17 times greater at 8 mm.Hg. in the Rhesus monkey than at 15 mm.Hg. The pressure dependancy of the pore resistance must therefore contribute to the stability of the intra-ocular pressure. Another result of the model is that pilocarpine has been shown to decrease the resistance through the pore by a factor of 7. The effect on pore resistance must therefore be at least a factor in the effectiveness of pilocarpine in the treatment of glaucoma. The use of the Venturi tube model should assist in the analysis of further experiments to determine the cause(s) of glaucoma and thus predict the effectiveness of different forms of treatment.

APPENDIX I

FORTRAN TEXT

```
C*****EYE MODEL IN CYLINDRICAL CO-ORDINATES, DIFFUSION FROM VITREOUS
C*****INTO SURROUNDING MEDIA, REMOVAL BY CHOROIDAL BLOOD FLOW
C*****INP IS INITIAL CENTRAL P CO-ORDINATE
C*****F IS BLOOD FLOW REMOVAL TERM
C*****TSTEP IS TIME INCREMENT, DSTEP IS DISTANCE INCREMENT
C*****D0 IS DIFFUSION COEFFICIENT OF SCLERA
C*****D1 IS DIFFUSION COEFFICIENT OF CHOROID + RETINA
C*****D2 IS DIFFUSION COEFFICIENT OF VITREOUS
C*****OUTPUT CONDITIONS: RMAX - PRINT BLOOD, MAX - FILE CON2,
C*****NAX - PRINT CON2
      INTEGER P,BN,BS,BE,BW,EXTRAP,Y,B,XX,EXL
      REAL MOS1,LI,LP,LL,LLL
      DIMENSION CON1(89,113),CON2(89,113)
      READ (5,71) RMAX,MAX,NAX
      READ (5,80) INP,F
      READ (5,4) TSTEP,DSTEP,D0,D1,D2
71    FORMAT(F5.1,I2,I2)
80    FORMAT(I2,F5.3)
4     FORMAT (F4.2,F5.3,3E8.2)
C*****SETS INITIAL DISTRIBUTION
      DO 261 I=1,89
      ISQ = (I-1)**2
      RI = I
      RISQ = (RI-1.0)**2
      DO 26 P=1,113
      LENS = ISQ+(P-143)**2
      LIMIT = ISQ+(P-89)**2
      IF((LIMIT.GT.7744).OR.(LENS.LT.3844))GO TO 26
      RP = P
      RLIM = RISQ+(RP-89.0)**2
      IF(RLIM.LT.6642.25) GO TO 23
      CON1(I,P) = 0.0
      GO TO 26
23    CON1(I,P) = 100.0
26    CONTINUE
261   CONTINUE
      WRITE(6,72)RMAX,MAX,NAX
      WRITE (6,81) INP,F
      WRITE (6,8) TSTEP,DSTEP,D0,D1,D2
72    FORMAT(//8H RMAX = ,F5.1,2X,7H MAX = ,I2,2X,7H NAX = ,I2)
81    FORMAT(7H INP = ,I2,5H F = ,F5.3)
8     FORMAT (9H TSTEP = ,F4.2,5H(SEC),/,9H DSTEP = ,F5.3,4H(CM),/,6H D0
     1 = ,E8.2,11H(CM**2/SEC),/,6H D1 = ,E8.2,11H(CM**2/SEC),/,6H D2 = ,
     2E8.2,11H(CM**2/SEC))
C*****PRINTS INITIAL DISTRIBUTION
      DO 24 I=1,89
      RI = I
      RISQ = (RI-1.0)**2
      X = SQRT(7744.0-RISQ)
      XX = INT(X)
      Y = 89-XX
      IF (I.GE.56) GO TO 6
      A = SQRT(3844.0-RISQ)
      AA = 143.0-A
      B = INT(AA)
      GO TO 7
```

```
6     IF (I.GE.86)GO TO 9
      B = 113
      GO TO 7
9     B = 89+XX
7     WRITE (6,57)I,Y
57    FORMAT (/,5H I = ,I2,13H P STARTS AT ,I2)
      WRITE (6,31) (CON1(I,P),P=Y,B)
31    FORMAT (20F6.1)
24    CONTINUE
      R0 = (TSTEP*D0)/DSTEP**2
      R1 = (TSTEP*D1)/DSTEP**2
      R2 = (TSTEP*D2)/DSTEP**2
      FF = 1.0-F
      BLOOD = 0.0
      MOS1 = 0.0
      MOS2 = 0
      N = 0
40    MOS1 = MOS1+TSTEP
C*****CALCULATION OF POINTS ON Z-AXIS
      DO 3 P=2,3
      CON2(1,P) = (1.0-4.0*R0)*CON1(1,P)+R0*(2.0*CON1(2,P)+CON1(1,P+1)+C
     1ON1(1,P-1))
3     CONTINUE
      DO 5 P=5,6
      CON2(1,P) = (1.0-4.0*R1)*CON1(1,P)+R1*(2.0*CON1(2,P)+CON1(1,P+1)+C
     1ON1(1,P-1))
5     CONTINUE
      DO 12 P=8,80
      CON2(1,P) = (1.0-4.0*R2)*CON1(1,P)+R2*(2.0*CON1(2,P)+CON1(1,P+1)+C
     1ON1(1,P-1)
12    CONTINUE
C*****CALCULATION OF OTHER POINTS
      DO 131 I=2,89
      ISQ = (I-1)**2
      RI = I
      RISQ = (RI-1.0)**2
      ISQN = I**2
      ISQS = (I-2)**2
      DO 13 P=1,112
      LIMIT = ISQ+(P-89)**2
      RP = P
      RLIM = RISQ+(RP-89.0)**2
      IF((LIMIT.GT.7744).OR.(RLIM.LT.7310.25))GO TO 15
      BN = ISQN+(P-89)**2
      BS = ISQS+(P-89)**2
      BE = ISQ+(P-88)**2
      BW = ISQ+(P-90)**2
      IF(BN.GT.7744.OR.BS.GT.7744.OR.BE.GT.7744.OR.BW.GT.7744)GO TO 13
      CON2(I,P) = (1.0-4.0*R0)*CON1(I,P)+R0*((1.0+0.5/RI)*CON1(I+1,P)+(1
     1.0-0.5/RI)*CON1(I-1,P)+CON1(I,P+1)+CON1(I,P-1))
      GO TO 13
15    IF ((RLIM.GE.7140.25).OR.(RLIM.LT.6806.25))GO TO 16
      CON2(I,P) = (1.0-4.0*R1)*CON1(I,P)+R1*((1.0+0.5/RI)*CON1(I+1,P)+(1
     1.0-0.5/RI)*CON1(I-1,P)+CON1(I,P+1)+CON1(I,P-1))
      GO TO 13
16    LENS = ISQ+(P-143)**2
      IF((RLIM.GE.6642.25).OR.(LENS.LT.3969)) GO TO 13
      CON2(I,P) = (1.0-4.0*R2)*CON1(I,P)+R2*((1.0+0.5/RI)*CON1(I+1,P)+(1
     1.0-0.5/RI)+CON1(I-1,P)+CON1(I,P+1)+CON1(I,P-1))
13    CONTINUE
131   CONTINUE
```

```
C*****CALCULATION OF BOUNDARY POINTS
      DO 171 I=1,89
      ISQ = (I-1)**2
      RI = I
      RISQ = (RI-1.0)**2
      LI = RI-1.0
      DO 17 P=1,112
      RP = P
      RLIM = RISQ+(RP-89.0)**2
      IF((RLIM.GE.7310.25).OR.(RLIM.LT.7140.25))GO TO 33
      IF (I.GT.1)GO TO 28
      CON2(I,P) = (D1*CON1(I,P+1)+D0*CON1(I,P-1))/(D0+D1)
      GO TO 17
28    IF (P.EQ.89) GO TO 21
      LP = ABS(RP-89.0)
      LL = LI/LP
      LLL = (1.0-LL)
      EXTRAP = ISQ-(P-89)**2
      IF(EXTRAP)29,29,19
29    CON2(I,P) = (D1*(LL*CON1(I-1,P-1)+LLL*CON1(I,P-1))+D0*(LL*CON1(I+1
     1,P-1)+LLL*CON1(I,P+1)))/(D0+D1)
      GO TO 17
19    IF (P.GT.89)GO TO 27
20    CON2(I,P) = (D1*(CON1(I-1,P+1)/LL-LLL*CON1(I-1,P)/LL)+D0*(CON1(I+1
     1,P-1)/LL-LLL*CON1(I+1,P)/LL))/(D0+D1)
      GO TO 17
21    CON2(I,P) = (D1*CON1(I-1,P)+D0*CON1(I+1,P))/D0+D1)
      GO TO 17
27    CON2(I,P) = (D1*(CON1(I-1,P-1)/LL-LLL*CON1(I-1,P)/LL)+D0*(CON1(I+1
     1,P+1)/LL-LLL*CON1(I+1,P)/LL))/(D0+D1)
      GO TO 17
33    IF((RLIM.GE.6806.25).OR.(RLIM.LT.6642.25))GO TO 17
      IF(I.GT.1)GO TO 34
      CON2(I,P) = (D2*CON1(I,P+1)+D1*CON1(I,P-1))/(D1+D2)
      GO TO 17
34    IF (P.EQ.89)GO TO 38
      LP = ABS(RP-89.0)
      LL = LI/LP
      LLL = (1.0-LL)
      EXTRAP = ISQ-(P-89)**2
      IF(EXTRAP)35,35,36
35    CON2(I,P) = (D2*(LL*CON1(I-1,P-1)+LLL*CON1(I,P-1))+D1*(LL*CON1(I+1
     1,P-1)+LLL*CON1(I,P+1)))/(D1+D2)
      GO TO 17
36    IF (P.GT.89) GO TO 39
37    CON2(I,P) = (D2*(CON1(I-1,P+1)/LL-LLL*CON1(I-1,P)/LL)+D1*(CON1(I+1
     1,P-1)/LL-LLL*CON1(I+1,P)/LL))/(D1+D2)
      GO TO 17
38    CON2(I,P) = (D2*CON1(I-1,P)+D1*CON1(I+1,P))/(D1+D2)
      GO TO 17
39    CON2(I,P) = (D2*(CON1(I-1,P-1)/LL-LLL*CON1(I-1,P)/LL)+D1*(CON1(I+1
     1,P+1)/LL-LLL*CON1(I+1,P)/LL))/(D1+D2)
17    CONTINUE
171   CONTINUE
C*****CALCULATION OF SCLERAL EDGE POINTS
      DO 411 I=1,89
      ISQ = (I-1)**2
      ISQN = I**2
      ISQS = (I-2)**2
      DO 41 P=1,112
      LIMIT = ISQ+(P-89)**2
      IF(LIMIT.GT.7744)GO TO 41
```

```
      BN = ISQN+(P-89)**2
      BS = ISQS+(P-89)**2
      BE = ISQ+(P-88)**2
      BW = ISQ+(P-90)**2
      IF(BN.LE.7744.AND.BS.LE.7744.AND.BE.LE.7744.AND.BW.LE.7744)GO TO 4
     11
      EXTRAP = ISQ-(P-89)**2
      IF(EXTRAP)42,42,43
42    CON2(I,P) = 2.0*CON2(I,P+1)-CON2(I,P+2)
      GO TO 53
43    CON2(I,P) = 2.0*CON2(I-1,P)-CON2(I-2,P)
53    IF(CON2(I,P))52,41,41
52    CON2(I,P) = 0.0
41    CONTINUE
411   CONTINUE
C*****CALCULATION OF ANTERIOR EDGE POINTS
      DO 44 I=56,85
      CON2(I,113) = 2.0*CON2(I,112)-CON2(I,111)
      IF(CON2(I,113))51,44,44
51    CON2(I,113) = 0.0
44    CONTINUE
C*****CALCULATION OF LENTICULAR EDGE POINTS
      DO 451 I=1,55
      ISQ = (I-1)**2
      DO 45 P=1,112
      LENS + ISQ+(P-143)**2
      IF(LENS.GE.3969.OR.LENS.LT.3844)GO TO 45
      EXL = ISQ-(P-143)**2
      IF(EXL)46,46,47
46    CON2(I,P) = 2.0*CON2(I,P-1)-CON2(I,P-2)
      GO TO 48
47    CON2(I,P) = 2.0*CON2(I+1,P)-CON2(I+2,P)
48    IF(CON2(I,P))49,45,45
49    CON2(I,P) = 0.0
45    CONTINUE
451   CONTINUE
C*****BLOOD FLOW REMOVAL
      DO 551 I=1,89
      RI = I
      RISQ = (RI-1.0)**2
      DO 55 P=1,113
      RP = P
      RLIM = RISQ+(RP-89.0)**2
      IF((RLIM.GE.7140.25).OR.(RLIM.LT.6972.25))GO TO 55
      BLOOD = BLOOD+F*CON2(I,P)
      CON2(I,P) = FF*CON2(I,P)
55    CONTINUE
551   CONTINUE
      IF(MOS1.LT.RMAX)GO TO 69
      MOS2 = 1+MOS2
      RMOS2 = MOS2
      RMOS3 = RMOS2+MOS1/60.0
      WRITE (6,32) RMOS3,BLOOD
32    FORMAT (//8H TIME = ,F5.1,5H(MIN),5X,9H BLOOD = ,E9.3)
C*****OUTPUT CONDITIONS
      N = N+1
      IF(N.LT.NAX)GO TO 54
      N = 0
      DO 54 I=1,89
      RI = I
      RISQ = (RI-1.0)**2
```

```
      X = SQRT(7744.0-RISQ)
      XX = INT(X)
      Y = 89-XX
      IF(I.GE.56)GO TO 10
      A = SQRT(3844.0-RISQ)
      AA = 143.0-A
      B = INT(AA)
      GO TO 11
10    IF(I.GE.86)GO TO 14
      B = 113
      GO TO 11
14    B = 89+XX
11    WRITE(6,58)I,Y
58    FORMAT (/,5H I = ,I2,13H P STARTS AT ,I2)
      WRITE (6,56) (CON2(I,P),P=Y,B)
56    FORMAT (20F6.1)
      IF(MOS2.LT.MAX)GO TO 54
      DO 70 P=Y,B
      WRITE(8,73)I,P,CON2(I,P)
73    FORMAT(I2,I3,E12.6)
70    CONTINUE
54    CONTINUE
      MOS1 = 0.0
      BLOOD = 0.0
69    DO 50 I=1,89
      DO 50 P=1,113
50    CON1(I,P) = CON2(I,P)
      IF(MOS2.LT.MAX)GO TO 40
      WRITE (6,22) R0,R1,R2
22    FORMAT (//,6H R0 = ,E12.5,/,6H R1 = ,E12.5,/,6H R2 = ,E12.5)
      STOP
      END
```

APPENDIX 2

Partial pressure distribution at nodal points in eye for diffusion of xenon from the vitreous with removal in choroidal blood flow.

Partial pressure = 100 within initial distribution and 0 elsewhere.

Initial mid-point p-value = 37. Normal blood flow.

Time = 20 min.

Results are presented with points having the same I-value grouped together (I = 1 is along z-axis) starting with the scleral points and moving towards the front of the eye (see fig. 4.10).

I = 1 P STARTS AT 1

0.1	0.1	0.2	0.2	0.3	1.2	2.4	3.2	4.2	5.4	6.6	7.8	9.0	10.2	11.4	12.6	13.8	15.0	16.1	17.3
18.4	19.4	20.5	21.4	22.4	23.2	24.0	24.8	25.5	26.1	26.6	27.1	27.5	27.8	28.0	28.2	28.3	28.3	28.2	28.0
27.8	27.4	27.1	26.6	26.1	25.5	24.9	24.2	23.5	22.7	21.9	21.0	20.2	19.3	18.4	17.5	16.6	15.7	14.8	13.9
13.0	12.2	11.3	10.5	9.7	8.9	8.2	7.5	6.8	6.1	5.5	4.9	4.3	3.7	3.1	2.6	2.1	1.6	1.1	0.5
0.0																			

I = 2 P STARTS AT 2

0.1	0.2	0.3	0.3	1.1	1.9	3.0	4.2	5.4	6.5	7.7	9.0	10.2	11.4	12.6	13.8	14.9	16.1	17.2	18.3
19.4	20.4	21.4	22.3	23.2	24.0	24.7	25.4	26.0	26.6	27.0	27.4	27.7	28.0	28.1	28.2	28.2	28.1	27.9	27.7
27.4	27.0	26.5	26.0	25.4	24.8	24.1	23.4	22.6	21.8	21.0	20.1	19.3	18.4	17.5	16.6	15.7	14.8	13.9	13.0
12.1	11.3	10.5	9.7	8.9	8.2	7.5	6.8	6.1	5.5	4.9	4.3	3.7	3.1	2.6	2.1	1.6	1.1	0.5	0.0

I = 3 P STARTS AT 2

0.1	0.2	0.3	0.3	1.0	1.8	2.9	4.1	5.3	6.5	7.7	8.9	10.1	11.3	12.5	13.7	14.8	16.0	17.1	18.2
19.3	20.3	21.2	22.2	23.0	23.8	24.6	25.3	25.9	26.4	26.9	27.3	27.6	27.8	28.0	28.0	28.0	27.9	27.8	27.5
27.2	26.8	26.4	25.9	25.3	24.7	24.0	23.3	22.5	21.7	20.9	20.0	19.1	18.3	17.4	16.5	15.6	14.7	13.8	12.9
12.1	11.2	10.4	9.6	8.9	8.1	7.4	6.7	6.1	5.4	4.8	4.2	3.7	3.1	2.6	2.1	1.6	1.1	0.6	0.1

I = 4 P STARTS AT 2

0.2	0.2	0.3	0.3	1.0	1.7	2.9	4.0	5.2	6.4	7.6	8.8	10.0	11.2	12.4	13.5	14.7	15.8	17.0	18.0
19.1	20.1	21.1	22.0	22.8	23.6	24.4	25.0	25.6	26.2	26.6	27.0	27.3	27.6	27.7	27.8	27.8	27.7	27.5	27.3
27.0	26.6	26.2	25.6	25.1	24.5	23.8	23.1	22.3	21.5	20.7	19.8	19.0	18.1	17.2	16.3	15.4	14.6	13.7	12.8
12.0	11.1	10.3	9.6	8.8	8.1	7.4	6.7	6.0	5.4	4.8	4.2	3.6	3.1	2.6	2.1	1.6	1.1	0.6	0.1

I = 5 P STARTS AT 2

0.2	0.2	0.3	0.3	1.0	1.6	2.8	3.9	5.1	6.3	7.4	8.6	9.8	11.0	12.2	13.4	14.5	15.6	16.7	17.8
18.9	19.8	20.8	21.7	22.6	23.4	24.1	24.8	25.4	25.9	26.3	26.7	27.0	27.3	27.4	27.5	27.5	27.4	27.2	27.0
26.7	26.3	25.9	25.4	24.8	24.2	23.5	22.8	22.1	21.3	20.5	19.6	18.8	17.9	17.0	16.1	15.3	14.4	13.5	12.7
11.8	11.0	10.2	9.4	8.7	8.0	7.3	6.6	6.0	5.3	4.7	4.2	3.6	3.1	2.6	2.0	1.5	1.1	0.6	0.1

I = 6 P STARTS AT 2

0.2	0.2	0.2	0.3	0.9	1.6	2.7	3.8	4.9	6.1	7.3	8.5	9.6	10.8	12.0	13.1	14.3	15.4	16.5	17.5
18.6	19.6	20.5	21.4	22.2	23.0	23.7	24.4	25.0	25.5	26.0	26.4	26.7	26.9	27.0	27.1	27.1	27.0	26.8	26.6
26.3	25.9	25.5	25.0	24.4	23.8	23.2	22.5	21.7	21.0	20.2	19.3	18.5	17.6	16.8	15.9	15.0	14.2	13.3	12.5
11.7	10.9	10.1	9.3	8.6	7.9	7.2	6.5	5.9	5.3	4.7	4.1	3.6	3.0	2.5	2.0	1.5	1.1	0.6	0.1

I = 7 P STARTS AT 2

0.2	0.2	0.2	0.2	0.9	1.5	2.6	3.7	4.8	5.9	7.1	8.2	9.4	10.6	11.7	12.9	14.0	15.1	16.2	17.2
18.2	19.2	20.1	21.0	21.9	22.6	23.3	24.0	24.6	25.1	25.5	25.9	26.2	26.4	26.6	26.6	26.6	26.6	26.4	26.2
25.9	25.5	25.1	24.6	24.0	23.4	22.8	22.1	21.4	20.6	19.8	19.0	18.2	17.3	16.5	15.6	14.8	13.9	13.1	12.3
11.5	10.7	9.9	9.2	8.4	7.7	7.1	6.4	5.8	5.2	4.6	4.0	3.5	3.0	2.5	2.0	1.5	1.1	0.6	0.1

I = 8 P STARTS AT 2

0.2	0.2	0.2	0.2	0.8	1.4	2.4	3.5	4.6	5.7	6.9	8.0	9.2	10.3	11.5	12.6	13.7	14.8	15.8	16.9
17.9	18.8	19.7	20.6	21.4	22.2	22.9	23.5	24.1	24.6	25.0	25.4	25.7	25.9	26.1	26.1	26.1	26.0	25.9	25.7
25.4	25.0	24.6	24.1	23.6	23.0	22.4	21.7	21.0	20.2	19.4	18.7	17.8	17.0	16.2	15.3	14.5	13.7	12.9	12.0
11.2	10.5	9.7	9.0	8.3	7.6	6.9	6.3	5.7	5.1	4.5	4.0	3.5	2.9	2.5	2.0	1.5	1.1	0.6	0.1

I = 9 P STARTS AT 2

0.3	0.2	0.2	0.2	0.7	1.2	2.2	3.3	4.4	5.5	6.6	7.8	8.9	10.0	11.1	12.3	13.3	14.4	15.5	16.5
17.4	18.4	19.3	20.1	20.9	21.7	22.4	23.0	23.6	24.1	24.5	24.9	25.1	25.4	25.5	25.6	25.6	25.5	25.3	25.1
24.8	24.5	24.1	23.6	23.1	22.5	21.9	21.2	20.5	19.8	19.0	18.2	17.4	16.6	15.8	15.0	14.2	13.4	12.6	11.8
11.0	10.2	9.5	8.8	8.1	7.4	6.8	6.1	5.5	5.0	4.4	3.9	3.4	2.9	2.4	2.0	1.5	1.1	0.6	0.2

I = 10 P STARTS AT 2

0.3	0.3	0.2	0.2	0.6	1.1	2.0	3.0	4.1	5.2	6.4	7.5	8.6	9.7	10.8	11.9	13.0	14.0	15.0	16.0
17.0	17.9	18.8	19.6	20.4	21.1	21.8	22.4	23.0	23.5	23.9	24.2	24.5	24.7	24.9	24.9	24.9	24.9	24.7	24.5
24.2	23.9	23.5	23.0	22.5	21.9	21.3	20.7	20.0	19.3	18.6	17.8	17.0	16.2	15.4	14.6	13.8	13.0	12.3	11.5
10.7	10.0	9.3	8.6	7.9	7.2	6.6	6.0	5.4	4.9	4.3	3.8	3.3	2.8	2.4	1.9	1.5	1.1	0.6	0.2

I = 11 P STARTS AT 2

0.3	0.3	0.3	0.3	0.3	1.0	1.6	2.8	3.9	5.0	6.1	7.2	8.3	9.4	10.4	11.5	12.6	13.6	14.6	15.6
16.5	17.4	18.2	19.1	19.8	20.5	21.2	21.8	22.3	22.8	23.2	23.6	23.9	24.1	24.2	24.3	24.3	24.2	24.0	23.8
23.6	23.2	22.8	22.4	21.9	21.3	20.8	20.1	19.5	18.8	18.1	17.3	16.6	15.8	15.0	14.2	13.5	12.7	11.9	11.2
10.4	9.7	9.0	8.3	7.7	7.0	6.4	5.8	5.3	4.7	4.2	3.7	3.2	2.8	2.3	1.9	1.5	1.1	0.7	0.2

I = 12 P STARTS AT 2

0.3	0.3	0.3	0.3	0.3	0.9	1.4	2.5	3.6	4.7	5.8	6.9	7.9	9.0	10.1	11.1	12.1	13.1	14.1	15.0
16.0	16.8	17.7	18.5	19.2	19.9	20.6	21.1	21.7	22.1	22.5	22.9	23.1	23.3	23.5	23.6	23.5	23.5	23.3	23.1
22.9	22.5	22.2	21.7	21.2	20.7	20.1	19.5	18.9	18.2	17.5	16.8	16.1	15.3	14.6	13.8	13.1	12.3	11.6	10.8
10.1	9.4	8.7	8.1	7.4	6.8	6.2	5.7	5.1	4.6	4.1	3.6	3.2	2.7	2.3	1.9	1.5	1.1	0.7	0.3

I = 13 P STARTS AT 2

0.3	0.3	0.3	0.2	0.2	0.8	1.3	2.3	3.4	4.4	5.5	6.5	7.6	8.6	9.7	10.7	11.7	12.6	13.6	14.5
15.4	16.3	17.1	17.9	18.6	19.3	19.9	20.4	21.0	21.4	21.8	22.1	22.4	22.6	22.7	22.8	22.8	22.7	22.6	22.4
22.1	21.8	21.4	21.0	20.6	20.0	19.5	18.9	18.3	17.6	16.9	16.3	15.5	14.8	14.1	13.4	12.6	11.9	11.2	10.5
9.8	9.1	8.5	7.8	7.2	6.6	6.0	5.5	5.0	4.5	4.0	3.5	3.1	2.6	2.2	1.8	1.4	1.1	0.7	0.3
0.0																			

I = 14 P STARTS AT 2

0.3	0.3	0.3	0.2	0.2	0.7	1.2	2.1	3.1	4.2	5.2	6.2	7.2	8.2	9.2	10.2	11.2	12.1	13.1	14.0
14.8	15.7	16.5	17.2	17.9	18.6	19.2	19.7	20.2	20.7	21.0	21.4	21.6	21.8	21.9	22.0	22.0	21.9	21.8	21.6
21.4	21.1	20.7	20.3	19.8	19.3	18.8	18.2	17.6	17.0	16.4	15.7	15.0	14.3	13.6	12.9	12.2	11.5	10.8	10.1
9.4	8.8	8.2	7.5	6.9	6.4	5.8	5.3	4.8	4.3	3.8	3.4	3.0	2.6	2.2	1.8	1.4	1.1	0.7	0.4
0.0																			

I = 15 P STARTS AT 3

0.3	0.3	0.2	0.2	0.6	1.0	1.9	2.9	3.9	4.9	5.9	6.8	7.8	8.8	9.8	10.7	11.6	12.5	13.4	14.2
15.0	15.8	16.5	17.2	17.8	18.4	19.0	19.4	19.9	20.2	20.5	20.8	21.0	21.1	21.2	21.2	21.1	21.0	20.8	20.6
20.3	19.9	19.5	19.1	18.6	18.1	17.6	17.0	16.4	15.7	15.1	14.4	13.8	13.1	12.4	11.7	11.1	10.4	9.7	9.1
8.5	7.9	7.3	6.7	6.1	5.6	5.1	4.6	4.1	3.7	3.3	2.9	2.5	2.1	1.7	1.4	1.1	0.7	0.4	0.1

I = 16 P STARTS AT 3

0.3	0.3	0.2	0.2	0.5	0.8	1.6	2.6	3.6	4.5	5.5	6.5	7.4	8.4	9.3	10.2	11.1	12.0	12.8	13.6
14.4	15.1	15.8	16.5	17.1	17.7	18.2	18.7	19.1	19.4	19.7	20.0	20.1	20.3	20.3	20.3	20.3	20.1	20.0	19.7
19.5	19.1	18.8	18.3	17.9	17.4	16.9	16.3	15.7	15.1	14.5	13.9	13.2	12.6	11.9	11.3	10.6	10.0	9.3	8.7
8.1	7.5	7.0	6.4	5.9	5.4	4.9	4.4	4.0	3.6	3.2	2.8	2.4	2.0	1.7	1.4	1.1	0.7	0.4	0.1

I = 17 P STARTS AT 3

0.3	0.3	0.2	0.2	0.3	0.7	1.2	2.3	3.2	4.2	5.1	6.1	7.0	7.9	8.8	9.7	10.5	11.4	12.2	13.0
13.7	14.4	15.1	15.8	16.4	16.9	17.4	17.8	18.2	18.6	18.9	19.1	19.3	19.4	19.4	19.4	19.4	19.3	19.1	18.9
18.6	18.3	18.0	17.6	17.1	16.6	16.1	15.6	15.0	14.5	13.9	13.3	12.6	12.0	11.4	10.8	10.2	9.5	8.9	8.3
7.8	7.2	6.7	6.1	5.6	5.2	4.7	4.2	3.8	3.4	3.0	2.7	2.3	2.0	1.6	1.3	1.0	0.8	0.5	0.2
0.0																			

I = 18 P STARTS AT 3

0.3	0.3	0.2	0.2	0.2	0.6	1.1	2.0	2.9	3.9	4.8	5.7	6.6	7.4	8.3	9.2	10.0	10.8	11.6	12.3
13.1	13.8	14.4	15.0	15.6	16.1	16.6	17.0	17.4	17.7	18.0	18.2	18.4	18.5	18.6	18.6	18.5	18.4	18.2	18.0
17.8	17.5	17.1	16.8	16.3	15.9	15.4	14.9	14.4	13.8	13.2	12.7	12.1	11.5	10.9	10.3	9.7	9.1	8.5	8.0
7.4	6.9	6.4	5.9	5.4	4.9	4.5	4.1	3.6	3.3	2.9	2.5	2.2	1.9	1.6	1.3	1.0	0.8	0.5	0.2
0.0																			

I = 19 P STARTS AT 3

0.3	0.3	0.2	0.2	0.2	0.6	0.9	1.8	2.7	3.5	4.4	5.3	6.1	7.0	7.8	8.6	9.4	10.2	11.0	11.7
12.4	13.1	13.7	14.3	14.8	15.3	15.8	16.2	16.6	16.9	17.1	17.4	17.5	17.6	17.7	17.7	17.6	17.5	17.4	17.2
16.9	16.6	16.3	16.0	15.6	15.1	14.7	14.2	13.7	13.1	12.6	12.0	11.5	10.9	10.3	9.8	9.2	8.7	8.1	7.6
7.1	6.5	6.1	5.6	5.1	4.7	4.3	3.9	3.5	3.1	2.8	2.4	2.1	1.8	1.5	1.3	1.0	0.8	0.5	0.3
0.0																			

I = 20 P STARTS AT 4

0.3	0.2	0.2	0.1	0.5	0.8	1.6	2.4	3.2	4.0	4.9	5.7	6.5	7.3	8.1	8.9	9.6	10.4	11.0	11.7
12.4	13.0	13.5	14.0	14.5	15.0	15.4	15.7	16.0	16.3	16.5	16.6	16.7	16.8	16.8	16.7	16.6	16.5	16.3	16.1
15.8	15.5	15.2	14.8	14.4	13.9	13.5	13.0	12.5	12.0	11.4	10.9	10.4	9.8	9.3	8.8	8.2	7.7	7.2	6.7
6.2	5.7	5.3	4.9	4.4	4.0	3.7	3.3	3.0	2.6	2.3	2.0	1.7	1.5	1.2	1.0	0.7	0.5	0.3	0.1

I = 21 P STARTS AT 4

0.3	0.2	0.2	0.1	0.3	0.6	1.3	2.1	2.9	3.7	4.5	5.3	6.1	6.8	7.6	8.3	9.0	9.7	10.4	11.0
11.7	12.2	12.8	13.3	13.7	14.2	14.5	14.9	15.2	15.4	15.6	15.7	15.8	15.9	15.9	15.8	15.8	15.6	15.4	15.2
15.0	14.7	14.3	14.0	13.6	13.2	12.7	12.3	11.8	11.3	10.8	10.3	9.8	9.3	8.8	8.3	7.8	7.3	6.8	6.3
5.9	5.4	5.0	4.6	4.2	3.8	3.5	3.1	2.8	2.5	2.2	1.9	1.7	1.4	1.2	1.0	0.7	0.5	0.3	0.1
0.0																			

I = 22 P STARTS AT 4

0.2	0.2	0.2	0.2	0.2	0.5	0.9	1.7	2.5	3.3	4.1	4.8	5.6	6.3	7.1	7.8	8.5	9.1	9.8	10.4
11.0	11.5	12.0	12.5	12.9	13.3	13.7	14.0	14.3	14.5	14.7	14.9	14.9	15.0	15.0	15.0	14.9	14.8	14.6	14.4
14.1	13.9	13.6	13.2	12.8	12.4	12.0	11.6	11.2	10.7	10.2	9.7	9.3	8.8	8.3	7.8	7.3	6.9	6.4	6.0
5.5	5.1	4.7	4.3	4.0	3.6	3.3	3.0	2.7	2.4	2.1	1.8	1.6	1.4	1.1	0.9	0.7	0.5	0.4	0.2
0.0																			

I = 23 P STARTS AT 4

0.2	0.2	0.2	0.1	0.1	0.4	0.7	1.4	2.2	2.9	3.7	4.4	5.1	5.9	6.6	7.2	7.9	8.5	9.1	9.7
10.3	10.8	11.3	11.7	12.2	12.5	12.9	13.2	13.5	13.7	13.8	14.0	14.1	14.1	14.1	14.1	14.0	13.9	13.7	13.5
13.3	13.1	12.8	12.4	12.1	11.7	11.3	10.9	10.5	10.1	9.6	9.2	8.7	8.3	7.8	7.4	6.9	6.5	6.0	5.6
5.2	4.8	4.5	4.1	3.7	3.4	3.1	2.8	2.5	2.2	2.0	1.7	1.5	1.3	1.1	0.9	0.7	0.5	0.4	0.2
0.0	0.0																		

I = 24 P STARTS AT 5

0.2	0.2	0.1	0.1	0.3	0.5	1.1	1.9	2.6	3.3	4.0	4.7	5.4	6.1	6.7	7.3	7.9	8.5	9.1	9.6
10.1	10.6	11.0	11.4	11.8	12.1	12.4	12.6	12.8	13.0	13.1	13.2	13.3	13.3	13.2	13.2	13.0	12.9	12.7	12.5
12.3	12.0	11.7	11.4	11.0	10.6	10.3	9.9	9.5	9.0	8.6	8.2	7.8	7.3	6.9	6.5	6.1	5.7	5.3	4.9
4.5	4.2	3.8	3.5	3.2	2.9	2.6	2.4	2.1	1.9	1.6	1.4	1.2	1.0	0.9	0.7	0.5	0.4	0.2	0.1
0.0																			

I = 25 P STARTS AT 5

0.2	0.1	0.1	0.1	0.1	0.5	0.8	1.5	2.2	2.9	3.6	4.3	4.9	5.6	6.2	6.8	7.4	7.9	8.4	8.9
9.4	9.9	10.3	10.6	11.0	11.3	11.6	11.8	12.0	12.2	12.3	12.4	12.4	12.4	12.4	12.3	12.2	12.1	11.9	11.7
11.5	11.2	10.9	10.6	10.3	10.0	9.6	9.2	8.9	8.5	8.1	7.7	7.3	6.9	6.5	6.1	5.7	5.3	4.9	4.6
4.2	3.9	3.6	3.3	3.0	2.7	2.5	2.2	2.0	1.7	1.5	1.3	1.2	1.0	0.8	0.7	0.5	0.4	0.3	0.1
0.0																			

I = 26 P STARTS AT 5

0.2	0.1	0.1	0.1	0.1	0.4	0.6	1.3	1.9	2.6	3.2	3.9	4.5	5.1	5.7	6.2	6.8	7.3	7.8	8.3
8.7	9.2	9.6	9.9	10.2	10.5	10.8	11.0	11.2	11.4	11.5	11.5	11.6	11.6	11.6	11.5	11.4	11.3	11.1	10.9
10.7	10.5	10.2	9.9	9.6	9.3	9.0	8.6	8.3	7.9	7.5	7.2	6.8	6.4	6.0	5.7	5.3	5.0	4.6	4.3
4.0	3.7	3.4	3.1	2.8	2.5	2.3	2.1	1.8	1.6	1.4	1.3	1.1	0.9	0.8	0.6	0.5	0.4	0.3	0.2
0.1	0.0																		

I = 27 P STARTS AT 5

0.1	0.1	0.1	0.1	0.1	0.3	0.5	1.0	1.6	2.2	2.9	3.5	4.1	4.6	5.2	5.7	6.2	6.7	7.2	7.7
8.1	8.5	8.9	9.2	9.5	9.8	10.0	10.2	10.4	10.6	10.7	10.7	10.8	10.8	10.8	10.7	10.6	10.5	10.4	10.2
10.0	9.8	9.5	9.2	9.0	8.7	8.4	8.0	7.7	7.4	7.0	6.7	6.3	6.0	5.6	5.3	4.9	4.6	4.3	4.0
3.7	3.4	3.1	2.9	2.6	2.4	2.1	1.9	1.7	1.5	1.4	1.2	1.0	0.9	0.7	0.6	0.5	0.4	0.3	0.2
0.1	0.0																		

I = 28 P STARTS AT 6

0.1	0.1	0.1	0.1	0.2	0.4	0.6	1.3	1.9	2.5	3.1	3.6	4.2	4.7	5.2	5.7	6.2	6.6	7.1	7.5
7.8	8.2	8.5	8.8	9.1	9.3	9.5	9.7	9.8	9.9	10.0	10.0	10.0	10.0	9.9	9.9	9.8	9.6	9.5	9.3
9.1	8.8	8.6	8.3	8.0	7.8	7.5	7.1	6.8	6.5	6.2	5.9	5.5	5.2	4.9	4.6	4.3	4.0	3.7	3.4
3.2	2.9	2.7	2.4	2.2	2.0	1.8	1.6	1.4	1.3	1.1	1.0	0.8	0.7	0.6	0.5	0.4	0.3	0.2	0.1
0.0	0.0																		

I = 29 P STARTS AT 6

0.1	0.1	0.1	0.1	0.1	0.3	0.5	1.1	1.6	2.2	2.7	3.2	3.8	4.3	4.8	5.2	5.7	6.1	6.5	6.9
7.2	7.6	7.9	8.1	8.4	8.6	8.8	8.9	9.1	9.2	9.2	9.3	9.3	9.3	9.2	9.1	9.0	8.9	8.8	8.6
8.4	8.2	8.0	7.7	7.5	7.2	6.9	6.6	6.3	6.0	5.7	5.4	5.1	4.8	4.5	4.2	4.0	3.7	3.4	3.2
2.9	2.7	2.5	2.2	2.0	1.8	1.7	1.5	1.3	1.2	1.0	0.9	0.8	0.7	0.6	0.5	0.4	0.3	0.2	0.1
0.1	0.0																		

I = 30 P STARTS AT 6

0.1	0.1	0.1	0.1	0.1	0.2	0.4	0.8	1.3	1.8	2.4	2.9	3.4	3.8	4.3	4.7	5.2	5.6	5.9	6.3
6.6	6.9	7.2	7.5	7.7	7.9	8.1	8.2	8.4	8.5	8.5	8.6	8.6	8.5	8.5	8.4	8.3	8.2	8.1	7.9
7.8	7.6	7.3	7.1	6.9	6.6	6.4	6.1	5.8	5.6	5.3	5.0	4.7	4.5	4.2	3.9	3.7	3.4	3.2	2.9
2.7	2.5	2.3	2.1	1.9	1.7	1.5	1.4	1.2	1.1	1.0	0.8	0.7	0.6	0.5	0.4	0.3	0.3	0.2	0.1
0.1	0.0	0.0																	

I = 31 P STARTS AT 7

0.1	0.1	0.1	0.1	0.1	0.3	0.5	1.0	1.5	2.0	2.5	3.0	3.4	3.9	4.3	4.7	5.1	5.4	5.7	6.1
6.4	6.6	6.9	7.1	7.3	7.4	7.6	7.7	7.8	7.8	7.9	7.9	7.9	7.8	7.8	7.7	7.6	7.4	7.3	7.1
7.0	6.8	6.6	6.3	6.1	5.9	5.6	5.4	5.1	4.9	4.6	4.4	4.1	3.8	3.6	3.4	3.1	2.9	2.7	2.5
2.3	2.1	1.9	1.7	1.6	1.4	1.3	1.1	1.0	0.9	0.8	0.7	0.6	0.5	0.4	0.3	0.3	0.2	0.1	0.1
0.0	0.0																		

I = 32 P STARTS AT 7

0.1	0.1	0.1	0.1	0.1	0.2	0.3	0.7	1.2	1.7	2.2	2.6	3.0	3.5	3.8	4.2	4.6	4.9	5.2	5.5
5.8	6.0	6.3	6.5	6.7	6.8	6.9	7.0	7.1	7.2	7.2	7.2	7.2	7.2	7.1	7.1	7.0	6.8	6.7	6.6
6.4	6.2	6.0	5.8	5.6	5.4	5.2	4.9	4.7	4.5	4.2	4.0	3.8	3.5	3.3	3.1	2.9	2.7	2.5	2.3
2.1	1.9	1.7	1.6	1.4	1.3	1.2	1.0	0.9	0.8	0.7	0.6	0.5	0.5	0.4	0.3	0.3	0.2	0.1	0.1
0.1	0.0	0.0																	

I = 33 P STARTS AT 8

0.1	0.1	0.1	0.0	0.1	0.2	0.4	0.9	1.4	1.8	2.3	2.7	3.1	3.4	3.8	4.1	4.4	4.7	5.0	5.3
5.5	5.7	5.9	6.1	6.2	6.3	6.4	6.5	6.6	6.6	6.6	6.6	6.6	6.5	6.5	6.4	6.3	6.1	6.0	5.8
5.7	5.5	5.3	5.1	4.9	4.7	4.5	4.3	4.1	3.9	3.7	3.4	3.2	3.0	2.8	2.6	2.4	2.3	2.1	1.9
1.7	1.6	1.5	1.3	1.2	1.1	1.0	0.8	0.7	0.7	0.6	0.5	0.4	0.4	0.3	0.2	0.2	0.1	0.1	0.1
0.0	0.0																		

I = 34 P STARTS AT 8

0.1	0.1	0.1	0.1	0.1	0.2	0.3	0.7	1.1	1.6	2.0	2.3	2.7	3.1	3.4	3.7	4.0	4.3	4.5	4.8
5.0	5.2	5.4	5.5	5.7	5.8	5.9	5.9	6.0	6.0	6.0	6.0	6.0	6.0	5.9	5.8	5.7	5.6	5.5	5.3
5.2	5.0	4.9	4.7	4.5	4.3	4.1	3.9	3.7	3.5	3.3	3.1	2.9	2.8	2.6	2.4	2.2	2.1	1.9	1.7
1.6	1.5	1.3	1.2	1.1	1.0	0.9	0.8	0.7	0.6	0.5	0.5	0.4	0.3	0.3	0.2	0.2	0.1	0.1	0.1
0.0	0.0	0.0																	

I = 35 P STARTS AT 8

0.1	0.1	0.1	0.0	0.0	0.1	0.2	0.5	0.9	1.3	1.7	2.0	2.4	2.7	3.0	3.3	3.6	3.8	4.1	4.3
4.5	4.7	4.9	5.0	5.1	5.2	5.3	5.4	5.4	5.5	5.5	5.5	5.5	5.4	5.4	5.3	5.2	5.1	5.0	4.9
4.7	4.6	4.4	4.3	4.1	3.9	3.7	3.6	3.4	3.2	3.0	2.9	2.7	2.5	2.3	2.2	2.0	1.9	1.7	1.6
1.5	1.3	1.2	1.1	1.0	0.9	0.8	0.7	0.6	0.5	0.5	0.4	0.4	0.3	0.3	0.2	0.2	0.1	0.1	0.1
0.0	0.0	0.0	0.0																

0.0	0.0	0.0	0.0	0.1	0.2	0.3	0.7	1.0	1.4	1.7	2.0	2.4	2.6	2.9	3.2	3.4	3.7	3.9	4.1
4.2	4.4	4.5	4.6	4.7	4.8	4.9	4.9	5.0	5.0	5.0	5.0	4.9	4.9	4.8	4.7	4.6	4.5	4.4	4.3
4.2	4.0	3.9	3.7	3.6	3.4	3.2	3.1	2.9	2.8	2.6	2.4	2.3	2.1	2.0	1.8	1.7	1.6	1.4	1.3
1.2	1.1	1.0	0.9	0.8	0.7	0.6	0.6	0.5	0.4	0.4	0.3	0.3	0.2	0.2	0.2	0.1	0.1	0.1	0.1
0.0	0.0	0.0																	

I = 37 P STARTS AT 9

0.0	0.0	0.0	0.0	0.0	0.1	0.2	0.5	0.8	1.1	1.4	1.8	2.0	2.3	2.6	2.8	3.0	3.3	3.5	3.6
3.8	3.9	4.1	4.2	4.3	4.4	4.4	4.5	4.5	4.5	4.5	4.5	4.4	4.4	4.3	4.3	4.2	4.1	4.0	3.9
3.8	3.6	3.5	3.4	3.2	3.1	2.9	2.8	2.6	2.5	2.3	2.2	2.1	1.9	1.8	1.7	1.5	1.4	1.3	1.2
1.1	1.0	0.9	0.8	0.7	0.7	0.6	0.5	0.5	0.4	0.3	0.3	0.3	0.2	0.2	0.2	0.1	0.1	0.1	0.1
0.0	0.0	0.0	0.0																

I = 38 P STARTS AT 10

0.0	0.0	0.0	0.0	0.0	0.1	0.2	0.6	0.9	1.2	1.5	1.7	2.0	2.2	2.5	2.7	2.9	3.1	3.2	3.4
3.5	3.6	3.8	3.8	3.9	4.0	4.0	4.0	4.1	4.1	4.0	4.0	4.0	3.9	3.9	3.8	3.7	3.6	3.5	3.4
3.3	3.2	3.0	2.9	2.8	2.6	2.5	2.4	2.2	2.1	2.0	1.9	1.7	1.6	1.5	1.4	1.3	1.2	1.1	1.0
0.9	0.8	0.7	0.7	0.6	0.5	0.5	0.4	0.4	0.3	0.3	0.2	0.2	0.2	0.1	0.1	0.1	0.1	0.1	0.0
0.0	0.0	0.0	0.0																

I = 39 P STARTS AT 10

0.0	0.0	0.0	0.0	0.0	0.1	0.2	0.4	0.7	1.0	1.2	1.5	1.7	1.9	2.2	2.4	2.6	2.7	2.9	3.0
3.1	3.3	3.4	3.4	3.5	3.6	3.6	3.6	3.6	3.6	3.6	3.6	3.6	3.5	3.5	3.4	3.3	3.2	3.1	3.1
2.9	2.8	2.7	2.6	2.5	2.4	2.3	2.1	2.0	1.9	1.8	1.7	1.6	1.4	1.3	1.2	1.1	1.1	1.0	0.9
0.8	0.7	0.7	0.6	0.5	0.5	0.4	0.4	0.3	0.3	0.2	0.2	0.2	0.2	0.1	0.1	0.1	0.1	0.1	0.0
0.0	0.0	0.0	0.0	0.0															

I = 40 P STARTS AT 11

0.0	0.0	0.0	0.0	0.0	0.1	0.2	0.5	0.7	1.0	1.2	1.5	1.7	1.9	2.1	2.2	2.4	2.5	2.7	2.8
2.9	3.0	3.1	3.1	3.2	3.2	3.2	3.3	3.3	3.3	3.2	3.2	3.2	3.1	3.0	3.0	2.9	2.8	2.7	2.6
2.5	2.4	2.3	2.2	2.1	2.0	1.9	1.8	1.7	1.6	1.5	1.4	1.3	1.2	1.1	1.0	0.9	0.9	0.8	0.7
0.6	0.6	0.5	0.5	0.4	0.4	0.3	0.3	0.3	0.2	0.2	0.2	0.1	0.1	0.1	0.1	0.1	0.0	0.0	0.0
0.0	0.0	0.0	0.0																

I = 41 P STARTS AT 11

0.0	0.0	0.0	0.0	0.0	0.1	0.1	0.3	0.5	0.8	1.0	1.2	1.4	1.6	1.8	1.9	2.1	2.2	2.4	2.5
2.6	2.7	2.7	2.8	2.8	2.9	2.9	2.9	2.9	2.9	2.9	2.9	2.8	2.8	2.7	2.7	2.6	2.5	2.4	2.4
2.3	2.2	2.1	2.0	1.9	1.8	1.7	1.6	1.5	1.4	1.3	1.2	1.2	1.1	1.0	0.9	0.8	0.8	0.7	0.6
0.6	0.5	0.5	0.4	0.4	0.3	0.3	0.3	0.2	0.2	0.2	0.1	0.1	0.1	0.1	0.1	0.1	0.0	0.0	0.0
0.0	0.0	0.0	0.0	0.0															

I = 42 P STARTS AT 12

0.0	0.0	0.0	0.0	0.0	0.1	0.1	0.3	0.6	0.8	1.0	1.2	1.4	1.5	1.7	1.8	2.0	2.1	2.2	2.3
2.3	2.4	2.5	2.5	2.6	2.6	2.6	2.6	2.6	2.6	2.5	2.5	2.5	2.4	2.4	2.3	2.3	2.2	2.1	2.0
2.0	1.9	1.8	1.7	1.6	1.5	1.4	1.4	1.3	1.2	1.1	1.0	1.0	0.9	0.8	0.7	0.7	0.6	0.6	0.5
0.5	0.4	0.4	0.3	0.3	0.3	0.2	0.2	0.2	0.2	0.1	0.1	0.1	0.1	0.1	0.1	0.0	0.0	0.0	0.0
0.0	0.0	0.0	0.0	0.0															

I = 43 P STARTS AT 12

0.0	0.0	0.0	0.0	0.0	0.0	0.1	0.1	0.4	0.6	0.8	1.0	1.1	1.3	1.4	1.6	1.7	1.8	1.9	2.0
2.1	2.1	2.2	2.2	2.3	2.3	2.3	2.3	2.3	2.3	2.3	2.2	2.2	2.2	2.1	2.1	2.0	1.9	1.9	1.8
1.7	1.7	1.6	1.5	1.4	1.4	1.3	1.2	1.1	1.1	1.0	0.9	0.9	0.8	0.7	0.7	0.6	0.6	0.5	0.5
0.4	0.4	0.3	0.3	0.3	0.2	0.2	0.2	0.2	0.1	0.1	0.1	0.1	0.1	0.1	0.1	0.0	0.0	0.0	0.0
0.0	0.0	0.0	0.0	0.0	0.0														

I = 44 P STARTS AT 13

0.0	0.0	0.0	0.0	0.0	0.0	0.1	0.2	0.4	0.6	0.8	0.9	1.1	1.2	1.3	1.5	1.6	1.7	1.7	1.8
1.9	1.9	2.0	2.0	2.0	2.0	2.0	2.0	2.0	2.0	2.0	1.9	1.9	1.9	1.8	1.8	1.7	1.7	1.6	1.5
1.5	1.4	1.3	1.3	1.2	1.1	1.1	1.0	0.9	0.9	0.8	0.8	0.7	0.6	0.6	0.5	0.5	0.4	0.4	0.4
0.3	0.3	0.3	0.2	0.2	0.2	0.2	0.1	0.1	0.1	0.1	0.1	0.1	0.1	0.0	0.0	0.0	0.0	0.0	0.0
0.0	0.0	0.0	0.0	0.0	0.0														

I = 45 P STARTS AT 13

0.0	0.0	0.0	0.0	0.0	0.0	0.1	0.1	0.3	0.4	0.6	0.8	0.9	1.0	1.1	1.3	1.3	1.4	1.5	1.6
1.6	1.7	1.7	1.7	1.8	1.8	1.8	1.8	1.8	1.8	1.7	1.7	1.7	1.7	1.6	1.6	1.5	1.5	1.4	1.4
1.3	1.2	1.2	1.1	1.1	1.0	0.9	0.9	0.8	0.8	0.7	0.7	0.6	0.6	0.5	0.5	0.4	0.4	0.4	0.3
0.3	0.3	0.2	0.2	0.2	0.2	0.1	0.1	0.1	0.1	0.1	0.1	0.1	0.0	0.0	0.0	0.0	0.0	0.0	0.0
0.0	0.0	0.0	0.0	0.0	0.0	0.0													

I = 46 P STARTS AT 14

0.0	0.0	0.0	0.0	0.0	0.0	0.0	0.1	0.3	0.4	0.6	0.7	0.8	1.0	1.1	1.2	1.2	1.3	1.4	1.4
1.5	1.5	1.5	1.5	1.6	1.6	1.6	1.6	1.6	1.5	1.5	1.5	1.5	1.4	1.4	1.3	1.3	1.2	1.2	1.1
1.1	1.0	1.0	0.9	0.9	0.8	0.8	0.7	0.7	0.6	0.6	0.5	0.5	0.5	0.4	0.4	0.3	0.3	0.3	0.3
0.2	0.2	0.2	0.2	0.1	0.1	0.1	0.1	0.1	0.1	0.1	0.1	0.0	0.0	0.0	0.0	0.0	0.0	0.0	0.0
0.0	0.0	0.0	0.0	0.0	0.0	0.0													

I = 47 P STARTS AT 14

0.0	0.0	0.0	0.0	0.0	0.0	0.0	0.1	0.2	0.3	0.4	0.6	0.7	0.8	0.9	1.0	1.1	1.1	1.2	1.2
1.3	1.3	1.3	1.4	1.4	1.4	1.4	1.4	1.4	1.3	1.3	1.3	1.3	1.2	1.2	1.2	1.1	1.1	1.0	1.0
1.0	0.9	0.9	0.8	0.8	0.7	0.7	0.6	0.6	0.6	0.5	0.5	0.4	0.4	0.4	0.3	0.3	0.3	0.3	0.2
0.2	0.2	0.2	0.1	0.1	0.1	0.1	0.1	0.1	0.1	0.1	0.0	0.0	0.0	0.0	0.0	0.0	0.0	0.0	0.0
0.0	0.0	0.0	0.0	0.0	0.0	0.0	0.0												

I = 48 P STARTS AT 15

0.0	0.0	0.0	0.0	0.0	0.0	0.0	0.1	0.2	0.3	0.4	0.5	0.6	0.7	0.8	0.9	1.0	1.0	1.1	1.1
1.1	1.2	1.2	1.2	1.2	1.2	1.2	1.2	1.2	1.2	1.1	1.1	1.1	1.1	1.0	1.0	1.0	0.9	0.9	0.8
0.8	0.8	0.7	0.7	0.6	0.6	0.6	0.5	0.5	0.4	0.4	0.4	0.4	0.3	0.3	0.3	0.2	0.2	0.2	0.2
0.2	0.1	0.1	0.1	0.1	0.1	0.1	0.1	0.1	0.0	0.0	0.0	0.0	0.0	0.0	0.0	0.0	0.0	0.0	0.0
0.0	0.0	0.0	0.0	0.0	0.0	0.0	0.0												

I = 49 P STARTS AT 16

0.0	0.0	0.0	0.0	0.0	0.0	0.0	0.1	0.2	0.3	0.4	0.5	0.6	0.7	0.7	0.8	0.9	0.9	0.9	1.0
1.0	1.0	1.0	1.0	1.0	1.0	1.0	1.0	1.0	1.0	1.0	0.9	0.9	0.9	0.9	0.8	0.8	0.8	0.7	0.7
0.7	0.6	0.6	0.6	0.5	0.5	0.5	0.4	0.4	0.4	0.3	0.3	0.3	0.3	0.2	0.2	0.2	0.2	0.2	0.1
0.1	0.1	0.1	0.1	0.1	0.1	0.1	0.0	0.0	0.0	0.0	0.0	0.0	0.0	0.0	0.0	0.0	0.0	0.0	0.0
0.0	0.0	0.0	0.0	0.0	0.0	0.0	0.0												

I = 50 P STARTS AT 16

0.0	0.0	0.0	0.0	0.0	0.0	0.0	0.0	0.1	0.2	0.3	0.4	0.5	0.5	0.6	0.7	0.7	0.8	0.8	0.8
0.9	0.9	0.9	0.9	0.9	0.9	0.9	0.9	0.9	0.9	0.8	0.8	0.8	0.8	0.8	0.7	0.7	0.7	0.6	0.6
0.6	0.5	0.5	0.5	0.5	0.4	0.4	0.4	0.3	0.3	0.3	0.3	0.2	0.2	0.2	0.2	0.2	0.1	0.1	0.1
0.1	0.1	0.1	0.1	0.1	0.1	0.0	0.0	0.0	0.0	0.0	0.0	0.0	0.0	0.0	0.0	0.0	0.0	0.0	0.0
0.0	0.0	0.0	0.0	0.0	0.0	0.0	0.0	0.0	0.0										

I = 51 P STARTS AT 17

0.0	0.0	0.0	0.0	0.0	0.0	0.0	0.0	0.1	0.2	0.3	0.4	0.4	0.5	0.6	0.6	0.6	0.7	0.7	0.7
0.8	0.8	0.8	0.8	0.8	0.8	0.8	0.8	0.7	0.7	0.7	0.7	0.7	0.7	0.6	0.6	0.6	0.6	0.5	0.5
0.5	0.4	0.4	0.4	0.4	0.3	0.3	0.3	0.3	0.3	0.2	0.2	0.2	0.2	0.2	0.1	0.1	0.1	0.1	0.1
0.1	0.1	0.1	0.1	0.0	0.0	0.0	0.0	0.0	0.0	0.0	0.0	0.0	0.0	0.0	0.0	0.0	0.0	0.0	0.0
0.0	0.0	0.0	0.0	0.0	0.0	0.0	0.0	0.0	0.0										

I = 52 P STARTS AT 18

0.0	0.0	0.0	0.0	0.0	0.0	0.0	0.0	0.1	0.2	0.3	0.3	0.4	0.5	0.5	0.5	0.6	0.6	0.6	0.6
0.7	0.7	0.7	0.7	0.7	0.7	0.7	0.6	0.6	0.6	0.6	0.6	0.6	0.5	0.5	0.5	0.5	0.5	0.4	0.4
0.4	0.4	0.3	0.3	0.3	0.3	0.3	0.2	0.2	0.2	0.2	0.2	0.2	0.1	0.1	0.1	0.1	0.1	0.1	0.1
0.1	0.1	0.0	0.0	0.0	0.0	0.0	0.0	0.0	0.0	0.0	0.0	0.0	0.0	0.0	0.0	0.0	0.0	0.0	0.0
0.0	0.0	0.0	0.0	0.0	0.0	0.0	0.0	0.0	0.0										

I = 53 P STARTS AT 19

0.0	0.0	0.0	0.0	0.0	0.0	0.0	0.0	0.1	0.2	0.3	0.3	0.4	0.4	0.4	0.5	0.5	0.5	0.5	0.6
0.6	0.6	0.6	0.6	0.6	0.6	0.6	0.5	0.5	0.5	0.5	0.5	0.5	0.5	0.4	0.4	0.4	0.4	0.4	0.3
0.3	0.3	0.3	0.3	0.2	0.2	0.2	0.2	0.2	0.2	0.1	0.1	0.1	0.1	0.1	0.1	0.1	0.1	0.1	0.1
0.0	0.0	0.0	0.0	0.0	0.0	0.0	0.0	0.0	0.0	0.0	0.0	0.0	0.0	0.0	0.0	0.0	0.0	0.0	0.0
0.0	0.0	0.0	0.0	0.0	0.0	0.0	0.0	0.0	0.0	0.0									

I = 54 P STARTS AT 19

0.0	0.0	0.0	0.0	0.0	0.0	0.0	0.0	0.0	0.1	0.2	0.2	0.3	0.3	0.4	0.4	0.4	0.4	0.5	0.5
0.5	0.5	0.5	0.5	0.5	0.5	0.5	0.5	0.5	0.4	0.4	0.4	0.4	0.4	0.4	0.4	0.3	0.3	0.3	0.3
0.3	0.3	0.2	0.2	0.2	0.2	0.2	0.2	0.1	0.1	0.1	0.1	0.1	0.1	0.1	0.1	0.1	0.1	0.1	0.0
0.0	0.0	0.0	0.0	0.0	0.0	0.0	0.0	0.0	0.0	0.0	0.0	0.0	0.0	0.0	0.0	0.0	0.0	0.0	0.0
0.0	0.0	0.0	0.0	0.0	0.0	0.0	0.0	0.0	0.0	0.0	0.0								

I = 55 P STARTS AT 20

0.0	0.0	0.0	0.0	0.0	0.0	0.0	0.0	0.1	0.1	0.2	0.2	0.3	0.3	0.3	0.3	0.4	0.4	0.4	0.4
0.4	0.4	0.4	0.4	0.4	0.4	0.4	0.4	0.4	0.4	0.4	0.3	0.3	0.3	0.3	0.3	0.3	0.3	0.2	0.2
0.2	0.2	0.2	0.2	0.2	0.1	0.1	0.1	0.1	0.1	0.1	0.1	0.1	0.1	0.1	0.1	0.1	0.0	0.0	0.0
0.0	0.0	0.0	0.0	0.0	0.0	0.0	0.0	0.0	0.0	0.0	0.0	0.0	0.0	0.0	0.0	0.0	0.0	0.0	0.0
0.0	0.0	0.0	0.0	0.0	0.0	0.0	0.0	0.0	0.0	0.0	0.0	0.0							

I = 56 P STARTS AT 21

0.0	0.0	0.0	0.0	0.0	0.0	0.0	0.0	0.1	0.1	0.2	0.2	0.2	0.3	0.3	0.3	0.3	0.3	0.3	0.3
0.4	0.4	0.4	0.3	0.3	0.3	0.3	0.3	0.3	0.3	0.3	0.3	0.3	0.3	0.2	0.2	0.2	0.2	0.2	0.2
0.2	0.2	0.1	0.1	0.1	0.1	0.1	0.1	0.1	0.1	0.1	0.1	0.1	0.1	0.0	0.0	0.0	0.0	0.0	0.0
0.0	0.0	0.0	0.0	0.0	0.0	0.0	0.0	0.0	0.0	0.0	0.0	0.0	0.0	0.0	0.0	0.0	0.0	0.0	0.0
0.0	0.0	0.0	0.0	0.0	0.0	0.0	0.0	0.0	0.0	0.0	0.0	0.0							

I = 57 P STARTS AT 22

0.0	0.0	0.0	0.0	0.0	0.0	0.0	0.0	0.1	0.1	0.1	0.2	0.2	0.2	0.3	0.3	0.3	0.3	0.3	0.3
0.3	0.3	0.3	0.3	0.3	0.3	0.3	0.3	0.3	0.3	0.2	0.2	0.2	0.2	0.2	0.2	0.2	0.2	0.2	0.1
0.1	0.1	0.1	0.1	0.1	0.1	0.1	0.1	0.1	0.1	0.1	0.1	0.0	0.0	0.0	0.0	0.0	0.0	0.0	0.0
0.0	0.0	0.0	0.0	0.0	0.0	0.0	0.0	0.0	0.0	0.0	0.0	0.0	0.0	0.0	0.0	0.0	0.0	0.0	0.0
0.0	0.0	0.0	0.0	0.0	0.0	0.0	0.0	0.0	0.0	0.0	0.0								

I = 58 P STARTS AT 22

0.0	0.0	0.0	0.0	0.0	0.0	0.0	0.0	0.0	0.1	0.1	0.1	0.2	0.2	0.2	0.2	0.2	0.2	0.2	0.2
0.3	0.3	0.3	0.2	0.2	0.2	0.2	0.2	0.2	0.2	0.2	0.2	0.2	0.2	0.2	0.2	0.2	0.1	0.1	0.1
0.1	0.1	0.1	0.1	0.1	0.1	0.1	0.1	0.1	0.1	0.0	0.0	0.0	0.0	0.0	0.0	0.0	0.0	0.0	0.0
0.0	0.0	0.0	0.0	0.0	0.0	0.0	0.0	0.0	0.0	0.0	0.0	0.0	0.0	0.0	0.0	0.0	0.0	0.0	0.0
0.0	0.0	0.0	0.0	0.0	0.0	0.0	0.0	0.0	0.0	0.0	0.0								

I = 59 P STARTS AT 23

0.0	0.0	0.0	0.0	0.0	0.0	0.0	0.0	0.0	0.1	0.1	0.1	0.2	0.2	0.2	0.2	0.2	0.2	0.2	0.2
0.2	0.2	0.2	0.2	0.2	0.2	0.2	0.2	0.2	0.2	0.2	0.2	0.2	0.1	0.1	0.1	0.1	0.1	0.1	0.1
0.1	0.1	0.1	0.1	0.1	0.1	0.1	0.0	0.0	0.0	0.0	0.0	0.0	0.0	0.0	0.0	0.0	0.0	0.0	0.0
0.0	0.0	0.0	0.0	0.0	0.0	0.0	0.0	0.0	0.0	0.0	0.0	0.0	0.0	0.0	0.0	0.0	0.0	0.0	0.0
0.0	0.0	0.0	0.0	0.0	0.0	0.0	0.0	0.0	0.0	0.0									

I = 60 P STARTS AT 24

0.0	0.0	0.0	0.0	0.0	0.0	0.0	0.0	0.1	0.1	0.1	0.1	0.1	0.1	0.2	0.2	0.2	0.2	0.2	0.2
0.2	0.2	0.2	0.2	0.2	0.2	0.2	0.2	0.1	0.1	0.1	0.1	0.1	0.1	0.1	0.1	0.1	0.1	0.1	0.1
0.1	0.1	0.1	0.1	0.1	0.0	0.0	0.0	0.0	0.0	0.0	0.0	0.0	0.0	0.0	0.0	0.0	0.0	0.0	0.0
0.0	0.0	0.0	0.0	0.0	0.0	0.0	0.0	0.0	0.0	0.0	0.0	0.0	0.0	0.0	0.0	0.0	0.0	0.0	0.0
0.0	0.0	0.0	0.0	0.0	0.0	0.0	0.0	0.0	0.0										

I = 61 P STARTS AT 25

0.0	0.0	0.0	0.0	0.0	0.0	0.0	0.1	0.1	0.1	0.1	0.1	0.1	0.1	0.1	0.1	0.1	0.1	0.1	0.1
0.1	0.1	0.1	0.1	0.1	0.1	0.1	0.1	0.1	0.1	0.1	0.1	0.1	0.1	0.1	0.1	0.1	0.1	0.1	0.1
0.1	0.1	0.0	0.0	0.0	0.0	0.0	0.0	0.0	0.0	0.0	0.0	0.0	0.0	0.0	0.0	0.0	0.0	0.0	0.0
0.0	0.0	0.0	0.0	0.0	0.0	0.0	0.0	0.0	0.0	0.0	0.0	0.0	0.0	0.0	0.0	0.0	0.0	0.0	0.0
0.0	0.0	0.0	0.0	0.0	0.0	0.0	0.0	0.0											

I = 62 P STARTS AT 26

0.0	0.0	0.0	0.0	0.0	0.0	0.0	0.0	0.1	0.1	0.1	0.1	0.1	0.1	0.1	0.1	0.1	0.1	0.1	0.1
0.1	0.1	0.1	0.1	0.1	0.1	0.1	0.1	0.1	0.1	0.1	0.1	0.1	0.1	0.1	0.1	0.1	0.1	0.0	0.0
0.0	0.0	0.0	0.0	0.0	0.0	0.0	0.0	0.0	0.0	0.0	0.0	0.0	0.0	0.0	0.0	0.0	0.0	0.0	0.0
0.0	0.0	0.0	0.0	0.0	0.0	0.0	0.0	0.0	0.0	0.0	0.0	0.0	0.0	0.0	0.0	0.0	0.0	0.0	0.0
0.0	0.0	0.0	0.0	0.0	0.0	0.0	0.0												

I = 63 P STARTS AT 27

0.0	0.0	0.0	0.0	0.0	0.0	0.0	0.0	0.1	0.1	0.1	0.1	0.1	0.1	0.1	0.1	0.1	0.1	0.1	0.1
0.1	0.1	0.1	0.1	0.1	0.1	0.1	0.1	0.1	0.1	0.1	0.1	0.1	0.1	0.1	0.0	0.0	0.0	0.0	0.0
0.0	0.0	0.0	0.0	0.0	0.0	0.0	0.0	0.0	0.0	0.0	0.0	0.0	0.0	0.0	0.0	0.0	0.0	0.0	0.0
0.0	0.0	0.0	0.0	0.0	0.0	0.0	0.0	0.0	0.0	0.0	0.0	0.0	0.0	0.0	0.0	0.0	0.0	0.0	0.0
0.0	0.0	0.0	0.0	0.0	0.0	0.0													

```
I = 64 P STARTS AT  28
  0.0  0.0  0.0  0.0  0.0  0.0  0.0  0.0  0.1  0.1  0.1  0.1  0.1  0.1  0.1  0.1  0.1  0.1  0.1  0.1
  0.1  0.1  0.1  0.1  0.1  0.1  0.1  0.1  0.1  0.1  0.1  0.0  0.0  0.0  0.0  0.0  0.0  0.0  0.0  0.0
  0.0  0.0  0.0  0.0  0.0  0.0  0.0  0.0  0.0  0.0  0.0  0.0  0.0  0.0  0.0  0.0  0.0  0.0  0.0  0.0
  0.0  0.0  0.0  0.0  0.0  0.0  0.0  0.0  0.0  0.0  0.0  0.0  0.0  0.0  0.0  0.0  0.0  0.0  0.0  0.0
  0.0  0.0  0.0  0.0  0.0  0.0
I = 65 P STARTS AT  29
  0.0  0.0  0.0  0.0  0.0  0.0  0.0  0.0  0.0  0.1  0.1  0.1  0.1  0.1  0.1  0.1  0.1  0.1  0.1  0.1
  0.1  0.1  0.1  0.1  0.1  0.1  0.1  0.0  0.0  0.0  0.0  0.0  0.0  0.0  0.0  0.0  0.0  0.0  0.0  0.0
  0.0  0.0  0.0  0.0  0.0  0.0  0.0  0.0  0.0  0.0  0.0  0.0  0.0  0.0  0.0  0.0  0.0  0.0  0.0  0.0
  0.0  0.0  0.0  0.0  0.0  0.0  0.0  0.0  0.0  0.0  0.0  0.0  0.0  0.0  0.0  0.0  0.0  0.0  0.0  0.0
  0.0  0.0  0.0  0.0  0.0
I = 66 P STARTS AT  30
  0.0  0.0  0.0  0.0  0.0  0.0  0.0  0.0  0.0  0.0  0.0  0.1  0.1  0.1  0.1  0.1  0.1  0.1  0.1  0.1
  0.1  0.0  0.0  0.0  0.0  0.0  0.0  0.0  0.0  0.0  0.0  0.0  0.0  0.0  0.0  0.0  0.0  0.0  0.0  0.0
  0.0  0.0  0.0  0.0  0.0  0.0  0.0  0.0  0.0  0.0  0.0  0.0  0.0  0.0  0.0  0.0  0.0  0.0  0.0  0.0
  0.0  0.0  0.0  0.0  0.0  0.0  0.0  0.0  0.0  0.0  0.0  0.0  0.0  0.0  0.0  0.0  0.0  0.0  0.0  0.0
  0.0  0.0  0.0  0.0
```

All other points 0.0

REFERENCES

AKHMETELI, L.M., KASAVINA, B.S. & PETROPAVLOVSKAJA, G.A. (1975)
Biochemical investigation of the subretinal fluid.
British Journal of Ophthalmology 59: 70-77.

ASCHER, K.W. (1942)
Aqueous-vein: preliminary note.
American Journal of Ophthalmology 25: 31-38.

ASHTON, N. (1951)
Anatomical study of Schlemm's Canal and aqueous vein by means of Neoprene casts. Part I: aqueous veins.
British Journal of Ophthalmology 35: 291-303.

ASHTON, N. (1952)
Anatomical study of Schlemm's Canal and aqueous veins by means of Neoprene casts. Part II: aqueous veins (continued).
British Journal of Ophthalmology 36: 265-267.

BAIRATI, A. & ORZALESI, N. (1963)
The ultrastructure of the pigment epithelium and of the photoreceptor-pigment epithelium junction in the human retina.
Journal of Ultrastructure Research 9: 484-496.

BALAZS, E.A. (1960)
Physiology of the vitreous body.
In Importance of the Vitreous Body in Retina Surgery with Special Emphasis on Re-operations, ed. Stephens, C.L., St. Louis: C.V. Mosby.

BALAZS, E.A. (1961)
Molecular morphology of the vitreous body.
In the Sturcutre of the Eye, ed. Smelser, G.K. pp 293-310., New York: Academic Press.

BALAZS, E.A., TOTH, L.Z.J. & MITCHELL, A.P. (1963)
Studies on the vitreous body, part XII, cytological and histochemical studies on the cortical tissue layer.
Experimental Eye Research 3: 57-71.

BARANY, E.H. (1964)
Simultaneous measurement of changing pressure and outflow facility in the vervet monkey by constant pressure infusion.
Investigative Ophthalmology 3: 135-143.

BASINGER, S., HOFFMAN, R. & MATTHES, M. (1976)
Photoreceptor shedding is initiated by light in the frog retina.
Science 194: 1074-1076.

BECKER, B. (1961)
Iodite transport by the rabbit eye.
American Journal of Physiology 200: 804-806.

BELCHER, E.H. (1971)
Measurement of radioactivity in vitro.
In Radioisotopes in Medical Diagnosis, ed. Belcher, E.H. & Vetter, H., pp 79-117. London: Butterworths.

BELLHORN, M.B., BELLHORN, R.W. & POLL, D.S. (1977)
Permeability of fluorescein-labelled dextrans in fundus fluorescein angiography of rats and birds.
Experimental Eye Research 24: 595-605.

BERGGREN, L. (1967)
The intraocular pressure in rabbits after lithium administration with comments on pressure effects of injections into the vitreous.
Acta. Ophthalmologica 45: 229-238.

BERMAN, E.R. (1969)
Mucopolysaccharides (Glycosaminoglycans) of the retina: identification, distribution and possible biological role.
Modern Problems in Ophthalmology 8: 5-31.

BERMAN, E.R. & MICHAELSON, I.C. (1964)
The chemical composition of the human vitreous body as related to age and myopia.
Experimental Eye Research 3: 9-15.

BERMAN, E.R. & VOADEN, M. (1970)
The vitreous body.
In Biochemistry of the Eye, ed. Graymore, C. Ch.6, pp 441-452 New York: Academic Press.

BERNSTEIN, M.H. (1961)
Architecture of retinal epithelium.
In The Structure of the Eye, ed. Smelser, G.K., pp 139-150. New York and London: Academic Press.

BILL, A. (1962)
Quantitative determination of uveal blood flow in rabbits.
Archives of Ophthalmology 67: 62-68.

BILL, A. (1965)
The aqueous humor drainage mechanism in the cynomolgus monkey (Macaca irus) with evidence for unconventional routes.
Investigative Ophthalmology 4: 911-919.

BILL, A. (1966a)
Conventional and uveo-scleral drainage of aqueous humour in the cynomolgus monkey (Macaca irus) at normal and high introcular pressures.
Experimental Eye Research 5: 45-54.

BILL, A. (1966b)
The routes for bulk drainage of aqueous humour in the vervet monkey (Corcopithecus ethiops).
Experimental Eye Research 5: 55-57.

BILL, A. (1966c)
Formation and drainage of aqueous humour in cats.
Experimental Eye Research 5: 185-190.

BILL, A. (1966d)
The routes for bulk drainage of aqueous humour in rabbits with and without cyclodialysis.
Documenta Ophthalmologica 20: 157-169.

BILL, A. (1970)
Scanning electron microscopic studies of the canal of Schlemm.
Experimental Eye Research 10: 214-218.

BILL, A. (1971)
Aqueous humor dynamics in monkeys (Macaca irus and Corcopithecus ethiops).
Experimental Eye Research 11: 195-206.

BILL, A. (1973)
The role of ciliary blood flow and ultrafiltration in aqueous humor formation.
Experimental Eye Research 16: 287-298.

BILL, A. (1974)
Some aspects of tissue fluid dynamics in the eye.
Proceedings of the Third William McKenzie Memorial Symposium, ed. Cant, J.S. pp 333-338. London: Henry Kimpton.

BILL, A. (1975)
The drainage of aqueous humour.
Investigative Ophthalmology 14: 1-3.

BILL, A. & BARANY, E.H. (1966)
Gross facility, facility of conventional routes, and pseudofacility of aqueous humor outflow in the cynomolgus monkey.
Archives of Ophthalmology 75: 665-673.

BILL, A. & HELLSING, K. (1965)
Production and drainage of aqueous humour in the cynomolgus monkey (Macaca irus).
Investigative Ophthalmology 4: 920-926.

BILL, A. & PHILLIPS, C. (1971)
Uveoscleral drainage of aqueous humour in human eyes.
Experimental Eye Research 12: 275-281.

BILL, A. & SVEDBERGH, B. (1972)
Scanning electron microscopic studies of the trabecular meshwork and the canal of Schlemm - an attempt to localize the main resistance to outflow of aqueous humour in man.
Acta Ophthalmologica 50: 295-320.

BILL, A. & WÅLINDER, P.E. (1966)
The effects of pilocarpine on the dynamics of aqueous humor in a primate (Macaca irus).
Investigative Ophthalmology 5: 170-175.

BITO, L.Z. & DAVSON, H. (1964)
Steady state concentrations of potassium in ocular fluids.
Experimental Eye Research 3: 283-297.

BITO, L.Z., DAVSON, H., LEVIN, E., MURRAY, M. & SNIDER, N. (1965)
The relationship between the concentrations of amino acids in the ocular fluids and blood plasma of dogs.
Experimental Eye Research 4: 374-380.

BLEEKER, G.M., van HAERINGEN, N.J. & GLASIUS, E. (1968a)
Urea and the vitreous barrier of the eye.
Experimental Eye Research 7: 30-36.

BLEEKER, G.M., van HAERINGEN, N.J., MAAS, E.R. & GLASIUS, E. (1968b)
Selective properties of the vitreous barrier.
Experimental Eye Research 7: 37-46.

BLUMENTHAL, M., BEST, M., GALIN, M.A. & WALD, N. (1971)
Volumetric studies of ophthalmic artery perfusion pressure and ocular rigidity.
Acta Ophthalmologica 49: 805-811.

CAGIANUT, B. & VERREY, F. (1949)
Essai de depistage du metabolisme hydrique dans les milieux transparents de l'oeil humain par injection d'eau lourde dans la chambre anterieure.
Annales d'Oculistique 182: 649-657.

CARSLAW, H.S. & JAEGER, J.C. (1947)
Conduction of Heat in Solids.
Oxford: Clarendon Press.

CASTREN, J.A. & LAAMANENEN, A. (1963)
The resorption speed of intravitreally injected traced proteins.
Acta Ophthalmologica 41: 689-692.

CHAWLA, H.B. (1977)
Reflections on subretinal fluid release.
Transactions of the Ophthalmological Society of the United Kingdom 97: 627-629.

CHIDSEY, C.A., FRITTS, H.W., HARDEWIG, A., RICHARDS, D.W. & COURNAND, A. (1959)
Fate of radioactive krypton (Kr-85) introduced intravenously in man.
Journal of Applied Physiology 14: 63-67.

CHIGNELL, A.H. (1974)
Retinal detachment surgery without drainage of subretinal fluid.
American Journal of Ophthalmology 77:1-5.

CHIORALAIA, G., SALMINEN, L., BAURMANN, H. & KREMER, F. (1976)
Fluorescein-labelled dextrans as tracer substance for experimental angiograms.
Acta Ophthalmologica 54: 665-667.

CHISHOLM, I.A., McLURE, E. & FOULDS, W.S. (1975)
Functional recovery of the retina after retinal detachment.
Transactions of the Ophthalmological Society of the United Kingdom 95: 167-172.

COLE, D.F. (1966)
Aqueous humour formation.
Documenta Ophthalmologica 21: 116-238.

COLE, D.F. (1974)
Comparative aspects of the intraocular fluids. In The Eye, ed. Davson, H. & Graham, L.T. Vol. 5, ch.2. New York and London: Academic Press

CRANK, J. (1956)
The Mathematics of Diffusion. Oxford: Clarendon Press.

CRISTIANSSON, J. & PALM, E. (1954)
The exchange of substances in the anterior part of the vitreous body, bordering upon the lens.
Acta Ophthalmologica 32: 197-212.

CUNHA-VAZ, J., DE ABREU, J.R.F., CAMPOS, A.J. & FIGO, G.M. (1975)
Early breakdown in the blood-retinal barrier in diabetes.
British Journal of Ophthalmology 59: 649-656.

CUNHA-VAZ, J.G. & MAURICE, D.M. (1967)
The active transport of fluorescein by the retinal vessels and the retina.
Journal of Physiology 191: 467-486.

DAVSON, H. (1949)
The penetration of some electrolytes and non-electrolytes into the aqueous humour and vitreous body of the cat.
Journal of Physiology 108: 203-217.

DAVSON, H. & LUCK, C.D. (1956)
A comparative study of the total carbon dioxide in the ocular fluids, cerebrospinal fluid and plasma of some mammalian species.
Journal of Physiology 132: 454-464.

DE GUILLEBON, H., DE LA TRIBONNIERE, M.M. & POMERANTZEFF, O. (1971)
Adhesion between retina and pigment epithelium: measurement by peeling.
Archives of Ophthalmology 86: 679-684.

DE GUILLEBON, H. & ZAUBERMAN, H. (1972)
Experimental retinal detachment: biophysical aspects of retinal peeling and stretching.
Archives of Ophthalmology 87: 545-548.

DOBBIE, J.G. (1963)
A study of the intraocular fluid dynamics in retinal detachment.
Archives of Ophthalmology 69: 53-58.

EISENLOHR, J.E., LANGHAM, M.E., & MAUMENEE, A.E. (1962)
Manometric studies of the pressure-volume relationship in living and enucleated eyes of individual human subjects.
British Journal of Ophthalmology 46: 536-548.

EVANS, A.L., BUSUTTIL, A., GILLESPIE, F.C. & UNSWORTH, J. (1974)
The rate of clearance of xenon from rat liver sections in vitro and its significance in relation to intracellular diffusion rates.
Physics in Medicine and Biology 19: 303-316.

FALLOT, P., AEBERHARDT, A. & MASSON, J. (1956)
Methodes de dosage de l'eau tritiee et ses applications en clinique humaine.
International Journal of Applied Radiation and Isotopes 1: 237-243.

FATT, I. (1975)
Flow and diffusion in the vitreous body of the eye.
Bulletin of Mathematical Biology 37: 85-90.

FATT, I. & GOLDSTICK, T.K. (1965)
Dynamics of water transport in swelling membranes.
Journal of Colloid Science 20: 962-989.

FATT, I. & HEDBYS, B.O. (1970)
Flow of water in the sclera.
Experimental Eye Research 10: 243-249.

FATT, I. & SHANTINATH, K. (1971)
Flow conductivity of retina and its role in retinal adhesion.
Experimental Eye Research 12: 218-226.

FEENEY, L. (1973)
The interphotoreceptor space. II. Histochemistry of the matrix.
Developmental Biology 32: 115-128.

FEENEY, L. & WISSIG, S. (1966)
Outflow studies using an electron dense tracer.
Transactions of the American Academy of Ophthalmology and Otolaryngology 70: 791-798.

FICK, A. (1855)
Ann. Phys. Lpz. 170: 59

FINE, B.S. (1964)
Observations of the drainage angle in man and rhesus monkey: A concept of the pathogenesis of chronic simple glaucoma.
Investigative Ophthalmology 3: 609-646.

FINE, B.S. (1966)
Structure of the trabecular meshwork and the canal of Schlemm.
Transactions of the American Academy of Ophthalmology and Otolaryngology 70: 777-790.

FINE, B.S. (1968)
Retinal structure: light and electronmicroscopic observations.
In New and Controversial Aspects of the Retinal Detachment, ed. McPherson, A. New York: Harper and Row.

FINE, B.S. & TOUSIMIS, A.J. (1961)
The structure of the vitreous body and the suspensory ligaments of the lens.
Archives of Ophthalmology 4: 95-110.

FINE, B.S. & ZIMMERMAN, L.E. (1963)
Observations on the rod and cone layer of the human retina.
Investigative Ophthalmology 2: 446-459.

FISCHER, F.P. (1930)
Ein Versuch den Energiewechsel des Auges zu bestimmen.
Bericht: Deutsche Ophthalmologische Gesellschaft 48: 95-99.

FISH, M.B. O'DAY, D.M. ARONSON, S.B., POLLYCOVE, M. & COON, A. (1971)
Disappearance of intravitreous xenon-133: Its relation to ocular blood flow.
Archives of Ophthalmology 86: 314-320.

FORBES, M. & BECKER, B. (1960)
The transport of organic anions by the rabbit eye. II, in vivo transport of iodopyracet (diodrast).
American Journal of Ophthalmology 50: 867-875.

FORRESTER, J.V., EDGAR, W., PRENTICE, C.R.M., FORBES, C.D. & WILLIAMSON, J. (1976)
Intravitreal fibrinolysis in experimental vitreous haemorrhage.
Experimental Eye Research 22: 181-188.

FORSYTHE, G.E. & WASOW, W.R. (1960)
Finite-difference Methods for Partial Differential Equations.
New York: John Wiley.

FOULDS, W.S. (1969)
Experimental detachment of the retina and its effect on the intra-ocular fluid dynamics.
Modern Problems in Ophthalmology 8: 51-63.

FOULDS, W.S. (1975)
Aetiology of retinal detachment.
Transactions of the Ophthalmological Society of the United Kingdom 95: 118-127.

FOULDS, W.S. (1976)
Clinical significance of trans-scleral fluid transfer.
Transactions of the Ophthalmological Society of the United Kingdom 96: 290-308.

FOULDS, W.S. (1979)
The retinal-pigment epithelial interface.
British Journal of Ophthalmology 63: 71-84.

FOURIER, J.B. (1822)
Theorie analytique de la chaleur. Oeuvres de Fourier.

FOWLKS, W.L. (1963)
Meridional flow from the corona ciliaris through the pararetinal zone of the rabbit vitreous.
Investigative Ophthalmology 2: 63-71.

FOY, J.M. & SCHNIEDEN, A. (1960)
Estimation of total body water (virtual tritium space) in rat, cat, rabbit, guinea-pig and man and of the biological half-life of tritium in man.
Journal of Physiology, London 154: 169-176.

FRIEDENWALD, J.S. & BECKER, B. (1956)
Aqueous humour dynamics: theoretical considerations.
American Journal of Ophthalmology 41: 383-398.

FRIEDMAN, E., KOPALD, H.H. & SMITH, T.R. (1964)
Retinal and choroidal blood flow determined in anaesthetised animals.
Investigative Ophthalmology 4: 1122-1125.

GARRON, L.K. & FEENEY, M.L. (1959)
Electron microscopic studies of the human eye. II.Study of the trabeculae by light and electron microscopy.
Archives of Ophthalmology 62: 966-973.

GILLESPIE, F.C. & UNSWORTH J. (1968)
Anoxia in radiobiology.
British Journal of Radiology 41: 640.

GLOOR, B.P. (1970)
Physiology of the vitreous.
In Adler's Physiology of the Eye. ed. Moses, R.A. Chp.8, pp 311-332.
Saint Louis: C.V. Mosby.

GRANT, M.W. (1958)
Further studies of facility of flow through the trabecular meshwork.
Archives of Ophthalmology 60: 523-533.

GREEN, K. & PEDERSON, J.E. (1973)
Aqueous humour formation.
Experimental Eye Research 16: 273-286.

GRIERSON, I. (1976)
The morphology of the outflow apparatus of the eye with particular reference to its structural appearance at various levels of intra-ocular pressure.
Ph.D. Thesis, University of Glasgow.

GRIERSON, I. & LEE, W.R. (1974)
Changes in the monkey outflow apparatus at graded levels of intra-ocular pressure: a qualitative analysis by light microscopy and scanning electron microscopy.
Experimental Eye Research 19: 21-33.

GRIERSON, I. & LEE, W.R. (1975a)
The fine structure of the trabecular meshwork at graded levels of intraocular pressure (1) pressure effects within the near-physiological range (8-30 mm Hg).
Experimental Eye Research 20: 505-521.

GRIERSON, I. & LEE, W.R. (1975b)
The fine structure of the trabecular meshwork at graded levels of intraocular pressure (2) pressures outside the physiological range (0 and 50 mm Hg).
Experimental Eye Research 20: 523-530.

GRIERSON, I. & LEE, W.R. (1975c)
Pressure-induced changes in the ultrastructure of the endothelium lining Schlemm's canal.
American Journal of Ophthalmology 80: 863-884.

GRIERSON, I., LEE, W.R. & ABRAHAM, S. (1977)
Pathways for the drainage of aqueous humour into Schlemm's canal.
Transactions of the Ophthalmological Society of the United Kingdom 97: 719-725.

GRIERSON, I., LEE, W.R. & ABRAHAM, S. (1978)
Effects of pilocarpine on the morphology of the human outflow apparatus.
British Journal of Ophthalmology 62: 302-313.

GRIERSON, I., LEE, W.R. & ABRAHAM, S. (1979)
The effects of topical pilocarpine on the morphology of the outflow apparatus of the baboon.
Investigative Ophthalmology 18: 346-355.

GRIERSON, I., LEE, W.R., MOSELEY, H. & ABRAHAM, S. (1979)
The trabecular wall of Schlemm's canal: a study of the effects of pilocarpine by scanning electron microscopy.
British Journal of Ophthalmology 63: 9-16.

GUGGENHEIM, I. & FRANCESCHETT, A. (1928)
Refraktometrische Untersuchugen des Glaskörpers von Kaninchen und Mensch unter physiologischen und pathologischen Bedingungen.
Archiv fur Augenheilk 98: 448-482.

HAPPEL, J. & BRENNER, H. (1965)
Low Reynolds Number Hydrodynamics. New Jersey: Prentice Hall.

HAYREH, S.S. (1966)
Posterior drainage of the intraocular fluid from the vitreous.
Experimental Eye Research 5: 123-144.

HAYREH, S.S. (1977)
Fluids in the anterior part of the optic nerve in health and disease.
Transactions of the Ophthalmological Society of the United Kingdom 97: 573-587.

HOFFMANN, F. & DUMITRESCU, L.(1971)
Schlemm's canal under the scanning electron microscope.
Ophthalmic Research 2: 37-45.

HOGAN, M.J. (1963)
The vitreous, its structure, and relation to the ciliary body and retina.
Investigative Ophthalmology 2: 418-445.

HOLMBERG, A. (1959)
The fine structure of the inner wall of Schlemm's canal.
Archives of Ophthalmology 62: 956-958.

HOLMBERG, A.S. (1965)
Schlemm's canal and the trabecular meshwork. An electron microscopic study of the normal structure in man and monkey.
Documenta Opthalmologica 19: 339-355.

HOSNI, F.A. (1964)
The effect of haemodilution on the ocular rigidity of the rabbit eye.
Experimental Eye Research 3: 262-265.

HUGHES, A. (1972)
A schematic eye for the rabbit.
Vision Research 12: 123-138.

INOMATA, H., BILL, A. & SMELSER, G.K. (1972)
Aqueous humour pathways through the trabecular meshwork and into Schlemm's canal in the cynomolgus monkey (Macaca irus).
American Journal of Ophthalmology 73: 760-789.

JOCSON, V.L. & GRANT, W.M. (1965)
Interconnections of blood vessels and aqueous vessels in human eyes.
Archives of Ophthalmology 73: 707-720.

JOHNSON, N.F. (1975)
Phagocytosis in the normal and ischaemic retinal pigment epithelium of the rabbit.
Experimental Eye Research 20: 97-107.

JOHNSON, N.F. & FOULDS, W.S. (1977)
Observations on the retinal pigment epithelium and retinal macrophages in experimental retinal detachment.
British Journal of Ophthalmology 61: 564-572.

JOHNSON, N.F. & GRIERSON, I. (1976)
Post-mortem changes in the rabbit retina.
Acta Ophthalmologica 54: 529-541.

JOHNSON, N.F., McNAUGHT, E.I. & FOULDS, W.S. (1977)
Effect of photocoagulation on the barrier function of the pigment epithelium. II. A study of electron microscopy.
Transactions of the Ophthalmological Society of the United Kingdom 97: 640-651.

JOHNSTONE, M.A. & GRANT, W.M. (1973)
Pressure-dependent changes in structures of the aqueous outflow system of human and monkey eyes.
American Journal of Ophthalmology 75: 365-383.

KAYES, J. (1967)
Pore structure of inner wall of Schlemm's canal.
Investigative Ophthalmology 6: 381-388.

KAYES, J. (1975)
Pressure gradient changes on the trabecular meshwork of monkeys.
American Journal of Ophthalmology 79: 340-345.

KINSEY, V.E., GRANT, M. & COGAN, D.G. (1942)
Water movement and the eye.
Archives of Ophthalmology 27: 242-252.

KINSEY, V.E. & PALM, E. (1955)
Posterior and anterior chamber aqueous humour formation.
Archives of Ophthalmology 53: 330-344.

KINSEY, V.E. & REDDY, D.V.N. (1959)
An estimate of the ionic composition of the fluid secreted into the posterior chamber inferred from a study of aqueous humour dynamics.
Documenta Ophthalmologica 13: 7-40.

KINSEY, V.E., REDDY, D.V.N. & SKRENTNY, B.A. (1960)
Intraocular transport of C^{14}-labelled urea and the influence of diamox on its rate of accumulation in aqueous humors.
American Journal of Ophthalmology 50: 1130-1141.

KLEINSTEIN, R.N. & FATT, I. (1977)
Pressure dependency of transcleral flow.
Experimental Eye Research 24: 335-340.

LASANSKY, A. & De FISCH, F.W. (1966)
Potential, current and ionic fluxes across the isolated retinal pigment epithelium and choroid.
Journal of General Physiology 49: 913-924.

LEAVER, P.K., CHESTER, G.H. & SAUNDERS, S.H. (1976)
Factors influencing absorption of aubretinal fluid.
British Journal of Ophthalmology 60: 557-560.

LEE, W.R. (1971)
The study of the passage of particles through the endothelium of the outflow apparatus of the monkey eye by scanning and transmission electron microscopy.
Transactions of the Ophthalmological Society of the United Kingdom 91: 687-705.

LEE, W.R. & GRIERSON, I. (1974)
Relationships between intraocular pressure and the morphology of the outflow apparatus.
Transactions of the Ophthalmological Society of the United Kingdom 94: 430-449.

LEE, W.R. & GRIERSON, I. (1975)
Pressure effects on the endothelium of the trabecular wall of Schlemm's canal : a study by scanning electron microscopy.
Albrecht von Graefes Archiv fur klinische und experimentelle Ophthalmologie 196: 225-265.

LEIBMAN, J., GOTCH, F.A. & EDELMAN, I.S. (1960)
Tritium assay by liquid scintillation spectrometry. Comparison of tritium and deuterium oxides as tracers for body water.
Circulation Research 8: 907-912.

LEVENE, R.Z. (1957)
Studies on ocular blood flow in the rabbit.
Archives of Ophthalmology 58: 19-24.

LEVENE, R.Z. (1958)
Osmolarity in the normal state and following acetazolamide.
Archives of Ophthalmology 59: 597-602.

LEVENE, R.Z., BLOOM, J.N. & KIMURA, R. (1976)
Fluorophotometry and the rate of aqueous flow in man. II. Primary open angle glaucoma.
Archives of Ophthalmology 94: 444-447.

LIEB, W.R. & STEIN, W.D. (1971)
Implications of two different types of diffusion for biological membranes.
Nature New Biology 234: 220-221.

LINNER, E. (1952)
Ascorbic acid as a test substance for measuring relative changes in the rate of plasma flow through the ciliary processes.
Acta Physiologica Scandanavica 26: 57-67.

MAHIN, D.T. & LOFBERG, R.T. (1966)
A simplified method of sample preparation for determination of tritium, carbon-14, or sulfur-35 in blood or tissue by liquid scintillation counting.
Analytical Biochemistry 16: 500-509.

MARMOR, M.F. (1975a)
Structure and function of the retinal pigment epithelium.
International Ophthalmology Clinics 15: 115-130.

MARMOR, M.F. (1975b)
The retinal pigment epithelium and ocular disease.
International Ophthalmology Clinics 15: 131-136.

MAURICE, D.M. (1957)
The exchange of sodium between the vitreous body and the blood and aqueous humour.
Journal of Physiology 137: 110-125.

MAURICE, D.M. (1959)
Protein dynamics in the eye studied with labelled proteins.
American Journal of Ophthalmology 47: 361-368.

MAURICE, D.M. & POLGAR, J. (1977)
Diffusion across the sclera.
Experimental Eye Research 25: 577-582.

MAURICE, D.M., SALMON, J. & ZAUBERMAN, H. (1971)
Subretinal pressure and retinal adhesion.
Experimental Eye Research 12: 212-217.

McEWEN, W.K. (1958)
Application of Poiseuille's law to aqueous outflow.
Archives of Ophthalmology 60: 290-294.

MEESMANN, A. (1930)
Blutgasanalysen am Kaninchenauge
Bericht: Deutsche Ophthalmologische Gesellschaft

MICHAELSON, I.C. (1965)
Intertissue vascular relationships in the fundus of the eye.
Investigative Ophthalmology 4: 1004-1012.

MILLER, S.S. & STEINBERG, R.H. (1977)
Active transport of ions across the frog retinal pigment epithelium.
Experimental Eye Research 25: 235-248.

MISHIMA, S. & MAURICE, D.M. (1961)
The oily layer of the tear film and evaporation from the corneal surface.
Experimental Eye Research 1: 39-45.

MOSES, R.A. (1970)
The aqueous
In Adler's Physiology of the Eye, ed. Moses, R.A. Ch.7, pp.297-310.

NAKAMURA, Y. & GOULSTINE, D. (1973)
The effect of intraocular pressure on the vortex vein blood flow.
Experimental Eye Research 15: 461-466.

OAKLEY, B.II. (1977)
Potassium and photoreceptor-dependent pigment epithelial hyperpolarization.
Journal of General Physiology 70: 405-425.

O'DAY, D.M., FISH, M.B., ARONSON, S.B., POLLYCOVE, M. & COON, A. (1971)
Ocular blood flow measurement by nuclide labelled microspheres.
Archives of Ophthalmology 86: 205-209.

O'ROURKE, J. (1976)
Nuclear Opthalmology. London: W.B. Saunders.

PALM, E. (1949)
The exchange of phosphate between the blood and the eye, studied with the aid of radio-autographs.
Acta Ophthalmologica 27: 267-274.

PARKES, G.D. (1967)
Mellor's Modern Inorganic Chemistry. London: Longmans.

PAUFIQUE, L., FAYET, M.T. & RAVAULT, M. (1959)
Etude comparative du vitre humain normal et lyophilise.
Annales d'Oculistique 192: 241-254.

PERKINS, E.S. & GLOSTER, J. (1957)
Distensibility of the eye.
British Journal of Ophthalmology 41: 93-102.

PEYMAN, G.A., SPITZNAS, M. & STRAATSMA, B.R. (1971)
Chorioretinal diffusion of peroxidase before and after photocoagulation.
Investigative Ophthalmology 10: 489-495.

PINSON, E.A. & LANGHAM, W.H. (1957)
Physiology and toxicology of tritium in man.
Journal of Applied Physiology 10: 108.

PRINCE, J.H. (1964a)
The Rabbit in Eye Research. Illinois: Charles C. Thomas.

PRINCE, J.H. (1964b)
Aqueous drainage. 3: Outflow.
In The Rabbit in Eye Research, ed. Prince, J.H. Ch.10, pp 336-339.
Springfield, Illinois: Charles C. Thomas.

PRINCE, J.H. (1964c)
Vitreous.
In The Rabbit in Eye Research, ed. Prince, J.H. Ch.6, pp 372-384.
Springfield, Illinois: Charles C. Thomas.

REDDY, D.V.N. & KINSEY, V.E. (1960)
Composition of the vitreous humor in relation to that of plasma and aqueous humors.
Archives of Ophthalmology 63: 715-720.

REDDY, D.V.N. & KINSEY, V.E. (1962)
Transport of alpha aminoisobutyric acid into ocular fluids and lens.
Investigative Ophthalmology 1: 41-51.

REDDY, D.V.N., ROSENBERG, C. & KINSEY, V.E. (1961)
Steady state distribution of free amino acids in the aqueous humors, vitreous body and plasma of the rabbit.
Experimental Eye Research 1: 175-181.

REDSLOB, E. (1932)
Le corps vitre. Son developpment, sa structure, ses proprietes, physicochimiques. Paris: Masson & Cie, Editeurs.

RICHMOND, C.R., LANGHAM, W.H. & TRUJILLO, T.T. (1962)
Comparative metabolism of tritiated water by mammals.
Journal of Cellular and Comparative Physiology, 59: 45-52.

RODRIGUEZ-PERALTA J. & LORENZO, A. (1968)
Hematic and fluid barriers of the retina and the vitreous body.
Journal of Comparative Neurology 132: 109-124.

ROHEN, J.W. (1969)
New studies on the functional morphology of the trabecular meshwork and the outflow channels.
Transactions of the Ophthalmological Society of the United Kingdom 89: 431-447.

ROHLICH, P. (1970)
The interphotoreceptor matrix: electron microscopic and histochemical observations on the vertebrate retina.
Experimental Eye Research 10: 80-96.

ROSENGREN, B. (1971)
Significance of subretinal absorption for effectiveness of buckling operations.
Acta Ophthalmologica 49: 866-872.

RUSKELL, G.L. (1961)
Aqueous drainage pathways in the rabbit.
Archives of Ophthalmology 66: 861-870.

RUSKELL, G.L. (1964)
Blood vessels of the orbit and globe.
In The Rabbit and Eye Research, ed. Prince, J.H. Ch.15, pp 514-553.
Springfield, Illinois: Charles C.Thomas.

SCHWARZ, W. (1961)
Electron microscopic observations of the human vitreous body.
In The Structure of the Eye, ed. Smelser, G.K.
New York: Academic Press

SEGAWA, K. (1973)
Pore structures of the endothelial cells of the aqueous outflow pathway: scanning electron microscopy.
Japanese Journal of Ophthalmology 17: 133-139.

SHABO, A.L., REESE, T.S. & GAASTERLAND, D. (1973)
Postmortem formations of giant endothelial vacuoles in Schlemm's canal of the monkey.
American Journal of Ophthalmology 76: 896-905

SHERMAN, S.H., GREEN, K. & LATIES, A.M. (1978)
The fate of anterior chamber fluorescein in the monkey eye. I. The anterior chamber outflow pathways.
Experimental Eye Research 27: 159-173.

SHIOSE, Y. (1969)
Electron microscopic studies on blood-retinal and blood-aqueous barriers.
Japanese Journal of Ophthalmology 14: 73-87.

SHIOSE, Y. (1970)
Electron microscopic studies on blood-retinal and blood-aqueous barrier.
Japanese Journal of Ophthalmology 14: 73-87.

SIDMAN, R.L. (1958)
Histochemical studies on photoreceptor cells.
Annals of the New York Academy of Sciences 74: 182-195.

SONDERMANN, R. (1932)
Experimentelle Untersuchungen uber die Durchblutungsgrosse des Auges bei normalen und abnormalen Drucke.
Arch. Augenkeilk. 105: 698-703.

STEINBERG, R.H. & MILLER, S.S. (1973)
Aspects of electrolyte transport in frog pigment epithelium.
Experimental Eye Research 16: 365-372.

STRANG, R. (1975a)
The measurement of choroidal blood flow using krypton-85.
Ph.D. Thesis. University of Glasgow.

STRANG, R. (1975b)
The measurement of the Ostwald solubility coefficient of krypton in blood and ocular tissues.
Physics in Medicine and Biology 20: 1025-1028.

STRANG, R. (1977)
The determination of the diffusion coefficient of krypton in rabbit ocular tissue.
Investigative Ophthalmology 16: 83-86.

STRANG, R., WILSON, T.M. & JOHNSON, N.F. (1974)
The effect of alterations in arterial carbon dioxide tensions on choroidal blood flow in rabbits.
Experimental Eye Research 18: 153-156.

SUGAYA, M. & NAGATAKI, S. (1978)
Kinetics of topical pilocarpine in the human eye.
Japanese Journal of Ophthalmology 22: 127-141.

SULLMANN, H. (1951)
Chemie des Auges.
Tabul. Biol. 22: 79-88.

SVEDBERGH, B. (1976)
Aspects of the aqueous humor drainage. Functional ultrastructure of Schlemm's canal, the trabecular meshwork and the corneal endothelium at different intraocular pressures.
Acta Universitatis Uppsaliensis Abstract of the Uppsala Dissertations in the Faculty of Medicine 256: 1-71.

SZIRMAI, J.A. & BALAZS, E.A. (1958)
Studies on the structure of the vitreous body. III. Cells in the cortical layer.
Archives of Ophthalmology 59: 34-48.

TONJUM, A.M. (1977)
Movement of horseradish peroxidase in the cornea, sclera and the anterior uvea.
Acta Ophthalmologica 55: 771-780.

TRIPATHI, R.C. (1968)
Ultrastructure of Schlemm's canal in relation to aqueous outflow.
Experimental Eye Research 7: 335-341.

TRIPATHI, R.C. (1971a)
Mechanism of the aqueous outflow across the trabecular wall of Schlemm's canal.
Experimental Eye Research 11: 116-121.

TRIPATHI, R.C. (1971b)
Ultrastructure of the exit pathway of the aqueous in lower mammals (a preliminary report on the "angular aqueous plexus").
Experimental Eye Research 12: 311-314.

TRIPATHI, R.C. (1974)
Comparative physiology and anatomy of the aqueous outflow pathway.
In The Eye, ed. Davson, H. & Graham, L.T. Vol5, Ch.3. New York and London: Academic Press.

TRIPATHI, R.C. (1977)
The functional morphology of the outflow system of ocular and cerebrospinal fluids.
Experimental Eye Research Suppl.: 65-116.

TRONCHE, P., MEYNIEL, G., ALFIERI, R., ROUHER, F. & PAGES, C. (1963)
Repartition et metabolisme du radiophosphore 32 injecte dans le gel vitreen.
Annales d'Oculistique 196: 159-179.

UDEKWU, F.A.O., KOZELL, D.D. & MEYER, K.A. (1963)
Determination of total body water with tritium oxide.
Journal of Nuclear Medicine 4: 60-65.

UNSWORTH, J. & GILLESPIE, F.C. (1970)
Diffusion coefficients of xenon and krypton in water from 0°C to 80°C and in biological tissues at 37°C.
In Proceedings of Thomas Graham Memorial Symposium. London: Gordon and Breech.

VAN ALPHEN, G.W. (1961)
On emmetropia and ametropia.
Ophthalmologica 142: 47-52.

VAN DER ZYPHEN, E. (1971)
Light and electron microscopic studies on the morphology of tissues involved in circulation of aqueous humour and cerebrospinal fluid.
In Altern und Entiwicklung, ed. Brant, H. & Rohen, J.W.
Band 2. Stuttgart and New York: F.K. Shattauer Verlag.

VIERNSTEIN, L.J. & COWAN, M. (1969)
Static and dynamic measurements of the pressure-volume relationship in living and dead rabbit eyes.
Experimental Eye Research 8: 183-192.

VISSER-HEEREMA, J. (1936)
Ueber das spezifische gewicht der beider operation von netzhautablosungen gewonnenen flussigkeit.
Arch. Augenheilk 109: 543-561.

VON ROSENBERG, D.U. (1969)
Methods for the Numerical Solution of Partial Differential Equations.
New York: American Elevier Publishing Company.

VON SALLMANN, L. & DILLON, B. (1950)
Studies of the eye with radioiodine autographs.
American Journal of Ophthalmology 33: 429-440.

VON SALLMANN, L., EVANS, T. & DILLON, B. (1949)
Studies of the eye with radiosodium autographs.
Archives of Ophthalmology 41: 611-626.

VON SALLMANN, L. & LOCKE, B.D. (1952)
Experimental study on early lens changes after roentgen irradiation: exchanges and penetration of radioactive indicators (Na^{24}, K^{42}, I^{131}, P^{32}) in normal and irradiated lenses of rabbits.
Archives of Ophthalmology 45: 431-444.

WANG, J.H. (1965)
Self-diffusion coefficients of water.
Journal of Physical Chemistry 69: 4412.

WEIDENTHAL, D.T. (1967)
Retinal reattachment without release of subretinal fluid.
American Journal of Ophthalmology 63: 108-112.

WITMER, R. (1975)
Retinal detachment surgery.
Canadian Journal of Ophthalmology 10: 15-24.

YOUNG, R.W. & BOK, D. (1969)
Participation of the retinal pigment epithelium in the rod outer segment renewal process.
Journal of Cell Biology 42: 392-403.

ZAUBERMAN, H. & de GUILLEBON, H. (1972)
Retinal traction in vivo and post mortem.
Archives of Ophthalmology 87: 549-554.

ZIMMERMAN, L.E. & EASTHAM, A.B. (1959)
Acid mucopolysaccharide in the retinal pigment epithelium and visual cell layer of the developing mouse eye.
American Journal of Ophthalmology 47: 488-498.